Alpaca, armadillo and cotton rat as new animal models for non-conventional T cells: Identification of cell populations and analysis of antigen receptors and ligands

Alpaka, Gürteltier und Baumwollratte als neue Tiermodelle für nicht-konventionelle T-Zellen: Identifikation von Zellpopulationen und Analyse von Antigenrezeptoren und Liganden

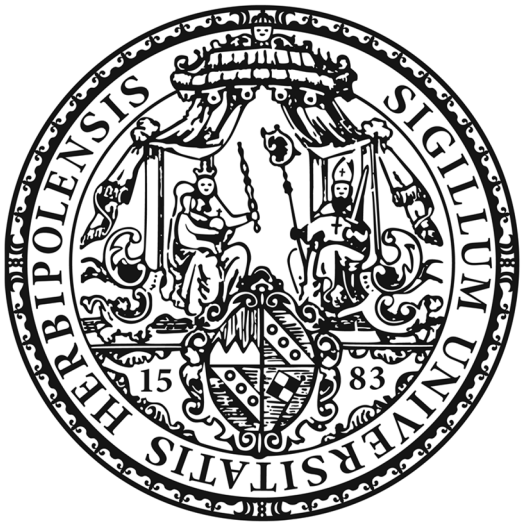

Doctoral thesis for a doctoral degree at the Graduate School of Life Sciences
Julius-Maximilians-Universität Würzburg
Section Infection and Immunity

submitted by
Alina Suzann Fichtner
from
Ingolstadt

Würzburg 2018

Submitted on: ……..…..

Office stamp

Members of the *Promotionskomitee*:

Chairperson:	Prof. Dr. Georg Gasteiger
Primary Supervisor:	Prof. Dr. Thomas Herrmann
2nd Supervisor:	PD Dr. Heike Hermanns
3rd Supervisor:	PD Dr. Niklas Beyersdorf

Date of Public Defence: ……..…

Date of Receipt of Certificates: ……..

Table of Contents

1 Introduction

The basic principles of immunology described in this thesis are based on the 8th edition of "Cellular and Molecular Immunology" by A. K. Abbas, A. H. Lichtman and S. Pillai [1] and the 9th edition of "Janeway's Immunobiology" by K. Murphy and C. Weaver [2]. The immunological principles are described for the human model system if not otherwise indicated.

1.1 Preface

For centuries, non-human species have been used as models for comparative medicine in medical research due to physiological and behavioral similarities to humans [3]. Today, animal models are used in most scientific fields including immunology, virology, oncology, infectious diseases and behavioral biology. The growing use of animal models was marked by the development of inbred mouse and rat strains that carry characteristic traits leading to increased or decreased susceptibility to certain malignancies or diseases. Moreover, the use of inbred strains allowed to ensure reproducibility of experimental procedures. Subsequently, small rodent models became the state-of-the-art to investigate biological and medical significance [3]. With the more recent application of genetic modifications, such as gene knock out mice, transgenic mouse strains and the development of humanized mice carrying human cells, tissues or a human immune system, the utility of the mouse model has increased even more. However, some aspects of immunological research cannot be covered by the sole use of mouse models, for example the study of functional relationships and coevolution. Therefore, other non-human animals like rats, cattle, pigs, sheep and zebrafish have been studied, and valuable insights into coevolution and immunity were gained. Some of these animals can be considered model organisms whereas others serve as subjects for basic research. The applicability of new animal models for distinct non-conventional T cell subsets will be investigated here. For this, two non-conventional T cell populations will be identified in these animals and ligands as well as restricting molecules for antigen recognition will be studied. This will allow to evaluate the potential use of these models in the study of both cell populations. Invariant natural killer T (iNKT) cells can modulate the immune response via rapid cytokine secretion and are characterized by a semi-invariant αβ T cell receptor (TCR). The conservation of this cell type is investigated in the cotton rat (*Sigmodon hispidus*), an organism susceptible to infections with human viruses like measles, influenza or respiratory syncytial virus (RSV). The second innate-like T cell subset uses a characteristic Vγ9Vδ2 TCR and was thought to be restricted to primates. Here, the conservation of these cells is investigated in the placental mammal species nine-banded armadillo (*Dasypus novemcinctus*) and alpaca (*Vicugna pacos*).

1.2 The vertebrate immune system

The immune system of vertebrates consists of two principal responses against pathogens: the innate and the adaptive immune response. The first line of defense is provided by the innate immune system and is characterized by a rapid recognition of invading pathogens mediated by germline-encoded receptors, the pattern recognition receptors (PRR). Innate responses are characterized by cellular mechanisms including neutrophils, dendritic cells (DC), macrophages and innate lymphoid cells, e.g. natural killer (NK) cells, and the activation of the complement system. Subsequently, the adaptive immune system mediates a strong pathogen-specific cellular and humoral response. A hallmark of the adaptive immune system of jawed vertebrates is the use of somatic recombination of immunoglobulin (Ig) genes to generate a diverse array of antigen receptors, more specifically B cell receptors (BCR) and T cell receptors, that are able to specifically recognize pathogenic antigens. The cell types of the adaptive immune system are B cells which provide the basis for a humoral response, consisting of antibody effector functions, and T cells mediating cellular responses. The adaptive immune system is able to form a memory response which can rapidly react to recurring pathogenic infections. This combination of effector mechanisms and the interplay of different cell types ensure an efficient response to pathogens. The cells of the immune system are called white blood cells (leukocytes) and arise from hematopoietic stem cells (HSC) in the bone marrow. Development and maturation of adaptive immune cells take place in the bone marrow (B cells) and thymus (T cells). Circulation of immune cells to tissues or secondary lymphoid organs occurs through the lymphatic system and the bloodstream.

1.3 T cells

T lymphocytes emerge from common lymphoid progenitors in the bone marrow and immature progenitors migrate to the thymus to complete their maturation. The T cell compartment can be divided into two types of T cells, γδ and αβ T cells, which are distinguishable by their T cell receptor. This receptor is a multiprotein complex characterized by two transmembrane proteins, γδ or αβ, linked by a disulfide bond or, in some cases, non-covalently associated, and is formed by somatic recombination (see 1.3.1). Each TCR chain possesses two extracellular Ig-like domains, the variable (IgV) and constant (IgC) region, a stalk segment, a transmembrane part and an intracellular tail. These polypeptides are associated with and stabilized by the Cluster of Differentiation 3 (CD3) complex which consists of two CD3 heterodimers, CD3δ:CD3ε and CD3γ:CD3ε, and two cytosolic ζ chains. These accessory molecules are essential for surface expression of the TCR, signal transduction and T cell activation.

TCR signaling is initiated by antigen recognition dependent on signals by the TCR and involves tyrosine phosphorylation of immunoreceptor tyrosine-based activation motifs (ITAM), which are cytoplasmic domains of the CD3 and ζ chains. Subsequently, a downstream cascade of signaling pathways leads to various changes in the cell, like the activation of transcription factors, cytoskeletal changes or metabolism, that enable effector functions of the activated T cell.

αβ and γδ T cells are distinct developmental lineages and are profoundly different in their way of antigen recognition and function. In general, the αβ T cell receptor recognizes peptide antigens which are processed and presented by major histocompatibility complex (MHC) molecules on special antigen-presenting cells in the case of MHC class II (MHC II) or all body cells in the case of MHC class I (MHC I). In contrast, γδ T cells are not restricted to the recognition of peptide:MHC complexes but consist of different cell subsets that recognize antigens by various mechanisms.

1.3.1 Generation of diversity in T cell receptors

A hallmark of adaptive immunity is the use of a diverse repertoire of antigen receptors able to recognize a wide range of pathogens. The antigen recognition site of TCRs is composed of parts of the IgV domain of both TCR chains and highly variable. The IgV domain is encoded by variable (*TRV*), diversity (*TRD*) and joining (*TRJ*) genes and the IgC domain by constant region (*TRC*) gene segments. Diversity in the antigen recognition site is mediated by somatic recombination of these genes in the germline of developing T lymphocytes in the thymus. The gene segments used for αβ and γδ chains are organized in three loci on different chromosomes. In humans, the α locus is located on chromosome 14 and contains all δ genes which are interspersed between α genes. The β and γ locus map to different arms of chromosome 7. Each locus is comprised of multiple *TRV*, *TRJ* genes and one or few *TRC* genes. The β and δ loci also contain *TRD* gene segments.

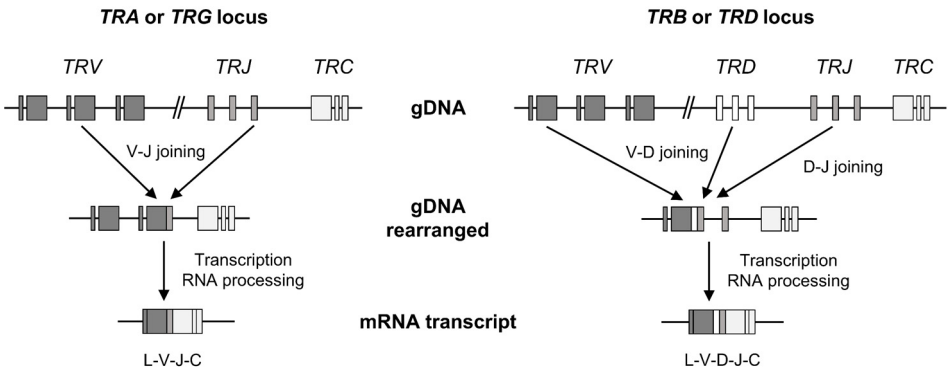

Figure 1.1 Somatic recombination of TCR gene segments. In the genomic DNA (gDNA) of an immature T lymphocyte a randomly chosen *TRV* segment, including the signal sequence, is joined with a randomly selected *TRJ* segment in the α (*TRA*) or γ (*TRG*) locus. *TRV* to *TRD* and *TRD* to *TRJ*, respectively, are joined in the β (*TRB*) or δ (*TRD*) locus. A primary rearranged transcript is formed in which the rearranged V(D)J exons are still separated from the C segment which is comprised of multiple exons. Following RNA splicing, a messenger RNA (mRNA) is formed that contains a signal sequence (L), *TRV* (V), *TRD* (D) *TRJ* (J) and *TRC* (C), in this order and is subsequently translated into the respective TCR chain.

An overview of the somatic recombination of TCR gene segments is depicted in **Figure 1.1**. In the TCR loci, random *TRV*, (*TRD*) and *TRJ* are joined by gene rearrangements and transcription of the rearranged germline DNA occurs. The signal sequence essential for translocation into the endoplasmic reticulum (ER) and *TRC* gene segments are joined in this transcript via splicing mechanisms during RNA processing. The joined *TRV* and *TRJ* gene segments encode for a polypeptide with a typical immunoglobulin fold (IgV). The structure of this domain is characterized by nine β sheets and loops between β sheet pairs. Those loops are called complementarity determining regions (CDR) and are essential for antigen recognition. CDR1 and 2 are encoded by *TRV*, while the *TRV*/*TRJ* junction encodes CDR3. *TRC* codes for the constant IgC domain and the transmembrane/intracellular part of the molecule.

Somatic recombination is only possible through the occurrence of flanking sequences of *TRV*, *TRD* and *TRJ* genes. These recombination signal sequences (RSS) are located directly at the end of *TRV* (3' end), the beginning and end of *TRD* (5' and 3' end) and the beginning of the *TRJ* gene segment (5' end). RSS sites consist of a conserved heptameric nucleotide (NT) sequence followed by a nonconserved spacer region of 12 or 23 base pairs (bp) and a second block of nine conserved nucleotides (nonamer). The conserved consensus sequences can vary among different gene segments and species. A reason for the conserved lengths of spacers could be the fact that one turn of the DNA helix is around 12 bp and two turns around 23 bp which is thought to bring both RSS sites onto the same side of the helix, enabling interactions with necessary proteins.

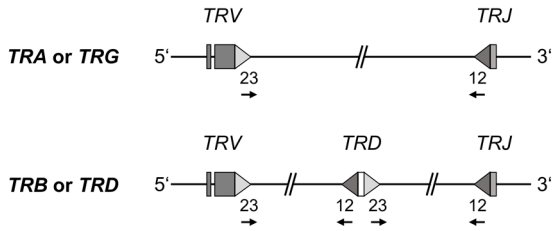

Figure 1.2 Location of RSS sites in TCR genes. The location of conserved RSS sites is indicated for *TRV*, *TRD* and *TRJ* genes of all loci and the orientation of the RSS is indicated (5' to 3': heptamer-spacer-nonamer, 3' to 5': nonamer-spacer-heptamer).

The distribution of 12/23 bp RSS sites in TCR gene segments (**Figure 1.2**) ensures proper rearrangement of *TRV*, (*TRD*) and *TRJ* gene segments as usually only 12 bp spacers join with 23 bp spacer RSS sites (12/23 rule). Typically, gene rearrangement occurs on the same chromosome. The addition of *TRD* gene segments between *TRV* and *TRJ* in the δ locus can lead to the use of more than one *TRD* gene segment or no *TRD* gene segment at all.

Somatic recombination is carried out by a complex of enzymes called the V(D)J recombinase. The first step of gene rearrangement is dependent on the RAG-1:RAG-2 recombinase, a complex of two RAG-1 and RAG-2 proteins each, only expressed in developing lymphocytes. The remaining enzymes used for somatic recombination are ubiquitously expressed members of the nonhomologous end joining pathway of double-strand DNA repair. This process is imprecise in nature and contributes to the junctional diversity of antigen receptors. RAG-1:RAG-2 recognizes two RSS sites and joins them following the 12/23 rule. Subsequently, the RAG complex introduces a single-strand DNA break 5' of the RSS site and a hairpin at the coding region is created. Next, the Ku70:Ku80 heterodimeric protein binds around the hairpin ends of both gene segments and initiates the formation of the DNA-dependent protein kinase (DNA-PK) through recruitment of complex members. Artemis, a complex protein with nuclease activity, mediates the opening of hairpins. This can occur at several locations, leading to sequence variability of the joints as hairpin overhangs create palindromic sequences known as P nucleotides. Nucleotides can be removed by DNA repair enzymes or are added by the lymphoid-specific terminal deoxynucleotidyl transferase (TdT). The addition of nucleotides by TdT is random and non-template dependent (N nucleotides). DNA ligase IV joins the modified ends, and remaining RSS sites are joined precisely to avoid chromosome breaks or genetic changes. This process of somatic recombination leads to high variability in the CDR3 region of TCR chains which is essential for antigen recognition. Moreover, two-thirds of rearranged gene segments lead to non-productive TCR chains, as the reading frame is disturbed by the addition of N or P nucleotides.

1.3.2 Antigen recognition by T cells

1.3.2.1 Antigen recognition by αβ T cells

Conventional αβ T cells recognize peptides presented by highly polymorphic MHC proteins on antigen-presenting cells (APC). These MHC molecules are encoded in the MHC region on human chromosome 6 which possibly extends over 7 million base pairs and contains more than 200 genes. These include three genes named human leukocyte antigen genes (HLA in humans) for each chain of the MHC classes I and II. Additional genes like β_2-microglobulin (β_2m) and multiple genes that resemble MHC molecules in structure and are called non-classical MHC or MHC class Ib genes (e.g. human: MIC-A, MIC-B; mouse: T10, T22) are also encoded in the MHC region. Other MHC class Ib genes, such as CD1 and MR1 genes, are not MHC-encoded. MHC molecules differ in their structural organization with MHC I using a single α chain consisting of three Ig-like domains (α1-3) and a non-covalently associated β_2-microglobulin, while MHC II is comprised of two associated chains, the α and β chain with two Ig-like domains each. The polypeptide chains of MHC molecules are anchored to the cell membrane with a transmembrane unit in the α chains of MHC I/II and the β chain of MHC II and possess an intracellular tail. Antigen presentation is mediated by binding of peptides in antigen-binding clefts which are comprised of the α1 and α2 domains in MHC I and the α1 and β1 domains in MHC II molecules. These regions are highly diverse and allow the binding of peptide fragments of particular length. The antigen binding cleft of MHC I molecules usually accommodates peptides of 8-10 amino acids (AA), whereas MHC II molecules present longer peptides that usually contain 13-17 amino acids. The αβ T cell population can be divided by their ability to be activated by MHC I or MHC II molecules. Expression of the co-receptors CD4 and CD8 determines MHC restriction of αβ T cells to MHC II or MHC I, respectively. MHC molecules are differentially expressed in various cell types. MHC I is expressed by nearly all somatic cells, whereas MHC II is only expressed by immune cells that carry out professional antigen-presenting functions like DCs, macrophages and B cells. Epithelial cells in the thymus (thymic cortical epithelial cells) and activated T cells are also able to express MHC II molecules. Antigen presentation by MHC I and MHC II molecules is dependent on different pathways of antigen loading and specialized for antigens of intracellular (MHC I) or extracellular origin (MHC II). MHC I molecules mediate direct presentation of antigenic peptides originating from the cytosol, including pathogenic, tumor or self-antigens. Newly synthesized MHC I α chains are translocated to the lumen of the ER where they are folded with the help of chaperones, like calnexin, and associated with β_2-microglobulin. Cytosolic peptides, which are partially degraded proteins mediated by proteasomal activity in the cytosol, are transported to the ER by the transporters associated with antigen processing-1 and -2 (TAP1 and TAP2). MHC I molecules possess an antigen-binding

cleft formed by the α1 and α2 domain of the α chain that can accommodate peptides of 8-11 amino acids. Therefore, antigenic peptides transported into the ER are trimmed before loading onto MHC I by the peptide-loading complex (PLC). Peptide:MHC I complexes are then expressed on the cell surface. The antigens presented by MHC II molecules are peptides internalized into endocytic vesicles by receptor-mediated endocytosis or phagocytosis of pathogens, infected or transformed cells. Pathogens that replicate in intracellular vesicles can also be detected in this way as well as self-peptides originating from protein turnover known as autophagy. Proteins are then degraded in the endosomes at low pH by proteases. The MHC II α and β chains are, like MHC I molecules, delivered to the ER for folding and transported to the cell surface. Peptide loading of the newly synthesized MHC II molecules in the ER is prevented by the class II-associated invariant chain peptide (CLIP) which binds the MHC II α:β heterodimer in a trimeric fashion. CLIP blocks the antigen-binding cleft formed by the α1 and β1 domains of MHC II and also directs MHC II molecules to low pH endosomal compartments. Subsequently, CLIP is cleaved and exchanged by peptide antigens via HLA-DM catalysis, a monomorphic MHC II-like protein. Peptide antigens presented by MHC II are usually 10-30 amino acids and therefore longer compared to MHC I antigens, as MHC II possesses an antigen-binding cleft with open ends. Binding of peptide:MHC complexes is dependent on germline-encoded and non-germline-encoded parts of the αβ TCR [4]. Usually, the CDR1 and CDR2 of the TCR α chain contact the MHC I α2 helix or the β helix of MHC II, whereas CDR1 and CDR2 of the β chain bind to the α1 helix of MHC I or the α helix of MHC II. The CDR3 regions of αβ TCRs are not germline encoded, highly variable and usually contact residues on the peptide. This pattern of interactions results in a diagonal binding mode of the TCR to MHC molecules.

1.3.2.2 Antigen recognition by γδ T cells

Antigen recognition of γδ T cells is very diverse in comparison to αβ T cells and the major difference to αβ T cells is the lack of MHC restriction in γδ T cells. Expression of co-receptors CD4 and CD8 does not seem to be essential for γδ T cell antigen recognition and most murine γδ T cells are $CD4^{-}CD8^{-}$. However, mouse intestinal intraepithelial T cells (iIEL) express CD8αα and certain human γδ T cell subsets express CD8 [5]. Also, CD8αβ expression was shown on rat γδ T cells but was not linked to MHC-dependent antigen recognition [6]. In contrast to αβ TCRs, γδ TCRs do not seem to be restricted in structure to recognize antigens presented by specific molecules, as CDR3 lengths, especially in the δ chain, vary substantially [7]. Their antigen recognition mode was described to share similarities with immunoglobulins rather than αβ TCR [8] and a wide range of structurally variable ligands has been shown for γδ T cells which is distinct from conserved peptide:MHC recognition of αβ T cells [9].

However, a restricting molecule could still exist, especially since distinct subsets of γδ T cells were identified that recognize a variety of antigens and can be considered either innate-like or adaptive [7]. Specific examples of γδ T cell ligands exist for mouse and human subsets and can sometimes be assigned to γδ TCRs using specific *TRGV* or *TRDV* gene segments. Certain MHC-related molecules can be recognized by γδ TCRs. The crystal structures of mouse γδ TCR with the non-classical MHC class Ib molecules T10/T22 have been reported and specificity is dependent on a motif in CDR3δ but not on ligands presented by these molecules [10, 11]. In addition, a murine Vγ2Vδ5 clone was reactive to an epitope of the mouse MHC II molecule I-E^k, again independent of peptide cargo [12]. Certain human γδ TCRs using Vδ1 or Vδ2 chains, are able to recognize MHC I-like MICA/B or ULBP family members, respectively [13-15]. The MHC-related molecule CD1d, a CD1 family member (see 1.5.2.1), was found to present sulfatide, a myelin glycosphingolipid, to γδ TCRs with a Vδ1 chain [16]. The phospholipids phosphatidylethanolamine [17-19] and cardiolipin [20] presented by CD1d were also recognized by γδ TCRs. This indicates MHC-like antigen presentation to γδ T cells. Another MHC-like molecule recognized by a human Vγ4Vδ5 T cell clone obtained from a cytomegalovirus (CMV)-infected patient, is the endothelial protein C receptor (EPCR) [21]. Apart from reactivity to self-MHC or MHC-like molecules, γδ TCRs from human, murine and bovine origin were reactive to the algal molecule phycoerythrin (PE), which is also a B cell antigen [22] and supports antibody-like antigen recognition modes of γδ T cells. Soluble proteins of pathogenic origin were also implied in the activation of certain γδ TCRs, e.g. the superantigen staphylococcal enterotoxin [23], herpes simplex virus (HSV) glycoprotein 1 [24] and tetanus toxoid [25, 26]. Moreover, small peptides were also recognized by γδ TCRs including a peptide originating from the mycobacterial heat shock protein HSP-65 which was detected by murine Vγ1$^+$ T cells in a TCR-dependent manner independent of antigen presentation [27-29]. The insulin-derived peptide B:9-23, also presented to CD4 T cells by MHC II I-A^{g7}, was found to activate murine Vγ1$^+$ T cell clones in non-obese diabetic mice independent of MHC [30]. Apart from this multitude of different ligands, non-peptide antigens of mycobacterial origin were observed that efficiently activate human Vγ9Vδ2 T cells [31]. The antigens involved where low-molecular-mass prenyl pyrophosphates, also termed phosphoantigens (PAg) [32]. The Vγ9Vδ2 T cell subset is described in more detail in chapter 1.6. The multitude of structurally different antigens and ligands for γδ T cells suggests diverse modes of antigen recognition by small or large subsets of γδ T cells. Moreover, a clear distinction of γδ and αβ T cells in terms of antigen recognition is evident. A detailed review of γδ T cell antigens was provided by Born et al. [9], Vantourout et al. [7], Adams et al. [33] and very recently by Vermijlen et al. [34].

1.3.3 Development of T cells

1.3.3.1 Thymic maturation of MHC-restricted αβ T cells

Lymphocyte development from progenitor cells to mature lymphocytes can be described by several essential events in the lymphoid organs, namely commitment to B or T cell lineage, proliferation, rearrangement of antigen receptors, selection and differentiation [2, 35]. Hematopoietic stem cells are pluripotent stem cells in the fetal liver and bone marrow and progenitor to all blood cell lineages, including lymphocytes. HSCs develop into common lymphoid progenitors which, if committed to the T cell lineage, leave the fetal liver and bone marrow to complete their maturation in the thymus. The two subsets of T cells can arise from different HSCs with αβ T cells originating from bone marrow-derived HSCs, and γδ T cells can emerge from both bone-marrow or fetal liver HSCs. The development of αβ T cells can be divided into distinct stages dependent on the surface expression of the co-receptors CD4 and CD8 important for T cell activation. These stages are the double-negative (DN) stages 1-4 ($CD4^-CD8^-$), the double-positive (DP) stage ($CD4^+CD8^+$) and the single-positive (SP) stage ($CD4^+CD8^-$ or $CD4^-CD8^+$) where CD3 expression can be detected. Rearrangement of the *TRB* locus occurs from stage DN2-DN3, and a preTCR using an invariant preTα chain is expressed. These cells undergo positive selection, a process ensuring self-peptide:self-MHC recognition and therefore functionality of the TCR while cells that fail to bind self-peptide:self-MHC undergo apoptosis. Following positive selection, only one of the co-receptors CD4 and CD8 is expressed (SP stage). A second selection process eliminates cells that strongly bind to self-antigens (negative selection). Single-positive αβ T lymphocytes leave the thymus and home to the periphery. These cells are still functionally immature and T cell activation by the antigen specifically recognized by individual clones and presented by professional APCs is required in secondary lymphoid organs.

1.3.3.2 Development of γδ T cells

The rearrangements of *TRD* and *TRG* loci precede *TRB* recombination, and successful *TRA* rearrangement eliminates the *TRD* locus which lies within *TRA*. Hence, γδ T cells usually emerge before αβ T cells and are major cell subsets in fetal development [36-38]. The γδ cell lineage develops first during embryonic development from DN2 stage progenitors common for all T cells [39-42], and this has raised the hypothesis of the increased importance of these cells in early life [43, 44]. The maturation of γδ T cells is different from αβ T cell maturation and can be controlled by the activity of certain transcription factors and is influenced by TCR signal strength and potentially by ligand interactions [45, 46].

Moreover, γδ T cell antigen recognition is very broad and not dependent on ligand:MHC interactions during selection. The influence of B7 receptor family-like butyrophilin (BTN) and butyrophilin-like (BTNL) molecules on the development of specific γδ T cell subsets like epithelial and circulating γδ T cell subsets (see 1.6) has been shown [47-49]. In the murine system, γδ T cell development starts at the DN stage of thymic precursors [43, 45, 46, 50, 51]. An important factor for the commitment to the γδ lineage in mice seems to be strong TCR signals [52]. As summarized by Prinz et al. [45], maturation of γδ T cells in the mouse can be described by functional γδ T cell waves that arise during windows of opportunity in fetal development. Dendritic epidermal T cells (DETC, Vγ5$^+$), which have been shown to be selected by the butyrophilin-like Skint1 molecule on medullary thymic epithelial cells, are the first subset developing in mice, followed by interleukin-17 (IL-17) producing γδ T cells (Vγ6$^+$, Vγ4$^+$ and sometimes Vγ1$^+$), γδ NKT cells and iIELs [45, 53, 54]. Distinct γδ T cell subsets show differential homing to and accumulation in lymphoid tissues or peripheral like the skin (DETCs) [53, 55-58]. Homing of γδ subsets depends on the action of various chemokines and their receptors whose expression is induced during maturation [45]. Notch signaling has been shown to influence γδ lineage commitment in humans [59, 60] and γδ T cell subsets can be roughly divided into Vδ1$^+$ γδ T cells that share similarities with murine iIELs and Vδ2$^+$ T cells which are a dominant cell population in the blood (see 1.6) [46]. Circulating γδ T cells can be detected at 12.5 weeks of gestation in humans, and high levels of Vγ9Vδ2 T cells were found around mid-gestation. Most γδ T cells acquire their effector functions during thymic development and show a pre-activated phenotype [61].

The overall frequency of γδ T cells varies in species leading to the assignment of "γδ low" species like mice and humans with 1-10% γδ T cells of circulating T cells and "γδ high" species like cattle, sheep, pigs and chicken with up to 40% γδ T cells in the blood [62, 63]. However, circulating γδ T cells do not fully recapitulate γδ T cell numbers as tissue-resident γδ T cells exist in many species [63]. Also, recirculation of γδ T cell populations between blood, skin/intestinal tissues and lymphatic tissues was shown in cattle and pigs [63, 64].

1.3.4 Effector functions of T cells

1.3.4.1 Effector responses of αβ T cell subsets

Naïve αβ T cells migrate continuously from the bloodstream through secondary lymphoid organs like lymph nodes, the spleen and mucosal-associated tissues (MALT) and back to sample peptide:MHC complexes on the surface of activated dendritic cells. Whenever αβ T cells encounter their specific antigen, presented by the appropriate MHC molecule

(MHC II for $CD4^+$; MHC I for $CD8^+$), the T cells are activated and undergo differentiation into effector T cells. This activation or priming is dependent on three signals: the first essential signal is the interaction of the peptide:MHC complex with the TCR complex, the second is provided by costimulatory signals that ensure the proliferation and survival and the third signal originates from cytokines that influence the direction of differentiation into effector subsets. Costimulatory molecules include the B7 receptor family molecules CD80 and CD86 on the APC and their ligand CD28 on T cells. The recognition of costimulatory molecules induces the expression of the cytokine IL-2 and a high-affinity IL-2 receptor which can increase cell proliferation and survival. Additional costimulatory signals through the inducible costimulator (ICOS, CD278) and ICOS ligand (ICOSL, CD275) and CD70 on DCs and CD27 on T cells are involved in the activation of naïve T cells. After activation, T cells proliferate for four to five days and become effector cells that do not depend on costimulation.

MHC restriction divides αβ T cells into two major lineages, $CD8^+$ T cells develop into cytotoxic effector cells that can kill target cells and $CD4^+$ T cells differentiate into distinct effector subsets with specialized functions, namely T helper 1 (T_H1), T helper 2 (T_H2), T helper 17 (T_H17), T follicular helper subsets (T_{FH}) or regulatory T cells (T_{reg}). While $CD8^+$ T cells always differentiate into cytotoxic T cells, differentiation of $CD4^+$ T cells into the main effector cell subsets is characterized by the type of pathogen targeted and their cytokine secretion. There is certain plasticity in T helper subsets indicated by the acquisition of some subsets to produce different cytokines in secondary infections [65]. The T_H1 subset is induced by an IL-12 cytokine milieu and is involved in the clearance of intracellular pathogens like mycobacteria species that can replicate and survive in phagocytes and evade killing mechanisms of those cells. T_H1 cells produce interferon-γ (IFN-γ) to activate microbicidal activities of macrophages further. The T_H2 subset requires IL-4 for differentiation and is a major subset in the control of extracellular parasites like helminths and promotes eosinophil and mast cell activity through IL-4, IL-5, IL-10 and IL-13 secretion [65]. In contrast, T_H17 cells are essential for the response to extracellular pathogens of bacterial or fungal origin and were observed to be heterogeneous in humans [65]. These cells are induced in a cytokine milieu with TGF-β, IL-1β, IL-6 and IL-23 dominance and produce IL-17 and/or IL-22 which promote barrier function of epithelial cells and induce production of antimicrobial peptides [65]. T follicular helper cells are important because they provide B cell help in germinal center reactions to produce high-affinity antibodies and are activated by most pathogens. The chemokine receptor CXCR5 is essential for localization of T_{FH} cells. Regulatory T cells have a completely different function as they limit the response of effector cells by the production of inhibitory cytokines like TGF-β and IL-10, expression of inhibitory costimulatory molecules like CTLA-4 and the fact that they sequester IL-2 from naïve T cells.

Cytotoxic T cells act by depleting cells infected by intracellular pathogens, especially viruses. The foreign peptides in the cytosol of infected cells are presented by MHC I and recognized by $CD8^+$ T cells. Cytotoxic T cells release granzymes which induce apoptosis, perforin which is involved in granzyme delivery into the cell and granulysin which is characterized by antimicrobial activity and induces apoptosis. Expression of Fas ligand (CD178) by $CD8^+$ T cells enables this cell subset to bind Fas (CD95) on target cells which leads to the extrinsic pathway of apoptosis. Production of IFN-γ by cytotoxic T cells inhibits viral replication and induces MHC I expression as well as activation of macrophages.

1.3.4.2 Effector responses of γδ T cell subsets

In contrast to αβ T cells, γδ T cells have been described as sentinels for infected and transformed cells that can rapidly react to activation without (w/o) the need for excessive clonal expansion and differentiation and can, therefore, be considered non-conventional or innate-like T cells as described in chapter 1.4 [7, 66, 67]. This is due to their pre-activated phenotype shown by expression of memory markers that enables fast induction of effector responses similar to innate cell types [67]. Effector functions include the elimination of infected or transformed cells, tissue repair and effects on epithelial cell barriers [66]. Killing of cells is mediated by engagement of death receptors like Fas and tumor necrosis factor-related apoptosis-inducing ligand (TRAIL) receptors as well as granzyme and perforin release and production of granulysin or defensins [68-71]. Interactions with other cells are mediated via chemokine production of γδ T cells. CXCL13, an important chemokine for B cell organization in follicles, is also produced by human Vγ9Vδ2 T cells [72]. Evidence was found that γδ T cells can regulate DC function and can actively present antigens to αβ T cells due to upregulation of MHC and costimulatory molecules [73-75]. Also, neutrophil recruitment by γδ T cells was shown. In general, a lymphoid stress surveillance is executed by γδ T cells, and these cells play a role in inflammation, infectious diseases, autoimmunity and tumor recognition [44, 66, 76-83]. Therefore, γδ T cells are an important target for immunotherapy [76, 84-87].

Murine γδ T cells are divided into IFN-γ and IL-17 producing effector cells. CD27 and TCR signals induce the development of IFN-γ producing cells during thymic differentiation [53, 88-90]. The human γδ T cell repertoire in the blood shows interindividual differences in numbers of naïve, effector/memory and differentiated γδ T cells [91, 92]. Most blood human γδ T cells are characterized by the expression of a Vδ2 chain and produce IFN-γ and TNF-α [46]. Differentiation is triggered by IL-2 or IL-15 *in vitro*, whereas TCR activation is not necessary [91]. The second major subpopulation uses a Vδ1 chain and is found in the thymus and peripheral tissues where these cells contribute to immune surveillance [7].

1.4 Non-conventional and innate-like T cells

Conventional αβ T cells recognize peptides presented in complex with the highly polymorphic MHC I or MHC II molecules. The somatic recombination of TCR genes and diversity at the junctional region of TCRs contribute to the complexity of this process. In theory, $1*10^{15}$ unique αβ TCRs can be generated in the mouse, however, only around $5*10^{6}$ are usually used by different individuals [93-97]. Due to this diversity, a wide array of peptide antigens can be detected, and infections are successfully cleared. Yet, unique naïve antigen-specific TCRs exist only in very small numbers, and activation, clonal expansion and effector cell differentiation take 7-10 days to complete [98]. Next to conventional MHC-restricted αβ T cells, other subsets of T cells exist that do not fit into this classical mode of antigen recognition and adaptive responses [98]. These non-conventional T cells exist in all individuals, recognize antigens different from classical peptide antigens and are not restricted to the polymorphic MHC molecules but rather to non-polymorphic antigen-presenting molecules [98]. A limited TCR repertoire is used by non-conventional T cells, and tissue-specific localization can be observed as well as higher frequencies of subsets compared to αβ clonotypes [98].

Non-conventional T cells are found in the αβ and γδ lineage. Studies of NKT cells revealed CD1d restriction, a member of the MHC I-like CD1 family of lipid-presenting antigens (see 1.5). Human T cells with a diverse TCR repertoire were found to be restricted to the CD1 family members CD1a [99], CD1b [100] and CD1c [101] presenting mycobacterial glycolipids. T cells restricted to the group I members of CD1 molecules (CD1a, CD1b and CD1c) have been described as autoreactive T cells and are found in frequencies of 0.1% to 10% of T cells [102-105]. CD1a-restricted T cells could be an early warning system of a disturbed skin barrier [98]. Another MHC I-like molecule implied in the activation of the non-conventional T cell subset of mucosal-associated invariant T (MAIT) cells is MR1 [106]. This molecule presents ligands like folate derivatives or molecules of the riboflavin pathway to MAIT cells which are defined by usage of *TRAV1-2*/*TRAJ33* in humans and mice [107-111]. The TCR α chain in MAIT cells is usually paired with β chains using *TRBV19* or *TRBV13* in mice and *TRBV6* or *TRBV20* in humans [107]. Frequencies of MAIT cells in mice are low compared to humans where they constitute 5% of blood T cells and 45% of liver T cells [98, 112-114]. MAIT cells were implied in protective immunity against *Mycobacterium tuberculosis* in a *TRAV1*/*TRAJ33* transgenic mouse model [114]. Acute infection with this pathogen in humans results in a reduction of MAIT cells in the blood and an increase of frequencies in the lung [114, 115]. MHC Ib molecules were reported to present peptides to $CD8^{+}$ T cells or modulate T cell responses [98]. Cells of the γδ T cell lineage are also characterized by a non-classical antigen recognition mode and several subsets with distinct functions exist (see 1.3.2.2 and 1.3.4.2).

1.5 The CD1d/iNKT cell system

1.5.1 NKT cells

Natural killer T cells were first mentioned in 1987 [116, 117] and the term "NKT cell" was first published in 1995 [118]. Three subgroups of NKT cells have first been described as $CD3^+CD4^-CD8^-$ T cells and later as a $NK1.1^+TCR^+$ cell population due to their expression of the NK cell marker NK1.1 [117, 119]. NKT cells comprise type I NKT cells, also termed classical or iNKT cells, type II non-classical NKT cells and NKT-like cells. Type II NKT cells use a diverse TCR repertoire [120], and NKT-like cells are a diverse pool of cells that is not necessarily reactive to CD1d or αGC but expresses the NK cell marker NK1.1 in mice or CD161 in humans [121].

The hallmark of iNKT cells is the expression of a semi-invariant αβ TCR using a Vα14Jα18 chain encoded by an *AV14/AJ18* rearrangement and the α chain constant region in mice and rats (IMGT: mouse *TRAV11/TRAJ23*) and a homologous *AV24/AJ18* gene rearrangement in humans (IMGT: *TRAV10/TRAJ18*) [122-127]. These α chains associate with a limited number of β chains using gene segments of the *BV8* (IMGT: *TRBV13*) family and *BV7* (IMGT: *TRBV29*) in mice and rats, as well as *BV2* (IMGT: *TRBV1*) in mice and *BV11* (IMGT: *TRBV11*) in humans [122-125, 128]. Although an invariant α chain is used by this cell population, there is still diversity in the β chain junctional region [123, 129, 130]. Classical iNKT cells are restricted by the antigen-presenting molecule CD1d which presents glycolipid antigens to the iNKT TCR and can influence immune responses by rapid cytokine secretion [126, 131-134]. This subset of T cells can modulate immune responses and plays a role in different diseases like microbial infections [135, 136], autoimmunity [137], allergies [138] and cancer [139]. Invariant NKT cells can have a protective character in these pathological states, or they can aggravate or even cause the disease [140]. Furthermore, a role of iNKT cells in the control of influenza virus in the lung has been indicated [141-144].

Frequencies of iNKT cells vary in different species, inbred strains of mice and rats and among individuals of the same species. Classical NKT cells in mice are most frequent as a proportion of T cells in the liver (30%) and the bone marrow (20-30%) [126, 145]. They represent 0.3-0.5% of all thymocytes and are also found in the spleen (3%), the lymph nodes (0.3%), the blood (4%) and the lung (7%) [145]. This cell population is about 10-100 times less frequent in humans although tissue distribution is less well studied in this model [126]. Genetic control of iNKT cell frequencies has been shown in mice, rats and humans [146-150]. Rat iNKT cells frequencies are more similar to humans, and 0.01% of splenocytes and 0.2% of intrahepatic lymphocytes (IHL) were identified as iNKT cells in F344 rats [149]. Identification of iNKT cells with the NK1.1 marker is not suitable as expression of this molecule varies [149, 151].

A reliable tool for the detection of iNKT cells are antigen-loaded CD1d oligomers [121, 149, 152, 153]. Mouse and human CD1d oligomers are cross-reactive to iNKT cells of other species, whereas rat CD1d oligomers are not cross-reactive to murine iNKT cells. [149, 154-156].

1.5.2 CD1d-mediated antigen recognition of iNKT cells

1.5.2.1 The CD1d molecule

The CD1 family of non-polymorphic glycoproteins presents lipids to T cells, shares structural and sequence homologies with MHC I molecules and those molecules are thus termed MHC I-like molecules [157-159]. The members of the CD1 family can be divided into group 1 containing CD1a, CD1b and CD1d, group 2 including CD1d and group 3 represented by CD1e [160, 161]. The three groups are similar in structure but differ in their trafficking and function. Group 1 molecules present lipid antigens to a diverse pool of CD1a-, CD1b- or CD1c-restricted T cells and CD1d molecules present glycolipid antigens to the NKT cell family, while CD1e modulates antigen-loading of the other isoforms [157, 162]. Expression of all CD1 isoforms was found in humans, whereas only CD1d is expressed in murid rodents. Two variants of CD1d exist in mice [163], CD1d1 and CD1d2, and only CD1d1 is found in rats [164-166].

The structure of CD1d is similar to MHC I molecules, with an α chain comprised of three domains (α1-3) associated with β_2-microglobulin through α3 [167, 168]. The domains α1 and α2 form an antigen-binding groove comprised of two deep hydrophobic pockets (A' and F'). Those are located between two antiparallel helices of the α1 and α2 domain and are situated on a β-pleated sheet, and a narrow portal (F' portal) serves as an access to these hydrophobic pockets [157, 167]. The α3 domain forms an Ig-like structure and anchors the molecule to the membrane with a transmembrane region including a short cytoplasmic tail [167]. The transmembrane and cytoplasmic domains vary among species indicative of differential functional or structural requirements [169]. While MHC I molecules present short peptides, CD1d can accommodate various glycolipid antigens of greater size with long alkyl chains [168, 170].

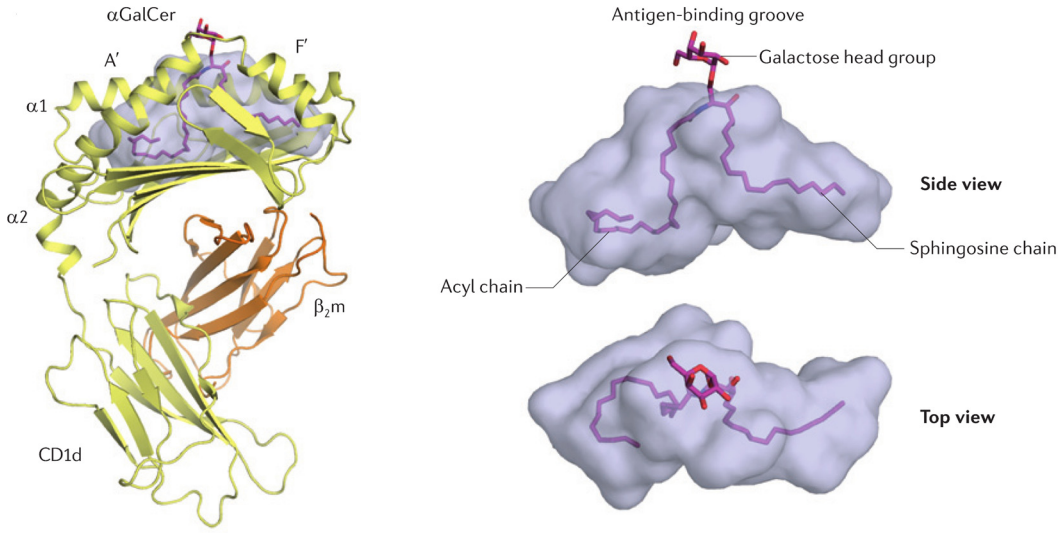

Figure 1.3 Glycolipid presentation by CD1d. The crystal structure of CD1d loaded with the glycolipid antigen αGC (left, PDB: 1ZT4) and positioning of αGC within the CD1d antigen-binding cleft (right). The galactose headgroup protrudes from the antigen-binding groove, and the lipid tails are inserted into the A' and F' pockets. Reprinted by permission from: Springer Nature, Journal: Nature Reviews Immunology [171].

As depicted in **Figure 1.3**, the hydrophobic channels beneath the surface of the CD1d molecule bind the alkyl chains and the hydrophilic head of the molecule protrudes from the molecular surface [157]. Hydrogen bonds stabilize these protruding parts of the antigen and contribute to the correct positioning of the glycolipid [157]. *In vivo* loading of CD1d has been reviewed by Barral et al. [157]. After translation and translocation of the CD1d α chain into the lumen of the ER, self-lipids like phosphatidylinositol or glycosylphosphatidylinositol are thought to be loaded onto CD1d [157, 172, 173]. A lipid transfer protein in the ER, the microsomal triglyceride transfer protein (MTP) was found to be essential for CD1d antigen presentation although the mechanism is unclear [174, 175]. The ER chaperones calnexin and calreticulin bind CD1d through glycosylation patterns and the molecule non-covalently associates with β_2-microglobulin and the thiol oxidoreductase ERp57 and is transported to the cell surface [176-178]. CD1d is internalized after expression on the plasma membrane into early or sorting endosomes using a clathrin-dependent pathway and trafficking to late endosomes or lysosomes occurs [179]. There, self-antigens are exchanged with other antigens and loaded CD1d molecules are transported back to the cell surface [157]. Membrane-perturbing sphingolipid activator proteins, known as saposins, seem to be essential tools for the presentation of endogenous lipid antigens for CD1 isoforms and deficiency leads to antigen-presenting defects of CD1d [180-182]. The surface expression of CD1d is constitutive on the surface of APCs like DCs, macrophages and B cells, especially marginal zone B cells [183, 184]. Cortical thymocytes, essential for the development of iNKT cells [185], Kupffer cells and endothelial cells lining liver sinusoids were also reported to express CD1d [186].

1.5.2.2 iNKT cell ligands and CD1d antigen presentation

The most widely used antigens for iNKT cell research are α-galactosylceramide (αGC) isolated from a marine sponge sample (*Agelas mauritianus*) and its derivatives [131, 140, 188]. A synthetic glycolipid and commonly used form of αGC is the compound KRN7000. The glycosphingolipid αGC is comprised of a polar sugar head group (galactose) α-linked to a ceramide base which consists of an 18-carbon phytosphingosine chain and a 26-carbon acyl chain shown in **Figure 1.4** [171]. In addition to the synthetic αGC antigen, which triggers production of T_H1 and T_H2 cytokines by iNKT cells, modified antigens have been developed that result in biased cytokine secretion (reviewed in [134, 189]). Modifications at the 6'-hydroxyl group resulted in promotion of T_H1 cytokine release, leading to reduced tumor growth in mice [190]. The compound OCH which possesses a truncated sphingosine chain results in T_H2-biased response [191, 192]. Another synthetic derivative of αGC is PBS57 which was also used in the experiments described in this thesis (see 3.1). In this compound, the 6-hydroxyl group was exchanged with an amide linked to a small molecule resulting in increased solubility while retaining the effect of αGC on iNKT cells [187]. Antigens of microbial origin have been identified for iNKT cells including antigens from *Sphingomonas* species, *Borrelia burgdorferi*, *Streptococcus pneumoniae*, group B *Streptococcus* and *Mycobacterium tuberculosis* [171]. These microbial antigens, except for mycobacterial phosphatidylinositol mannosides, use a glycosyl head group connected in an α-linkage to a ceramide or a diacylglycerol base [171]. Mammalian glycolipids are usually not α-linked and include β-linked glycolipids and phospholipid antigens [171]. Isoglobotrihexosylceramide (iGb3) is such an antigen resulting in a moderate binding to iNKT cells with controversial importance for iNKT cell development [193-195]. Other antigens have been investigated, but it is possible that there is not just one but several self-lipid antigens that are important for iNKT cell development [171, 189].

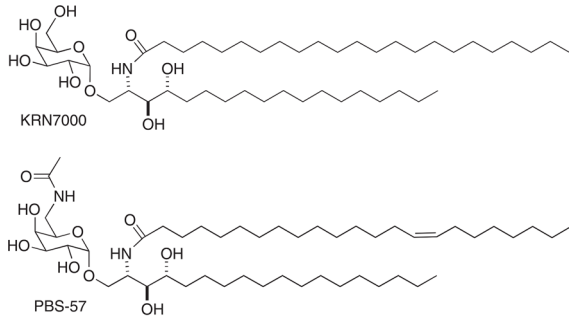

Figure 1.4 Structure of the glycolipid antigen αGC/KRN7000 and its derivative PBS57. Reprinted from Liu et al. 2006 [187] with permission from Elsevier.

Antigen presentation of lipid antigens to the iNKT TCR occurs in a distinct conformation. Crystal structures of human and mouse CD1d in complex with αGC revealed the positioning of this antigen within CD1d (see **Figure 1.3**) [196-198]. **Figure 1.5** shows the human NKT cell receptor binding to CD1d presenting a glycolipid antigen. The iNKT TCR contacts both molecules in a tilted parallel position above the F' pocket of CD1d [171]. The same docking mode was described for the mouse iNKT TCR [199], and the docking mode does not seem to change in different species with variable TCR β chain usage or the nature of the bound antigen [200]. In contrast, conventional αβ T cells contact the peptide:MHC complex in a diagonal docking mode. Usually, the CDR1 and CDR2 of both TCR chains contact the MHC. The CDR3 regions of αβ TCRs contact residues on the peptide. In iNKT TCRs, the germline encoded CDR1α and CDR2β, which only contacts the α1-helix of CD1d, are used for the binding of iNKT cells to CD1d in complex with αGC [200]. CDR3α is almost invariant and only the third nucleotide of the triplet encoding for the amino acid in position 93 is not germline encoded. Contacts to the antigen are made by CDR1α and CDR3α binds both antigen and CD1d [201]. Variations in the TCR β chain cause subtle changes in the conformation of the α chain and indirectly contribute to the iNKT/CD1d binding [199, 202].

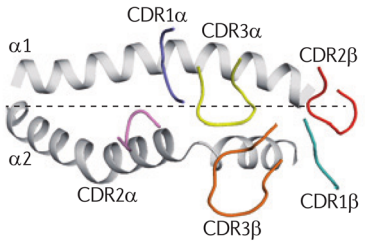

Figure 1.5 Docking mode of the iNKT TCR-lipid-CD1d complex. View of the antigen-binding cleft and the TCR chains contacting the antigen-presenting molecule. A dashed line indicates the overall docking mode. Reprinted by permission from: Springer Nature, Journal: Nature Reviews Immunology [171].

1.5.3 Development of iNKT cells

Precursors of iNKT cells are defined to be $CD4^+CD8^+$ (DP) thymocytes which also give rise to conventional αβ T cells [203, 204]. More recently, an alternative pathway of iNKT cell development was described that originates from DN thymocytes and bypasses the DP stage [205]. The classical pathway of iNKT development is initiated by the semi-invariant *AV14/AJ18* rearrangement which occurs randomly and is followed by positive selection mediated by cortical thymocytes [185, 206]. Positive selection depends on self-antigen:CD1d complexes and identified self-antigens were mostly β-linked glycolipids like β-glucosylceramide [193, 207, 208] or structurally similar antigens [126, 209-211]. The lack of α-transferases in mammals was seen as a cause for the lack of α-linked lipid self-antigens. However, recently α-glycosylceramide was described as a major self-antigen in thymus and periphery [212]. Upon engagement of the TCR, signaling through the SLAM family of surface receptors is characteristic for iNKT cell development and not found in conventional αβ T cells [213-216]. SLAM signaling together with

TCR signaling triggers activation of the NF-κB signaling cascade leading to cell survival and proliferation [132]. Autoreactivity of iNKT cells is limited by the negative selection of highly reactive clones [217-219]. Directly after positive selection the transcription factor promyelocytic leukaemia zinc finger protein (PLZF) is induced and was implied in the control of the developmental pathway in iNKT cells [220]. In mice iNKT cell maturation is divided into four stages, starting with stage 0 ($CD24^{+}CD44^{low}NK1.1^{low}$) during which no proliferation takes place, and cells are $CD4^{+}$ and mostly $CD8^{-}$ [203]. Type I NKT cells proliferate after downregulation of CD24 and enter stage 1 ($CD24^{low}CD44^{low}NK1.1^{low}$). In the subsequent stage 2, proliferation and up-regulation of CD44 were observed [221]. Upregulation of NK cell receptors is characteristic for stage 3 which includes reduced proliferation and a $CD24^{lo}CD44^{hi}NK1.1^{hi}$ phenotype [203] and cytokine secretion varies throughout the different developmental stages [221]. The exit of mature iNKT cells from the thymus occurs before stage 3, and iNKT cells preferentially home to the liver and spleen, in contrast to αβ T cells which are abundant in lymph nodes [132, 152, 222].

1.5.4 Activation and effector functions of iNKT cells

After selection and maturation in the thymus, mature iNKT cells exert diverse effector functions including responses against pathogens, tumors, tissue grafts and involvement in autoimmune and inflammatory diseases [223]. They resemble effector memory T cells and can rapidly secrete cytokines upon activation [224]. Ligand recognition of iNKT cells triggers a cascade of events that can lead to the recruitment of APCs and many other bystander cells such as NK, B, and T cells [129]. As summarized by Reilly et al. [225], several mechanisms can activate iNKT cells. Classical activation is initiated by TCR engagement of lipid:CD1d complexes and the cytokines IL-12, IL-18 or IFN-α important for conventional αβ T cells are not necessary for the initial activation of iNKT cells [226]. Secretion of IL-4, IFN-γ and IL-17 is observed in distinct subsets of iNKT cells, defined by CD4 or NK1.1 expression. Lack of agonistic glycolipids in the case of *Mycobacterium tuberculosis* or *Staphylococcus aureus* infections leads to activation by recognition of self-antigens presented by pathogen-activated DCs [227, 228]. Activation by this pathway leads to significant IFN-γ secretion. In contrast, activation of iNKT cells can also occur without TCR engagement and activation through IL-12 and IL-18 [229-231].

1.5.5 The cotton rat as an animal model

Hispid cotton rats (*Sigmodon hispidus*) are native to parts of the United States, Mexico and Central America and are assigned to the order Rodentia, the family Muridae, and the subfamily Sigmodontinae [232]. This animal model was first used by Dr. Charles Armstrong in 1939 as a model for poliovirus infections [232]. Until 1979, cotton rats were established as a model for polio and later filariasis research [232]. Moreover, cotton rats are susceptible to a number of human pathogens and can be applied for pre-clinical testing of antiviral reagents and vaccines [232, 233]. The susceptibility to infections with human respiratory viruses, e.g., influenza virus, human parainfluenza virus (HPIV), RSV, measles virus [234] and infections with HSV [232] renders this animal an ideal model for human respiratory virus infections [235]. However, in comparison to other rodent models, a profound lack of reagents and methods hampers research in this animal model. Tools to study the immune system of cotton rats include cotton rat-specific antibodies for CD3, CD4 and CD8 and cytokines like IFN-γ and IL-4 [235]. Commercially available reagents for chemokine or cytokine studies have been developed, and studies of immune responses after virus infections and the sequencing of cotton rat genes enabled more in-depth research [235]. In contrast to other model organisms, the whole genome of the cotton rat is not readily available. The cotton rat is a developing model organism and an alternative for research with mice or rats especially in the study of host-pathogen interactions [232].

1.6 The BTN3/Vγ9Vδ2 T cell system

1.6.1 Vγ9Vδ2 T cells

The major γδ T cells subset in human peripheral blood (up to 5% of T cells) is the Vγ9Vδ2 T cell subset which is characterized by a Vγ9JP (*TRGV9*/*TRGJP*) rearrangement paired with a Vδ2 chain using *TRDV2* gene segments [32, 236-238]. Length restriction of the junctional region and a restricted repertoire of the Vγ9 chain are typical for Vγ9Vδ2 T cells, whereas the Vδ2 chain shows higher diversity [239, 240]. This cell subset is activated in an MHC-unrestricted fashion by phosphoantigens, the phosphorylated metabolites of isoprenoid synthesis pathways in the context of BTN3 (CD277) molecules (see 1.6.2 and 1.6.3) [32, 48, 49, 241-243]. Phosphoantigen-independent *in vitro* or *ex vivo* activation of Vγ9Vδ2 T cells can be induced by the BTN3 (CD277)-specific agonistic antibody 20.1 [48, 244]. Characteristic features of PAg-reactive Vγ9Vδ2 T cells include germline-encoded lysine residues in the JP segment of the Vγ9 chain, varying CDR3 lengths of Vδ2 chains, the conserved Vδ2 residues R51, E52

and the presence of a hydrophobic amino acid (L, I, V) at position δ97 [241, 245-247]. In general, most Vγ9Vδ2 T cells that carry a Vγ9JP chain were found to react to PAg [248]. Human PAg-reactive effector Vγ9Vδ2 T cells are a major T cell subset in fetal blood (<30 weeks of gestation) with a dominance of the germline-encoded Vγ9 clonotype (CDR3: ALWEVQELGKKIKV) [38]. Moreover, shared clonotypes (public) that occur in unrelated healthy adults are characteristic for Vγ9 chains (reviewed in [240]). The Vγ9Vδ2 T cell repertoire is shaped by extrathymic selection, decreasing complexity in adult life and arises during embryonal development [240]. Cell-cell contact was found to be necessary for PAg-mediated activation of Vγ9Vδ2 T cells and activation is modulated by additional receptors like NK cell inhibitors or activating receptors (e.g. NKG2D) [71, 249-253]. Activation and proliferation of Vγ9Vδ2 T cells have been shown in infections with *Mycobacterium tuberculosis* [254-259], *Mycobacterium leprae* [260], *Listeria monocytogenes* [261] and in malaria [262] as well as toxoplasmosis [263]. This cell subset was found in rheumatoid arthritis and multiple sclerosis conditions [264-266]. Vγ9Vδ2 T cells also mount effector responses against several lymphoma cell lines [240]. This T cell subset shows characteristics of NK cells, T_H1 and $CD8^+$ T cells after isolation and can differentiate into T_H17-like cells in culture [267-269]. However, T_H2- and T_{reg}-like effector functions have also been observed [270, 271]. Activated human Vγ9Vδ2 T cells can rapidly release cytokines and to kill transformed or infected cells by perforin and granzyme release, TCR-mediated and NKG2D-dependent mechanisms as well as Fas-Fas ligand interactions [272, 273]. They proliferate upon activation and can expand to frequencies of up to 50% of circulating T cells [274]. Vγ9Vδ2 T cells can carry out APC-like functions due to upregulation of MHC II and costimulatory molecules upon activation [73] and can provide B cell help [275]. Moreover, they engage in crosstalk with NK cells, DCs and monocytes [276-278]. In summary, Vγ9Vδ2 TCR act like PRRs in their immunosurveillance function and can sense changes in cell metabolism, microbial infections and drug-treated cells due to the accumulation of endogenous or exogenous phosphoantigens. As reviewed before [7, 85, 279, 280], these features enabled the use of Vγ9Vδ2 T cells as therapeutic targets in immunotherapy, and these γδ T cells are currently investigated in clinical trials.

1.6.2 Phosphoantigens

Antigens for Vγ9Vδ2 T cells were first identified in extracts from pathogens and were found to be low molecular weight non-peptide antigens [168]. Later, alkyl phosphates were shown to be the chemical components activating this T cell subset [281]. Prenyl pyrophosphate antigens are metabolites of isoprenoid synthesis, play a multitude of roles in cell metabolism and are

involved in the downstream synthesis of cholesterol, steroids, ubiquinones, vitamins and various other compounds [32, 282]. The antigen isopentenyl pyrophosphate (IPP) was initially isolated from mycobacteria [283], and two distinct pathways for IPP synthesis were found in eukaryotic and prokaryotic organisms [284]. Whereas eukaryotes use the cytoplasmic mevalonate (MVA) pathway of isoprenoid synthesis, most eubacteria, protozoa, cyanobacteria and plant chloroplasts use a pathway termed 2-C-methyl-D-erythritol 4-phosphate (MEP), 1-deoxy-D-xylulose 5-phosphate (DOXP) or non-mevalonate pathway, characteristic for the chloroplast-related apicoplast organelle present in those species [32, 285]. Both pathways including their intermediates and enzymes involved up to the antigenic metabolite IPP are shown in **Figure 1.6**.

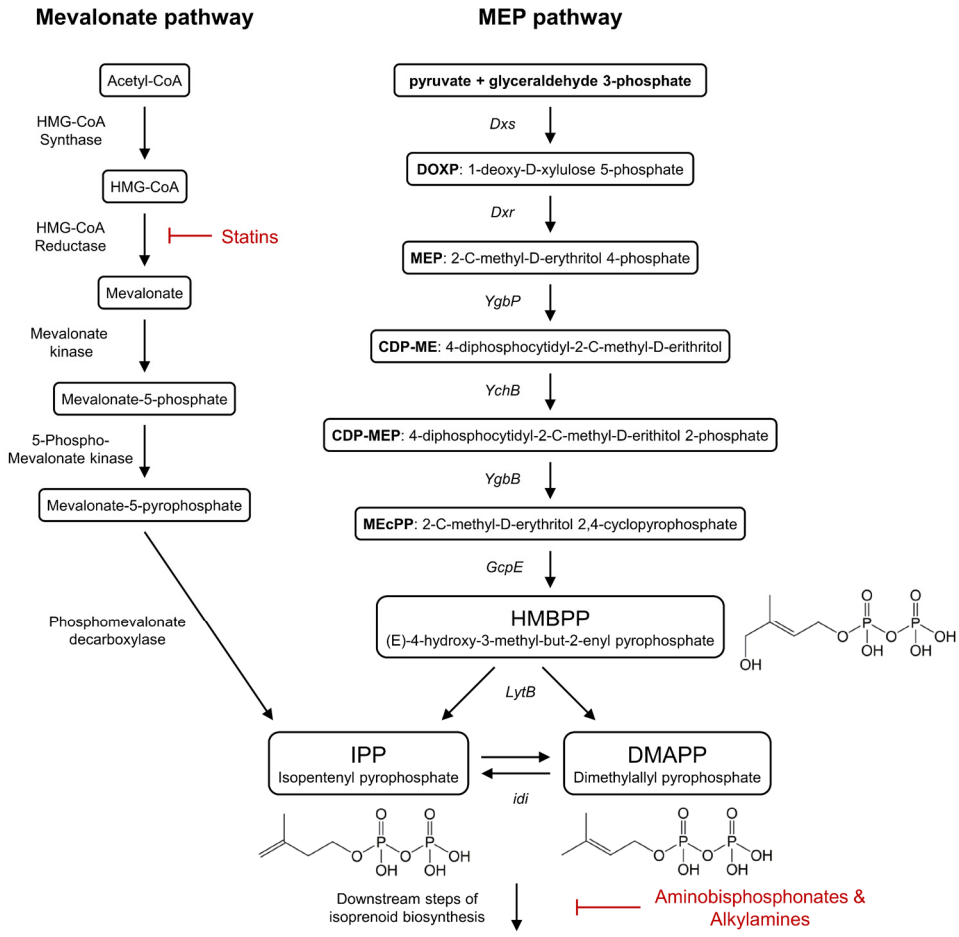

Figure 1.6 Eukaryotic and prokaryotic isoprenoid biosynthesis pathways. The first steps of the eukaryotic mevalonate and the prokaryotic MEP pathway leading to the synthesis of isoprenoids are shown. Enzymes involved in this pathway are indicated, and inhibitors are marked in red. The chemical structures of HMBPP, IPP and DMAPP were designed using ChemDraw. Overview adapted from [32].

The ubiquitous mevalonate pathway involves the substrate Acetyl coenzyme A (Acetyl-CoA) which is in several steps converted to IPP. An important intermediate in this process is mevalonate, and the key enzyme β-hydroxyl-β-methylglutaryl-coenzyme A (HMG-CoA) can be

targeted by inhibitors like statins to modulate Vγ9Vδ2 T cell activation upstream of IPP synthesis [32, 286]. In contrast, the MEP/DOXP pathway is absent in mammals and uses pyruvate and glyceraldehyde 3-phosphate as substrates. The intermediates DOXP and MEP as well as IPP and its precursor molecule (E)-4-hydroxy-3-methyl-but-2-enyl pyrophosphate (HMBPP) are produced by the action of seven enzymes [32]. As reviewed before [32, 274, 287], most eubacteria like mycobacteria, and gram-negative bacteria like *Pseudomonae*, *Salmonellae*, *Escherichiae* and *Clostridia* use the MEP/DOXP pathway for isoprenoid synthesis. Other species use both pathways (e.g., *Listeria monocytogenes* [288] and *Streptomyces* [289, 290]), whereas *Staphylococci* and *Streptococci* only use the MVA pathway. Detection by Vγ9Vδ2 T cells is mediated by IPP which is produced in all cells, its isomer Dimethylallyl pyrophosphate (DMAPP) and HMBPP. Those antigenic molecules have been termed "phosphoantigens" along with other synthetic variants [32, 273, 287, 291, 292]. In contrast to the weaker IPP which can accumulate in cells after infection, transformation or drug treatment, HMBPP is a more potent activator of Vγ9Vδ2 T cells [273, 287, 293]. As reviewed by Morita et al. [32], drug-induced accumulation of IPP can be mediated by aminobisphosphonates (e.g. zoledronate) which are used in the treatment of osteoporosis, Paget's disease and bone malignancies and by alkylamines. These drugs act by inhibiting farnesyl pyrophosphate synthase (FPPS) which is important for downstream processing of IPP and thus an accumulation of endogenous IPP ensues [32].

1.6.3 BTN3A1 – an essential molecule for phosphoantigen reactivity

Butyrophilin molecules are type I receptor glycoproteins which are encoded in the MHC on human chromosome 6 and show some structural similarity to the superfamily of B7 receptors [244, 294-296]. The family members of BTN3 (CD277) consist of two extracellular Ig-like domains (BTN3-V and BTN3-C), a single transmembrane domain (TM), a short intracellular juxtamembrane domain (JM) and a large B30.2 (PRY/SPRY) domain at the C-terminus [296, 297]. Three members of BTN3 termed BTN3A1, BTN3A2 and BTN3A3 have been identified in humans, whereas rodents do not carry homologs for this molecule [298, 299]. The structure of those isoforms is depicted in **Figure 1.7** and varies slightly as BTN3A1 and BTN3A3 express a B30.2 domain, whereas BTN3A2 has lost most of the intracellular regions including B30.2 [294]. In addition, BTN3A3 molecules possess a longer cytoplasmic tail compared to BTN3A1 [294]. BTN3-V and BTN3-C domains are highly conserved between the three isoforms and show gene homogenization in the BTN3-V domain [298, 299]. Evolutionary analysis revealed two successive duplications of the *BTN3* locus in primates and a primate-specific concerted evolution by homogenization of *BTN3* genes [298, 300]. Concerted evolution describes the observation that paralogues in one species, e.g. certain domains of *BTN3A1-3* in primates, are more similar to each other than to their homologs in related species. All three BTN3 isoforms are present in the Catharrhini group which includes Hominoids and Old World monkeys, two *BTN3* genes are expressed in New World monkeys (*BTN3A1*-like and *BTN3A2/3* co-ortholog) and only one isoform in Prosiminians like *Otolemur garnettii* [298]. This primordial *BTN3*-like gene in *Otolemur garnettii* possesses a B30.2 domain which indicates a specific loss of B30.2 in *BTN3A2* [298]. BTN3 is ubiquitously expressed on lymphocytes in human peripheral blood including T cells, B cells, NK cells, immature and mature DCs and surface expression has been shown to be higher on T cells compared to B cells and monocytes [244, 301, 302]. Moreover, the BTN3A1 isoform has been shown to be essential for PAg-mediated activation of Vγ9Vδ2 T cells [48, 49, 303, 304]. Two general models for the function of BTN3A1 in phosphoantigen recognition have been proposed. The first model described the BTN3A1 molecule as an antigen-presenting molecule which binds phosphoantigen in a shallow groove in the BTN3-V domain which is formed by the residues E37, K39, R61, Y100, Q102 and Y107 [304]. However, mutational studies of this groove did not support this model of direct presentation [305]. The second model presents BTN3A1 as a phosphoantigen sensor and involves the recognition of phosphoantigens by the intracellular B30.2 domain, the translation of the signal to the outside and thus an activation

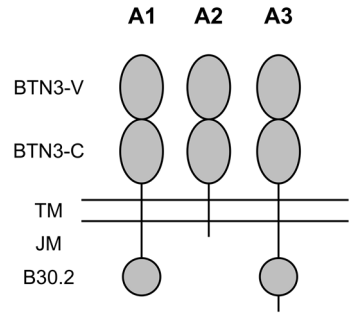

Figure 1.7 Structure of human BTN3 isoforms.

of the Vγ9Vδ2 TCR either by direct or indirect recognition of BTN3A1 [48, 49, 305-310]. The structure of the B30.2 domain of BTN3A1 and A3 resembles an Ig-domain and contains layered antiparallel β sheets and loops of variable lengths [307]. As reviewed by Rhodes et al. [296], B30.2 domains are also used by tripartite motif molecules (TRIM) where they act similar to PRRs which recognize pathogen- or damage-associated molecular patterns (PAMP or DAMP). A similar function for the B30.2 domain of BTN3A1 is indicated by the finding of phosphoantigen binding to a pocket composed of the residues H351, H378, K393, R412, R418 and R469 in the B30.2 domain of BTN3A1 (see **Figure A.2**) [306-308]. Interestingly, the B30.2 domain can distinguish phosphoantigens from other non-antigenic small molecules [311]. Other studies also implied a role for W350 and W391 as well as Y352 and the juxtamembrane domain of BTN3A1 [307, 312, 313]. The B30.2 domain of BTN3A3 shows one critical amino acid change (H351R) which results in loss of PAg binding [307, 308]. Furthermore, conformational changes were observed in the B30.2 domain and juxtamembrane domain upon PAg binding [309, 312]. The amino acids T297 and T304 were shown to be essential for binding of PAg to the juxtamembrane domain and interactions of PAg with the B30.2 domain followed by a conformational change and clamping of PAg:B30.2 onto the juxtamembrane domain were proposed [309]. Surface expression of BTN3 isoforms as dimers or monomers was investigated and homodimers of BTN3A1 were observed to occur in two conformations *in vitro*, a "V-shaped" conformation allowing binding of mAb 20.1 and oligomerization as well as a "head-to-tail" conformation [303]. The V-shaped conformation is adopted at resting state and locking BTN3A1 homodimers in this position was shown to diminish PAg-mediated activation of Vγ9Vδ2 T cells which indicates the need for conformational changes of the extracellular domains [312]. BTN3A1, however, is not sufficient for full activation of Vγ9Vδ2 T cells and a requirement for BTN3A2 and/or BTN3A3 has been shown by using BTN3 knock out cell lines indicating that heterodimer formation is essential for PAg-mediated Vγ9Vδ2 T cell activation [307, 310]. These heterodimers interact via the BTN3-C domain and ER retention motifs are crucial for subcellular localization and correct surface expression as well as functional efficacy [310]. Therefore, a PAg-sensing function of BTN3A heterodimers most likely implies recognition of PAg via the B30.2 domain of BTN3A1, subsequent structural changes in the molecule and help of BTN3A2 or BTN3A3. How this signal initiated by PAg recognition is converted to the cell surface and to the Vγ9Vδ2 TCR is unclear. A role of the cytoskeletal adaptor protein periplakin has been suggested and activity of the GTPase RhoB has been observed which could assist in mediating inside-out signaling [307, 314]. Studies with permanent rodent cell lines revealed the necessity of other molecules except BTN3 in the antigen-presenting cell that are located on human chromosome 6 and not conserved in rodents which lack the BTN3/Vγ9Vδ2 T cell system [300, 315].

1.6.4 Coevolution of *TRGV9*, *TRDV2* and *BTN3* in placental mammals

The occurrence of a functional BTN3/Vγ9Vδ2 T cell system has generally been thought to be specific to monkeys and hominids [49, 303, 316] as no evidence of homologous cells and molecules was found in rodent models, cattle, pigs or horses [267]. Karunakaran et al. investigated this apparent lack of other species carrying this phosphoantigen-reactive T cells subset and this study will be summarized below [317]. Their approach included the genome-wide search of 39 placental mammal species to find homologous genes for *TRGV9*, *TRDV2* and *BTN3* encoding essential parts of this system.

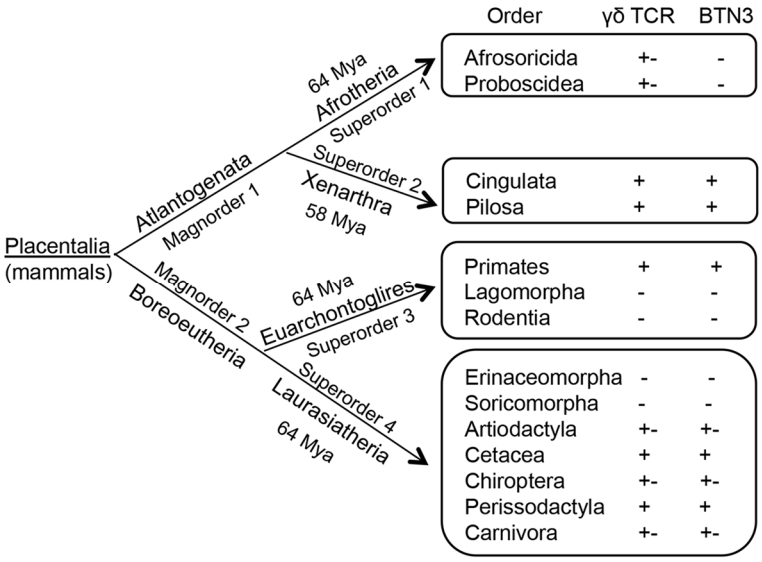

Figure 1.8 Distribution of *TRGV9*, *TRDV2* and *BTN3* (*BTN3-V* and *BTN3-C*) genes among placental mammals. The magnorders and superorders of Placentalia are shown as well as orders where genomic information was available. Conservation of genes among all species of one order is indicated (+) as well as complete absence of genes in all species (-). The heterogenous conservation in one order is indicated as +-. This figure was reprinted by permission from: Springer Nature, Immunogenetics and was initially published by Karunakaran et al. [317].

The presence of homologous genes with a nucleotide identity of more than 60% and at least 90% query coverage could be observed in multiple species belonging to both eutherian magnorders, Atlantogenata and Boreoeutheria but no homologs were found in non-eutherian mammals (**Figure 1.8**). However, some orders like Lagomorpha (including rabbits and pikas), Rodentia (rodents), Erinaceomorpha (containing hedgehogs), and Soricomorpha (shrews) completely lost the genes encoding Vγ9, Vδ2 and the extracellular region of BTN3. Conservation of the investigated genes in the sister taxa Afrotheria and Xenarthra [318, 319] was heterogeneous, and *TRDV2* was the only gene conserved in afrotherian species (includes elephants, manatees and cape golden mole). In contrast, homologs of all three genes were present in sloth (*Choleopus hoffmanni*) and nine-banded armadillo (*Dasypus novemcinctus*) which belong to the superorder Xenarthra. The higher primate species investigated by

Karunakaran and colleagues show conservation of the genes for the BTN3/Vγ9Vδ2 T cell system. The superorder Laurasiatheria comprises the orders Eulipotyphla, which includes Erinaceomorpha and Soricomorpha, and Scrotifera including the remaining clades shown in the superorder Laurasiatheria (**Figure 1.8**). Species in the Eulipotyphla order were characterized by a lack of all three genes, whereas Scrotifera included species carrying all of them. Mostly, species that lacked *TRGV9* and *TRDV2* also lacked *BTN3* genes, and *TRGV9* genes were well conserved among distantly related species. Since both magnorders of Placentalia contain species conserving all three genes, coevolution of *TRGV9*, *TRDV2* and *BTN3* genes with placental mammals seems evident and further proves a functional relationship of those genes.

1.6.5 Non-primate candidates for the BTN3/Vγ9Vδ2 T cell system

Coevolution of the genes necessary for a functional BTN3/Vγ9Vδ2 T cell system was proposed by Karunakaran et al. [317]. Through genome-wide searches for the three important genes of this system, Karunakaran et al. identified the following nine mammalian species of seven families that carry *TRGV9*, *TRDV2* and *BTN3* genes which are *in silico* translatable: sloths (*Choleopus hoffmanni*), nine-banded armadillos (*Dasypus novemcinctus*), gray mouse lemurs (*Microcebus murinus*), Aye-ayes (*Daubentonia madagascariensis*), humans (*Homo sapiens*), alpacas (*Vicugna pacos*), bottlenose dolphins (*Tursiops truncatus*), killer whales (*Orcinus orca*) and horses (*Equus caballus*). The *TRGV9* and *TRDV2* genes in horses show mutations that disturb the formation of immunoglobulin domains. The alpaca *TRGV9*, *TRDV2* and *BTN3* genes were more closely characterized in the same study [317]. Expression of all genes was shown on the cDNA level and characteristic features of human Vγ9Vδ2 T cells and BTN3A1 are conserved. First of all, *TRGV9* rearranged preferentially with a *TRGJP* homolog which was found to be expressed in different variants (JPA, JPB and JPC) and carried germline-encoded lysine residues, namely K108 and K111, with K108 being essential for PAg recognition [241, 242, 246]. K108 was in some cases substituted with arginine which is also observed in phosphoantigen-reactive Vγ9 chains of rhesus monkeys [320]. The third lysine residue K109 was substituted with threonine. CDR3 lengths in the alpaca were conserved with a variation of ± 2 amino acids, corresponding to findings in human Vγ9 chains [241]. Alpaca *TRDV2* was preferentially rearranged with *TRDJ4*, rarely with *TRDJ2* and shows substitution of a conserved arginine residue to glutamine (R51Q) and carries a conserved glutamic acid (E52) characteristic for PAg-reactive human Vδ2 chains [241, 245, 246]. It is noteworthy that only *TRDJ1-3* were shown in human PAg-reactive Vδ2 chains so far [241]. Prevalence of the amino acids leucine, isoleucine or valine (L, I, V) at position δ97 has been shown in human PAg-reactive Vδ2 chains, and alanine substitutions at this position abolish PAg recognition [241].

High diversity of CDR3δ lengths was found in alpacas which was also observed for human Vδ2 chains [241]. Pairing of alpaca Vγ9 and Vδ2 TCR chains was successful, and functionality by anti-CD3 stimulation was shown by expression of TCR chains in a TCR-negative mouse cell line. Moreover, cloning of the full-length alpaca BTN3-like molecule revealed conservation of extracellular and intracellular PAg-binding sites [304, 308, 321]. This BTN3-like molecule is the only isoform expressed in alpacas and can be viewed as a more primordial form of BTN3 [298]. This makes the alpaca a likely candidate to possess a functional BTN3/Vγ9Vδ2 T cell system and an outgroup allowing the study of functional similarities to humans [267]. The second non-primate candidate for a functional BTN3/Vγ9Vδ2 T cell system was the nine-banded armadillo, the only animal model susceptible to infections with the HMBPP-producing pathogen *Mycobacterium leprae* which shows neurological involvement and dissemination similar to human leprosy [322-324]. The armadillo possesses *in silico* translatable genes for *TRGV* and *TRDV* and a *BTN3-V* region, however, the only B30.2 domain was more closely linked to *BTN2A2* [267, 317]. From an evolutionary standpoint, conservation of the genes of the BTN3/Vγ9Vδ2 T cell system in species of the Atlantogenata superorder which is distinct from Boreoeutheria (see **Figure 1.8**) supports the existence of these genes in a common placental ancestor [267]. Apart from alpaca and armadillo, productive rearrangements of *TRGV9*- and *TRDV2*-like genes have been found in the bottlenose dolphin (*Tursiops truncatus*) [325], and a predicted *BTN3A3*-like gene can be found in the NCBI databases (GenBank: XM_004332447.2).

1.7 Aim of the thesis

This project aims to prove the existence and further investigate non-conventional T cell subsets in new animal models. This thesis is divided into two distinct projects attempting to elucidate the roles of iNKT cells in the cotton rat (*Sigmodon hispidus*) and Vγ9Vδ2 T cells in the non-primate candidate species nine-banded armadillo (*Dasypus novemcinctus*) and alpaca (*Vicugna pacos*). The results obtained for the CD1d/iNKT cell system in cotton rats [169] and the BTN3/Vγ9Vδ2 T cell subset in armadillos [326] have already been published.

The αβ T cell subset of iNKT cells is involved in infectious and autoimmune diseases, and cotton rats (*Sigmodon hispidus*) are an excellent model for different virus infections. A role for iNKT cells in virus infections is presumed but can so far not be further examined in the cotton rat. The investigation of the iNKT cell subset of αβ T cells in the cotton rat is limited due to a lack of reagents and methods to identify and characterize iNKT cells. Also, no complete genome of this species is available. However, there is evidence for reactivity to glycolipids, and thus iNKT cells are presumably present in cotton rats. Here, established methods used in the mouse and

rat model are examined and the molecular basis of the CD1d/iNKT cell system, the CD1d molecule and iNKT TCR, will be determined in the cotton rat. The aim of these experiments is to take the first step to identify cotton rat iNKT cells in a manner that allows the study of this cell type during virus infections.

A functional BTN3/Vγ9Vδ2 T cell system is so far only proven for primate species. However, the genes necessary for all parts of this system are conserved in some placental mammals. The candidate species armadillo and alpaca have been chosen to investigate Vγ9Vδ2 T cells in this setting. Armadillos are a valuable tool for *Mycobacterium leprae* research and provide the only animal model in which a disease similar to human leprosy can be observed. Here, the expression of functional *TRGV9*, *TRDV2* rearrangements and *BTN3* molecules is investigated to determine whether this candidate possesses the prerequisites for a functional BTN3/Vγ9Vδ2 T cell system. The second candidate species, *Vicugna pacos*, has been proven to possess functional rearrangements of *TRGV9* and *TRDV2* TCR gene segments and a BTN3-like molecule. Characteristic features of human phosphoantigen-reactive Vγ9Vδ2 TCR chains and BTN3 are conserved in those molecules. In this setting, new functional data will be provided to support the existence of a functional Vγ9Vδ2 T cell subset and a phosphoantigen-sensing BTN3-like molecule. This is investigated using approaches like the development of hybridomas specific for alpaca surface molecules, *in vitro* stimulation assays of peripheral blood monocytic cells (PBMCs) and permanent cell lines and repertoire analysis.

2 Material and Methods

2.1 Materials

2.1.1 Software and websites

Software	Company
BioEdit 7.2.5	Tom Hall
CellQuest Pro	BD
ChemDraw Professional 17.0	PerkinElmer
ChromasLite 2.1.1	Technelysium
Endnote X8	Clarivate Analytics
FlowJo 7.6.5 and 8.8.7	Tree Star
GIMP	GIMP team
Magellan™	Tecan
Microsoft Office 2016	Microsoft
Prism	GraphPad
SerialCloner 2.6.1	SerialBasics

Website/URL
http://www.ncbi.nlm.nih.gov/ (NCBI: BLAST [327, 328], PubMed)
http://www.imgt.org/ (IMGT database [329])
http://www.imgt.org/3Dstructure-DB/doc/IMGTDomainGapAlign.shtml (IMGT/DomainGapAlign [330-332])
http://www.ensembl.org/index.html (Ensembl database [333])
http://www.ebi.ac.uk/Tools/msa/clustalo/ (Clustal Omega [334])
http://web.expasy.org/translate/ (DNA to AA Translate tool [335])
http://www.umd.be/HSF3/HSF.shtml (Human Splicing Finder [336])
http://www.itb.cnr.it/rss/analyze.html (RSS site prediction [337])

2.1.2 Laboratory Equipment

Device	Company
5519 MicroCentrifuge	ThermoForma
ABI PRISM 3100 Genetic Analyzer	Applied Biosystems
Adjustable volume pipettes	Brand/Eppendorf/Gilson/Rainin
AlphaImager®	AlphaInnotech
Autoclave	Melag
C1000™ Thermal Cycler	Bio Rad
Centrifuge 5430R (Microcentrifuge)	Eppendorf
FACSAria™ III cell sorter	BD
FACSCalibur™ flow cytometer	BD
FACScan™ flow cytometer	BD
Gene Pulser® II	BioRad
General Purpose Centrifuge	ThermoForma
Heating block (1.5 ml)	Liebisch
Heating block TDB-120 (2 ml)	Thermostat
Ice machine	Scotsman
Incubator	Hotpack
Laminar flow cabinet	Heraeus

Light microscope	Labovert
Micropipette 0.5-1.5 ml	Socorex
Mini-PROTEAN® 3 cell	BioRad
Multi-channel (8-channel) pipette	Brand/Eppendorf
NanoDrop 1000 Spectrophotometer	Thermo Scientific
NanoDrop 2000c Spectrophotometer	Thermo Scientific
pH meter	Pulse
Pipetting aid	Brand
RC5C Ultracentrifuge	Sorvall Instruments
Scale	Scaltec
Shaker Certomat	Biotech International
Sunrise™ Microplate Reader	Tecan
Thermocycler	Eppendorf
Thermostat (water bath)	MT Lauda
Transfer pipette 10-50 µl	Brand
VMax Kinetic ELISA Microplate Reader	Molecular Devices
Vortex-Genie 2	Scientific Industries

2.1.3 Consumables

Product	Company
12 well plate flat bottom tissue culture	Greiner/Nalgene Nunc
24 well plate flat bottom tissue culture	Greiner/Nalgene Nunc
48 well plate flat bottom tissue culture	Greiner/Nalgene Nunc
6 well plate flat bottom tissue culture	Greiner/Nalgene Nunc
96 well plate flat bottom suspension culture	Greiner/Nalgene Nunc
96 well plate flat bottom tissue culture	Greiner/Nalgene Nunc
96 well plate round bottom suspension culture	Greiner
96 well plate twin tec™ (#0030133.404)	Eppendorf
Bacterial tubes	Fisherbrand
Big Flask T175	Nalgene Nunc
Cell culture flasks (50/200 ml)	Greiner
Cell culture petri dish (Ø 10 cm)	Greiner
Cell culture petri dish (Ø 6 cm)	Sarstedt
Cell strainer 100 µm	BD
Cryogenic vials	Sarstedt
Cyto One High Flow 0.2 µm Bottle Top Filter	Starlab
Dialysis tubes Membra-Cel™ (MWCO: 14000 kDa)	Roth
Dynabeads pan mIgG	Life technologies
Electroporation cuvette (0.4 cm)	BioRad
Express™ Plus 0.22 µm Bottle Top Filter	Millipore
Falcon 15 ml	Greiner/Nalgene Nunc
Falcon 50 ml	Greiner/USA Scientific
Fisherbrand™ Petri dish 10 cm^2	Fisher Scientific
Glas pasteur pipettes filtered/unfiltered (1.5 ml)	Distributed by Laborbedarf Scheller
Medium Flask T75	Nalgene Nunc
Minisart® Syringe Filters (0.2/0.45 µm)	Sartorius Stedim Biotech
Non-tissue culture petri dish (Ø 9 cm)	Greiner
Pipette tips filtered/unfiltered	Starlab/Roth/Rainin
Plastic pipettes (5/10/25 ml)	Greiner
Poly-Prep® chromatography column (9 cm)	BioRad
Polystyrene half-area 96 well plate	Corning Incorporated

Reaction tubes (0.5/1.5/2 ml)	Eppendorf/USA Scientific
Single-use syringes (2/5/10 ml)	BD
Small flask T25	Nalgene Nunc
Syringe filters (0.2/0.45 µm)	Whatman
Tissue culture plates 10 cm^2	Nalgene Nunc
Vivaspin 20 ml 50.000 MW column	Sartorius Stedim Biotech

2.1.4 Reagents

Product	Company
2-Mercaptoethanol	Sigma
Acetic acid	AppliChem
Acrylamide 4K-Solution (30%) – 37.5:1 (AA)	AppliChem
Advanced RPMI Medium 1640	Gibco
Agarose NEEO	Roth
Agarose	Fisher Scientific
Amicon® Ultra-4 10K Centrifugal Filter Devices	Merck Millipore
Ammonium persulfate (APS)	Roth
Ampicillin	Fisher Scientific/Gibco BLR
Betaine Solution 5 M	Sigma
Biozym LE GP Agarose	Biozyme
Bovine Serum Albumin (BSA) protease-free	MP Biomedicals/Roth
Calcium chloride ($CaCl_2$)	Roth
Concanavalin A C201 type IV (ConA)	Sigma
Coomassie R250	Sigma
Diethylamine	Sigma
Difco® LB Agar, Lennox	Fisher Scientific
Difco® LB Broth, Lennox	Fisher Scientific
Dimethlysulfoxide (DMSO)	AppliChem/Fisher Scientific
Disodium phosphate (Na_2HPO_4)	Roth
DMEM (1x) + GlutaMAX™-I	Gibco
DMEM (1x)	Gibco
DPBS (10x)	Gibco
DPBS (1x)	Gibco
Ethanol	AppliChem/Fisher Scientific
Fetal calf serum (FCS)	Atlantic Biologicals/Sigma
Ficoll-Paque™ Plus	GE Healthcare
Fixable Viability Dye eFluor® 660	eBioscience
G418	Biochrom
GelRed®	Genaxxon
GeneRuler 1 kb DNA Ladder	Thermo Scientific
GeneRuler 100 bp DNA Ladder	Thermo Scientific
GlutaMAX™ Supplement	Gibco
Glycerol	AppliChem
HAT Media Supplement Hybri-Max™ (50x)	Sigma
HEPES	Roth
Hexadimethrine bromide/Polybrene (10 mg/ml)	Sigma-Aldrich
hIL-2 (Proleukin® S $18*10^6$ I.E.)	Novartis Pharma
Histopaque®-1077	Sigma
HMBPP	Sigma
HT Media Supplement Hybri-Max™ (50x)	Sigma
ISF-1 Medium	Biochrom

Isopropanol	AppliChem/Fisher Scientific
Kanamycin sulfate	Gibco
KRN 7000 (αGC)	Enzo Life Sciences
LB-Broth	AppliChem
Lipofectamine® 2000	Invitrogen
Loading Dye (6x)	Fisher Scientific
Magnesium chloride ($MgCl_2$*6H2O)	Ferak
Magnesium sulfate ($MgSO_4$)	AppliChem
PEG 1500	Roche Diagnostics
Penicillin-Streptomycin (10,000 U/ml)	Gibco
Percoll	GE Healthcare
Potassium chloride (KCl)	AppliChem
Protein A-Sepharose® 4B Conjugate	Invitrogen
Protein G Sepharose™ 4 Fast Flow	GE Healthcare
rhIL-6 (10 µg/ml)	ImmunoTools
RPMI 1640 (1x)	Gibco
S.O.B. (Super Optimal Broth)	AppliChem
SDS (Sodium dodecyl sulfate)	Sigma
Sodium azide (NaN_3)	Roth/Sigma
Sodium bicarbonate ($NaHCO_3$)	Merck?
Sodium butyrate	Roth
Sodium carbonate (Na_2CO_3)	Merck?
Sodium chloride (NaCl)	AppliChem
Sodium phosphate (NaH_2PO_4)	AppliChem
Sulfuric acid (H_2SO_4)	AppliChem/Sigma
TAE Buffer (50x)	National Diagnostics
TE Buffer pH 8	Qiagen
Tetramethylethylenediamine (TEMED)	Roth
TrackIt™ 1 kb Plus DNA Ladder	Invitrogen
TrackIt™ 100 bp DNA Ladder	Invitrogen
Tris ultrapure	AppliChem
Triton™ X-100	Sigma
Trypan Blue	Gibco/Sigma
Tween® 20	Sigma
Tyloxapol	Sigma
UltraPure™ 10 mg/ml Ethidium Bromide (EtBr)	Invitrogen
UltraPure™ DNase/RNase-Free Distilled Water	Gibco
α-Galactosylceramide derivate PBS44/PBS57	provided by Dr. Paul Savage [187]
α-Galactosylceramide (αGC)	GC Alexis Biochemicals
β-Mercaptoethanol	Gibco BLR

2.1.5 Cell culture media, buffers and solutions

Cell culture	Recipe
ATV	80 g NaCl 4 g KCl 10 g D-(+)-Glucose 5.8 g $NaHCO_3$ 5 g Trypsin 2 g EDTA fill to 10 l with dH_2O

BSS I	50 g Glucose 3 g KH_2PO_4 11.9 g NaH_2PO_4 0.4 g Phenol red fill to 5 l with dH_2O take 110 ml and fill to 1 l with dH_2O
BSS II	9.3 g $CaCl_2$ 20 g KCl 400 g NaCl 10 g $MgSO_4 \cdot H_2O$ 10 g $MgCl_2 \cdot 6H_2O$ fill to 5 l with dH_2O take 110 ml and fill to 1 l with dH_2O
BSS/BSA	0.2% BSA in BSS
Bulk fusion medium	47.5 ml RPMI+SC 2.5 ml FCS 5 µl $5*10^5$ U/ml rhIL-6 (10 µg/ml, stable 1 week at 4°c)
Cell freezing medium	50% FCS 40% RPMI 1640 10% DMSO
DMEM+ (cotton rat)	DMEM (1x) with 10% FCS 1x GlutaMAX™ Supplement
DMEM+	DMEM (1x) with 50 ml FCS and with or without 1.2 ml Streptomycin-Penicillin
HAT/HT (50x)	10 ml of RPMI used to dissolve HAT or HT powder (aliquot, stable for two weeks at 4°C)
HAT- or HT-medium (1x)	46.5 ml RPMI+SC 2.5 ml FCS 5 µl rhIL-6 (10 µg/ml, stable for 1 week at 4°c) 1 ml HAT or HT (50x)
RPMI++ (cotton rat primary cells)	RPMI 1640 10% FCS, 1x GlutaMAX™ supplement, 1x Penicillin-Streptomycin, 10^{-5} M β-Mercaptoethanol
RPMI+++ (cotton rat primary cells)	RPMI 1640 10% FCS, 1x GlutaMAX™ supplement, 1x Penicillin-Streptomycin, 10^{-5} M β-Mercaptoethanol, 2.5 M HEPES
RPMI+SC	RPMI 1640 with 40 ml SC supplement
RPMI++	RPMI 1640 with 25 ml FCS and 40 ml SC supplement

SC supplement	50% heat-inactivated FCS 10% 100 mM sodium pyruvate 10% nonessential amino acids 10% Penicillin-Streptomycin (10 kU/ml) 5.84% Glutamine (5% solution) 0.5% 50 mM β-Mercaptoethanol
Transfection medium	DMEM (1x) + GlutaMAX-I Supplement with 50 ml of FCS and with or without addition of 1.2 ml Streptomycin-Penicillin
Penicillin-streptomycin	5 g Streptomycin 5 g Penicillin dissolve in 50 ml dH_2O

Bacterial cell culture	Recipe
Agarose plates	25 g LB-Broth 15 g Agarose 1 l dH_2O autoclave and add ampicillin (final concentration 100 µg/ml) at 50°C, 20 ml per 9 cm non-tissue culture dish
Ampicillin (100 mg/ml	100 mg ampicillin powder in 1 ml 70% ethanol
Competent *E. coli*	chemically competent cells (α-select, Bioline)
S.O.C. medium	25.5 g Super Optimal Broth (SOB) dissolve in H_2O and set pH to 7 fill to 980 ml with H_2O add 20 ml glucose (1M)
LB-medium	25 g Lysogeny broth (LB) powder Fill to 1 l with dH_2O, autoclave

Buffers and Solutions	Recipe
Ammonium sulfate (saturated)	761 g ammonium sulfate slowly added to 1 l H_2O
ELISA coating buffer (0.1 M Bicarbonate buffer)	0.84 g $NaHCO_3$ (0.1 M) 0.356 g Na_2CO_3 (33.59 mM) Fill to 100 ml with dH_2O and set to pH 9.5
ELISA blocking buffer	PBS 5% FCS
ELISA washing buffer	1 l PBS with 500 µl Tween20®
ELISA reagent diluent (cotton rat)	DPBS 1% BSA (protease free), 0.2 µm filtered
ELISA washing buffer (cotton rat)	DPBS 0.05% Tween® 20
Elution buffer (Protein G)	50 mM Diethylamine, pH 11

Elution buffer (Protein A)	50 mM Trisodium citrate 100 mM NaCl set to pH 3.0
Flow cytometry buffer	PBS 0.1% BSA, 0.05% NaN_3
2x HBS	50 mM HEPES pH 7.1 10 mM KCl 12 mM Glucose 280 mM NaCl 1.5 mM Na_2HPO_4 Filtration (45 µM), pH 7.1
High salt buffer (Protein purification)	2.5 M NaCl 1.5 M Glycine set pH to 8.6
Neutralization buffer (Protein G)	2 M Tris base, pH 6
PBS	0.2 g KCl 0.2 g KH_2PO_4 0.05 g $MgCl_2$ 8 g NaCl 1.15 g Na_2HPO_4 0.167 g $CaCl_2 \cdot 2H_2O$ 0.1 g $MgCl_2 \cdot 6H_2O$ fill to 10 l with dH_2O
SDS-PAGE Destaining solution	12.5% Isopropanol 10% Acetic acid 77.5% dH_2O
SDS-PAGE Staining solution	12.5% Isopropanol 10% Acetic acid 0.25% Coomassie Brilliant Blue R250
Storage buffer (Protein G)	PBS 0.9% NaN_3
50x TAE	40 mM Tris base 20 mM Acetic acid 1 mM EDTA
TE	10 mM Tris-HCl pH 8 1 mM EDTA pH 8
5x TGS	15.1 g Tris base 94 g Glycin 50 ml SDS (10%) fill to 1 l with dH_2O
1.0 M Tris (pH 6.8)	121.1 g Tris base dissolve in 700 ml dH_2O, set pH fill to 1 l with dH_2O

1.5 M Tris (pH 8.8)	181.65 g Tris base dissolve in 700 ml dH_2O, set pH fill to 1 l with dH_2O
Washing buffer (Protein G)	PBS 1 M NaCl

2.1.6 Commercially available kits

Product	Company
BD Calibrite™ 3-color kit	BD
BD OptEIA™ Mouse IL-2 ELISA Set	BD
BD OptEIA™ TMB Substrate Reagent Set	BD
BigDye Term v3.1 CycleSeq Kit	Applied Biosystems
DNase I Kit	Thermo Scientific
dNTP Mix (10mM)	Invitrogen
ELISA Cotton Rat IFN-γ DuoSet	R&D Systems
ELISA Cotton Rat IL-4 DuoSet	R&D Systems
First Strand cDNA Synthesis Kit	Thermo Scientific
Foxp3/Transcription Factor Staining Buffer Set	eBioscience
GeneJET™ Plasmid Miniprep Kit	Thermo Scientific
GeneRacer™ Kit	Invitrogen
High Pure RNA Isolation Kit	Roche
innuPREP Plasmid Mini Kit 2.0	Analytik Jena
JETquick DNA Clean Up Spin Kit 50	Genomed
JETsorb Gel Extraction Kit/150	Genomed
JETstar 2.0 Plasmid Midiprep Kit	Genomed
Lentivector Expression Systems LV500-A1	System Biosciences
MiniElute™ Gel Extraction Kit	Quiagen
Mouse IgG1 ELISA Quantitation Set	Bethyl
Mouse IL-2 Uncoated ELISA Kit	Invitrogen
Mouse Monoclonal Antibody Isotyping Test Kit	BioRad
NucleoSpin® Gel and PCR Clean-up	Macherey-Nagel
One Shot® TOP10 Chemically Competent E. coli	Invitrogen
OneStep RT-PCR Kit	Qiagen
Pierce™ BCA Protein Assay Kit	Thermo Scientific
Plasmid Maxi Kit	Qiagen
PureLink™ HiPure Plasmid Midiprep Kit	Invitrogen
QIAamp DNA Mini Kit	Qiagen
QIAprep Spin Miniprep Kit	Qiagen
QIAquick Gel Extraction Kit	Qiagen
QIAquick PCR Purification Kit	Qiagen
QIAshredder	Qiagen
RNeasy Micro Kit	Qiagen
RNeasy Mini Kit	Qiagen
Substrate Reagent Pack	R&D Systems
SuperScript™ First-Strand Synthesis Kit for RT-PCR	Invitrogen
TOPO® TA Cloning® Kit for Sequencing	Invitrogen
Zenon® AlexaFluor 680® Rabbit IgG Labeling Kit	Molecular Probes
In-Fusion® HD Cloning Kit	Takara Bio

2.1.7 Enzymes

Product	Company
AmpliTaq Gold™ DNA Polymerase	Applied Biosystems
PCR Master Mix Taq DNA Polymerase	Thermo Scientific
Phusion™ High-Fidelity DNA-Polymerase	Thermo Scientific
Platinum® Taq DNA Polymerase (5U/µl)	Invitrogen
Platinum® Taq DNA Polymerase High Fidelity (5U/µl)	Invitrogen
Q5® Hot Start High-Fidelity DNA Polymerase	New England Biolabs
Restriction enzymes	Thermo Scientific
T4 DNA Ligase (1U/µl)	Invitrogen/Fermentas
Taq DNA Polymerase (5U/µl)	Invitrogen

2.1.8 Oligonucleotides

The Oligonucleotides used in this thesis were purchased from Sigma-Aldrich and are depicted in a 5' to 3' orientation. Potential restriction sites appear underscored and forward (fwd) or reverse (rev) orientation of oligonucleotides is indicated. The oligonucleotides were designed based upon alignments, database entries or other sequence information. All primers were used in 10 µM dilutions. Degenerate primer symbols are indicated next to the primer sequence.

1. Cotton rat

Name	Sequence
A1 crBV8 5'RACE rev 2	CTGTCTGAGAGGGGGAGGCCATCT
A100 crBC2 BamHI rev	ATAGGATCCTCAGGAATTCTTTTTCTTGACCA
A2 crBV8 5'RACE rev	TCACTGCTAGCACAGAAGTACACAGC
A3 crBC 3'RACE fwd	AGCCCACCCACAGTCAACTTGTTTGA
A7 crBC 3'RACE fwd 2	GTGCAGTTCTATGGGCTTACAG
A98 crBV8.2 PagI fwd	CTATTCATGAGCCGCCACCCCTGAGATGGGCTTCAGGCTC
A99 crBC1 BamHI rev	ATAGGATCCTCAGGAATTCTTTCTTTTGACCA
cr1 crBV8.2 fwd	AACATGTACTGGTATCGGCAG
cr2 crBV8.2 fwd 2	TGGTCTGAGGCTGATCCATTA
cr3 crBCrev	CCTTGTAGGCCTGAGGGTC
cr4 crBCrev 2	ACACGAGGGTAGCCTTTTGTT
crAC rev	ACTGACAGGTTTTGAAAGTTTAG
crAV14 fwd	AAGACCCAAGTGGAGCAGAGT
crAV14 RACE3' fwd	AAGGCCATAAGCAATTGGTATGTCATGT

crAV14 RACE5' rev	GCATCTTCATCCAGAGCTGCTGAGTATC
crAV14BamHI rev	ATGCGGATCCTCAACTGGACCATAGCCGCAGCGTCATGAG
crAV14EcoRI fwd	GGGCTAGAATTCAGTAGAACAACAATGGAGAAG
crAV14gDNA BamHI rev	GCATGGATCCGGCAGTGTCCTCAAACTGGG
crAV14gDNA EcoRI fwd	GCATGAATTCAGAGCCCCAAGTTCCTGACT
crCD1d fwd nested	GCCTGTGTGGGTGATGTGGA
crCD1d fwd	AACCAGCTTTACCAGGGACAT
crCD1d RACE3' fwd	AAGGCCATAAGCAATTGGTATGTCATGT
crCD1d RACE5' rev	ATTCTCAGAGTACACTTCACATCCTACA
crCD1d rev nested	ATCCACATCACCCACACAGG
crCD1d rev	TCTCCAGCCTCCACATCCAG
crCD1dBamHI rev	GCATGGATCCCTATTGGATGCTTTGATAGGAG
crCD1dNcoI fwd	GCATCCATGGCGGCGCTATGGGGCTCCTCCCGTGC
pXIg 3' XhoI rev	GGTCACTCGAGCCAATAGAGGATGATGTCTTGGT
pXIg 5' MluI fwd	GGTCCACGCGTCGCAGCAAAAGAATTCCACCTTC
S65T fwd	CAAAGTAGACGGCATCGCAGCTTG
S65T rev	TGATATTGTTGAGTCAAAACTAGAGC

2. Armadillo

Name	Sequence
A103 CγRACE3'fwd	TGTTTCTTCCTTCAATTGCTGAAACACAT
A104 CγRACE3'fwd2	AGGATGGCAATACGATTCTGGAATCC
A118 Vδ2RACE5'rev	CAGTGATGCCTCACGAATCTCGAGTA
A119 Vδ2RACE5'rev2	TAAACGCTGCCACGGAACCTGCTCT
A122 BTN3panIgVfwd	TTCCAAGATGACAACTTCTATGA
A123 BTN3panIgCrev	AGAGCCCTCCCCAGAGCC
A163 BTN3RACE3'panIgVfwd	CATCGTGGCCATGGTGGGTGAGGA
A164 BTN3RACE3'panIgVfwd2	CCAGGCTCAGGCAGGTGGTGGA
A165 BTN3RACE5'panIgVrev	CCATGGCTTTCTCATAGAAGTTGTCAT
A166 BTN3RACE5'panIgVrev2	ATAACACAGGTAGTGTCCACTGTCAGA

A167 BTN3RACE3'panIgCfwd	GCGCTGGGCTCTGATCTCCACATT
A168 BTN3RACE3'panIgCfwd2	CTGTGATGGTGAAAGGCGGCTCT
A17 Vγ9fwd	CTAGAGCAACCTCGACTTTCTA
A19 CγEx1rev	TCCCATTCACGGTCAGCCAG
A193 Vδ2pMSCV fwd	CTAGGCGCCGGAATTCGCCGCCACCATGCAAAGGATCTGCTGTCTC
A194 Vδ2pMSCV rev	CGAGCAATTGGGATCCTTAAAAGAAAAGTAACTTGGCAGT
A21 Vδ2fwd	GCCATTGTGTTGGTGCCTGAA
A23 CδEx1rev	AGACGACGATAGCAGGGTCAA
A23 CδEx1rev	AGACGACGATAGCAGGGTCAA
A27 Vγ9fwd3	GGACAAATTTGAGGTGGACAAG
A28 CγEx1rev2	TTGAAGGAAGAAACACAGTGGG
A29 Vδ2fwd3	TTCCGTGGCAGCGTTTATAGTT
A30 CδEx1rev2	CAACTTTCGTCTCATTTTTCATGA
A66 Vγ9fwd2	TGTGTGGTATCTGGAGTAACAAT
A67 Cγ1-3Ex1rev	ACACATTTGTGTTCTTCATCCAT
A67 Cγ1-3Ex1rev	ACACATTTGTGTTCTTCATCCAT
A68 Cγ1-3Ex1rev2	TGGGATTCCAGAATCGTATTGC
A71 Vδ2fwd2	TAGTGACCGTGACTGTGGGAA
A72 CδEx1rev3	TTTGTCTTCAATTCAAAGTCAGAG
A73 CδEx1rev4	CATTATTGTGTTGAACTGAACATG
A78 Cγ4Ex1rev	CTCCTCTATTATCTTCATGTTTGA
A86 CγRACE5'rev	TGTCTGACCACACATTTGTGTTCTTC
A87 CγRACE5'rev2	GGATTCCAGAATCGTATTGCCATCCT
A92 Vγ9RACE3'fwd2	CAGGTTTTCTAGAGCAACCTCGACTT
A93 Vγ9RACE3'fwd	CCCGCCTGGAATGTGTGGTATCT
A94 Vδ2RACE3'fwd	GTAGTGACCGTGACTGTGGGAAAGT
A95 Vδ2RACE3'fwd2	GAGCGATGCGTAACTACTACATGAA
IRES rev	GCATTCCTTTGGCGAGAG
pLXSN 5'	CCCTTGAACCTCCTCGTTCGACC
pMImCherry II for	GTCAAGCCCTTTGTACACCCT

3. Alpaca

Name	Sequence
129 phNGFRmCh huA1 BglII rev	CTATAGATCTCGCTGGACAAATAGTCAGGGC
156pEGZVγ9_ins1Ecofwd	GGACCATCCTCTAGAGAATTCGCCGCCACCATGCTGTCACTGTTCCCGC
157 pEGZ Vγ9_ins1 rev	TGGTGAGGGTAGACGTCGAAGTGTCAGGCG
158 pEGZ Vγ9_ins2 fwd	TTCGACGTCTACCCTCACCATTCACAGTGT
158 pEGZ Vγ9_ins2 rev	TGATGGTGTTTCCCTGCTGGGATTCCAGA
160 pEGZ Vγ9_ins3 fwd	CCAGCAGGGAAACACCATCATGACGAATGATAC
162 pEGZ Vγ9_ins3BamHI rev	GGGGGAGGGAGAGGGGGATCCTCACGAGCCCTTCCCGTG
162 pIH Vd2Jd2_ins1Eco fwd	GGACCATCCTCTAGAGAATTCGCCGCCACCATGCAGAGGGTCTGCTCCC
163 pIH Vd2Jd2_ins1 rev	TCTCTGATGCCTTGAGGATCTCCAGCAGGACC
164 pIH Vd2Jd2_ins2 fwd	GATCCTCAAGGCATCAGAGAGAGACAAAGGATC
165 pIH Vd2Jd2_ins2 rev	GACCGAGCTTGATGGCACTGTACCTCCCAC
166 pIH Vd2Jd2_ins3 fwd	CAGTGCCATCAAGCTCGGTCAGTATGAAGATTCCG
167 pIH Vd2Jd2_ins3BamHI rev	GGGGGAGGGAGAGGGGGATCCTTAGAAGAAAAATAACTTGGTAGTC
178 pIH Vd2Jd2_ins1-3Eco fwd	GATCGAATTCGCCGCCACCATGCAGAGGGTCTGCTCCCT
179 pIH Vd2Jd2_ins1-3Bam rev	GATCGGATCCTTAGAAGAAAAATAACTTGG
200 huBTN3 EcoRI fwd	CTATGAATTCGCCGCCACCATGAAAATGGCAAGTTTCCTGGC
275 vpBTN3 MfeI fwd	CTATCAATTGGCCGCCACCATGAAAACGGCCAGGTCCCTAGA
281 hu/vpBTN3 IgC rev	GGCGCTCCTGAAGAAGGGGTCTGC
282 hu/vpBTN3 ID fwd	GCAGACCCCTTCTTCAGGAGCGCC
67 vpVγ9 fwd	GTGCAGGTCATCTAGAGCAACCGC
68 vpVδ2 fwd	GTCAGCAGATGTGTTGGTGCCTCA
69 vpCγ rev	TCCATTGACTTTTCAGGCACGGTCA
70 vpCδ rev	CCAGCACCGAGAGGGACATCATGT
A173 SCPCRVpVg9 fwd	TCGAGAAAGGCCCGGTCAAG
A174 SCPCRVpCg rev	GGGGCCATGTCTGCATCAAG
A175 SCPCRVpVd2 fwd	ATCAAGTAAACAACCAGGTCCT
A176 SCPCRVpCd rev	TGACAAAGACAGATGGTGTGG
A195 vpCgRACE5deg rev1	TCCRTWGACTTTTCAGGCACGGTCA (R=A+G; W=A+T)

A198 vpCdRACE5 rev1	AGTGCCTTTGGTTTTGGAGTCACTG
A199 vpCdRACE5 rev2	GAGAGACGACGATAGCAGGGTCATA
A96 vpBTN3 Mfe1rev	ATAGCAATTGCTAGGCAGGGACAAGCAAGGAT
A97 vpBTN3mCherry BglII rev	ATAGAGATCTGGCAGGGACAAGCAAGGATGTTA
M13 fwd	GTAAAACGACGGCCAG
M13 rev	CAGGAAACAGCTATGAC

2.1.9 Vectors

Name	Description
pczVSV-G	Vector encoding the env protein of the vesicular stomatitis virus (kindly provided by D. Lindemann [338]).
pEGN	pEGZ vector with a neomycin resistance gene instead of a zeocin gene (EGFP-neomycin fusion gene) (kindly provided by I. Berberich [339]).
pEGN huVγ9 MOP	pEGN vector with a full-length human Vγ9 chain (GenBank: KC170727.1).
pEGZ	pIZ vector with an additional EGFP gene (EGFP-zeocin fusion gene) located 3' of an internal ribosomal entry site (kindly provided by I. Berberich [339]).
pEGZ vpBTN3	pEGZ vector containing the complete coding sequence of alpaca BTN3 (GenBank: MG029164). Cloned by L. Starick using the restriction sites MfeI/BglII for insert and EcoRI/BamHI for pEGZ.
pEGZ huBTN3A1	pEGZ vector containing the complete coding sequence of human BTN3A1. Cloned by L. Starick using the restriction sites EcoRI/BglII for insert and EcoRI/BamHI for pEGZ.
pEGZ vpVγ9	pEGZ vector containing a full-length alpaca Vγ9 chain and parts of the 5' and 3' UTRs. Alpaca Vγ9 was cloned into pEGZ by M. Karunakaran using EcoRI and BamHI restriction enzymes [317].
pHIT 60	Vector encoding the gag and pol proteins of the murine leukemia virus (MoMLV) (kindly provided by D. Lindemann [340]).

phNGFR mCherry	phNGFR vector (kindly provided by I. Berberich) and modified by L. Starick. The phNGFR gene and IRES sequence were removed through a BamHI and Kpn21 digestion and replaced with a multiple cloning site (MCS) followed by a linker sequence, a Kozak sequence, EcoRI, SmiI, and BamHI restriction sites and a mCherry gene. Cloning of mCherry fusion proteins requires the stop codon to be removed to achieve transcription of the gene of interest in frame with mCherry.
pIH vpVδ2 cl. 8/9	pIH vector containing a full-length alpaca Vδ2 chain (clone 8 or 9). This gene was cloned into pIH by M. Karunakaran using EcoRI and BamHI restriction sites [317].
pIH	pIZ vector with a hygromycin resistance gene (kindly provided by I. Berberich).
pIZ	Retroviral vector originating from the murine leukemia virus (MuLV). This vector can be used for the constitutive MuLV-mediated expression of inserted genes. pIZ contains a zeocin resistance gene with an IRES promotor (kindly provided by I. Berberich [341]).
pMIG II mCD3 δ-F2A-γ-T2A-ε-P2A-ζ	Retroviral vector encoding all four subunits of WT mouse CD3 linked by F2A, T2A and P2A linker sequences and co-expressed with an EGFP gene [342]. This vector contains an ampicillin resistance gene for bacterial selection.
pXIg	Vector to produce CD1d mIgG dimers which contains MluI and XhoI restriction sites. An IgG1 heavy chain is encoded in this vector. The signal sequence is located 5' of the MluI site, and the IgG1 heavy chain gene starts with the variable domain 3' of the XhoI site [343]. The vector was derived from the pSN-RCR2 plasmid encoding a mouse IgG1 heavy chain specific for the hapten NP [344].
S65T CDR(2+4)	In this vector, the original SFP-GFP coding fragment was replaced by a rat TCR β chain [345].
SFG-GFP (S65T)	Retroviral expression vector coding for a GFP gene fragment located between the NcoI and BamHI restriction interfaces [346].

2.1.10 Cell lines

Name	Description
293T	(ACC 635, DSMZ) Human Embryonic Kidney (HEK) 293 cell line transformed with the SV40 large T antigen with neomycin resistance. Used to produce pseudovirus particles during retroviral transduction and as a cell line for stable overexpression of surface molecules.
53/4	Mouse/rat T cell hybridoma cell line, sister clone of 35/4, specific for guinea pig myelin basic protein (gpMBP68-88) with $RT1B^1$ restriction [345].
53/4 r/mCD28	53/4 cells transduced with a rat/mouse chimeric CD28 molecule to enhance the response to the antigen in the presence of counter-ligands on the antigen-presenting cell (e.g. CD80) [156, 345, 347].
53/4 huVγ9Vδ2	53/4 cells transduced with a rat/mouse chimeric CD28 molecule and expressing a human Vγ9Vδ2 TCR (GenBank: KC170727.1/KC196073.1) encoded by the vectors pEGN huVγ9 MOP and pIZ huVδ2 MOP.
53/4 vpVγ9vpVδ2 cl.8/9	53/4 r/m CD28 cells overexpressing an alpaca TCR (pEGZ vpVγ9) and an alpaca Vδ2 chain (pIH vpVδ2 cl. 8 or 9) [317, 321].
BW 5417 gal1	TCR-negative mouse T cell hybridoma cell line, used for PEG-mediated fusion.
BW58	(ATCC TIB-233) TCR-negative AKR/J mouse T cell hybridoma cell line, derived from Do-11.10.7 hybridoma cell line [348]. Used as a target cell line for retroviral transduction.
BW58 r/mCD28	BW58 transduced with a rat/mouse chimeric CD28 molecule [347].
BW rat S6 93A	BW58 r/mCD28 overexpressing a rat iNKT TCR. The Vα14 S6 chain is encoded by the vector pEGN rAV14 S6 93A, and the Vβ chain is encoded by S65T CDR2+4 L14V [156, 349].
BW huVγ9vpVδ2 cl.8/9	BW58 r/m CD28 cells overexpressing a TCR with a human Vγ9 TCR chain (pEGN huVγ9 MOP) and an alpaca Vδ2 chain (pIH vpVδ2 cl. 8 or 9) [321].
CHO huCD80	Chinese hamster ovary (CHO) cells retrovirally transduced with a human CD80 gene in the S65T vector.
CHO chr.6 huCD80	(GM11580, Coriell Institute for Medical Research) CHO cells monosomal for human chromosome 6 [350] (provided by Human Genetic Cell Repository, Coriell Institute, Camden, New Hampshire). CHO chr.6 cells were transduced with S65T containing human CD80.

J558L	Mouse B myeloma cell line, a variant of J558 cells derived from BALB/c. with spontaneous loss of the heavy chain [351].
J558L pXIg huCD1d	J558L cell line transduced with human CD1d, used for production of mCD1d dimers [349].
J558L pXIg mCD1d	J558L cell line transduced with mouse CD1d, used for production of mCD1d dimers [148].
J558L pXIg rCD1d	J558L cell line transduced with rat CD1d, used for the production of mCD1d dimers [148].
L929	Mouse fibroblast cell line used for overexpression of vpBTN3 and vpVγ9Vδ2 TCRs [352].
LGK-1-R	(CCLV-RIE 1224) Fibroblast-like, polymorph primary kidney cell line (*Vicugna pacos*) provided by M. Lenk, Friedrich-Löffler-Institute, Insel Riems, Germany.
M12	M12.4.1C3 mouse B cell lymphoma cell line used for overexpression of vpVγ9Vδ2 TCRs [353].
Raji	(ATCC® CC1-86™) Human Burkitt-lymphoma cell line.
Raji RT1B^1	Raji cell line transduced with RT1B^1 a rat MHC class II molecule [345].
SP2/0 (Ag14)	(ATCC® CRL-1581™) HAT-sensitive non-Ig-producing mouse myeloma cell line used as a fusion partner for monoclonal antibody production.

2.1.11 Antibodies and secondary reagents

Primary antibodies

Antigen	Clone	Conjugation	Isotype	Company
BoWC1	GB45A	purified	mIgG1	[354]
crIgG (Fc)	14-106FF1,IFA	purified	rabbit	[169]
huBTN3	103.2	purified	mIgG2a, κ	[48, 244]
huBTN3	20.1	purified	mIgG1, κ	[244]
huCD3ε	CD3-12	FITC	rIgG1	AbD serotech
huCD80	L307.4	PE	mIgG1, κ	BD Pharmingen
huVγ9	B3	PE	mIgG1, κ	BD Pharmingen
huVδ2	B6	PE	mIgG1, κ	BD Pharmingen
Isotype mIgG1	P3.6.2.8.1	purified	mIgG1, κ	Affymetrix
Isotype mIgG2a		FITC	mIgG2a,κ	BD Pharmingen
Isotype mIgG2a	eBM2a	purified	mIgG2a, κ	Affymetrix
Isotype mIgG2a	X39	PE	mIgG2a,κ	BD Pharmingen
Isotype haIgG1	anti-TNP	bio	haIgG1,κ	BD Pharmingen
LaCD5	LT3A	purified	mIgG1	[354]
LaCD8	LT5A	purified	mIgG2a	[354]
LC1	LT10A	purified	mIgG2a	[354]
m/r I-Ek (MHC II)	14-4-4S	purified	mIgG2a,κ	Affymetrix
mCD1d	1B1	PE	mIgG2b,κ	BD [183]

mCD3ε	145-2C-11	bio	haIgG1,κ	BD Pharmingen
MHCII	LT1A	purified	mIgG2a	[354]
mNK1.1	PK136	PE	mIgG2a,κ	BD Pharmingen
rCD1d	WTH-1	pur./bio	mIgG2a,κ	[355, 356]
rCD1d	WTH-2	pur./bio/FITC	mIgG2a,κ	[355, 356]
rCD28	JJ319	purified	mIgG1	Exbio
vpBTN3	189	purified	mIgG2b,κ	see 3.2.2.2.2
vpVδ2Jδ4	118.7	purified	mIgG1,κ	see 3.2.2.2.1

Secondary antibodies

Antigen	Name	Conjugation	Company
mIgG	F(ab')$_2$ Fragment Donkey α-Mouse IgG (H+L)	R-PE	Jackson ImmunoResearch
mIgG	Goat α-Rabbit IgG (H+L) FITC		Invitrogen
mIgG	F(ab')$_2$ Fragment Donkey α-Mouse IgG (H+L)	FITC	Jackson ImmunoResearch
mIgG1	AffiniPure Fab Fragment Goat α-Mouse IgG1 (Fcγ)	R-PE	Jackson ImmunoResearch
mIgG1	Goat α-Mouse IgG1 Cross-Adsorbed sec. Ab	AF647	Invitrogen
mIgG2b	Goat α-Mouse IgG2b	R-PE	BioRad

Secondary reagents

Reagent	Specific for	Conjugation	Company
Streptavidin	Biotin	APC	BD Pharmingen

2.1.12 Animals and human samples

Inbred hispid cotton rats (*Sigmodon hispidus*) and inbred C57BL/6 mice (Harlan Laboratories, Indianapolis, IN) were used at six to twelve weeks of age and bred in the animal facility located in the Department of Psychology of The Ohio State University in Columbus Ohio. The Vivarium was used by the Department of Veterinary Biosciences. Animal experiments were reviewed by the Institutional Animal Care and Use Committee at the Ohio State University.

BALB/cAnNCrl mice used for hybridoma development were bred at the Institute for Virology and Immunobiology (Julius-Maximilians-Universität, Würzburg). Breeding pairs were provided by Charles River, Sulzfeld, Germany. Mice were kept and samples collected in accordance with the German regulations (Tierschutzgesetz) under protocols approved by the District of Lower Franconia (55.2-2531.01-81/14).

Armadillos (*Dasypus novemcinctus*) were kept and samples collected in accordance with the ethical guidelines of the U.S. Public Health Service under protocols approved by the IACUC of the National Hansen's Disease Program, assurance number A3032-1.

Alpacas (*Vicugna pacos*) were bred in the animal facility of the Ludwig-Maximilians-Universität in Munich, Germany and provided by Prof. Dr. Thomas Göbel. Blood samples were collected according to local regulations (Permission Regierung von Oberbayern: Az. 55.2-1-54-2532.3-11-11). Adult animals were between one and eight years of age and female or male.

Human PBMCs were prepared from healthy donors as a byproduct of platelet concentrates obtained with leukoreduction system chambers (LRS-C; Gambro Trima Accel aphaeresis apparatus, Pall Corp) and provided by Clinical Transfusion Medicine, University of Würzburg.

2.2 Methods

2.2.1 Molecular biology and Microbiology

2.2.1.1 Agarose gel electrophoresis and purification of DNA

Agarose Gel electrophoresis was carried out using 1% agarose gels with GelRed (1:40000) or EtBr (0.3 µg/ml) and buffer 1x TAE. The samples were loaded using 1x Loading Dye (6x) and the molecular standards GeneRuler 100 bp or 1 kb or TrackIt™ 1 Kb Plus or 100 bp DNA Ladder. The applied voltage was 120 V for 30-60 min to separate DNA of different lengths and UV-light was used to visualize DNA. Gel extraction of DNA was performed with the QIAquick Gel Extraction Kit or MiniElute™ Gel Extraction Kit following the manufacturers' manuals. Alternatively to gel extraction, PCR products were purified after PCR reactions with QIAquick PCR Purification Kit (Qiagen) or the NucleoSpin® Gel (Macherey-Nagel).

2.2.1.2 Restriction enzyme digestion and ligation of inserts and plasmids

Restriction enzyme digestion was carried out using plasmid DNA or PCR products after PCR clean up or Gel extraction. A single or double digestion was performed for 2 h, and conditions and buffers were chosen accordingly. The digested DNA sample was purified as described in 2.2.1.1 and stored at -20°C in the provided elution buffer. The ligation of the digested insert and vector for cloning was conducted with a T4 DNA Ligase according to the manual at 10°C overnight. Vector and insert were used in a molar ratio of 1:5-6.

2.2.1.3 Transformation of competent *E.coli* with plasmid DNA

Escherichia coli (*E.coli*) were transformed with plasmid DNA using the heat shock method. Chemically competent cells (α-select chemically competent cells, Bioline) were thawed on ice, and 1-2 µl of a ligation mix or 5 ng of plasmid was added. Following an incubation period of 10-30 min on ice, a 30 s heat shock was carried out at 42°C, and after 2 min on ice 150 µl S.O.C medium was added. The bacterial culture was incubated in the bacterial shaker for 1 h. The cells were then spread on agar plates containing 100 µg/ml ampicillin and left o.n. in a dry incubator at 37°C.

2.2.1.4 Bacterial cultures

Usually, bacterial cultures were performed in the presence of 100 µg/ml ampicillin using the appropriate volume of LB medium. Cultures were incubated overnight in a bacterial shaker.

2.2.1.5 Plasmid DNA isolation (Mini/Midi)

An amount of 3-5 ml LB Broth with ampicillin was used as culture media for mini-cultures and 50 ml for midi cultures. Single clones were picked from incubated agar plates after transformation or spreading of frozen bacterial stocks. After incubation of mini-cultures 1 ml bacterial stocks containing 15% glycerol were frozen at -80°C. The mini preparation was either carried out using the innuPREP Plasmid Mini Kit following the provided protocol or following the "Quick Method" protocol. For this, 2 ml of the dense bacterial mini culture were spun down at 10621 x g (10000 rpm) at RT for 2 min. The cell pellet was then resuspended with 250 µl E1 solution (JETstar 2.0 Midiprep Kit) and 250 µl lysis buffer E2 were added. The reaction tubes were inverted several times, and lysis did not exceed 5 min at RT. To neutralize, 250 µl of buffer E3 were added and the tube was inverted. After centrifugation at 17949 x g (13000 rpm) at RT for 10 min, the supernatant was transferred to a new tube, and a volume fraction of 0.7 isopropanol was added. The DNA was pelleted at 17949 x g (13000 rpm) at 4°C for 15 min, and the pellet was washed for 5 min with 500 µl 70% ethanol. DNA pellets were then dried at RT and dissolved in 50 µl TE buffer. Midi preparations were carried out using the JETstar 2.0 Midiprep Kit following the manufacturer's instructions, and the eluted DNA was frozen at -20°C.

2.2.1.6 RNA/DNA isolation from primary cells and cell lines

RNA was isolated from primary cells or cell lines using either the Qiagen RNeasy Mini Kit, the Qiagen RNeasy Micro Kit or the Roche High Pure RNA Isolation Kit following the instructions in the respective manuals. If the RNeasy Mini Kit was used, approximately $4*10^6$ cells were lysed and disrupted using RLT buffer with 1% β-Mercaptoethanol and passed through a 20-gauge needle (at least five times) or were homogenized using QIAshredder columns. After the following column-based RNA binding and washing steps, RNA was eluted with 40 µl or less elution buffer. An additional DNase digestion to decrease DNA contamination was performed using the DNase I kit. DNA isolation was performed from at least $1*10^6$ cells (primary or cell lines) and the QIAamp DNA Mini Kit (Qiagen) was used according to the manufacturer's protocol.

2.2.1.7 Spectrophotometric determination of RNA and DNA amounts

The quantity and purity of DNA and RNA amounts were measured using the spectrophotometer NanoDrop 1000 at the wavelengths 260 nm and 280 nm following the manual provided by the manufacturer.

2.2.1.8 First Strand cDNA synthesis

First Strand cDNA synthesis was carried out using either the SuperScript™ First Strand Synthesis Kit for RT PCR (Invitrogen) or the First Strand cDNA Synthesis Kit (Fermentas) following the protocol provided with the kit. The primers applied for RT PCR were Random Primers or Oligo dT Primers, and the amount of RNA was 1 µg or the maximum amount available. To minimize DNA contamination, RNA was digested with the DNase I Kit before cDNA synthesis, according to the manual.

2.2.1.9 RNA-ligase mediated rapid amplification of cDNA ends (RLM-RACE)

Amplification of 5' and 3' ends of unknown genes was performed using the GeneRacer™ Kit. This procedure is based on RNA-ligase-mediated (RLM) oligo-capping rapid amplification of cDNA ends (RACE). 5' RACE ready cDNA required the RNA to be dephosphorylated at the 5' end, decapped and ligated to an RNA Oligo with a known priming sequence for GeneRacer PCR primers. The cDNA synthesis was carried out with Random Primers and the SuperScript™ III RT. For 3' RACE-ready cDNA, the cDNA synthesis was conducted with the provided 3' Oligo dT primer. This primer also provides a known priming site after the 3' polyA tail of the mRNA. The 5' or 3' RACE-ready cDNA was digested with RNaseH and used in subsequent PCR reactions with gene-specific primers (GSP) and GeneRacer Primers provided with the kit. Amplification of 5' and 3' ends was achieved by Touchdown-PCR, and if needed a nested PCR, with Q5 Hot Start Polymerase or Platinum® Taq DNA Polymerase following the manufacturers' recommendations.

1. Q5 PCR Mix (50 µl):

Q5 Reaction Buffer (5x)	10 µl
dNTP Mix (10 µM)	1 µl
GeneRacer 5'/3'	4.5 µl
Primer GSP (10 µM)	2.5 µl
Q5 Hot Start Polymerase	0.5 µl
(Betaine	10 µl)
cDNA (RACE-ready)	1-2 µl
H_2O	to 50 µl

2. Platinum Taq PCR Mix (50 µl):

PCR Buffer (10x)	5 µl
dNTP Mix (10 µM)	1 µl
GeneRacer 5'/3'	3 µl
Primer GSP nested (10 µM)	1 µl
Platinum Taq Polymerase	0.5 µl
$MgCl_2$ (50 mM)	2 µl
cDNA (RACE-ready)	1-2 µl
H_2O	to 50 µl

Q5 PCR program Touchdown PCR (Platinum Taq PCR Program):

Initial Denaturation	5 min (2 min)	98°C (94°C)	
Denaturation	30 s	98°C (94°C)	] 5x
Annealing/Extension	1 min/kb	72°C (72°C)	
Denaturation	30 s	98°C (94°C)	] 5x
Annealing/Extension	1 min/kb	70°C (70°C)	
Denaturation	30 s	98°C (94°C)	] 20-25x
Annealing	30 s	65-70°C	
Extension	1 min/kb	72°C (72°C)	
Final Extension	10 min	72°C	
Hold	∞	4°C	

3. nested Q5 PCR Mix:

Q5 Reaction Buffer (5x)	10 µl
dNTP Mix (10 µM)	1 µl
GeneRacer 5'/3' nested	2.5 µl
Primer GSP nested	2.5 µl
Q5 Hot Start Polymerase	0.5 µl
(Betaine	10 µl)
PCR product (Touchdown)	1 µl
H_2O	to 50 µl

4. nested Platinum Taq PCR Mix:

PCR Buffer (10x)	5 µl
dNTP Mix (10 µM)	1 µl
GeneRacer 5'/3' nested	1 µl
Primer GSP nested (10 µM)	1 µl
Platinum Taq Polymerase	0.5 µl
$MgCl_2$ (50 mM)	1.5 µl
PCR product (Touchdown)	1 µl
H_2O	to 50 µl

nested Q5 PCR program (nested Platinum Taq PCR program):

Initial Denaturation	30 s (2 min)	98°C (94°C)	
Denaturation	10 s (30 s)	98°C (94°C)	] 25-35x
Annealing	30 s	55-65°C	
Extension	30 s/kb (1 min/kb)	72°C (72°C)	
Final Extension	2 min (10 min)	72°C (72°C)	
Hold	∞	4°C	

2.2.1.10 Polymerase Chain Reaction (PCR)

Polymerase chain reactions were carried out using either the Platinum® Taq DNA Polymerase or the PCR Master Mix Taq DNA Polymerase w/o proof-reading function. The Phusion™ High-Fidelity DNA-Polymerase or the Platinum® Taq DNA Polymerase High Fidelity were used whenever proof-reading was necessary. The 2x PCR Master Mix Taq DNA Polymerase consists of 0.05 U/µL Taq DNA polymerase, reaction buffer, 4 mM $MgCl_2$ and 0.4 mM of each dNTP (dATP, dCTP, dGTP and dTTP). The Phusion HF Buffer provides $MgCl_2$ at a final concentration of 1.5 mM. As standard, 50 µl reactions were used for Phusion or Platinum® Taq PCR and 20 µl reactions for Taq Polymerase and the PCR programs were standard programs. Temperatures for annealing and extension were chosen depending on the primers and the expected product length. In the case of moderate to strong secondary structures of the primers, Betaine (N,N,N-trimethylglycine) solution was added at a final concentration of 1 M. This isostabilizing agent facilitates strand separation was used to reduce the formation of those structures. PCR products were analyzed using agarose gel electrophoresis according to 2.2.1.1.

1. Platinum Taq PCR Mix (50 µl):

10x PCR Buffer	5 µl
$MgCl_2$ (50 mM)	1.5 µl
dNTP Mix (10 mM)	1 µl
Primer forward (10 µM)	1 µl
Primer reverse (10 µM)	1 µl
Platinum Taq (5 U/µl)	0.5 µl
Template	1-2 µl
H_2O	to 50 µl

Platinum Taq PCR program:

Initial Denaturation	10 min	94°C	
Denaturation	30 s	94°C	30-35x
Annealing	30 s	52-62°C	
Extension	1 min/kb	72°C	
Final Extension	10 min	72°C	
Hold	∞	4°C	

2. Platinum Taq HF PCR Mix (50 µl):

10x PCR Buffer	5 µl
$MgSO_4$ (50 mM)	2 µl
dNTP Mix (10 mM)	1 µl
Primer forward (10 µM)	1 µl
Primer reverse (10 µM)	1 µl
Platinum Taq (5 U/µl)	0.2 µl
Template	1-2 µl
H_2O	to 50 µl

Platinum Taq HF PCR program:

Initial Denaturation	2 min	94°C	
Denaturation	30 s	94°C	30-35x
Annealing	30 s	52-62°C	
Extension	1min/kb	68°C	
Final Extension	10 min	68°C	
Hold	∞	4°C	

3. Phusion PCR Mix (50 µl):

5x Phusion HF Buffer	10 µl
dNTP Mix (10 mM)	1 µl
Primer forward (10 µM)	2.5 µl
Primer reverse (10 µM)	2.5 µl
Phusion Polymerase (2 U/µl)	0.5 µl
(Betaine (5 M)	10 µl)
Template (10 ng)	1 µl
H_2O	to 50 µl

Phusion PCR program:

Initial Denaturation	30 s	98°C	
Denaturation	10 s	98°C	25-35x
Annealing	30 s	55-65°C	
Extension	30 s/kb	72°C	
Final Extension	10 min	72°C	
Hold	∞	4°C	

4. Taq PCR Mix (20 µl):

Master Mix (2x)	10 µl
Primer forward (10 µM)	1 µl
Primer reverse (10 µM)	1 µl
(Betaine (5 M)	10 µl)
Template (10 pg - 1 µg)	1 µl
H_2O	to 20 µl

Taq PCR program:

Initial Denaturation	4 min	92°C	
Denaturation	1 min	92°C	25-35x
Annealing	1 min	55-65°C	
Extension	1 min/kb	60°C	
Final Extension	10 min	72°C	
Hold	∞	4°C	

2.2.1.11 TOPO TA cloning for sequencing

The TOPO TA Cloning Kit for Sequencing was used to analyze heterogeneous PCR products of the same size or the junctional diversity of various TCR chains. A tailing was performed with Taq Polymerase on a fresh PCR product for 15 min at 72°C in a thermocycler. The A-tailed insert was ligated into the linearized pCR™4-TOPO® vector supplied with the kit together with Salt Solution for 20 min at RT. A transformation of the ligation into chemically competent *E.coli* was performed according to 2.2.1.3, and mini-cultures were prepared (see 2.2.1.4 and 2.2.1.5) to analyze single bacterial clones.

A tailing:

PCR product	7.8 µl
dNTP Mix (10 mM)	0.2 µl
$MgCl_2$ (25 mM)	0.8 µl
Taq Buffer $(NH_4)_2SO_4$ (10x)	1 µl
Taq Polymerase (5U/µl)	0.2 µl

TOPO vector ligation:

PCR product (A tailed)	4 µl
Salt Solution	1 µl
pCR™4-TOPO® vector	1 µl

2.2.1.12 Sequencing

Sanger-based sequencing was performed using the BigDye® Terminator v3.1 CycleSeq Kit and samples were purified and analyzed in a ABI 3100 Sequence Analyzer after PCR.

Sequencing reaction:

Purified DNA/PCR product	3 µl (plasmids: 750 ng)
Primer (10 µM)	0.5 µl
BigDye® Terminator 3.1 Buffer (5x)	0.5 µl
BigDye® Terminator 3.1	1 µl

Sequence PCR program:

Initial Denaturation	30 s	96°C	
Denaturation	10 s	96°C	⎫
Annealing	5 s	50°C	⎬ 25x
Extension	4 min	60°C	⎭
Final Extension	10 min	60°C	
Hold	∞	4°C	

2.2.1.13 Cloning

1. Cotton rat CD1d in pXIg

The cloning of cotton rat CD1d in pXIg was described before [357]. The cotton rat CD1d sequence was determined using the primers crCD1d fwd (nested) and crCD1d rev (nested) in a Platinum® Taq PCR experiment as in 2.2.1.10. The primers crCD1d RACE5' rev and crCD1d

RACE3' fwd were designed using a partial CD1d sequence and were used together with the Gene Racer Primers to amplify the unknown 5' and 3' ends of crCD1d as described in 2.2.1.9. The extracellular domains of crCD1d were subsequently cloned into pXIg to generate a vector expressing a crCD1d-mIgG fusion gene. The primers pXIg 5' MluI fwd and pXIg 3' XhoI rev with cotton rat spleen cDNA were used in a Platinum® Taq HF PCR (see 2.2.1.10) and the restriction enzymes XhoI and MluI were used to digest vector and insert. Ligation of vector and insert was performed according to 2.2.1.2.

2. Cotton rat CD1d in pEGZ

The complete coding sequence of crCD1d was cloned into the pEGZ plasmid using the restriction sites SwaI and BamHI. CD1d was amplified from the plasmid pCDH CMV-MCS-EF1-copGFP crCD1d using the primers crCD1dNcoI fwd and crCD1dBamHI rev in a Phusion PCR (see 2.2.1.10, Annealing 62°C, 30x). The insert was digested with NcoI and BamHi, and the vector pEGZ was digested with EcoRI and BamHI. Vector and insert were ligated according to 2.2.1.2, and the EcoRI restriction site was destroyed during ligation.

3. Cotton rat Vα14Jα18 chain in pEGN

A first partial sequence of cotton rat *AV14*/*TRAC* transcripts of the cotton rat was amplified from cotton rat IHL cDNA with the primers crAV14 fwd and crAC rev in a Platinum® Taq PCR reaction. To determine the 5' and 3' end of the Vα14Jα18 chain RACE-ready cDNA was generated from spleen cDNA and the primers crAV14 RACE5' rev and crAV14 RACE3' fwd were used in a touchdown PCR (2.2.1.9) to determine the 5' and 3' ends. The complete Vα14Jα18 chain transcript was amplified from IHL cDNA with the primers crAV14EcoRI fwd and crAV14BamHI rev in a Phusion PCR (see 2.2.1.10, Annealing 60°C, 40x). The α chain was then cloned into pEGN using EcoRI and BamHI.

4. Cotton rat genomic *AV14* in pEGN

The cotton rat *AV14* gene segment was amplified from cotton rat genomic DNA isolated from the ear using the primers crAV14gDNA EcoRI fwd and crAV14gDNA BamHI rev in a Phusion PCR (see 2.2.1.10, Annealing 64°C, 30 cycles). The *AV14* PCR product was then cloned into pEGN using the restriction sites EcoRI and BamHI (see 2.2.1.2).

5. Cotton rat Vβ8 chain in pS65T

A partial fragment of the *BV8* homolog of the cotton rat was first amplified from cotton rat spleen cDNA with the primers cr1 and cr3 (nested PCR: cr2 and cr4) and RACE primers were designed based on this sequence with subsequent RACE PCRs from RACE-ready spleen cDNA

according to 2.2.1.9. Amplification of the 5' end included a 5' RACE PCR with the primers GeneRacer™ 5' Primer and A2, and a nested PCR with primers GeneRacer™ 5' Nested Primer and A1. The 3' end was determined with a RACE PCR using A3 and GeneRacer™ 3' Primer. Both, 5' and 3' RACE PCR products were analyzed following TOPO TA cloning. The complete coding sequence of cotton rat *BV8* was amplified in a Phusion PCR (see 2.2.1.10, Annealing 64°C, 30 cycles) with the primers A98 introducing a PagI site upstream of the leader sequence and A99 or A100 adding a BamHI site after the end of *BV8*. The reverse primers A99 and A100 are specific for two isoforms of the *TRBV* constant region. The full-length PCR product was ligated into the NcoI and BamHI sites of the vector S65T.

6. Armadillo Vδ2 chains in pMSCV-IRES-mCherry FP

Full-length armadillo Vδ2 chains were amplified and cloned into pMSCV-IRES-mCherry FP (a gift from Dario Vignali, Addgene plasmid #52114) using the In-Fusion® HD Cloning Kit (Takara Bio). The primers A193 and A194 were used for amplification and cloning was performed using the provided protocol.

7. Alpaca BTN3 in pMIG II and phNGFR mCherry

For cloning of vpBTN3 in pMIG II, the coding sequence of alpaca BTN3 was amplified in a Phusion PCR from pEGZ vpBTN3 with the primers 275 and A96 (2.2.1.10, Annealing 64°C, 30 cycles) and the restriction enzyme MfeI was used. The mouse CD3 encoded in the vector pMIG II CD3dgezWT-2A was excised with EcoRI and MfeI and dephosphorylated to prevent religation. Subsequently, alpaca BTN3 was digested with restriction enzymes and inserted into pMIG II as described in 2.2.1.2. Cloning of alpaca BTN3 in phNGFR mCherry was performed using the restriction enzymes MfeI and BglII, and for the amplification of BTN3 from pEGZ vpBTN3, the primers 275 and A97 were used in a Phusion PCR (see 2.2.1.10, Annealing 64°C, 30 cycles). It is important to note that the stop codon of BTN3 needs to be changed to allow expression of a mCherry fusion protein. The vector phNGFR mCherry was digested with EcoRI and BamHI.

8. Alpaca and human BTN3 chimeric molecules in phNGFR mCherry

Two chimeric molecules of vpBTN3 and huBTN3A1, comprised of the human extracellular domains (ED: IgV and IgC) of BTN3A1 and the alpaca intracellular part (ID) downstream of IgC (hu/vpBTN3) or vice versa (vp/huBTN3), were amplified in a two-step PCR experiment. For the first step, the single domains were amplified from the plasmids pEGZ huBTN3A1 and pEGZ vpBTN3.

Two fragments, each amplified in a Phusion PCR (2.2.1.10, Annealing 64°C, 30 cycles) with the primers 200 and 281 (huED) or 282 together with A97 (vpID) were used as templates (1 µl of

each purified PCR product) for the generation of the hu/vpBTN3. This was performed in a second Phusion PCR (Annealing 64°C, 30 cycles) with the primers 200 and A97. The insert thus carried restrictions sites for EcoRI and BglII and was inserted into the EcoRI and BamHI sites of the phNGFR mCherry plasmid.

The second chimeric molecule, vp/huBTN3, was generated using the same strategy. The first two fragments were amplified with the primers 275 and 281 (vpED) or 282 and 129 (huID) in a Phusion PCR (Annealing 64°C, 30 cycles) using the pEGZ huBTN3A1 or pEGZ vpBTN3 as template. The joining of both fragments was achieved in a second Phusion PCR (Annealing 64°C, 30 cycles) with the primers 275 and 129 and the purified fragments as templates. The restriction sites introduced into the vp/huBTN3 insert were MfeI and BglII, using the EcoRI and BamHI sites of the phNGFR mCherry vector for ligation again.

9. Cloning of alpaca Vγ9 TCR chain in pEGZ

A full-length alpaca Vγ9 TCR chain with a CDR3 length of 14aa (Vγ9_14aa) was cloned into the pEGZ vector from the pEGZ vpVγ9 vector [317] and pCR™4-TOPO® clone 19 of 118.7^{+} HMBPP-stimulated cells of animal 1 (see 3.2.2.5) with the CDR3+*TRGJ* region "ALWDARADGRTIKVFGSGTRLIVT". Cloning was performed by L. Starick using the In-Fusion® HD Cloning Kit (Takara Bio). To obtain a full-length Vγ9 sequence, three fragments were amplified in a PCR reaction using CloneAmp HiFi PCR Premix following the provided protocol and using the templates pEGZ vpVγ9 (insert 1 and 3) or pCR™4-TOPO® clone 19 (insert 2). Insert 1 spanned most of Vγ9 and the primers 156 and 157 were used, insert 2 spanned parts of Vγ9, the junctional region and parts of the constant region (primers 158 and 159) and insert 3 comprised the rest of the constant region (primers 160 and 161). The ligation reaction was performed according to the manual using the pEGZ vector pre-cut with EcoRI and BamHI restriction enzymes. The plasmid DNA clone pEGZ vpVγ9_14aa cl.16 was selected for subsequent expression in permanent cell lines.

10. Cloning of alpaca Vδ2Jδ2 TCR chain in pIH

An alpaca Vδ2Jδ2 TCR chain (vpVδ2Jδ2) was cloned into the pIH vector from pIH vpVδ2 cl.8 [317] and pCR™4-TOPO® clone 23 of 118.7^{-} HMBPP-stimulated cells of animal 1 (see 3.2.2.5) with the CDR3+*TRDJ* region "ATHIRVGGRTGDLTAQLIFGKGTQLIVEP". Cloning was performed by L. Starick, and three inserts were amplified from pIH vpVδ2 cl.8 (insert 1 and 3) and pCR™4-TOPO® clone 23 (insert 3) with inserts spanning the Vδ2, junctional and constant region, respectively. The primers used were 162+163 for insert 1, 164+165 for insert 2 and 166+167 for insert 3. Amplification was performed according to the manual of the In-Fusion® HD Cloning Kit (Takara Bio). Ligation of inserts and vector was not performed with the kit, but a full-length

insert was amplified with a second round of PCR with the primers 178 and 179 using all three inserts as templates and EcoRI/BamHI-mediated restriction digestion for ligation into the vector pIH.

2.2.1.14 Single-cell PCR

Single-cell PCR amplifications were performed by L. Starick according to a protocol described before [358, 359]. Alpaca PBMCs were stained with 118.7 mAb specific for alpaca Vδ2/Jδ4 TCR chains and detected with the secondary antibody DαM R-PE (1 µg/ml, Jackson ImmunoResearch). Cell viability was measured by using the Fixable Viability Dye eFluor® 660 (1:1000, eBioscience). The cells were single-cell sorted for 118.7 expression on a FACSAria III cell sorter by L. Starick or C. Linden. Single-cells were sorted into 96 well plates (twin tec, #0030133.404, Eppendorf) containing 6 µl 1x PBS, sealed with adhesive plate seals and frozen at -80°C. Cell lysis was mediated by freezing and heating to 65°C for 2 min. The cells were placed on ice, and combined cDNA synthesis and amplification of Vγ9 and Vδ2 transcripts was performed with the OneStep RT-PCR Kit (Qiagen). The reagents were prepared as a master mix and added to the wells already containing RNA in 6 µl 1x PBS.

OneStep reaction Mix:

5x Buffer	5 µl
dNTP Mix (10 mM)	1 µl
Primer A173 (*TRGV9* fwd)	1 µl
Primer A174 (*TRGC* rev)	1 µl
Primer A175 (*TRDV2* fwd)	1 µl
Primer A176 (*TRDC* rev)	1 µl
Enzyme Mix	1 µl
RNA in 1x PBS	6 µl
H_2O	8 µl

cDNA synthesis	30 min	50°C	
Initial Denaturation	15 min	95°C	
Denaturation	30 s	94°C	30-35x
Annealing	30 s	60°C	
Extension	1 min	72°C	
Final Extension	10 min	72°C	
Hold	∞	4°C	

A second round of PCR amplifications was performed using the PCR product of the OneStep RT-PCR reaction (1:10 dilution). The AmpliTaq Gold™ DNA Polymerase (Applied Biosystems) was used for second round PCR. Here, two separate PCR reaction were performed per RNA sample for amplification of *TRGV9*/*TRGC* (Primers A173 + A174) or *TRDV2*/*TRDC* (Primers: A175 + A176), respectively.

AmpliTaq Gold PCR Mix:

10x PCR Buffer II	4 µl
$MgCl_2$ (25 mM)	2.4 µl
dNTP Mix (10 mM)	1 µl
Primer forward (10 µM)	1.2 µl
Primer reverse (10 µM)	1.2 µl
AmpliTaq Gold (5 U/µl)	0.2 µl
Template (1:10 diluted)	5 µl
H_2O	to 40 µl

AmpliTaq Gold PCR program:

Initial Denaturation	10 min	95°C	
Denaturation	30 s	94°C	30x
Annealing	1 min	63°C	
Extension	45 s	72°C	
Final Extension	7 min	72°C	
Hold	∞	4°C	

The PCR products were analyzed on a 1% agarose gel and purified with the PCR purification kit (Qiagen). Subsequent sequencing was performed according to chapter 2.2.1.12 using the primers applied in the PCR amplifications.

2.2.2 Protein biochemistry

2.2.2.1 SDS-PAGE

SDS-Polyacrylamide gel electrophoresis (SDS-PAGE) was used to separate proteins in an electric field according to their respective molecular weights. The sample originating from either purified protein solutions or cell culture supernatant was incubated for 5 min at 100°C with reducing loading buffer. The running (12%) and stacking gel (3%) were cast between two glass plates in a BioRad gel caster. Voltage was applied at 120 V during electrophoresis, and proteins were stained for 3 h in SDS-PAGE staining solution and destained with SDS-PAGE destaining solution overnight.

Running Gel (5 ml):

AA/Bis-AA	2 ml
1.5 M Tris (pH 8.8)	1.25 ml
10% SDS	50 µl
ddH2O	1.675 ml
TEMED	5 µl
10% APS	25 µl

Stacking Gel (3 ml):

AA/Bis-AA	390 µl
1 M Tris (pH 6.8)	375 µl
10% SDS	30 µl
ddH2O	1.85 ml
TEMED	7 µl
10% APS	20 µl

2.2.2.2 ELISA

2.2.2.2.1 Cotton rat IFN-γ ELISA

The cotton rat IFN-γ ELISA assay was performed in a 96 well plate according to the protocol provided by R&D Systems. Supernatants of primary cell stimulations were used, and 50 µl of the sample were added undiluted or in 5-/25-fold dilutions. A recombinant IFN-γ standard starting with a high concentration of 8000 pg/ml (1:2 dilutions) was used, and a five-parameter standard curve was calculated with the Magellan program.

2.2.2.2.2 Cotton rat IL-4 ELISA

The cotton rat IL-4 ELISA experiment followed the protocol provided by the R&D systems, and 50 µl sample was used undiluted or 5-/25-fold diluted. A five-parameter standard curve was calculated with the Magellan program.

2.2.2.2.3 Mouse IL-2 ELISA

Determination of mouse IL-2 concentrations in cell culture supernatants was achieved using a mouse IL-2 sandwich ELISA. Here, either the BD OptEIA™ Mouse IL-2 ELISA Set (BD) was used together with the BD OptEIA™ TMB Substrate Reagent Set (BD) or the Mouse IL-2 Uncoated ELISA Kit (Invitrogen) was used following the manual. Optic densities (ODs) were then measured at 450 nm in a Vmax Kinetic Microplate Reader.

2.2.2.2.4 Mouse IgG1 ELISA

Mouse IgG1 in cell culture supernatants or cell lysates was measured using the Mouse IgG1 ELISA Quantitation Set and the BD OptEIA™ TMB Substrate Reagent Set according to the enclosed protocols. The plates were subsequently measured at 450 nm in a Vmax Kinetic Microplate Reader.

2.2.3 Cell biology

2.2.3.1 Routine cell culture

Cell lines were cultured under sterile conditions in incubators providing a temperature of 37°C with 5% CO_2, and an H_2O saturated atmosphere. Suspension cells were kept in RPMI++ medium and adherent cells in RPMI++ (L929 and CHO cell lines), DMEM+ (293T cell lines) or DMEM+ without Pen/Strep (LGK-1-R). For the passaging of adherent cells, ATV was used as a detaching agent. Cell numbers were determined by counting of cells in a hemocytometer using a 1:2 or 1:10 ratio of cell suspension to trypan blue (10% solution).

2.2.3.2 Freezing and thawing of cell lines

To freeze cells, the cell suspension (1-5*10^6 cells) was centrifuged with 346-461 x g (1600 rpm) for 5 min, and the supernatant was aspirated completely. The cells were resuspended in 1 ml freezing medium (50% FCS, 40% RPMI, 10% DMSO), transferred to a cryogenic vial and frozen immediately at -80°C. PBMCs were frozen in an isopropanol chamber at -80°C.

Cells were thawed as quickly as possible in their respective culture medium. The cells were washed in cell culture medium for 5 min at 346-461 x g (1600 rpm) prior to plating. The cell pellet was resuspended in the medium of choice and plated in a suitable plate or flask.

2.2.3.3 Isolation of primary cells from different tissues

For the isolation of primary cells from different tissues, organs were prepared after the sacrifice of the animal and kept in DPBS 0.1% FCS on ice until further use. Usually the spleen, thymus and lymph nodes were taken. The organs were rubbed through a 100 µm cell strainer in a petri dish, and the cell suspension was transferred to a suitable vessel for centrifugation which was carried out at 300 rcf for 10 min at RT. The cell pellet was subsequently washed twice with DPBS 0.1% FCS. Afterward, the cells were resuspended in DPBS 0.1% FCS and counted.

2.2.3.4 Isolation of intrahepatic lymphocytes

This protocol for the isolation of IHLs from cotton rat livers was adapted from the protocol for the isolation of mouse and rat IHLs described by Monzon-Casanova in 2010 [148]. A few alterations were made due to the availability of certain reagents and utensils.

After the excision of other organs like the spleen or the thymus, a 5 ml syringe was used to draw as much blood as possible from the heart to reduce the blood flowing in the animal. Following this, the heart was punctured several times, and the liver was perfused using a 60 ml syringe and a 20-gauge needle filled with DPBS 0.1% FCS. The syringe was inserted into the portal vein, and the liver was flushed until it appeared pale. The organ was removed and kept at 4°C in DPBS 0.1% FCS until further use. The liver was then cut into small pieces and homogenized in a 15 ml glass homogenizer. The resulting homogenate was passed through a 100 µm cell strainer in a 50 ml falcon and filled up to 50 ml with DPBS 0.1% FCS. The suspension was centrifuged at 300 x g (1200 rpm) at RT for 10 min. A 90% Percoll solution was prepared with 10x DPBS. The pellet containing the cells was resuspended in 16.8 ml RPMI 5% FCS and 11.2 ml 90% Percoll solution which resulted in a Percoll concentration of 36%. The cell suspension was layered over a 72% Percoll solution prepared with 10 ml 90% Percoll solution and 2.5 ml RPMI 5% FCS. Centrifugation was carried out at 2440 rcf with no brakes for 20 min at RT. The top layer containing tissue debris was removed using a Pasteur pipette or vacuum. The lymphocytes were harvested from the interphase, transferred in a 50 ml tube, the tube was filled with RPMI 5% FCS to wash the cells and centrifuged with 300 rcf for 10 min at RT. The cell pellet was washed twice more, resuspended in RPMI 5% FCS, counted, and kept on ice until further use.

2.2.3.5 Isolation of peripheral blood monocytic cells (PBMCs)

Peripheral blood monocytic cells were isolated from alpaca blood samples kindly provided by Prof. Dr. Thomas Göbel (Institute for Animal Physiology, Ludwig-Maximilians-Universität, Munich). Blood samples were shipped at RT in EDTA and processed as soon as possible. Blood was layered over Histopaque® with a density of 1.077 g/ml in a 50 ml falcon tube and the gradient was centrifuged at 400 x g (1491 rpm) for 30 min. PBMCs were carefully aspirated from the interphase of the gradient and washed three times at 461 x g (1600 rpm) for 5 min with 15 ml PBS. Counting and freezing of cells were carried out as described in 2.2.3.1 and 2.2.3.2.

2.2.3.6 Retroviral transfection and transduction of cell lines

Stable overexpression of molecules in eukaryotic cells was achieved via infection with viral supernatants obtained from calcium-phosphate-mediated transfection of 293T cells using a transient three-plasmid expression system [340].

Day 1: Plating of $1.5*10^6$ 293T cells in transfection medium using a 6 cm tissue culture petri dish.

Day 2: The medium was exchanged with 4 ml DMEM+ medium (37°C) and incubated for 1 h. Three plasmids (pVSV-G, pHIT60, and expression plasmid) were used at 5 µg each for transfection of 293T cells, and 62 µl $CaCl_2$ (2 M) was added to the DNA-mix. The sample was filled to 500 µl with sterile H_2O and 500 µl 2x HBS were added to a second sterile reaction tube. The DNA-mix was added dropwise to the 2x HBS, mixed on a vortex device and the mixture was incubated for 15 min at RT. The precipitation mix was then dropped carefully to the 293T cells in DMEM+ medium and incubated for 6-8 h at 37°C. The medium was exchanged after the incubation period with prewarmed Transfection medium.

Day 3: The medium was exchanged with 5 ml Transfection medium with 10 mM sodium butyrate prewarmed to 37°C. After 6-7 h the medium was aspirated and 5 ml prewarmed Transfection medium were added.

Day 4: Infection was performed with $1*10^5$ target cells and 3 ml viral supernatant (45 µm syringe filter) was added. Polybrene at a concentration of 4 µg/ml was used to increase transduction efficiency, and the mixture was centrifuged with 871 x g (2200 rpm) for 3 h at 32°C. The supernatant was aspirated, and the infected cells were plated in the appropriate cell culture medium.

2.2.3.7 Stimulation assays

1. CD1d antigen presentation [169]

To analyze the antigen-presenting capacities of CD1d dimers, 4 µg/ml CD1d dimers were diluted in PBS with 4 µg/ml anti-rat CD28 mAb JJ319 (Exbio). Antigen-loaded CD1d dimers were combined with vehicle-loaded dimers to reach 4 µg/ml. The combinations of PBS57 dimers/DMSO dimers were the following: 4/0, 2/2, 1/3, 0.5/3.5, 0.25/3.75, 0.125/3.875 and 0/4 µg/ml. The positive control for this assay comprised an anti-mouse CD3ε antibody (BD Pharmingen) together with JJ319, both at 4 µg/ml. These dilutions at 50 µl per well were added to 96 well U-bottom suspension culture plates and incubated at 4°C overnight. After washing with PBS (3x), $5*10^4$ mouse T cell hybridoma cells expressing a rat iNKT TCR (BW rat S6 93A) were added to each well in RPMI++ medium. The stimulation assay was incubated at 37°C, 5% CO_2 for 22 h. The supernatants were analyzed with a mouse IL-2 ELISA (BD) as described in 2.2.2.2.3.

2. Stimulation of cotton rat primary cells

Primary cotton rat splenocytes were harvested according to 2.2.3.3, and $1*10^6$ cells per well were plated in 96 well plates (round bottom) using RPMI++ (cotton rat). The antigens αGC/KRN7000 (Enzo Life Sciences, 50 µg/ml) or PBS57 ([187],50 µg/ml) were used in 10-fold dilutions from 100 ng/ml to 0.1 ng/ml and Concanavalin A served as a positive control at 2 µg/ml. The cells were cultured for 24 h at 37°C, 5% CO_2 and supernatants were analyzed with cotton rat IFN-γ and IL-4 ELISA as described in 2.2.2.2.1 and 2.2.2.2.2.

3. Stimulation of permanent cell lines

TCR transductants or T cell hybridomas growing as permanent cell lines were stimulated using APCs and a murine responder cell line transduced with TCR chains, together with different stimulating agents. The read-out of those stimulations was the amount of mIL-2 produced by the mouse responder cells and detected in the cell culture supernatant. If adherent APCs were used, $1*10^4$ cells per well were plated in 50 µl cell culture medium in 96 well flat bottom TC plates and incubated overnight. Suspension APCs or responder cells ($5*10^4$) were added on the next day in 50 µl cell culture medium. Stimulating agents like antigens or agonistic antibodies were prepared 2x concentrated, and 100 µl of the dilutions were added to the APC-responder cell mixture. Incubation time of stimulation plates was 24 h and supernatants were tested with a mIL2-ELISA as described in 2.2.2.2.3 using appropriate dilutions. The same approach was used for stimulations with plate-bound anti-mCD3 antibody.

4. Stimulation of PBMCs

Peripheral blood mononuclear cells were isolated from blood samples as described in 2.2.3.5. These cells were then stimulated with HMBPP in the presence of hIL-2 (Novartis Pharma) for seven/eight days. One type of stimulation required the seeding of $1*10^5$ PBMCs in 200 µl RPMI++ medium in a 96 well flat bottom suspension culture plate with the desired amount of hIL-2 (usually 50 U/ml) and HMBPP. The second assay was performed using $3*10^5$ cells cultured in 1 ml of RPMI++ in a 48 well tissue culture plate with the appropriate stimuli. The PBMCs were tested on day 7/8 in a flow cytometry experiment (see 2.2.3.8) and in some cases sorted on $118.7^{+/-}$ cells as described in 2.2.3.9.

2.2.3.8 Flow cytometry

Flow cytometry was performed on a FACSCalibur flow cytometer and data was analyzed with the FlowJo software. Usually, $1*10^5$ cells were used for each sample and kept in Flow cytometry buffer during staining and acquisition of samples. Centrifugation was carried out at 755 x g (2000 rpm) for 5 min at 4°C. Stainings with multiple antibodies were usually performed in the following order: 1. unconjugated primary antibody, 2. secondary antibody, 3. blocking of secondary antibody with NmIg (mouse serum IgG), 4. fluorochrome-labeled/Fab fragment-labeled antibody and biotinylated antibody, 6. fluorochrome-labeled streptavidin, 7. Intracellular staining. Extracellular stainings with antibodies were incubated for 15-30 min at 4°C and CD1d dimer stainings for 30 min at RT. Fab fragments (Jackson ImmunoResearch) were incubated with purified antibodies prior to stainings for 30 min at RT following the enclosed protocol. Intracellular stainings were carried out using the Foxp3/Transcription Factor Staining Buffer Set following the manual.

2.2.3.9 Cell sorting

Fluorescence-activated cell sorting (FACS) was performed on a FACSAria™ III cell sorter by C. Linden or L. Starick. Transduced cells were sorted using either the fluorescence emitted by vectors, e.g., GFP or mCherry, or antibodies specific for the desired surface molecule. Staining of cells prior to FACS was performed according to 2.2.3.8 and cells were kept in Flow cytometry buffer. After sorting the cells were washed with the appropriate cell culture medium and cultivated or used directly for downstream experiments such as RNA isolation and cDNA synthesis.

2.2.4 Production of crCD1d-mIgG fusion proteins

2.2.4.1 Electroporation and selection of dimer-producing cells

To produce crCD1d-mIgG fusion proteins, the pXIg vector containing the extracellular domains of CD1d was transfected into J558L cells, which express a λ immunoglobulin light chain but no heavy chain [343]. These cells can produce high levels of Ig-like proteins after electroporation with plasmids containing the relevant genes [343]. Electroporation was carried out using the Gene Pulser® II system. Ten million cells were mixed with 10 µg pXIg crCD1d in 200 µl PBS and incubated for 10 min on ice in an electroporation cuvette (0.4 cm) and subsequently overlaid with 600 µl PBS. The cuvette was reused and cleaned with distilled water and ethanol under sterile conditions, followed by UV sterilization for 30 min. The electroporation was carried out at 280 V, 950 µF, 0.5-1 kV for 13.9 ms. The suspension was incubated on ice for 20 min, washed with RPMI++ and cultured in 24 fractions at 1 ml each. After 24 h, 1 mg/ml G418 was added to select cells positive for pXIg crCD1d. Following G418 selection, the supernatants of different fractions were tested with a mouse IgG1 ELISA (2.2.2.2.4) in 5-fold dilutions, and the clones with the highest IgG1 production were selected.

2.2.4.2 Purification of crCD1d dimers

After selecting one or more suitable clones according to 2.2.4.1, the transduced J558L cell culture was grown in roller bottles until the cells reached high densities in 1.5 l ISF-1 medium containing 10 mM HEPES and 1 mg/ml G418. The cell suspension was subsequently centrifuged at 3175 x g (4200 rpm) at 4°C for 30 min, and the supernatant was passed through a folded filter and a 20 µm bottle-top filter. Additionally, NaN_3 was added at a final concentration of 0.05%, and the mIgG1 fusion proteins were purified from the cell culture supernatant using Protein G Sepharose.

<u>Protein purification with Protein G Sepharose</u>

Poly-Prep columns (9 cm) with 1 ml Protein G Sepharose were stored with an additional 8 ml of storage buffer (PBS 0.09% NaN_3) at 4°C. Before use, 10 ml Diethylamine (50 mM, pH 11) followed by 10 ml PBS were applied to the column to wash away residual proteins. The cell culture supernatant was added to the Poly-Prep columns at a rate of 1 ml/min at 4°C. The loaded columns were then washed with 15 ml PBS and 8 ml PBS 1 M NaCl and the dimers bound to Protein G were eluted with 5 ml Diethylamine (50 mM, pH 11). Six fractions of 1 ml were collected in tubes containing 62 µl Tris (2 M, pH 6). The Poly-Prep column was then washed with 20 ml PBS and stored at 4°C with storage buffer. To maximize the yield, the procedure

was repeated, and the protein content of the six fractions was tested via SDS-PAGE and 0.02% NaN_3 was added for prolonged storage. Selected fractions were then concentrated and rebuffered into PBS using the Vivaspin 20 50.000 MW columns according to the provided manual. The protein concentration was measured with spectrophotometric methods using the NanoDrop 2000c (IgG1) and verified with SDS-PAGE. For storage, dimer solutions were always mixed with NaN_3 at a final concentration of 0.02%.

2.2.4.3 Antigen loading of crCD1d dimers

Purified mouse, rat or human CD1d dimers were loaded with αGC/KRN7000 at a concentration of 250 µg/ml and a 40x molar excess of lipid antigen at 37°C for 24 h in PBS 0.05% Triton X-100. Cotton rat dimers were loaded with αGC/KRN7000 without Triton X-100. All dimers were loaded with PBS57 in the absence of Triton X-100.

2.2.5 Hybridoma Development

2.2.5.1 Immunization of BALB/c mice

Immunizations of female BALB/c mice at 12 weeks of age to induce an immune response and the generation of plasma cells against a specific surface molecule were performed intraperitoneally (i.p.) once per week for five successive weeks with $10*10^6$ cells overexpressing the target molecule. After three weeks an intravenous (i.v.) boost with $5*10^6$ cells per mouse was carried out three days prior to the PEG-mediated fusion.

2.2.5.2 PEG-mediated cell fusion and HAT-mediated selection

Hybridoma cell lines were generated from the PEG-mediated fusion of SP2/0 cells with spleen cells from BALB/c mice. SP2/0 cells were thawed at least one week before fusion and grown in RPMI++ medium.

Day 1: SP2/0 cells were washed three times in 10 ml serum-free RPMI 1640, resuspended in 10 ml serum-free RPMI and counted. One immunized BALB/c mouse, three days post i.v. boost was sacrificed, blood was drawn from the heart, and the spleen was excised and kept on ice in a plate filled with BSS. The blood was centrifuged at 17949 x g (13000 rpm) for 2 min, and serum was frozen at -20°C. The spleen was passed through a 70 µM nylon mesh with a syringe plunger, and spleen cells were transferred into a 50 ml falcon tube. The tube was filled with

BSS, centrifuged at 461 x g (1600 rpm) for 5 min, and the cells were washed twice more with serum-free RPMI. The cells were then resuspended in 10 ml serum-free RPMI and counted. SP2/0 cells and spleen cells were mixed at a 1:5 (SP2/0: splenocytes) ratio and washed with serum-free medium. The supernatant was aspirated entirely, and the cell pellet was loosened carefully. While holding the tube containing the cells in the water bath heated to 37°C, 1 ml prewarmed PEG 1500 per $1*10^8$ spleen cells was added to the cells over the course of 1 min under constant stirring. In the same manner, 5 ml of prewarmed serum-free RPMI were added (1 ml/min) followed by 10 ml serum-free RPMI (2 ml/min). Slowly, 30 ml of RPMI++ were added to the mixture, and the fusion mix was incubated in the water bath for 30 min. The fused cells were pelleted at 461 x g (1600 rpm) for 5 min and carefully resuspended in Bulk fusion medium ($2.5*10^6$ cells/ml or 50 ml per $1*10^8$ spleen cells) and incubated in 250 ml tissue culture flasks (50 ml per bottle) overnight.

Day 2: The fused cells were aspirated from the tissue culture flasks and centrifuged at 461 x g (1600 rpm) for 5 min. The cell pellet was carefully dissolved in HAT medium (1x) containing rhIL-6 (final concentration 1 ng/ml, 130 ml per $1*10^8$ spleen cells) and carefully plated in 96 well plates (flat bottom, cell suspension). Two drops were pipetted with a 10 ml pipette per well which amounts to roughly 125 µl.

Day 5-x: As needed and depending on the density of cells in the 96 well plates and the color of the cell culture medium, the HAT medium was aspirated partially, and fresh HAT medium (1x) was added dropwise to the plates.

The fused cells under HAT selection were observed daily, and supernatants were tested as soon as the medium in the wells turned yellow and clones were visible. Clones usually grew up starting at week two after HAT selection. Screening for positive antibody-producing hybridomas was performed using flow cytometry. The supernatants (50 µl) were used to stain cell lines overexpressing the target molecule mixed with non-transduced cells, and DαM R-PE was used to detect potential specific immunoglobulins (see 2.2.3.8). Positive hybridomas were transferred to 48 well plates, further cultivated in HT medium and later in RPMI++ or ISF-1, frozen and subjected to single-cell dilutions. Single-cell clones of positive hybridomas were tested for their antibody production after removing HT or rhIL-6, and antibodies were purified from cell culture supernatants.

2.2.5.3 Purification of monoclonal antibodies (mAbs)

For antibody purification, single-cell clones of hybridomas were grown at high densities in RPMI++ medium with 5% FCS or ISF-1 medium. Hybridomas that could be grown in ISF-1 medium without losing their ability to produce antibody were scaled up to a 1 l culture in a roller bottle and supernatants were spun down at 3175 x g (4200 rpm) for 30 min at 4°C. The supernatant was filtered through a folded filter and a 20 µM bottle top filter. The protein was purified from the prepared supernatant using Protein G Sepharose™ 4 Fast Flow for mIgG1 and Protein A Sepharose® 4B conjugate for IgG2a/b. Hybridomas that could not be grown successfully in ISF-1 medium were grown in RPMI+ 5% FCS and the culture was scaled up to 1 l in a roller bottle. Supernatants were prepared the same way as for ISF-1 and subjected to a protein precipitation step to remove FCS or directly purified.

Ammonium sulfate precipitation

The filtered supernatant was mixed slowly under constant stirring with 33.3% ammonium sulfate solution with 500 ml saturated ammonium sulfate solution per 1 l supernatant. This step was necessary to remove non-Ig proteins from the supernatant. The mixture was incubated overnight at 4°C under constant stirring and centrifuged at 3175 x g (4200 rpm) for 30 min at 4°C to pellet and remove the FCS from the culture supernatant. The supernatant was again mixed with 500 ml ammonium sulfate, now approximately 50%, and incubated overnight at 4°C. The mixture was centrifuged again, and the pellet containing the precipitated antibodies was dissolved in a small volume of 0.1 M Tris-HCl buffer for mIgG2a/b, high salt buffer for mIgG1 (Protein A) or PBS for mIgG1 (Protein G). The suspension was filled in dialysis tubes and dialyzed with H_2O as a buffer solution for 4 h and with 0.1 M Tris-HCl, high salt buffer or PBS overnight. The dialysis tubes (Roth) were boiled for 5 min in 0.02 M EDTA, washed twice with PBS and stored at 4°C in PBS. The dialysis was repeated twice on day 2 with 0.1 M Tris-HCl buffer and for 4 h on day 3 with Tris-HCl. The rebuffered sample was then collected and centrifuged at 4°C with 17548 x g (12000 rpm) for 10 min. The supernatant was transferred to a new falcon tube and filtered with a 0.2 µm sterile filter. The concentrated antibody solution was stored at 4°C until the antibodies were purified from the solution with Protein G or A Sepharose.

Protein A Sepharose

Poly-Prep columns with 1 ml Protein A Sepharose® 4B conjugate were equilibrated with 20 ml 0.1 M Tris-HCl for mIgG2a/b or high salt buffer for mIgG1; the filtered supernatant was drained through the column at 0.5 ml/min and retained. The Poly-Prep column now loaded with antibodies was washed once with 15 ml Tris-HCl and eluted with 5 ml elution buffer

(Protein A). Fractions of 500 µl were collected in tubes containing 50 µl Triethanolamine (1 M, pH 8) to neutralize the elution buffer and tested with a Bradford Protein Assay. For this, 90 µl test reagent was added to a 96 well plate containing 10 µl of each fraction and blue color indicated protein in the solution. The fractions with the highest protein concentrations were combined and rebuffered in PBS using the Vivaspin 20 50.000 MW columns according to the provided manual, and NaN_3 (0.02%) was added. Protein concentrations were determined with a spectrophotometric measurement.

Protein G Sepharose

Purification of mIgG1 with Protein G Sepharose™ 4 Fast Flow was carried out according to 2.2.4.2 except for the elution step from the Poly-Prep column. Here, the antibodies were eluted from the column with 5 ml elution buffer (Protein G) and 500 µl fractions were collected in tubes containing 32 µl Tris (2 M, pH 6). The fractions were not tested with SDS-PAGE but with a Bradford Protein assay and rebuffered as described for Protein A Sepharose.

2.2.6 Data analysis and statistical interpretation

Sequence data were analyzed using Chromas Lite 2.1.1 for AB1 files, Clustal Omega for DNA and protein alignments and NCBI Basic Local Alignment Search Tool (BLAST) for alignment calculations and database analysis. Sequence alignments were modified with BioEdit and color-coded with the default settings of the program. Ensembl and IMGT databases were used as resources for sequence data and homology analysis. The program SerialCloner 2.6.1 was applied for cloning and restriction site analysis and FlowJo 7.6.5 and 8.8.7 for analysis of flow cytometry data. Statistical analysis was carried out using Graph Pad Prism.

3 Results

The thesis "Alpaca, armadillo and cotton rat as new animal models for non-conventional T cells: Identification of cell populations and analysis of antigen receptors and ligands" is divided into two projects. The first one describes the newly identified CD1d/iNKT cell system in cotton rats (*Sigmodon hispidus*) and has previously been published [169]. The second project focuses on the coevolution of Vγ9Vδ2 T cells with BTN3 in two non-primate candidate species. The first part describes the armadillo (*Dasypus novemcinctus*) as a witness for the coevolution of Vγ9Vδ2 T cell together with BTN3 molecules. The second part introduces the alpaca (*Vicugna pacos*) as a non-primate species with a functional BTN3 molecule and a Vγ9Vδ2 T cell subset.

3.1 The CD1d/iNKT cell system in cotton rats

An important subset of adaptive cells bridging the innate and adaptive immune system are invariant natural killer T cells. The hallmark of this cell subset is the rapid recognition of glycolipid antigens presented by the MHC I like molecule CD1d [157]. The existence of a functional subset of iNKT cells and the antigen-presenting molecule CD1d was studied in the cotton rat, a model organism for infections with measles virus and human RSV. The results of this study and proof of functional homologous molecules for CD1d and the iNKT cell α chain in the cotton rat has been published [169]. The figures and figure legends first published in the article "Function and expression of CD1d and invariant natural killer T-cell receptor in the cotton rat (*Sigmodon hispidus*)" by Fichtner et al. are printed under a license agreement with the publisher John Wiley and Sons.

3.1.1 The antigen-presenting molecule CD1d is conserved in cotton rats

3.1.1.1 The CD1d homolog in cotton rats

Before this study, a complete gene homologous to rat (rCD1d) and mouse CD1d (mCD1d) has been amplified from cotton rat spleen cDNA [169, 357]. This cotton rat CD1d-like molecule (crCD1d) was compared to the corresponding mRNA and amino acid sequences of Chinese hamster (*Cricetulus griseus*), rat (*Rattus norvegicus*) and mouse (*Mus musculus*) in **Figure 3.1**.

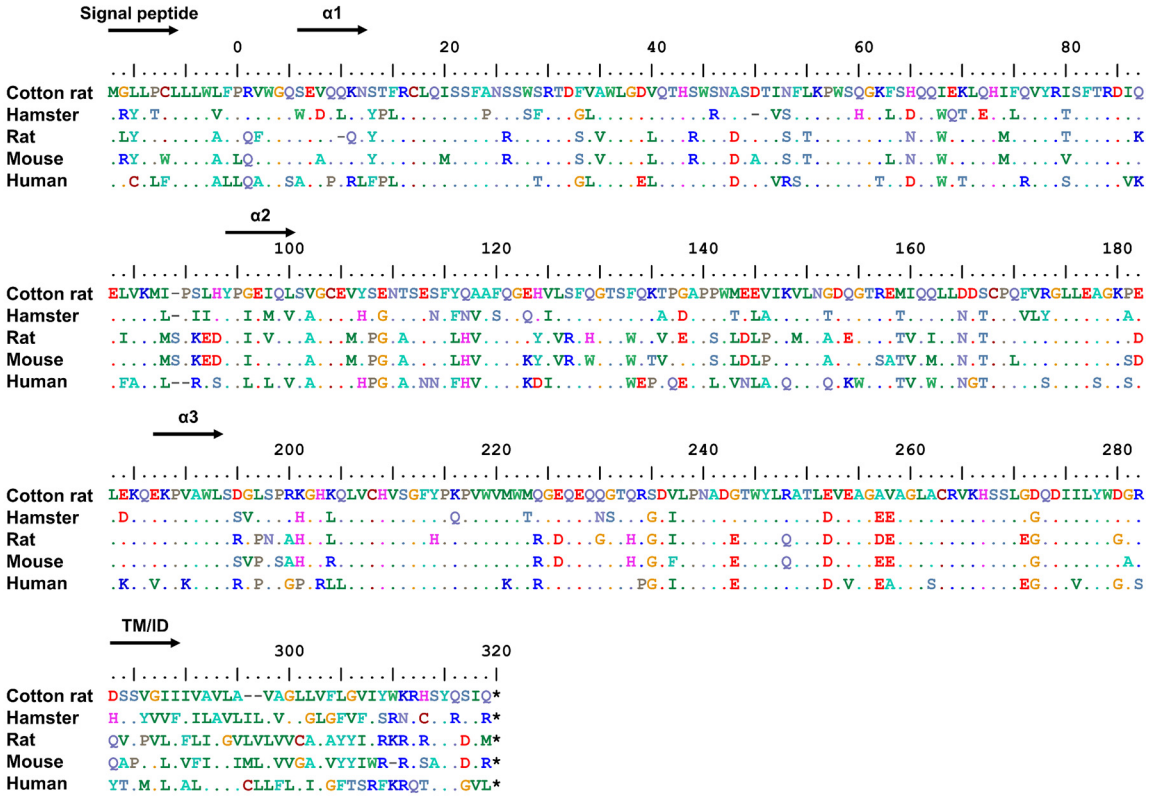

Figure 3.1 CD1d is conserved in different species. Cotton rat CD1d (GenBank: KM_267558) was compared to chinese hamster (GenBank: XM_007644702.1), rat (GenBank: KM_267558), mouse (GenBank: NM_007639.3) and human CD1d (GenBank: NM_001766.3). The alignment was calculated with Clustal Omega. Identical amino acids (dots), gaps (dashes) and stop codons (*) are indicated. The different regions are depicted in this order: signal peptide, extracellular regions α1, α2, α3 and transmembrane/intracellular regions (TM/ID). Figure and figure legend adapted from [169].

The conservation of the CD1d protein sequence among the analyzed species varied with their evolutionary proximity and in the domains of this molecule (**Figure 3.1**). Higher conservation was observed in the extracellular domains α1-3 which are essential for the recognition of iNKT cell antigens. The transmembrane and intracellular parts of CD1d were less alike among the considered animals. Sequence identities were calculated manually to analyze the conservation of all domains of CD1d between cotton rat and hamster, rat, mouse and human. For this, the number of identical amino acids or nucleotides was divided by the total length of the alignment and identities were given as rounded percentages.

Table 3.1 Extracellular domains of CD1d share higher conservation among species. Identical nucleotides or amino acids of CD1d sequences were counted, and the overall identity was calculated as the ratio of identical nucleotides/amino acids to the length of the alignment, therefore including gaps, and are given in rounded percentages. Figure and figure legend adapted from [169].

Cotton rat CD1d to	CD1d		α1-α3		Signal peptide		α1/α2/α3		TM/ID	
	% NT	% AA	% NT	% AA	% NT	% AA	% NT	% AA	% NT	%AA
Hamster	80	**71**	83	**76**	78	**78**	82/81/85	**71/71/85**	58	**32**
Rat	76	**69**	80	**74**	80	**72**	83/76/82	**77/67/78**	43	**30**
Mouse	78	**69**	81	**74**	78	**67**	84/76/84	**76/65/80**	50	**28**
Human	73	**62**	76	**66**	63	**50**	78/71/78	**67/57/74**	53	**32**

Closer inspection of nucleotide and amino acid identities in **Table 3.1** confirm the correlation of evolutionary relationship and conservation of CD1d on the nucleotide and amino acid level. Cotton rat CD1d shares the highest identities with Chinese hamster, being 71% of the whole amino acid sequence and 80% of the complete coding mRNA sequence. The complete CD1d sequences of human and cotton rat still share 62% identical amino acids and 73% nucleotides. The extracellular domain α1 of cotton rat CD1d is more similar to rat and mouse than to hamster CD1d α1. The most conserved domain of CD1d is the extracellular domain α3 with amino acid identities of 74%-85% among all species considered here. In contrast to this, the transmembrane and intracellular domains are relatively diverse.

3.1.1.2 Cross-reactivity of mAbs with cotton rat CD1d

Due to a lack of reagents applicable for the study of cotton rat CD1d, cross-reactivity of available monoclonal CD1d antibodies to crCD1d was analyzed. For this purpose, the two mouse anti-rat mAbs WTH-1 and WTH-2 and the rat anti-mouse mAb 1B1 were used to stain crCD1d [183, 355, 356]. The WTH-1 and WTH-2 antibodies originate from B cell hybridomas of BABL/c CD1d$^{-/-}$ mice immunized with M12.4.1.C3 cells transduced with the F344 rat CD1d allele [356] and a similar avidity to mouse and rat CD1d has been shown [355]. The 1B1 mAb, however, is not cross-reactive to rat CD1d [183].

Comparison of the staining differences mAbs on cotton rat CD1d was achieved using Raji cells overexpressing CD1d molecules. Cotton rat CD1d was cloned into the vector pEGZ as described in chapter 2.2.1.13 and overexpressed in Raji cells according to chapter 2.2.3.6. The vector pEGZ contains an enhanced GFP (EGFP) gene downstream of an internal ribosomal entry site (IRES) rendering it possible to correlate GFP expression with expression of the transduced molecule. Therefore, Raji crCD1d cells were sorted on the highest EGFP fluorescence (see 2.2.3.9). Raji cells overexpressing mouse and rat CD1d were available [156, 355]. The biotinylated antibodies WTH-1 and WTH-2 and 1B1 PE were used in saturating concentrations

to stain Raji rCD1d, mCD1d or crCD1d and WTH-1 and WTH-2 were detected with streptavidin-allophycocyanin (SA-APC) in a flow cytometry staining as described in chapter 2.2.3.8. Representative stainings of Raji cells overexpressing rat, mouse or cotton rat CD1d and similar EGFP expression are depicted in **Figure 3.2**.

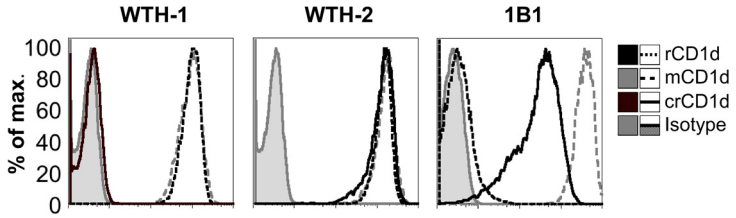

Figure 3.2 WTH-2 and 1B1 but not WTH-1 monoclonal CD1d antibodies are cross-reactive to cotton rat CD1d. Representative data of one out of two experiments in total are shown. The biotinylated monoclonal mouse anti-rat antibodies WTH-1 and WTH-2 (each 125 ng/ml), detected with SA-APC (400 ng/ml, BD Pharmingen), and rat anti-mouse 1B1 PE (2 µg/ml, Affymetrix) were applied to stain Raji cells overexpressing rat, mouse or cotton rat CD1d. Staining intensities are compared to isotype controls. Figure and figure legend adapted from [169].

WTH-1 readily detected mouse and rat CD1d molecules overexpressed on the cell surface of Raji cells with the same fluorescence intensity, whereas cotton rat CD1d was not stained by this mAb (**Figure 3.2**). However, the WTH-2 antibody stains the CD1d molecules of all three species in an equal fashion and can therefore be considered a cross-reactive with cotton rat CD1d. This similar staining was verified for lower, non-saturating conditions (data not shown). 1B1, the last antibody tested, was not able to recognize rat CD1d and stained cotton rat CD1d with much lower intensity (~15x) compared to mouse CD1d. Accordingly, WTH-2 is a suitable monoclonal antibody to analyze the expression levels of cotton rat CD1d in cotton rat tissues.

3.1.1.3 Expression patterns of crCD1d in different tissues

CD1d expression has been studied in rats and mice with WTH-1 and WTH-2 antibody stainings, and it was shown that all hematopoietic cells constitutively express this surface molecule [355]. LEW rats and C57BL/6 mice express similar levels of CD1d on thymocytes and the majority of splenocytes [355]. The surface expression of CD1d in cotton rat tissues has not yet been studied and was therefore compared to mouse CD1d expression using WTH-2 stainings. Thus, primary cells were prepared as described in chapter 2.2.3.3 and stained according to chapter 2.2.3.8 with WTH-2 FITC or isotype control and representative data of three stainings are shown in **Figure 3.3**.

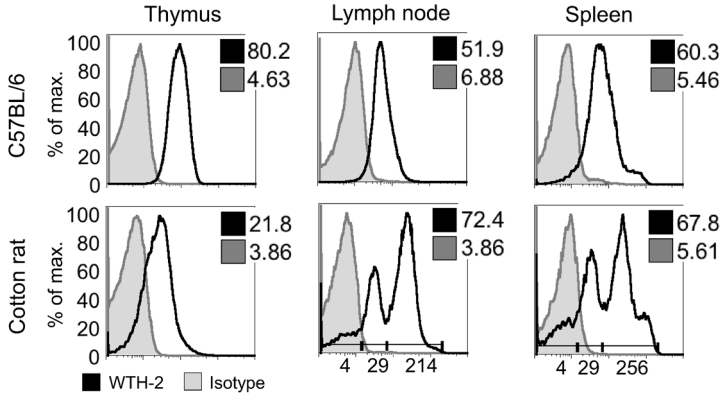

Figure 3.3 Expression patterns of mCD1d and crCD1d in different tissues. Representative data for a total of three experiments are shown. Cells ($5*10^5$) isolated from mouse or cotton rat tissues were stained with the mAb WTH-2 FITC (2 µg/ml) or isotype control. Geometric means (GM) of isotype control (tinted gray) or CD1d staining (black) are indicated in each graph. Additionally, GMs of different expression levels (cotton rat lymph node and spleen) are indicated below the histogram. Figure and figure legend adapted from [169].

As previously shown [355], mouse and rat CD1d is expressed in equal levels in the thymus, lymph node and spleen. However, as seen in **Figure 3.3**, cotton rat CD1d was only homogenously expressed in thymocytes with a staining intensity reaching only 20-25% of mouse CD1d expression. In cotton rat lymph nodes, three levels of CD1d expression could be detected with about 10% of the cells being $CD1d^-$. Approximately 30% of $CD1d^+$ cells were stained with lower intensity compared to mouse lymph node cells, and 60% expressed higher levels compared to mouse cells. In mouse spleen cells, homogeneous expression of CD1d could be confirmed with a small population (~3%) of cells expressing very high levels of CD1d. Those CD1d very high-expressing cells are mostly marginal zone B cells [355]. Cotton rat splenocytes show, like cotton rat lymph node cells, a CD1d expression divided into three peaks. One population of 10% is $CD1d^-$, the other two populations express intermediate (38%) and elevated levels (40%) of cotton rat CD1d. Here, as described for mouse splenocytes, a small foothill of cells expressing high CD1d levels (12%) was detected. Due to the lack of this small population in the lymph node and the similarities to the mouse, it can be assumed that this subpopulation contained marginal zone B cells.

Further characterization of the two distinct CD1d expression levels was performed using antibodies cross-reactive for cotton rat CD1d, MHC class II (specific for H2E and RT1D), and IgG molecules (see 2.2.3.3 and 2.2.3.8). Representative stainings are shown in **Figure 3.4**.

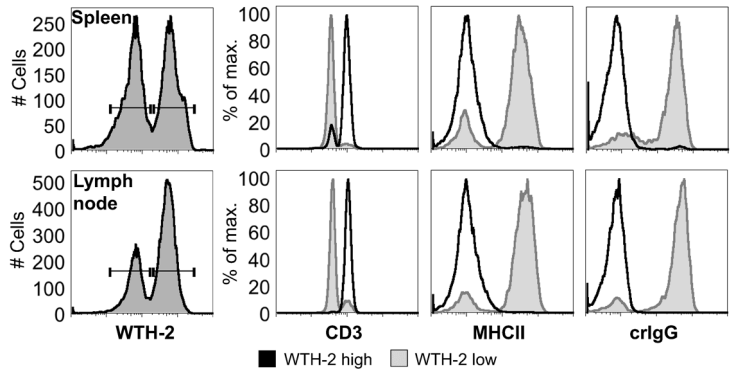

Figure 3.4 Two distinct CD1d expressing populations in cotton rat spleen and lymph node. Primary cells (5 *10^5) were stained with biotinylated WTH-2 (36 µg/ml) and antibodies against huCD3ε (2 µg/ml, Abd Serotech), MHC II (5 µg/ml, GαM R-PE from Jackson ImmunoResearch) and cotton rat IgG (10 µg/ml, GαR FITC from Invitrogen). WTH-2-positive cells from cotton rat spleen and lymph node were divided into low and high expression and CD3ε, MHC class II and cotton rat IgG (crIgG) expression of those populations are compared in histograms. Representative data for two independent experiments are shown. Figure and figure legend modified from [169].

Double stainings of cotton rat spleen and lymph node cells with WTH-2 together with CD3, MHC II and crIgG antibodies, respectively, showed distinct differences between the two subpopulations observed in **Figure 3.3** and **Figure 3.4**. In both organs, most cells expressing intermediate or low levels of CD1d were found to be negative for CD3 expression and vice versa, $CD1d^{high}$ expression correlated with CD3 expression. MHC II or crIgG were expressed almost exclusively by $WTH\text{-}2^{low}$ cells with one exception in the spleen. Here, a small population of $CD3^-$ cells could be observed and could reflect the small foothill of WTH-2 very high cells and potentially marginal zone B cells in **Figure 3.3**. Apparently, cotton rat T cells express CD1d at higher levels compared to non-T cells which were not observed in mice or rats. In those species, $CD3^+$ cells were associated with lower expression of CD1d [355]. It seems evident that expression levels of CD1d in cotton rats differ substantially from CD1d expression in mice and rats.

3.1.2 Evidence of an iNKT cell-like subpopulation in cotton rats

3.1.2.1 Production of crCD1d-mIgG fusion proteins

Invariant natural killer T cells can be detected using their specificity for glycolipids presented by CD1d [126, 149, 152, 153, 360]. MHC I, MHC II and CD1d molecules can be fused onto a mIgG antibody structure as a base for dimerization [155, 343, 361, 362]. This method has been applied before by E. Monzon-Casanova and D. Paletta for rat, mouse and human CD1d dimers, respectively [148, 149, 349]. To produce cotton rat CD1d dimers, the pXIg vector which encodes a mIgG heavy chain, was used [343]. A pXIg vector construct with the extracellular domains of cotton rat CD1d was already available (see 2.2.1.13 and [357]) and this plasmid was used to produce CD1d dimers in J558L cells which express a λ light chain [343].

Electroporation and selection of clones were performed according to chapter 2.2.4.12.2.4, and CD1d-mIgG protein quantities were measured using a mIgG1 ELISA as described in chapter 2.2.2.2.4. The clones A2 and B4 were selected as highest-producing cells and cotton rat CD1d dimers were purified following the procedures in chapter 2.2.4.2. Loading with antigens like αGC/KRN7000 or PBS57 as well as the vehicle DMSO was performed as previously described (see 2.2.4.3 and [187]).

The ability of cotton rat CD1d to present glycolipids to iNKT TCRs was analyzed using a stimulation of rat iNKT TCR expressing cells (BW rat S6 93A) with immobilized antigen-loaded CD1d dimers (see 2.2.3.7). Rat or cotton rat CD1d dimers were loaded with PBS57 or DMSO as a vehicle control. The results of this stimulations are given as percentages of the CD3 control including mean and standard deviation of three experiments in **Figure 3.5**.

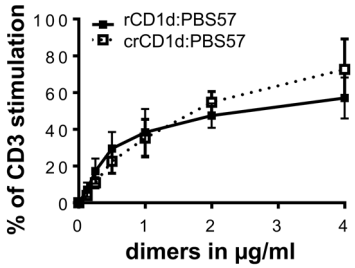

Figure 3.5 Cotton rat CD1d presents glycolipids. CD1d dimers loaded with PBS57 were diluted with CD1d vehicle-loaded dimers (DMSO) to CD1d:PBS57 concentrations of 4, 2, 1, 0.5, 0.25, 0.125 and 0 µg/ml. An α-mCD3 mAb was used as a positive control (4 µg/ml), and α-rCD28 mAb (4 µg/ml) was added to every sample. The dilutions were coated on a 96 well plate overnight. BW rat S6 93A cells ($5*10^4$) were added and cultured for 22 h. Supernatants were analyzed by mIL-2 ELISA. The results are given as a percentage of IL-2 production following stimulation with α-CD3. Three independent experiments were carried out, and mean+SD were calculated with GraphPad Prism. Figure and figure legend adapted from [169].

PBS57-loaded and immobilized cotton rat CD1d dimers were able to present the antigen to iNKT TCR expressing transductants in correlation with dimer concentrations (4 µg/ml to 0.125 µg/ml) (**Figure 3.5**). Vehicle-loaded cotton rat CD1d dimers did not induce an activation of the TCR transductants and therefore no IL-2 was detected. In comparison with rat CD1d dimers, cotton rat CD1d dimers were presenting the glycolipid PBS57 in a similarly effective fashion. Thus, the functionality of cotton rat CD1d dimers concerning the presentation of iNKT cell antigens seems evident.

The application of the newly produced crCD1d dimers to stain iNKT TCR in flow cytometry assays was tested with the same cell line used in **Figure 3.5**. The dimer staining was carried out with 4 µg/ml rat or cotton rat CD1d dimers stained for 30 min at RT, followed by detection with a Donkey anti-mouse R-PE (DαM R-PE) secondary antibody (see 2.1.11 and 2.2.3.8).

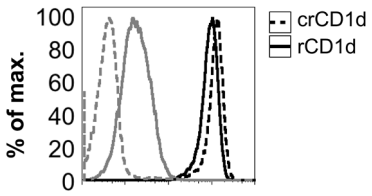

Figure 3.6 Cotton rat CD1d dimers are cross-reactive to rat iNKT TCR. Cotton rat CD1d dimers loaded with PBS57 (4 µg/ml, black) were used to stain cells expressing rat iNKT TCR and detected with DαM R-PE secondary antibody (1 µg/ml, Jackson ImmunoResearch). Dimers loaded with the vehicle DMSO (gray) served as a negative control. GMs were: rat CD1d:DMSO 17, rat CD1d:PBS57 851, crCD1d:DMSO 4, crCD1d:PB57 1192. The staining is representative for three experiments. Figure and figure legend adapted from [169].

Rat iNKT TCR could be detected with rat and cotton rat CD1d dimers as shown in **Figure 3.6**. The R-PE fluorescence of the secondary antibody showed a distinct peak in the histogram for each of the stainings with crCD1d:DMSO, crCD1d:PBS57, rCD1d:DMSO and rCD1d:PBS57. Cotton rat CD1d dimers loaded with the antigen PBS57 bound to rat iNKT TCR with a slightly higher affinity compared to antigen-loaded rat CD1d dimers. The background of crCD1d:DMSO dimers was less pronounced than the one generated by rCD1d:DMSO dimers. In summary, cotton rat CD1d dimers were able to present glycolipids to rat iNKT TCR and can be applied for flow cytometry stainings.

3.1.2.2 Identification of iNKT cells with crCD1d-mIgG fusion proteins

Detection of iNKT cells *ex vivo* was possible with the use of cotton rat CD1d dimers. Those were applied in flow cytometry stainings of splenocytes isolated according to chapter 2.2.3.3 and following the flow cytometry staining as described in chapter 2.2.3.8. The dimers were detected with a Goat anti-mouse secondary antibody labeled with R-PE (GαM R-PE) and co-stained with an intracellular rat anti-human CD3ε antibody linked to FITC (AbD Serotech).

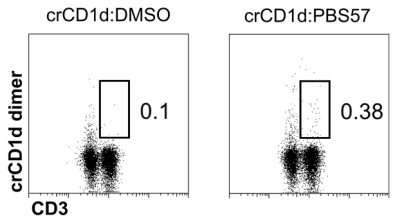

Figure 3.7 Identification of a crCD1d dimer-positive cotton rat splenocyte population. Splenocytes were stained with PBS57-loaded or control crCD1d dimers (detected with GαM R-PE, Jackson ImmunoResearch) followed by intracellular staining of CD3ε (AbD Serotech). Gates on CD3-positive, crCD1d dimer$^+$ cells were set to indicate iNKT cells. The experiment is representative of three individual experiments, the overall frequency of iNKT cells was 0.23%. Figure and figure legend from [169].

A small population of crCD1d-mIgG dimer-positive cells (0.28% of live cells) could be identified in cotton rat splenocytes (**Figure 3.7**). Staining with the anti-CD3 antibody resulted in two distinct cell populations when gating on live cotton rat splenocytes. The background of dimer staining with crCD1d:DMSO dimers amounted to 0.1% of live cells, and a small population of about 0.38% of live cells could be observed with crCD1d:PBS57 dimers. The mean frequency of iNKT cells in non-stimulated splenocytes was 0.23% ± 0.05 from three independent experiments. This population could also be seen in stainings with rat CD1d dimers, supporting the cross-reactivity of rat and cotton rat found in chapter 3.1.2.1.

3.1.2.3 Cytokine response of cotton rat cells to typical iNKT cell antigens

One of the most important effector functions of iNKT cells is the rapid production of cytokines in response to glycolipid recognition [126]. A unique capacity of iNKT cells is the release of high amounts of IFN-γ and IL-4 after activation by the presentation of an antigen like αGC or PBS57 on CD1d. To test whether cotton rat cells possess the ability to react to glycolipid antigens, cotton rat splenocytes (see 2.2.3.3) were stimulated with αGC or PBS57 as described in 2.2.3.7. The cytokine release was measured by cotton rat IFN-γ and IL-4 ELISA following the protocol in the chapters 2.2.2.2.1 and 2.2.2.2.2, respectively.

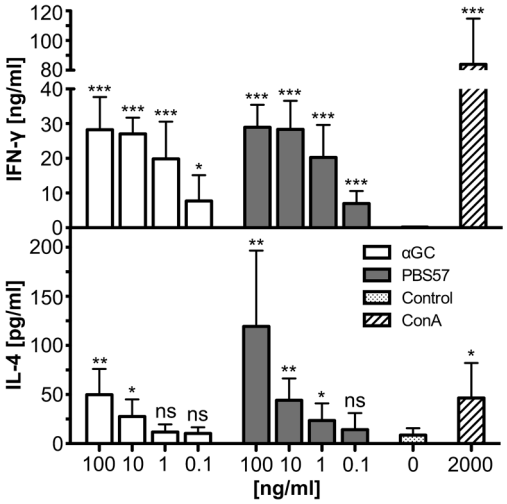

Figure 3.8 Cotton rat splenocytes produce cytokines in response to typical glycolipid antigens. Splenocytes ($1*10^6$) were stimulated with different concentrations of the glycolipids αGC or PBS57 ranging from 100 to 0.1 ng/ml. Media was used as a negative control, 2 µg/ml ConA as a positive control. Stimulations were carried out in duplicates, and cytokine production was measured with cotton rat IFN-γ and IL-4 ELISA. Three experiments were carried out in total, and mean+SD were calculated using GraphPad Prism. Statistical analysis is indicated above columns in comparison to negative control as ns: $p > 0.05$, *$p < 0.05$, **$p < 0.005$, ***$p < 0.0005$, unpaired Student's t-test. Figure and figure legend adapted from [169].

Stimulation of cotton rat splenocytes with αGC and PBS57 resulted in the release of a significant amount of IFN-γ and a less pronounced production of IL-4 as depicted in the histograms of **Figure 3.8**. The response was dose-dependent for both cytokines, and a near saturation could be shown for INF-γ at antigen concentrations higher than 10 ng/ml. No difference could be observed between the INF-γ production in response to either αGC or PBS57, and the highest measurement of IFN-γ was about 35 ng/ml. The IFN-γ release after ConA stimulation was considerable with concentrations of more than 100 ng/ml. The IL-4 release was lower with a maximum of roughly 225 pg/ml. Here, the recognition of PBS57 induced higher IL-4 production compared to αGC. Those results indicate a glycolipid recognition on the cellular level in spleen cells which hints at the presence of iNKT cells in the cotton rat spleen.

3.1.3 The cotton rat iNKT TCR

3.1.3.1 Multiple *AV14* family members in cotton rats

The invariant *AV14/AJ18* rearrangement typical for iNKT cell receptors has been partially amplified before using a RACE PCR approach [357]. The missing 5' UTR region was amplified in this study (see 2.2.1.9 and 2.2.1.13) and subsequently, a complete coding sequence for an iNKT TCR α chain has been amplified from spleen cDNA [169]. This TCR α chain (GenBank: KT367785) was compared to homologous sequences from Chinese hamster, rat, mouse and human using Clustal Omega to calculate an amino acid sequence alignment (**Figure 3.9**).

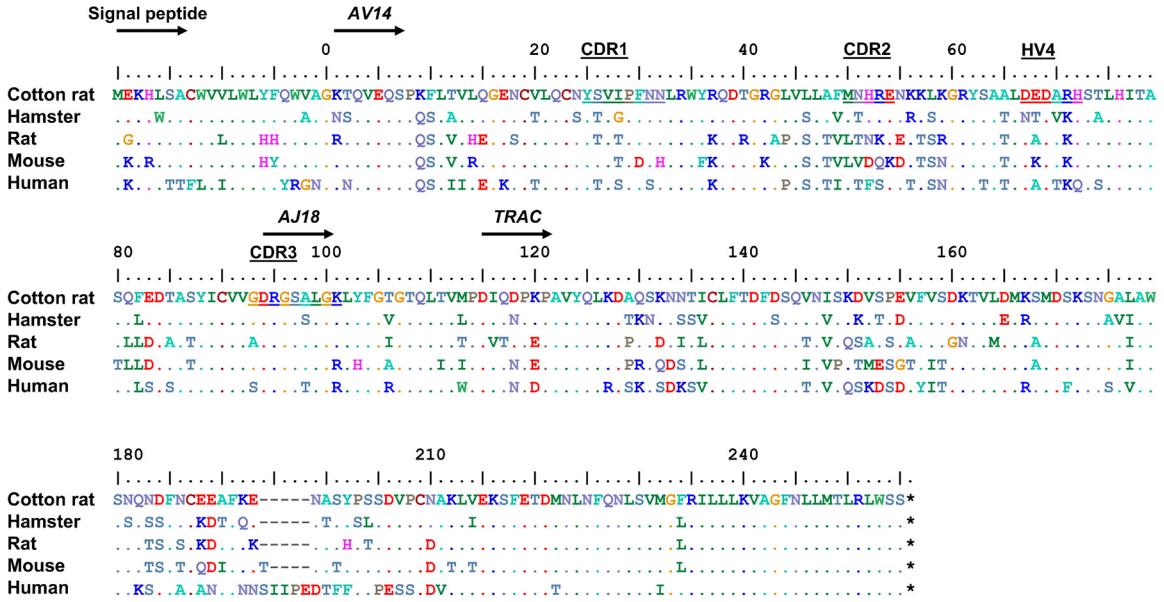

Figure 3.9 iNKT α chain amino acid sequence alignment of different species. A full-length cotton rat α chain (pEGN crAV14/AJ18 clone 1, GenBank: KT367785) was compared to Chinese hamster, designed from genomic sequences, GenBank: NW_003615069.1 and NW_003614213.1), rat (GenBank: ABC69268.1), mouse (GenBank: AAA40180.1), and human α chains (GenBank: ABC72374.1). The alignment was calculated with Clustal Omega. Identical amino acids (dots), gaps (dashes) and stop codons (*) are indicated. The different regions of the TCR α chain are labeled (signal peptide, *AV14*, *AJ18* and constant region). The regions CDR1, CDR2, hypervariable region 4 (HV4), and CDR3 appear underlined.

The alignment of one cotton rat Vα14Jα18 T cell receptor chain with homologous α chains from Chinese hamster, rat, mouse and human is shown in **Figure 3.9**. The conservation of the invariant iNKT TCR α chains is especially evident in the CDR3 encoded by the *AV14/AJ18* junction and in the C-terminal regions of the constant region. Closer examination of the homologies of *AV14, AJ18* and *TRAC* was performed by calculating the nucleotide and amino acid identities between cotton rat and the other species.

Table 3.2 Homologies of iNKT TCR α chains of different species. Identical nucleotides or amino acids of the sequences were counted, and the overall identity was calculated as the ratio of identical nucleotides/amino acids to the length of the alignment, therefore including gaps, and are given in rounded percentages. Figure and figure legend adapted from [169].

Cotton rat iNKT α chain 1 to	Vα14Jα18 chain cl.1		Signal peptide		*AV14*		*AJ18*		*TRAC*	
	% NT	% AA	% NT	% AA	% NT	% AA	% NT	% AA	% NT	% AA
Hamster	86	**80**	92	**90**	85	**78**	83	**86**	85	**79**
Rat	83	**75**	87	**81**	78	**65**	84	**90**	83	**79**
Mouse	83	**74**	86	**81**	80	**68**	83	**76**	82	**76**
Human	75	**66**	70	**52**	77	**65**	83	**81**	74	**66**

Analogous to the sequence analysis of cotton rat CD1d in **Table 3.1**, the cotton rat Vα14Jα18 TCR chain is most like the Chinese hamster homolog in all domains but *AJ18* (see **Table 3.2**). The *AJ18* gene segment of cotton rats more closely resembles the rat homologous sequence, sharing 90% amino acids and 84% nucleotides with rat *AJ18* but is the most conserved gene segment among cotton rat, hamster, rat, mouse and human. The signal peptide, *AV14* and *TRAC* region of the cotton rat iNKT TCR show homologies to the other analyzed species according to their evolutionary relationship. The constant region is rather conserved among rodents in this analysis with more than 80% nucleotide identities and 76-79% amino acid identities.

One peculiarity of rats is the use of multiple *AV14*-family members in expressed iNKT TCRs [125, 149, 349, 363]. Whether cotton rats share this characteristic of rat iNKT TCR α chains was analyzed in this study. For the analysis of cDNA transcripts, multiple single-cell clones of cotton rat *AV14/AJ18* TCR chain transcripts cloned into the pEGN vector were analyzed. To determine the genomic *AV14* family members, *AV14* was amplified from cotton rat genomic DNA and cloned into pEGN as described in chapter 2.2.1.13 and single-cell clones were analyzed (see 2.2.1.5). An alignment of unique *AV14* sequences and *AV14/AJ18* rearrangements is shown below.

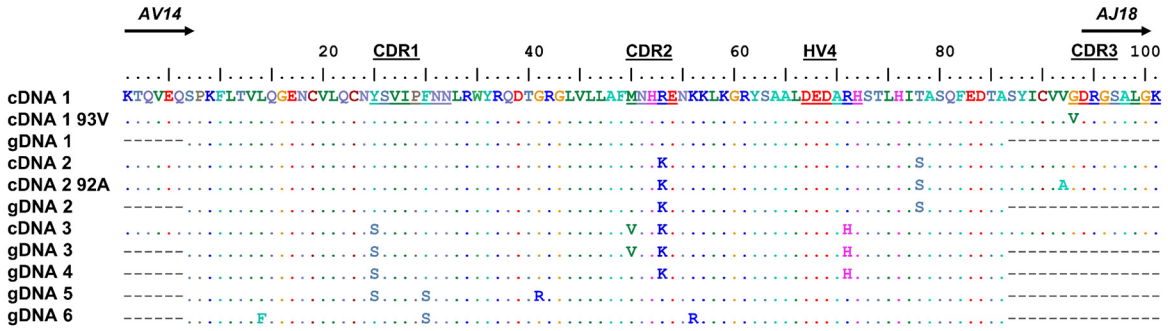

Figure 3.10 Cotton rats possess multiple *AV14*-family members with canonical iNKT TCR rearrangements. Cloning of IHL iNKT TCR α chains amplified from cDNA into pEGN was used to identify different *AV14*-family members. Cloning of the genomic *AV14* sequences into pEGN was applied to analyze genomic isoforms of *AV14*. The alignment was calculated with Clustal Omega. Dots indicate identical amino acids. The different regions are indicated and depict the protein sequences of *AV14* and the first part of *AJ18*. The CDR1-3 regions and hypervariable region 4 (HV4) are underlined in the top row of the alignment. The frequencies of the different members in the pool of sequenced clones were as follows: cDNA1 5/17, cDNA1 93V 1/17, gDNA1 2/20, cDNA2 3/17, cDNA2 92A 1/17, gDNA2 4/20, cDNA3 7/17, gDNA3 1/20, gDNA4 8/20, gDNA5 2/20, gDNA6 3/20.

The analysis of *AV14* on the genomic level revealed the existence of six unique cotton rat *AV14* family members (**Figure 3.10**). Those *AV14* gene segments show differences in the CDR1, CDR2, hypervariable region 4 and at three other locations in the protein sequence. The specific positions of differences observed on the protein level of *AV14* family members were L/F14, Y/S25, F/S30, G/R41, M/V50, R/K53, K/R56, R/H71, T/S78. The expression of three genomic *AV14* variants could be confirmed on the mRNA level. The genomic *AV14* family members 1, 2 and 3 had corresponding cDNA sequences with two cDNA carrying variations at the positions 91 and 92 in the CDR3. The expression of gDNA 4-6 could not be confirmed in this setting.

3.1.3.2 Identification of *BV8*-like family members in cotton rats

Invariant NKT α chains are preferentially associated with members of the *BV8* β chain family of TCR chains in rats and mice (IMGT: *TRGV13-2*) [123, 125]. Four members of this family have been identified in rats (*BV8.1*, *8.2*, *8.3/8.5* and *8.4*) [364-366] and three in mice (*BV8.1*, *8.2* and *8.3*) [367]. The homologous gene segment in humans is the *BV11* gene (IMGT: *TRGV25*). To verify the expression of such β chains and their ability to form functional iNKT TCRs, a cotton rat homolog was amplified from cotton rat spleen cDNA using primers for *BV8.2* and cloned into the S65T vector (see 2.2.1.13). Two cotton rat β chains containing distinct *BV8.2* homologs were compared to *BV8.2* carrying β chains of rat, mouse and human (*BV11*) in **Figure 3.11**.

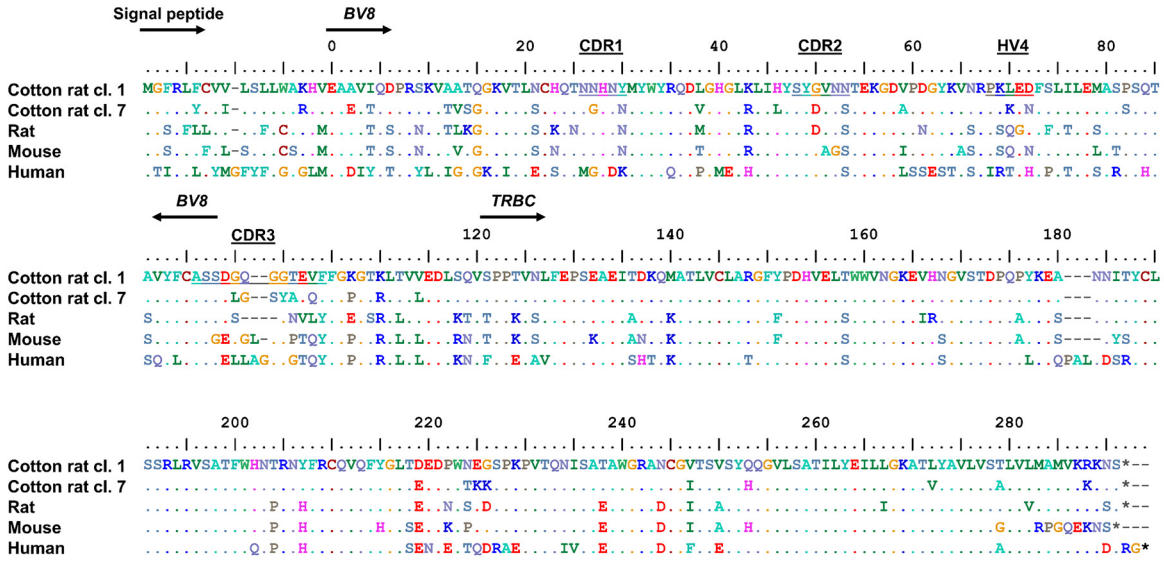

Figure 3.11 iNKT β chain amino acid sequence alignment of different species. Two full-length cotton rat β chains (S65T crBV8 clone 1 and 7) were compared to rat (GenBank: AY228549.1), mouse (GenBank: DQ340294.1), and human β chains (GenBank: DQ341462.1). The alignment was calculated with Clustal Omega. Identical amino acids (dots), gaps (dashes) and stop codons (*) are indicated. The different regions of the TCR β chain are labeled (Signal peptide, *BV8* and constant region). The regions of CDR1, CDR2, hypervariable region 4 (HV4), and CDR3 are underlined in the top row of the alignment.

The most conserved parts of *BV8*-carrying TCR β chains in different species are located in the constant region as illustrated in the alignment in **Figure 3.11**. The CDR3 regions of the analyzed TCR β chains show high diversity concerning sequence and length. To further investigate the homologies of *BV8* β chains, sequence identities were calculated.

Table 3.3 Conservation of Vβ8 TCR chains in cotton rat, rat and mouse. Identical nucleotides or amino acids of the cotton rat Vβ8 chains 1 and 7 to rat, mouse and human Vβ8 chains were counted, and the overall identity was calculated as the ratio of identical nucleotides/amino acids to the length of the alignment, therefore including gaps, and are given in rounded percentages.

Cotton rat iNKT β chain 1/7 to	Vβ8 chain cl.1/7		Signal peptide cl. 1/7		*BV8* cl. 1/7		*TRBC* cl.1/7	
	% NT	% AA	% NT	% AA	% NT	% AA	% NT	% AA
Rat	82/81	**78/77**	81/76	**61/50**	80/81	**75/77**	87/84	**86/84**
Mouse	81/83	**74/75**	81/78	**61/50**	83/84	**75/76**	84/86	**78/80**
Human	68/64	**65/66**	57/57	**21/21**	59/61	**55/54**	78/81	**76/76**

The full-length cotton rat iNKT β chains 1 and 7 shared amino acid sequence homologies of 74-78% with other rodents analyzed in this setting (**Table 3.3**). Conservation of cotton rat β chains with the human counterpart was less pronounced (65-66% AA). The most conserved region of β chains is *TRBC* (> 76% AA identity). The variable region is conserved in a comparable manner in cotton rats and rats/mice with nucleotide/amino acid homologies of 80-84%/75-77%. Signal peptide sequences are less conserved, with cotton rat and human sharing only 21% of amino acids in this part of the β chains.

Evidence for multiple *BV8.2* homologous genes was found in cotton rats during sequencing and cloning of cotton rat *BV8*. To investigate this, 16 single-cell clones of S65T crBV8 were sequenced and analyzed. Out of these sequences, nine β chains carried productive *BV8/TRBJ* rearrangements and were fully translatable.

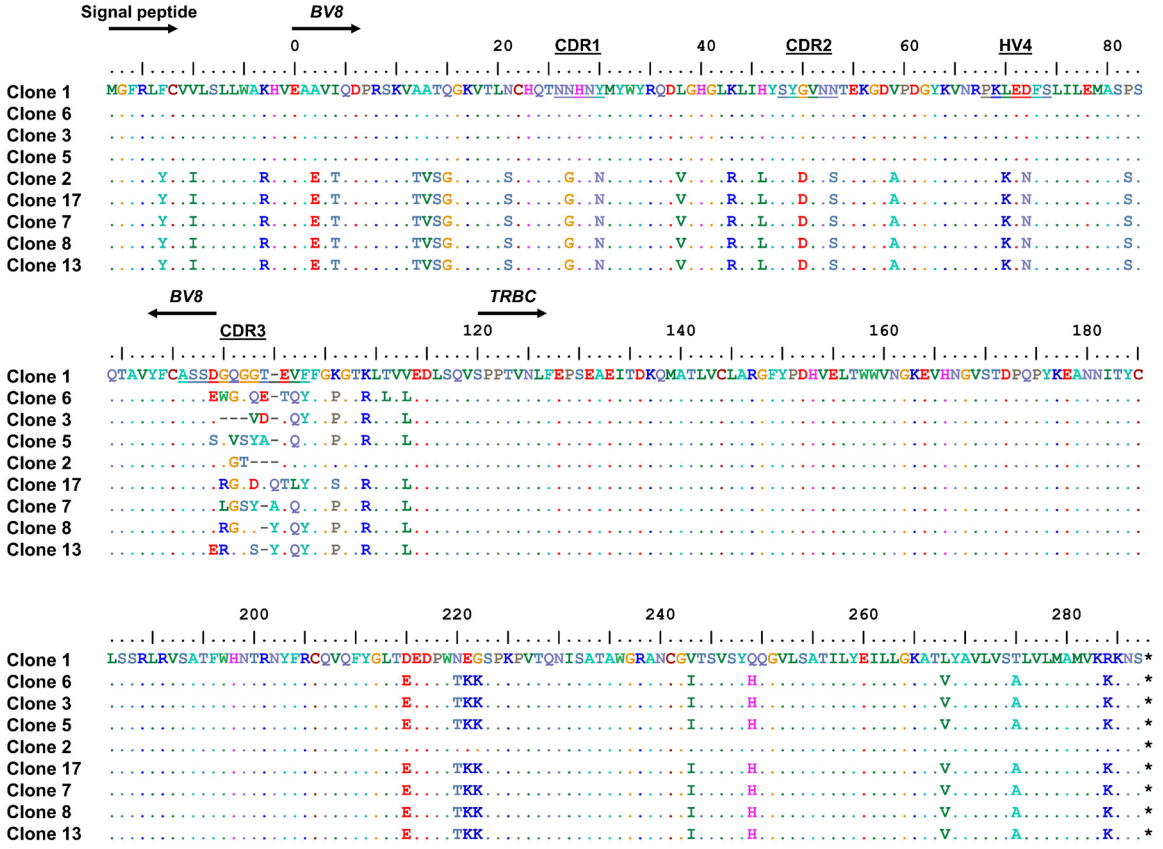

Figure 3.12 Cotton rats express distinct Vβ8-like β chains. Nine unique *in silico* translatable clones obtained from the analysis of S65T crBV8 clones were aligned using Clustal Omega. Identical amino acids (dots), gaps (dashes) and stop codons (*) are indicated. The different regions of the TCR β chain are labeled (Signal peptide, *BV8* and *TRBC*). The regions of CDR1, CDR2, hypervariable region 4 (HV4), and CDR3 are underscored in the top row of the alignment.

The analysis of nine unique and fully translatable S65T crBV8 clones depicted in **Figure 3.12** proves the existence of at least two distinct *BV8* segments in the cotton rat. The cotton rat *BV8* regions in this alignment share 89% of their nucleotides and 81% amino acids. IMGT/DomainGapAlign analysis revealed homology of 78.9% for the *BV* region of clone 1 and 80% for the one of clone 7 to the mouse *BV8* allele *BV8.1* (IMGT nomenclature: *TRBV13-3*01*). Both *BV8* homologs are rearranged with different *TRBJ* segments and CDR3 diversity was observed. The cotton rat expresses two distinct *TRBC* regions which share a 94% nucleotide identity and differ in their amino acid usage at nine locations (95% amino acid identity). The usage of *TRBC* in clone 1 and 2 could be linked to the rearranged *TRBJ* region only observed in these two clones. Otherwise, *TRBC* usage did not seem to be restricted to a certain *BV8* gene.

The analysis of the non-translatable clones of S65T crBV8 revealed the existence of two more *BV8* family members (data not shown) and one non-productive *BV8*/*TRBJ* rearrangement. The two distinct *BV8*-like gene segments can be considered pseudogenes as they carried an insertion of 22 nucleotides in the signal sequence which disrupts the reading frame and leads to the termination of translation.

3.1.3.3 *In vitro* expression of cotton rat iNKT TCRs

Cotton rat iNKT TCR α and β chains were overexpressed in a permanent cell line to prove the pairing of cotton rat invariant *AV14* and *BV8* family members and glycolipid recognition of these iNKT-like TCRs. Of the *AV14* group 1 described in chapter 3.1.3.1, two clones differing only in the amino acid at position 93 (clone 1: G, clone 8: V) were selected. The role of this position in modulating rat and mouse iNKT TCR glycolipid recognition has been described [349]. Valine at this position led to a decreased functionality shown by decreased affinity to CD1d multimers. The β chains amplified from cotton rat cDNA showed usage of two distinct *BV8*-like gene segments (see 3.1.3.2). Two clones were chosen with differential *BV8* and *TRBJ* usage (clone 1 and 7). Accordingly, the selected cotton rat α and β chains were selected and transduced in all combinations in the mouse cell line L929 already carrying the vector pMIG II mCD3 δ-F2A-γ-T2A-ε-P2A-ζ which encodes for all mouse CD3 subunits linked with 2A peptides and thus enabling expression of a complete TCR complex (see 2.2.3.6). The cells were subsequently sorted on mouse CD3 expression (see 2.2.3.9) and stained with rat CD1d tetramers and cotton rat CD1d dimers as described in chapter 2.2.3.8.

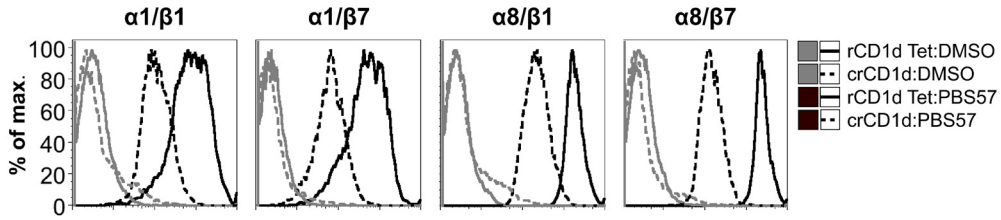

Figure 3.13 Surface expression of cotton rat iNKT TCRs. The cotton rat iNKT Vα14Jα18 chains 1 or 8 (pEGN crAV14 clone 1/8) were used to transduce L929 mCD3 cells (pMIG II mCD3 δ-F2A-γ-T2A-ε-P2A-ζ) cells, together with the cotton rat iNKT Vβ8 chain 1 or 7 (S65T crBV8 clone 1/7). Transductants were stained with 1 µg each rat CD1d tetramers labeled with PE and loaded with PBS57 (black) or DMSO (dashed black) or crCD1d dimers loaded with PBS57 (gray) or DMSO (dashed gray) detected with DαM R-PE (1 µg/ml, Jackson ImmunoResearch). The cells were co-stained with α-mCD3ε bio detected with SA-APC (400 ng/ml, BD Pharmingen). Cells were gated on live, $CD3^+$ cells and GMs of the CD1d dimer/tetramer stainings were (crCD1d:DMSO/:PBS57; rCD1d Tet:DMSO/:PBS57): α1/β1 (3.49/108; 3.29/689), α1/β7 (2.33/60.4; 2.38/444), α8/β1 (3.71/218; 2.65/1829), α8/β7 (2.72/143; 2.88/2430).

The surface expression and CD1d dimer or tetramer detection of cotton rat iNKT TCR chains could be shown in **Figure 3.13**. Each combination of *AV14* and *BV8*-using TCR chains could successfully be detected at the surface of the transduced L929 cells. However, the signal detected with rat CD1d tetramers was far superior to the one measured in stainings with cotton rat CD1d dimers. In addition, tendencies for differential staining intensities were more pronounced using tetramers, and therefore the application of CD1d tetramers was more sensitive and should be preferred. The pairing of the Vα14Jα18 chain clone 8 with β chain clone 1 led to a 3-fold increase of staining intensity (rat tetramer) compared to Vα14Jα18 clone 1 and to a more than 5-fold increase in combination with β chain clone 7. This difference in staining intensity of distinct combinations of cotton rat iNKT TCR α and β chains was not further investigated, but implies a dependence of glycolipid recognition on α and β chain usage in cotton rats.

3.2 Coevolution of Vγ9Vδ2 T cells with BTN3

The major γδ subset in human blood [32, 238] expresses a Vγ9Vδ2 T cell receptor with a *TRVG9/TRGJP* rearrangement in the TCR γ chain and a δ chain using the *TRDV2* gene. These TCRs are rapidly activated upon phosphoantigen recognition [32] and exert a multitude of effector functions. The antigen recognition mode has been shown to be independent of MHC molecules [32], and the molecule BTN3A1 has been proven essential for PAg sensing in humans [308]. For long, Vγ9Vδ2 T cells have been thought to be primate-specific cells, however, coevolution of *TRGV9*, *TRDV2*, and *BTN3* genes with placental mammals has been suggested [267, 317]. Two of the candidate species suggested by Karunakaran et al. [317] are the alpaca (*Vicugna pacos*) and the armadillo (*Dasypus novemcinctus*). Both species possess genes for *TRGV9*, *TRDV2* and *BTN3*, and the expression of them in alpacas has been proven before [317]. In this study, the expression of *TRGV9*, *TRDV2* and *BTN3* genes is analyzed in armadillos and the alpaca Vγ9Vδ2 T cell subset is characterized further. The results obtained for the armadillo BTN3/Vγ9Vδ2 T cell system have been published in the article "The Armadillo (*Dasypus novemcinctus*): A Witness but Not a Functional Example for the Emergence of the Butyrophilin 3/Vγ9Vδ2 System in Placental Mammals" by Fichtner et al. [326]. Contents are adapted and printed under the terms of the Creative Commons Attribution License.

3.2.1 The armadillo: a witness for the BTN3/Vγ9Vδ2 T cell system

3.2.1.1 Genomic organization of *BTN3* orthologs in non-primate candidate species

The existence of one homologous region each to the extracellular IgV-like *BTN3* region (*BTN3-V*) and the intracellular B30.2 domain of human *BTN3A1* was shown in 2014 by M. Karunakaran and T. Herrmann [267]. However, the in-depth analysis of those two regions in the armadillo genome resulted in a closer evolutionary relationship to human BTN3A3. This was confirmed by the comparison of armadillo *BTN3*-encoding regions to the human genome using the NCBI Blast [328]. Subsequently, the human *BTN3A3* coding region (GenBank: NM_006994.4) was used to identify other *BTN3*-like genomic sequences in the *Dasypus novemcinctus* whole genome shotgun database (wgs) retrieved from the NCBI database (BioProject: PRJNA12594/PRJNA196486; BioSample: SAMN02953623; GenBank: gb|AAGV00000000.3). Whole genome shotgun databases contain contigs with unique accession numbers and contain incomplete non-annotated genomic sequence information. The analysis of the armadillo wgs database resulted in the identification of three genomic regions homologous to *BTN3-V* and three regions homologous to the IgC-like *BTN3* region (*BTN3-C*).

Additionally, the *BTN3*-like genes of two other non-primate candidate species, alpaca (*Vicugna pacos*) and bottlenose dolphin (*Tursiops truncatus*) were analyzed. Predicted coding sequences of alpaca and dolphin *BTN3* were already published in the NCBI nucleotide databases (GenBank alpaca: XM_015251744.1, dolphin: XM_004332447.2). These database entries were used to map the locations of alpaca and dolphin *BTN3* in whole genome shotgun contigs as no complete genomic assembly of both species was available (**Figure 3.14**). The corresponding nucleotide and amino acid sequence alignments are shown in **Figure A.1-A.5**.

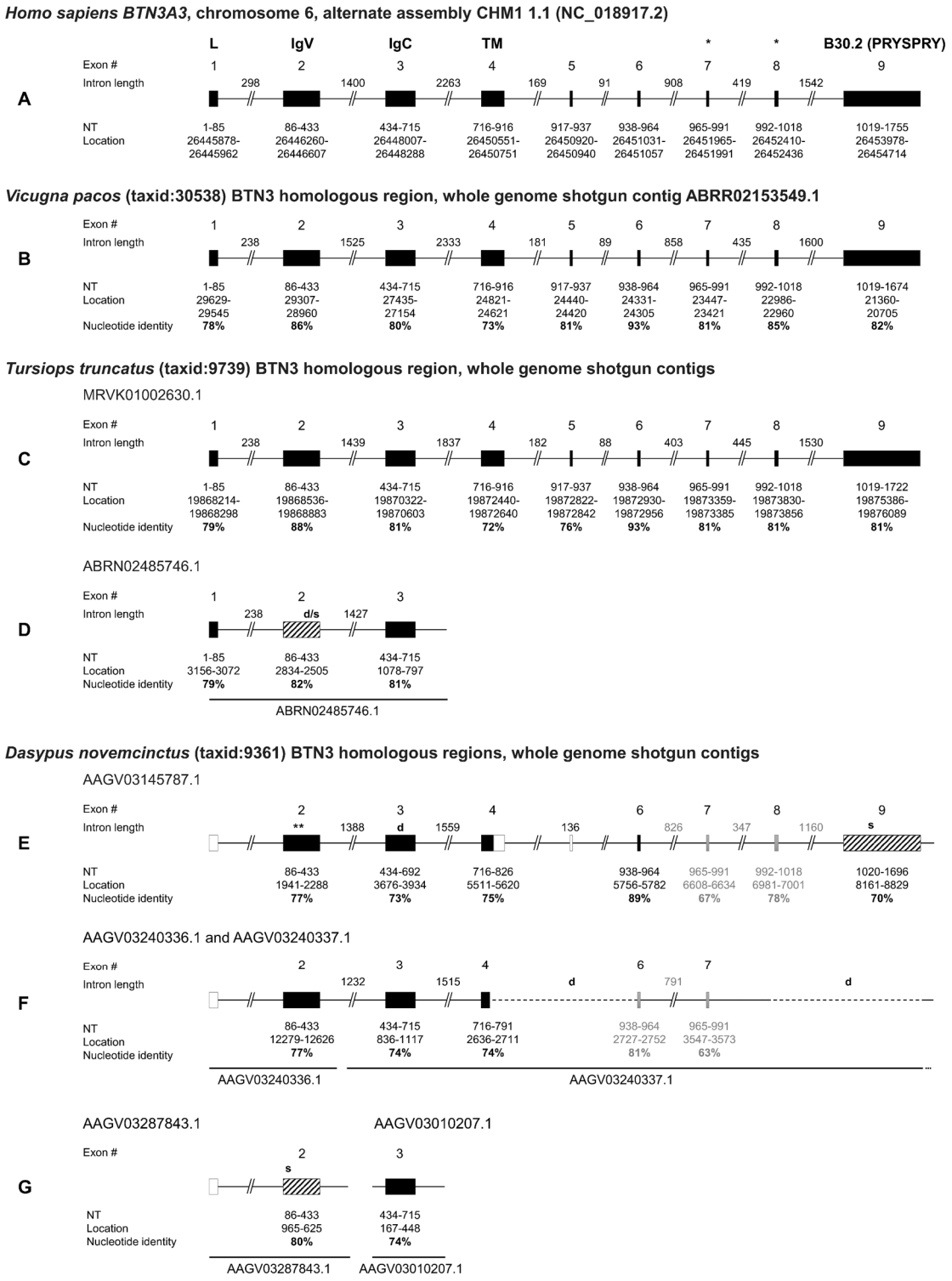

Figure 3.14 Genomic organization of *BTN3* loci in different species. Human *BTN3A3* locus (**A**) determined by NCBI megablast of *BTN3A3* (GenBank: NM_006994.4) to Human G+T database (GenBank: NC_018917.2). Alpaca *BTN3*-like locus (**B**) was mapped using NCBI blastn of the predicted alpaca *BTN3A3* (XM_015251744.1) to *Vicugna pacos* wgs database. Dolphin *BTN3*-like loci (**C**-**D**) were identified using NCBI blastn of the predicted dolphin *BTN3A3* (XM_004332447.2) to *Tursiops truncatus* wgs. Armadillo *BTN3* homologous regions (**E**-**H**) were identified by NCBI blastn of human *BTN3A3* to *Dasypus novemcinctus* wgs (taxid: 9361). Exons represented by boxes: translatable (solid black), non-translatable (striped black), missing (solid white) found by intron homologies (solid gray). Exon size, location in assembly/contig, and nucleotide identity to human *BTN3A3* (bold) are indicated. Intron lengths are indicated, and putative deletions shown by dashed lines and "d". Stop codons are indicated by "s" at approximate location (*location of proposed juxtamembrane motif [313]; **location of putative ATG at nt 1982). Figure and figure legend adapted from [326].

The full or partial reconstruction of *BTN3* encoding genomic regions of human, alpaca, dolphin and armadillo is depicted in **Figure 3.14**. The mapping of human *BTN3A3* to the fully assembled human genome in **Figure 3.14A** clearly shows the existence of nine distinct exons encoding for the *BTN3A3* regions BTN3-V (exon 2), BTN3-C (exon 3) and B30.2 domain (exon 9) [309]. The exons 4-8 encode the transmembrane region and intracellular stretches N-terminal of the B30.2 domain [309].

A striking resemblance to this genomic organization could be observed for the single *BTN3* molecule found in alpaca (**Figure 3.14B**), showing sequence conservation of 73-93% and conserved intron lengths. The intracellular B30.2 domain of the alpaca *BTN3*-like molecule was 81 nucleotides shorter than its human homolog. Splicing of alpaca *BTN3* exons was predicted using eukaryotic consensus splice donor and acceptor sequences and *in silico* translation was performed. Sequence identities of the armadillo *BTN3*-like sequence to human *BTN3A3* were 81% on the nucleotide and 72% on the amino acid level. The expression of an alpaca *BTN3*-like gene (GenBank: MG029164) with 81% identical nucleotides and 73% identical amino acids to human *BTN3A3* has been confirmed on the mRNA level [321]. Minor differences between the genomic sequence and the BTN3 derived from alpaca mRNA (**see Figure A.1 and A.2**) are possibly due to interindividual polymorphisms also reported for human BTN3 molecules [298]. Predicted residues reported to be essential for phosphoantigen recognition in the human BTN3A1-V (E37, K39, R61, Y100, Q102 and Y107) and the BTN3A1 B30.2 domain (H351, H378, K393, R412, R418, R469) [304, 308] were conserved in both the genomic and the expressed alpaca *BTN3* analyzed in this study (see **Figure A.2**) [267, 317].

Dolphins express *TRGV9*- and *TRDV2*-like TCR transcripts [325] but *BTN3* expression has not been confirmed in these animals. However, one complete *BTN3*-like locus could be identified here, which contains nine exons of a previously published *BTN3*-like molecule (GenBank: XM_004332447.2) and is depicted in **Figure 3.14C**. This locus is remarkably like the human and alpaca *BTN3* loci and nucleotide conservation in its exons is 72-93% compared to human *BTN3A3*. The intron lengths corresponded mostly to the ones observed in the human locus with one exception being the intron between exon 6 and 7 (~50% of the human intron). Moreover, the dolphin B30.2-like region was 33 nucleotides shorter than the human B30.2 domain. The splicing and translation of the dolphin homolog was predicted and resulted in a nucleotide identity of 81% and an amino acid identity of 73% to the human *BTN3A3* (see **Figure A.1 and A.2**). Phosphoantigen-binding residues of the human BTN3A1 molecule were completely conserved in the dolphin B30.2 domain [308], and five out of six residues were present in the translated dolphin *BTN3-V*, with K39T being the only substitution (**Figure A.2**) [304]. A second locus with regions homologous to human *BTN3A3* exons (**Figure 3.14D**) could be identified in

the dolphin wgs database. Due to its length, only a *BTN3* signal sequence, the *BTN3-V* and *-C* were comprised in this contig. The second exon of this locus was shorter than the one of the complete dolphin BTN3-like locus (**Figure 3.14C**) and in-frame translation of this *BTN3-V* lead to a termination codon. Therefore, this dolphin locus seems to comprise a *BTN3* pseudogene.

The armadillo genome encodes homologous regions to human *BTN3A3*, three homologs for each, *BTN3-V* and *BTN3-C*, and one B30.2 homolog were found in the armadillo wgs database. One complete *BTN3*-like locus is comprised in one contig (AAGV03145787.1) and could thus be reconstructed (**Figure 3.14E**). This genomic stretch contained homologs to the human *BTN3A3* exons 2-4, 6 and 9 with exon 4 being only half the length of the corresponding human sequence. Two other small exons (exon 7 and 8) encoding for transmembrane or intracellular *BTN3A3* regions in humans could be identified by comparing surrounding armadillo and human intron sequences. Sequence conservation of the armadillo homologs found in this contig (**Figure 3.14E** and **Figure A.5A**) was more than 70% on the nucleotide level compared to human *BTN3A3* and intron lengths were mostly conserved. The second and third *BTN3-V* homolog were located in different armadillo wgs contigs (AAGV03287843.1 and AAGV03240336.1) as was the case for the other two *BTN3-C* homologs (AAGV03240337.1 and AAGV03010207.1). One of the *BTN3-C* encoding contigs (AAGV03240337.1) showed a truncated transmembrane homolog (exon 4) directly followed by a homolog to exon 6 and did not include a B30.2-like domain (**Figure 3.14F** and **Figure A.5B**). Comparison of this contig and contig AAGV03145787.1 which comprises a complete *BTN3*-like locus (**Figure 3.14E**) showed two possible sites of deletion in AAGV03240337.1. The first deletion results in a fusion of a truncated exon 4 and exon 6, the second spans exon 8 and the B30.2 domain encoded by exon 9. The third contig comprising an armadillo *BTN3-C* homolog was too short to contain a downstream B30.2 homolog (**Figure 3.14G**). Identification of B30.2 homologous regions in the armadillo wgs database located in other contigs was hindered due to the abundant use of PRY/SPRY domains in other molecules [297]. Conserved signal sequences (exon 1) and homologous regions to exon 5 could not be found in this analysis. It is noteworthy, that those regions were also not identified by gene prediction tools like Gnomon which was used for a predicted armadillo *BTN3A3* database entry (GenBank: XM_012528284.1) or FGENESH+ [368] (reference protein: huBTN3A1/2/3; GenBank: NM_007048.5/ NM_007047.4/ NM_006994.4) which failed to predict a leader sequence in the contig AAGV03145787.1. Additionally, the start codon of the predicted *BTN3A3* homologs was located within the *BTN3-V* region (exon 2) as indicated in **Figure 3.14E**. Translation of nucleotide sequences to amino acids was performed *in silico* and resulted in the complete translation of two *BTN3-V*-like regions (**Figure A.3A**). One *BTN3-V* homolog carried a termination codon when translated in the same frame (**Figure 3.14G**). The three *BTN3-C* homologs in the armadillo genomic sequences could be translated.

However, the *BTN3-C* homolog in contig AAGV03145787.1 exhibited a nucleotide deletion which leads to a frameshift (**Figure 3.14E** and **Figure A.3B**). The single B30.2 domain was previously described by Karunakaran et al. to be fully translatable [267], but closer inspection with regard to the reading frame revealed several stop codons when the human B30.2 domain was used as a template (**Figure A.4**). All codons for the six predicted phosphoantigen-binding residues [308] were conserved in the armadillo B30.2 domain on the nucleotide level. Conservation of four out of six codons for the predicted phosphoantigen-binding regions in the extracellular *BTN3-V* domain [304] could be confirmed in the *BTN3-V*s in AAGV03240336.1 and AAGV03287843.1, and three of six codons were conserved in AAGV03145787.1 (**Figure A.3A**).

Database analysis of armadillo *BTN3* genes was followed by expression analysis of potential *BTN3* homologs in the cDNA of armadillo PBMCs. Those were provided by the National Hansen's Disease Program (Baton Rouge, Louisiana, USA) and used for RNA isolation (see 2.2.1.6) and cDNA synthesis (see 2.2.1.8 and 2.2.1.9), PCR amplification and TOPO TA cloning of PCR products (see 2.2.1.11). RACE PCR amplification of the 5' end of *BTN3-V* (primers: A165, A166) and the 3' end of *BTN3-V* (primers: A163, A164) and *BTN3-C* (primers: A167, A168) according to the protocol described in 2.2.1.9 were not successful. Partial amplification of *BTN3* from *BTN3-V* to *BTN3-C* was performed in a Phusion PCR following the protocol in 2.2.1.10 with primers specific for all three regions (A122 and A123) and resulted in no specific PCR product from armadillo cDNA (2.2.1.1 and 2.2.1.12). However, amplification with the same primers from genomic liver DNA (provided by the National Hansen's Disease Program) resulted in five clones of two types after TOPO TA cloning (GenBank: MG600558-MG600561). In one subset, a *BTN3-V* remarkably similar to the one encoded in the contig AAGV03240336.1 was contained followed by an intron and *BTN3-C* from contig AAGV03240337.1 and both contigs could therefore be linked (**Figure 3.14F**). The three clones of this type (MG600558-MG600560) were not completely identical on the nucleotide level. The two clones of the second subtype of genomic *BTN3-V*/*BTN3-C* sequences were nucleotide identical (MG600561) and only 92-95% identical to the predicted *BTN3* loci and could not be mapped to the armadillo wgs database. Therefore, the existence of more *BTN3* loci or polymorphisms could not be excluded. In summary, a striking similarity of *BTN3* loci of different species was observed, and no evidence for expression of a functional armadillo *BTN3*-like gene was found.

3.2.1.2 Expression of Vδ2-like TCR chains in armadillo

Expression analysis of the characteristic *TRDV2* rearrangement used in Vγ9Vδ2 T cells was performed with armadillo PBMC cDNA and liver genomic DNA as described before in 3.2.1.1.

TRDV2/*TRDC* was amplified in a Phusion PCR (see 2.2.1.10) with the primers A21 and A72 using armadillo cDNA as template. Additionally, the 3' end of *TRDV2* rearrangements was analyzed in a 3' RACE PCR (see 2.2.1.9) with the primers A94 and A95. The unknown 5' end of *TRDV2* transcripts, including the signal sequence, was identified using the RACE PCR approaches and the primers A118 and A119 were used. The PCR products were subsequently cloned as in described in chapter 2.2.1.11 and sequences of clones were analyzed. In addition, full-length armadillo Vδ2 chains were amplified from cDNA using the primers A193 and A194 and cloned into the pMSCV-IRES-mCherry FP vector using the In-Fusion® HD Cloning Kit (Takara Bio) as described in chapter 2.2.1.13 and clones were analyzed.

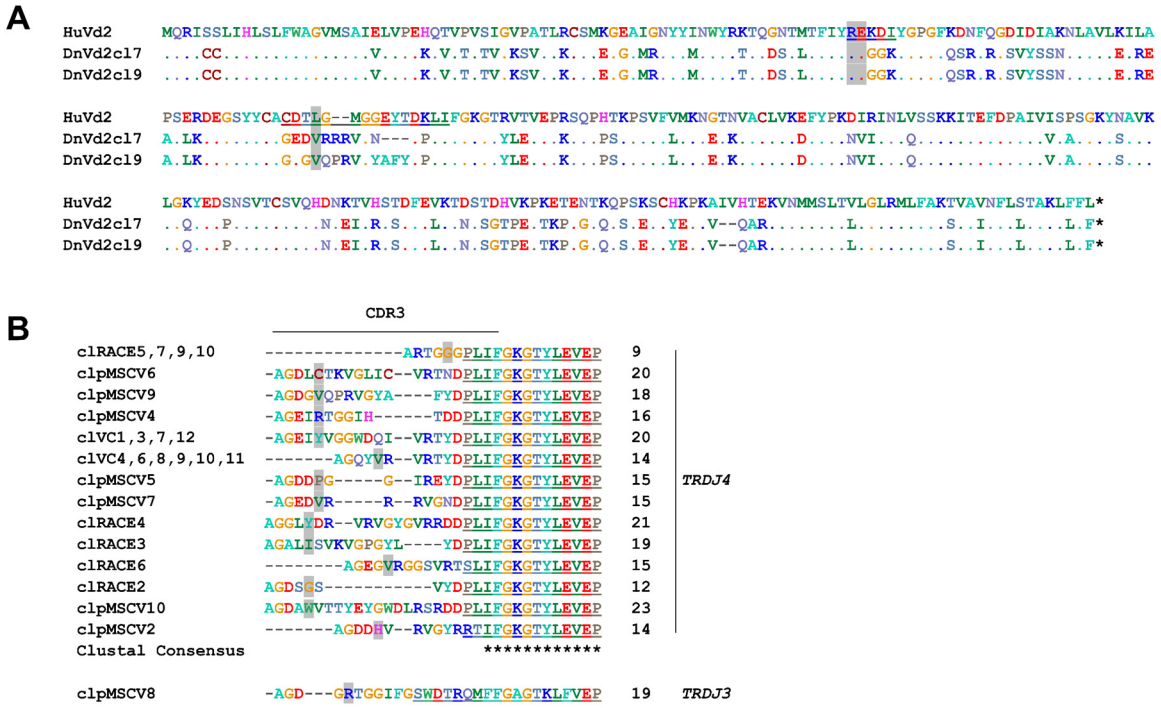

Figure 3.15 *In silico* translatable Vδ2 chains are expressed in *Dasypus novemcinctus* PBMCs. (**A**) Alignment of human G115 Vδ2 chain (PDB: 1HXM_A) [245] and two representative armadillo Vδ2 chains (pMSCV-IRES-mCherry FP dnVδ2 cl.7/9). (**B**) CDR3 regions of *TRDV2* clones obtained by *TRDV2/TRDC* (clVC1, 3, 4 and 6-12), *TRDV2* 3' RACE PCR (cl2-7, 9, 10) and cloning into pMSCV-IRES-mCherry FP (clpMSCV2, 4-10). CDR3 lengths as well as *TRDJ* usage are indicated. Identical amino acids (dots), gaps (dashes) and CDR1-3 (underscored) are indicated. The conserved positions δ51/52 [241, 245, 246] and δ97 [247] are highlighted in gray. GenBank accession numbers: cl2 (MG021118); clVC1 (MG021131); clVC4 (MG021132); cl3 (MG021127); cl4 (MG021128); cl5 (MG021129); cl6 (MG021130); clpMSCV2 (MG807648); clpMSCV4 (MG807649); clpMSCV5 (MG807650); clpMSCV6 (MG807651); clpMSCV7 (MG807652); clpMSCV8 (MG807653); clpMSCV9 (MG807654); clpMSCV10 (MG807655). Figure and figure legend adapted from [326].

As shown in **Figure 3.15A**, two clones obtained from the cloning of full-length armadillo Vδ2 chains in an expression vector showed amino acid sequence conservation of 65% to the human G115 Vδ2 TCR chain [245]. The *TRDV* region shared a 77% nucleotide and 59% amino acid identity with the human Vδ2 TCR chain, and the *TRDJ* region was 88% (NT) and 82% (AA) identical to the human *TRDJ4*. One clone was found to be rearranged with a *TRDJ3* homolog

with identities of 88% (NT) and 89% (AA) to the human counterpart (**Figure 3.15B**). Only the human *TRDJ1-3* gene segments have been reported to be used in phosphoantigen-reactive Vδ2 chains [241], however, alpacas preferentially use *TRDJ4* genes (see 3.2.2.1, 3.2.2.5 and [317]). Human phosphoantigen-reactive Vγ9Vδ2 T cells use *TRDV2* rearrangements with certain conserved features like varying CDR3 lengths and the encoded residues R51 [241, 245, 246] and E52 [245]. Additionally, the presence of a hydrophobic amino acid (L, I, V) at position δ97 was reported to be critical for phosphoantigen-dependent activation of Vγ9Vδ2 T cells [241, 247]. To investigate this, eight clones of the 3' RACE PCR product, ten clones of the *TRDV2*/*TRGC* amplification and eight clones from the cloning of Vδ2 in pMSCV-IRES-mCherry FP were analyzed. All of them were productive rearrangements, *in silico* translatable and CDR3 lengths varied from 9 to 23 amino acids (**Figure 3.15B**). The positions R51 and E52 were conserved in all clones and 5 of 15 unique CDR3 sequences carried a valine (V) or isoleucine (I) at position δ97.

Two Vδ2 clones (pMSCV-IRES-mCherry FP dnVδ2 cl7 and 9) were co-expressed with the human Vγ9 MOP TCR chain (pEGN huVγ9 MOP) in the TCR-negative mouse cell line BW58 r/mCD28 [347, 348]. Surface expression was verified using the vector-encoded fluorescent proteins EGFP (pEGN) and mCherry (pMSCV-IRES-mChery FP) and surface staining of huVγ9, huVδ2 and mouse CD3.

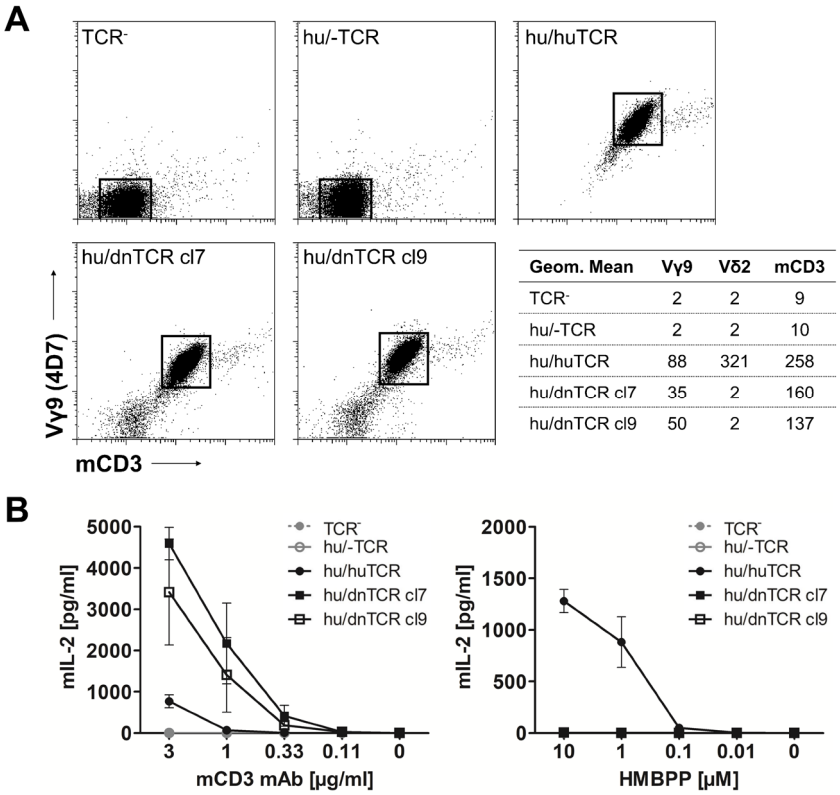

Figure 3.16 Surface expression of a functional armadillo Vδ2 TCR chain. (**A**) Armadillo Vδ2 TCR chains (pMSCV-IRES-mCherry FP dnVδ2 cl.7/9) were retrovirally transduced into TCR-negative murine cell lines (BW58 r/mCD28). The human Vγ9Vδ2 TCR MOP chain (pEGN huVγ9 MOP, GenBank: KC170727.1) was co-transduced, and TCR surface expression was confirmed by flow cytometry stainings of human Vγ9, Vδ2, and mouse CD3. Dotplots of Vγ9 (Y-axis, log) and CD3 (X-axis, log) co-stainings are shown, and GM of Vγ9, Vδ2, and CD3 stainings are indicated. (**B**) BW58 r/mCD28 cells and TCR transductants were cultured for 22 h in 96 well plates coated with α-mCD3 mAb or with RAJI-RT1B^{1} cells in the presence of increasing amounts of HMBPP. Mean+SEM of three independent experiments is shown for each cell line. Stimulation of hu/huTCR with 10 µg/ml α-mCD3 mAb resulted in 651 pg/ml mIL-2 (SEM: 129). Figure and figure legend adapted from [326].

Surface expression of human TCRs (pEGN huVγ9 MOP and pIZ huVδ2 MOP) and successful pairing of human Vγ9 and armadillo Vδ2 in hu/dnTCR cl7/9 (pEGN huVγ9 MOP and pMSCV-IRES-mCherry FP dnVδ2 cl7/9) was shown by staining of Vγ9, Vδ2 and CD3 (**Figure 3.16A**). In contrast, no surface TCR was detected on BW58 r/mCD28 cells (TCR^{-}) or cells transduced with huVγ9 alone. Expression of Vγ9 and CD3 for heteromeric hu/dnTCRs was lower compared to expression of hu/huTCRs. Signaling of hu/dnTCRs was tested in stimulation assays using plate-bound anti-mouse CD3 antibody [317, 369] and substantial mIL-2 production was measured for hu/huTCR and hu/dnTCR expressing cell lines (**Figure 3.16B**). Saturation of huTCR transductants was reached at 3 µg/ml mAb as tested by additional stimulations with 10 µg/ml mAb. No CD3-mediated activation of control cells was observed. Reactivity of responder cells with hu/dnTCRs to HMBPP was not observed in co-culture with RAJI-RT1B^{1} cells, however, human Vγ9Vδ2 TCRs readily reacted to HMBPP. Therefore, productively rearranged Vδ2 chains of armadillos can be reported that pair with human Vγ9 chains to form a functional TCR but show no cross-reactivity to human BTN3.

3.2.1.3 Functional TCRγ chain rearrangements lack homologs to human *TRGV9*

The existence of an *in silico* translatable *TRGV9* segment in the armadillo genome (Accession: AAGV03121505.1 nt402-695) has been discussed before [267, 317] and this gene shares a nucleotide identity of 80% and an amino acid identity of 69% with the *TRGV9* segment of the human G115 TCR [245]. Database analysis revealed four different *TRG* constant regions homologous to the first exon of human *TRGC* in the armadillo wgs database that are subsequently referred to as *TRGC-A*, *-B*, *-C* and *-D*. The armadillo *TRGC-A*, *-B* and *-C* (Accession: *TRGC-A* Ex1 AAGV03121543.1; *TRGC-B* Ex1 AAGV03121550.1; *TRGC-C* Ex1 AAGV03121548.1) were fully translatable, the *TRGC-D* sequence (Accession: *TRGC-D* Ex1 AAGV03173223.1 nt672-373), however, can be considered a pseudogene. *TRGC-A* and *TRGC-B/C* were 94% identical on the nucleotide level, *TRGC-B* and *TRGC-C* shared 98% of their nucleotides. All armadillo *TRGC* exons are 80% identical to the nucleotide sequence of the first exon of the human *TRGC1*. Expression analysis of this armadillo *TRGV* segment was attempted with the PCR of *TRGV9*/*TRGC* and 3' RACE PCR from *TRGV9* using various primer combinations. The template DNA used for these amplifications was cDNA synthesized from armadillo PBMC RNA as described in chapter 3.2.1.1 and primers in the *TRGC* region were specific for *TRGC-A/B/C* or *TRGC-D*. The 3' end of the *TRGC* regions *-A*, *-B* and *-C* was amplified in a 3' RACE PCR with the primers A103 and A104. All PCR products obtained were subjected to TOPO TA cloning according to chapter 2.2.1.11, and single-cell sequences were analyzed.

Here we report that no evidence of transcripts of productive *TRGV9* rearrangements was detected in armadillo cDNA using these approaches. The amplification of 3' and 5' end of the armadillo constant regions *TRGC-A*, *-B* and *-C*, however, confirmed only the expression of *TRGC-A* and *-B* in armadillo PBMC cDNA. Mapping of *TRGC-A* to armadillo wgs contigs revealed the organization of this gene in three exons all located in the contig AAGV03121543.1 (Ex1: nt3646-3953, Ex2: nt7499-7548, Ex3: nt9731-9871). In contrast, comparison of the 3' end of *TRGC-B* to armadillo wgs contigs via NCBI BLAST identified not only the location of the remaining exons 2-4 of *TRGC-B* but also the location of four *TRGC-C* exons. The contigs comprising these sequences were AAGV03121550.1 (*TRGC-B* Ex1: nt3170-347; Ex2: nt7125-7178), AAGV03121548.1 (*TRGC-C* Ex1: nt6277-6590; Ex2: nt7441-7491), AAGV03121549.1 (*TRGC-B/C* Ex3: nt101-152; Ex4: nt 2384-2525) and AAGV03121551.1 (*TRGC-B/C* Ex3: nt1733-1784; Ex4: nt3978-4119). Additionally, the existence of other armadillo *TRG* transcripts was tested with a 5' RACE PCR from *TRGC* with the primer A86 and the inner primer A87.

A

V regions of *TRGC* 5'RACE clones	Name	*D. novemcinctus* wgs Location	*D. novemcinctus* wgs Identities %	*Homo sapiens* homologs	*Bos taurus* homologs
AAGV03121491.1 (2/23)	*TRGV2*	1977-2285	100	TRGV2 46%	TRGV8-1 47%
AAGV03121484.1 (3/23)	*TRGV4.1*	40190-40506	99/100	TRGV4 48%	TRGV8-3 46%
AAGV03121485.1 (4/23)	*TRGV4.2*	6942-7251	98/99/100	TRGV4 48%	TRGV8-1 45%
AAGV03121495.1 (6/23)	*TRGV4.3*	4127-4438	99/100	TRGV4 46%	TRGV8-1 51%
AAGV03121497.1 (1/23)	*TRGV8.1*	7075-7385	100	TRGV8 54%	TRGV9-2 53%
AAGV03121496.1 (4/23)	*TRGV8.2*	20045-20356	99	TRGV8 50%	TRGV9-2 48%
	TRGV8.4	20045-20356	90	TRGV8 46%	TRGV5-1 49%
AAGV03121492.1 (2/23)	*TRGV8.3*	14807-15113	100	TRGV8 47%	TRGV5-1 43%
AAGV03121542.1 (1/23)	*TRGmV6*	2171-2485	100	IGLV3-12 38%	TRGV10-1 64% *Canis lupus* TRGV5-2 65% *Mus musculus* TRGV6 56%

B

J Regions of *TRGC* 5'RACE clones	Name	*D. novemcinctus* wgs Location	*D. novemcinctus* wgs Identities %	*Homo sapiens* homologs	Other species
AAGV03121547.1 (6/23)	*TRGJ-A*	2929-2991	97/98/100	TRGJP1 71% (73%) TRGJP2 63% (84%)	79% *Myotis davidii* (GenBank: ELK34092.1, 100%)
AAGV03121549.1 (15/23)	*TRGJ-B*	14544-14609	96/98/100	TRGJP 80% (52%) TRGJP1 73% (57%)	79% *Ovis aries* (PIR: S36294, 73%)
AAGV03121543.1 (2/23)	*TRGJ-C*	184-238	94/98	TRGJP 75% (60%)	72% *Tursiops truncatus* (GenBank: CDG24288.1, 90%)

Figure 3.17 *TRG* transcripts homologous to human IMGT subgroup TRGV1 are expressed in armadillo PBMCs. (**A**) *Dasypus novemcinctus TRG* transcripts obtained by 5' RACE PCR from *TRGC* (Accession: *TRGC-A* Ex1 AAGV03121543.1; *TRGC-B* Ex1 AAGV03121550.1; *TRGC-C* Ex1 AAGV03121548.1) with associated wgs accession numbers based on sequence homologies and location in the respective contigs. Armadillo *TRGV* segments were labeled according to their closest homolog in human or mouse. Varying nucleotide identities to genomic sequences and putative amino acid homologs in human and other species are indicated. Amino acid homologs were determined with the IMGT/DomainGapAlign tool [330-332]. (**B**) *TRGJ* regions of *TRGC* 5' RACE clones with location in wgs contigs and identities. Designations of J regions of the armadillo are random as distinct homologs to human *TRGJ* could not be determined. Homologies were determined by NCBI blastp to AA sequence of human germline encoded J regions or the NCBI non-redundant protein sequence database for other species. Figure and figure legend adapted from [326].

Out of 23 clones obtained from a 5' RACE PCR of *TRGC* only eight sequences were fully translatable TCR γ chains. The location of the *TRGV* and *TRGJ* gene segments in armadillo wgs contigs and the identity to those genomic database entries was determined using the NCBI BLAST tool (**Figure 3.17A**). All *TRGV* regions used in the TOPO TA sequences could be assigned to be homologous to genes of the human TRGV1 (*TRGV1-8*) subgroup of *TRGV* genes. Amino acid identities to the human homologs were determined with the IMGT/DomainGapAlign webtool and ranged from 46% to a maximum of 54% amino acids. Interestingly, higher sequence identities were found for *Bos taurus TRGV* (43-64%). One armadillo *TRGV* transcript was not detected to be homologous to any human *TRGV* but shared 56% identity with mouse *TRGV6*. The V regions in all clones were rearranged with *TRGJ* segments of three subtypes (*TRGJ-A*, *TRGJ-B* and *TRGJ-C*) as listed in **Figure 3.17B**. Homologies of translated *TRGJ* varied from 63-80% amino acid identity to translated human *TRGJ* sequences and query cover ranged from 52-84% making a prediction of homologies difficult.

Gene usage *in silico* translatable clones		
TRGV	***TRGJ***	***TRGC***
TRGV4.2	*TRGJ-A*	*TRGC-B/C*
TRGV2 (2x)	*TRGJ-B*	*TRGC-B/C*
TRGV4.1	*TRGJ-B*	*TRGC-B/C*
TRGV8.4 (2x)	*TRGJ-B*	*TRGC-B/C*
TRGV8.1	*TRGJ-C*	*TRGC-A*
TRGmV6	*TRGJ-C*	*TRGC-A*

Table 3.4 Gene usage of *in silico* translatable *TRGC* 5' RACE clones. Eight out of 23 clones obtained from 5' RACE PCR from armadillo *TRGC* with indicated gene usage according to homologies to human and mouse. Homologies were determined by NCBI blastp to AA sequence of human germline encoded J regions or the NCBI non-redundant protein sequence database for other species. Figure and figure legend adapted from [326].

Interestingly, the *TRGJ-A* and *TRGJ-B* segments in the armadillo seemed to associate with *TRGV* different from the ones found in rearrangements with *TRGJ-C* (**Table 3.4**). Additionally, the *TRGC* usage of *TRGJ-C* was apparently restricted to *TRGC-A* in contrast to the other J segments that potentially used *TRGC-B* or *-C*. These two constant regions could, however, not be distinguished in this experimental setup. A bias in *TRGC* usage is typical for a *TRG* locus organized in a cassette structure, as seen in artiodactyls or the bottlenose dolphin (IMGT-Locus representations). In summary, due to the lack of evidence for a productive *TRGV9* rearrangement in armadillos and the expression of other TCR γ chains we propose a lack of Vγ9Vδ2 TCRs in *Dasypus novemcinctus*.

3.2.2 The alpaca: the first non-primate species with functional Vγ9Vδ2 T cells

3.2.2.1 *TRG* and *TRD* repertoire of alpaca PBMCs

Study of the alpaca γδ TCR repertoire is hampered by lack of annotated genomic information. The main focus of this study in alpacas are the previously identified Vγ9 and Vδ2 chains and the proof of functional Vγ9Vδ2 T cells [317]. In addition, a more in-depth analysis of the whole array of *TRGV* and *TRDV* segments used in this animal model was pursued to gain more information on the γδ repertoire of *Vicugna pacos*. For this purpose, unstimulated alpaca PBMCs were used for generation of RACE-ready cDNA as described in the chapters 2.2.1.6 and 2.2.1.9, followed by 5' RACE PCR with primers located in the γ and δ constant regions (see 2.1.8). TOPO TA cloning of RACE PCR products was used to study single clones in these PCR products containing γ and δ chain transcripts (see 2.2.1.11). These experiments were part of a student's project and performed by M. Englert.

Amplification of γ chain transcripts was performed with the GeneRacer 5' Primer and the A195 primer specific for the first exon of three distinct genomic *TRGC* regions determined by NCBI Blast. A total of 39 out of 49 clones, generated from TOPO TA cloning, carried *TRGV*-like rearrangements. *In silico* translation of these rearrangements confirmed productive rearrangements in 37 clones. The coding sequences of 39 clones were compared to the currently available genomic information on *Vicugna pacos*, which included the whole genome shotgun database available in the NCBI database (BioProject: PRJNA30567/PRJNA233565, BioSample: SAMN01096418/SAMN02996813) and information retrieved from the Ensembl genome browser (vicPac1 assembly). Nucleotide identities of more than 98%, due to potential polymorphisms and alleles, were considered a genomic match. One *Vicugna pacos* wgs contig (JEMW01012530.1) contained a complete *TRG*-like locus and was therefore used as a reference for genomic organization. In order to determine the genomic organization of the γ chain constant regions, a known and functional constant region used by a Vγ9-chain (GenBank: KF734082) was used for an NCBI blastn search in the alpaca wgs database. Three γ chain constant regions were mapped in Ensembl scaffolds and JEMW01012530.1.

TRGC	Ensembl	JEMW01012530.
C-A Ex1	15900:667-996	165211-165540
C-A Ex2	n.a.	169147-169182
C-A Ex 3	n.a.	170759-170902
C-B Ex 1	5798:30769-31102	207438-207771
C-B Ex 2	n.a.	213021-213164
C-C Ex 1	n.a.	234327-234655
C-C Ex 2	n.a.	239976-240119

Table 3.5 Genomic organization of three distinct constant regions used in alpaca TCR γ chains. Location in the *Vicugna pacos* whole genome shotgun contig JEMW01012530.1 (NCBI blastn) and Ensembl vicPac1 assembly (BLASTN) was determined using the NT sequence of a full-length alpaca Vγ9 chain (GenBank: KF734082). Ensembl scaffold number and location in the scaffold are indicated. "n.a." indicates a failure to identify scaffolds/locations due to BLASTN or database limitations. *TRGC* genes were randomly labeled as *-A*, *-B*, *-C*.

The constant regions used by alpaca γ chain were labeled as *TRGC-A*, *TRGC-B* and *TRGC-C* due to inconclusive homologies to the human *TRGC1* and *TRGC2* genes (**Table 3.5**). The alpaca *TRGC-A* gene was comprised of three exons, whereas for *TRGC-B* and *-C* only two exons homologous to the constant region within the database entry KF734082 could be assigned. The first exon of *TRGC-A* was 80% and 82% nucleotide-identical to the first exons of *TRGC-C* and *TRGC-B*, respectively. Exon 1 of *TRGC-B* and *TRGC-C* shared 92% nucleotide identity. Exon 3 of *TRGC-A* and the second exons of *TRGC-B* and *TRGC-C* were completely nucleotide identical. Closer analysis of all isoforms revealed that one exon of *TRGC-B* and *TRGC-C*, corresponding to exon 2 of *TRGC-A*, was probably not found through homology searches. There is no indication of defects in the *TRGC-B* or *TRGC-C* gene so far, but reconstruction of a complete *TRGC-B* or *TRGC-B* constant region was not possible in this setting. Human *TRGC1* encodes for a cysteine residue in exon 2 which leads to the covalent linkage of γδ TCRs. *TRGC2* does not encode for this cysteine, and γδ TCRs using this constant region are non-covalently associated [370, 371]. This cysteine residue is conserved in *TRGC-A,* but the corresponding exon could have been overlooked for *TRGC-B* and *TRGC-C*.

The genomic organization of *TRGJ* segments used by alpaca constant region 5' RACE clones was determined by NCBI blastn and Ensembl BLASTN and mapped in the wgs contig JEMW01012530.1 and different Ensembl scaffolds. Recombination signal sequences of *TRGJ* genes were predicted using the human model for 12 bp spacer RSS sites of the webtool RSSsite [337] and consensus splice donor sites at the 3' end of J segments were predicted using the Human Splicing Finder web tool [336].

TRGJ	Ensembl	JEMW01012530.1	Human *TRGJ* % AA
JP	2184:236674-236739 or 15900:6254-6313	159577-159636	*TRGJP*01* 68%
JP1	15900:7263-7322	158567-158626	*TRGJP1*01* 68%
(F) J1/2-B	134788:148-197	163176-163225	*TRGJ1*01/J2* 01* 56%
JP2	5798:23833-23892	200499-200558	*TRGJP2*01* 63%
J1/2-A	41580:1685-1733	231383-231431	*TRGJ1*01/J2* 01* 63%

Table 3.6 Genomic organization of *TRGJ* homologs in *Vicugna pacos*. *TRGJ* segments used in unstimulated alpaca PBMCs were mapped in the *Vicugna pacos* whole genome shotgun contig JEMW01012530.1 (NCBI blastn) and Ensembl vicPac1 assembly (BLASTN). Locations are indicated, and amino acid sequence identities to homologous human *TRGJ* segments were calculated based on Clustal Omega alignments.

Five distinct *TRGJ* segments homologous to human *TRGJP*, *-JP1*, *-JP2* and *-J1* or *J2* (IMGT) were used by alpaca γδ cells in this experiment (**Table 3.6**). Amino acid identities with the human homologs were 68% for *TRGJP* and *TRJP1* and 63% for *TRGJP2* and *TRGJ1/2-A*. One *TRGJ* segment was found by NCBI Blastn of the alpaca *TRGJ1/2-A* gene segment to the contig JEMW01012530.1. Recombination signal sequence analysis revealed a functional RSS site, however, the nucleotides 8-10 after the RSS site code for a termination codon. Therefore, this gene could potentially represent a pseudogene and was assigned *TRGJ1/2-B* due to 83% nucleotide identity to alpaca *TRGJ1/2* and no conclusive homology to human *TRGJ*. This gene segment was not found in any clone. Expression of productive Vγ9 and Vδ2 chains was first described by Karunakaran et al. in *Vicugna pacos,* and different variants of *TRJP* were described (*TRGJP-A*, *-B*, *-C*) [317]. *TRGJP* usage of the clones in this experiment was *TRGJP-B* (genomic variant) in all cases but for clone 18 which used *TRGJP-A*. This usage of very similar *TRGJP* gene segments hints at the existence of different alleles for *TRGJP* in the alpaca and usage of both chromosomes for rearrangements (see 3.2.2.5). In the following, the nomenclature of *TRJP-A*, *-B* and *-C* will be used to assign alpaca *TRJP* gene segments [317]. Other *TRGJ* gene segments were described (JP1, JP2, J1). Here, we could confirm the existence of the JP, JP1 (now assigned *TRGJ1/2-A* according to revised homologies with human) and JP2 (now assigned *TRGJP1*) gene segments in the alpaca *TRG* locus. The last gene segment described by M. Karunakaran as J1 was used by a single clone in that study and could not be assigned to a genomic counterpart [317]. It is shorter than but identical to *TRGJP-B,* and the occurrence of this gene segment could be explained by higher exonuclease activity in this clone.

In the same fashion, variable regions used by all 39 clones were assigned to scaffolds in the vicPac1 assembly and the JEMW01012530.1 contig. Homologies to human variable genes were determined by NCBI blastn of all human *TRGV* genes (IMGT Repertoire human *TRG*), and homologs in other species were identified in published amino acid sequences using NCBI blastp (Non-redundant protein sequence database) or the IMGT/DomainGapAlign web tool [330, 332].

Table 3.7 *TRGV* homologs and *TRGJ* usage of unstimulated alpaca PBMCs. *TRGV* genes used in unstimulated alpaca PBMCs were determined by NCBI blastn (*Vicugna pacos* wgs database) and Ensembl BLASTN (vicPac1 assembly). Locations in the NCBI contig JEMW01012530.1 and various Ensembl scaffolds are indicated. Homologies to human IMGT *TRGV* genes were calculated, and homologs in other species were determined by [1]NCBI blastp (Non-redundant protein sequence database) or the [2]IMGT/DomainGapAlign Tool [330, 332]. The *TRGJ* and *TRGC* usage of clones are indicated as well as clone numbers and identifiers. "/" indicates clones with identical nucleotide sequences, *clones with non-productive rearrangements.

TRGV	Ensembl	JEMW01012530.1	Human *TRGV* % NT/AA	Other species % AA	*TRGJ/TRGC*	# clones (unique)	clone #
V9	2184:228836-229155	136909-137228	*TRGV9*01* 77/73%	[1]*C. ferus* (GenBank: EPY80787.1, 91%) [1]*T. truncatus* (GenBank: CDG24291.1, 76%)	*JP-B / C-A*	2 (1)	23/39
V10	229312:605-922	143970-144287	*TRGV10*01* 78/62%	[1]*C. ferus* (GenBank: EPY80788.1, 95%) [2]*Bos taurus* (IMGT: *TRGV3-1*01*, 74%)	*JP-A / C-A*	1 (1)	18
V11	285425:290-606	149393-149709	*TRGV11*01* 70/52%	[2]*B. taurus* (IMGT: *TRGV7-1*01*, 71%)	*JP-B / C-A*	8 (8)	6, 7, 15, 19, 29*, 33, 42, 50
					JP1 / C-A	9 (8)	3, 5, 11, 20, 31, 32/35, 34, 49
V8-A	43587:1320-1633	186209-186522	*TRGV8*01* 66/47%	[2]*C. dromedarius* (IMGT: *TRGV1*01*, 78%) [2]*B. taurus* (IMGT: TRGV8-3*02, 57%)	*JP2 / C-B*	2 (2)	4, 45*
					J1/2 / C-C	2 (1)	10/16
V8-B	5798:18529-18839	190702-191012	*TRGV8*01* 67/46%	[2]*C. dromedarius* (IMGT: *TRGV1*01*, 79%) [2]*B. taurus* (IMGT: *TRGV8-1*01*, 60%)	-	-	-
V8-C	-	195191-195501	*TRGV8*01* 71/53%	[2]*C. dromedarius* (IMGT: *TRGV1*01*, 68%) [2]*B. taurus* (IMGT: *TRGV8-1*01*, 65%)	*JP2 / C-B*	11 (6)	1/14/41, 17/21, 24/28/30, 36, 37, 44
VA	149312:1-255	223265-223572	*TRGVA*01* 55/49%	[2]*C. dromedarius* (IMGT: *TRGV2*01*, 96%) [2]*B. taurus* (IMGT: *TRGV6-2*01*, 65%)	*J1/2 /C-C*	4 (4)	22, 26, 27, 38

As listed in **Table 3.7**, the usage of seven distinct *TRGV* genes could be verified in alpaca unstimulated PBMCs. One homolog each for human *TRGV9*, *TRGV10*, *TRGV11* and *TRGVA* were assigned to alpaca variable genes. The most conserved variable gene segment was the *TRGV9* homolog with amino acid conservation of 73% to human *TRGV9*. In contrast, *TRGV10*-, *TRGV11*-, and *TRGVA*-like genes were 49-62% homologous to their human counterparts. Three distinct *TRGV8*-like genes were identified with amino acid identities of around 50% to human *TRGV8*. These genes were labeled *TRGV8-A*, *-B* and *-C*. Identities of alpaca variable genes to published amino acid sequences of *Camelus* species were above 90% for *TRGV9*, *TRGV10* and *TRGVA* and somewhat lower for *TRGV8*-like genes (68-79% AA). No published *TRGV11*-like sequence was found for camels, however, a genomic counterpart to alpaca *TRGV11* (~95% nt) was found in *Camelus* species whole genome shotgun sequences (NCBI blastn).

The same experimental approach was applied to generate 5' RACE clones of δ chain transcripts in unstimulated alpaca PBMCs. Here, PCR amplification of RACE-ready cDNA with the GeneRacer 5' Primer and a primer specific for the alpaca *TRDC* gene (A198 or A199) were performed. After TOPO TA cloning of the PCR product, 43 out of 47 clones carried a *TRDV*/*TRDD*/*TRDJ* rearrangement (A198: clone 51-91; A199: clone 92-99). *In silico* translation revealed one clone with a non-productive rearrangement and two clones using distinct leader sequences that lead to a frameshift and termination codon after splicing. Those 43 clones were compared to the alpaca whole genome shotgun databases available at the NCBI website

(BioProject: PRJNA30567/PRJNA233565, BioSample: SAMN01096418/SAMN02996813) and the Ensembl vicPac1 assembly. Again, nucleotide identities of more than 98% were considered a match. In contrast to the γ chain, only one δ chain constant region was found in the alpaca. This was already published as part of a Vδ2 chain (GenBank: KF734083/KF734084) and in this study, the genomic organization was determined. The constant region *TRDC* is comprised of three exons which could be found within the NCBI wgs contig JEMW01030915.1 (Ex1: nt170716-170994; Ex2: 171560-171625; Ex3: 171952-172064). Three distinct *TRDJ* segments were found in the alpaca genome with two of them being used in rearrangements of 5' RACE clones. The third gene segment (*TRDJ3*) was used by one clone mentioned in chapter 3.2.2.5.

TRDJ	Ensembl	JEMW01030915.1	Human *TRDJ* % AA
J2	1276:31558 -31611	165759-165812	*TRDJ2*01* 94%
J3	1276:33869 -33928	168095-168154	*TRDJ3*01* 84%
J4	1276:30142 -30194	164341-164393	*TRDJ4*01* 73%

Table 3.8 Genomic organization of alpaca *TRDJ* homologs. *TRDJ* segments of unstimulated alpaca PBMCs were mapped in the *Vicugna pacos* wgs contig JEMW01030915.1 (NCBI blastn) and Ensembl vicPac1 assembly (BLASTN). Locations are indicated, and amino acid sequence identities to homologous human *TRDJ* segments were calculated based on Clustal Omega alignments.

The *TRDJ* genes of *Vicugna pacos* could be assigned to be homologs of human *TRDJ2* (94% AA), *TRDJ3* (84% AA) and *TRDJ4* (73% AA) and were all located in one Ensembl scaffold and in one NCBI wgs contig (**Table 3.8**). The identification of *TRDD* genes used in alpaca unstimulated PBMCs was performed by NCBI blastn of the whole gene unit of the human *TRDD1-3* genes (IMGT database). Four distinct *TRDD*-like gene units were found in the NCBI wgs contig JEMW01030915.1 (D1: 126342-126352; D2: 136567-136578; D3: 144955-144965; D4: 157458-157468) and assigned numbers, as no conclusive homology of the D genes to human *TRDD* could be determined. *TRDD* gene segments were assigned to clones where possible as depicted in **Table A.1**.

In contrast to humans, a multitude of *TRDV* segments was found to be used in alpaca PBMCs. For this, all 43 δ chains were assigned to scaffolds of the vicPac1 assembly (Ensembl) and various contigs of the NCBI wgs database. Homologies to human *TRDV* genes (IMGT) were determined by NCBI blastn, and amino acid homologies to published *TRDV* genes of *Camelus dromedarius* [372] were determined (see **Table 3.9**).

Table 3.9 *TRDV* homologs and *TRDJ* usage of unstimulated alpaca PBMCs. *TRDV* genes used in unstimulated alpaca PBMCs were determined by NCBI blastn (*Vicugna pacos* wgs database) and Ensembl BLASTN (vicPac1 assembly). Locations in the indicated NCBI contigs and various Ensembl scaffolds are given. Homologies to human *TRDV* genes were calculated, and homologs in other species were determined by NCBI blastp to published *C. dromedarius* genomic variable genes [372] or the [1]non-redundant protein sequence database. The *TRDJ* usage of clones is indicated as well as clone numbers and identifiers. Clones that could not be assigned a genomic equivalent are marked in gray and the closest match is indicated. "/" indicates clones with identical nucleotide sequences, *clones with non-productive rearrangements, **clones with leader sequences that lead to termination of translation in V region.

TRDV	BioProject PRJNA30567	BioProject PRJNA233565	Ensembl	Human *TRDV* % NT/AA	Other species % AA	*TRDJ*	# clones (unique)	clone #
V2	ABRR02141948.1: 63361-63658	JEMW01030915.1: 102335-102632	3124:1425 39-142836	*TRDV2*01/03* 75/56%	[1]*T. truncatus* (GenBank: CEF90299.1, 67%)	*J4*	1 (1)	94
V3	ABRR02141954.1: 5113-4805	JEMW01030915.1: 176680-176372	1276:4186 5-42173	*TRDV3*01* 80/68%	*C. dromedarius TRDV4*01* (GenBank: CAX65622.1, 93%)	*J4*	7 (6)	63/68, 72, 85**, 92, 95**, 98
cdV2	ABRR02325124.1: 1-209	JEMW01030914.1: 66955-67253	6090:4848 0-48778	*TRAV33*01* 71/%	*C. dromedarius TRDV2.1*01* (GenBank: CAX65619.1, 92%)	*J4*	4 (3)	53, 56/76, 58
V1-A	-	JEMW01030914.1: 3223-3520	-	*TRDV1*01* 78/71%	*C. dromedarius TRDV1.1*01* (GenBank: CAX65611.1, 84%)	-	-	-
V1-B	-	JEMW01030914.1: 38201-38498	-	*TRDV1*01* 78/71%	*C. dromedarius TRDV1.3*01* (GenBank: CAX65614.1, 88%)	*J4*	1 (1)	55
V1-B2	-	96% JEMW01030914.1: 38201-38498	-	*TRDV1*01* 77/69%	*C. dromedarius TRDV1.3*01* (GenBank: CAX65614.1, 89%)	*J4*	7 (6)	57, 59, 61, 66, 69/75, 77
V1-C	-	JEMW01019339.1: 1413-1719	-	*TRDV1*01* 76/68%	*C. dromedarius TRDV1.6*01* (GenBank: CAX65618.1, 86%)	-	-	-
V1-C2	-	94% JEMW01019339.1: 1413-1719	-	*TRDV1*01* 76/67%	*C. dromedarius TRDV1.1*01* (GenBank: CAX65611.1, 82%)	*J4*	1 (1)	67
V1-D	-	JEMW01027781.1: 12331-12035	288753:30 9-606	*TRDV1*01* 76/67%	*C. dromedarius TRDV1.1*01* (GenBank: CAX65611.1, 87%)	*J4*	2 (1)	96/99
V1-E	ABRR02169533.1: 1-256	JEMW01028483.1: 19804-19507	17284:305 7-3354	*TRDV1*01* 80/70%	*C. dromedarius TRDV1.1*01* (GenBank: CAX65611.1, 82%)	*J4*	2 (2)	62, 83
V1-F	ABRR02163404.1: 5702-5998		11492:399 0-4286	*TRDV1*01* 78/72%	*C. dromedarius TRDV1.6*01* (GenBank: CAX65618.1, 90%)	-	-	-
V1-G	ABRR02165380.1: 1331-1628	-	5546:5026-5323	*TRDV1*01* 76/69%	*C. dromedarius TRDV1.3*01* (GenBank: CAX65614.1, 93%)	*J2*	2 (1)	74/87
						J4	5 (4)	73/86, 81*, 93, 97
V1-H	ABRR02173114.1: 3028-2731	-	-	*TRDV1*01* 77/70%	*C. dromedarius TRDV1.1*01* (GenBank: CAX65611, 84%)	*J4*	8 (7)	51, 52, 60, 64/70, 65, 71, 78
V1-K	ABRR02258994.1: 135-432		180136:54 0-837	*TRDV1*01* 78/71%	*C. dromedarius TRDV1.6*01* (GenBank: CAX65618.1, 86%)	*J4*	2 (1)	80/82
V1-K2	96% ABRR02258994.1: 135-432	-	96% 180136:54 0-837	*TRDV1*01* 76/67%	*C. dromedarius TRDV1.6*01* (GenBank: CAX65618.1, 84%)	*J4*	1 (1)	84

A total of 15 distinct variable genes were found in the alpaca genome and δ chain 5' RACE clones (see **Table 3.9**). Single genes homologous to human *TRDV2* (56% AA identity) and *TRDV3* (68% AA identity) and a multimember family of *TRDV1*-like genes (67-72% AA identity) were identified. *TRDV1* genes were labeled alphabetically in no specific order. One variable gene, *cdV2*, could not be identified as a human *TRDV*-like gene segment but shows 92% amino acid conservation to the *Camelus dromedarius TRGV2*01* gene and thus named accordingly. In contrast to the *TRGV* genes of 5' RACE clones, some *TRDV* gene segments used by δ chain clones could not be assigned to a genomic *TRDV* (*TRDV1-B2*, *-C2* and *-K2*). In addition, genomic information of different databases did not completely overlap (< 98% conservation in contigs/scaffolds). This could be due to incomplete genomic information, allelic differences or polymorphisms in the alpaca.

In addition to studies of homology and genomic organization, the *TRGV*/*TRGJ* and *TRDV*/*TRDJ* usage of clones and their frequency was analyzed. Assignment of *TRDD* gene segments in each clone was omitted due to the usage of multiple D segments in some clones and D segments shortened by exonuclease activity.

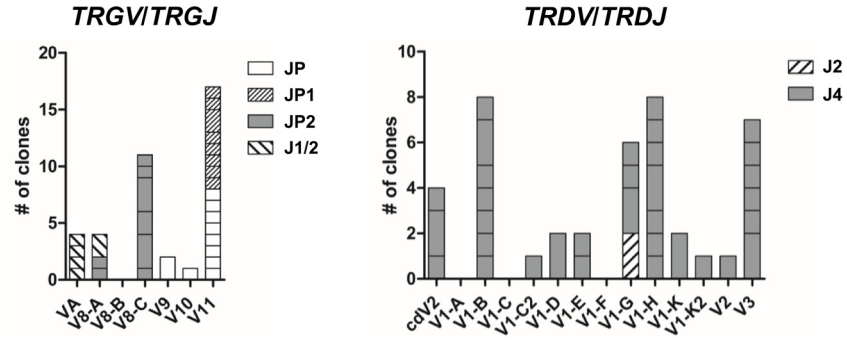

Figure 3.18 *TRV/TRJ* usage among alpaca constant region 5' RACE clones. *TRVs* used by 5' RACE clones as described in **Table 3.7** and **Table 3.9** were coded for *TRJ* usage as indicated. Boxes represent unique rearrangements and multiple clones with the same rearrangement are indicated by the size of distinct boxes.

The frequency of distinct *TRV/TRJ* combinations in unstimulated alpaca γδ T cells in the blood is shown in **Figure 3.18**. In the case of γ chains, a preference for *TRGV8-C* and *TRGV11* gene segments and a very low prevalence of *TRGV9* and *TRGV11* gene segments with one unique clone each could be observed. *TRGV8-C* was exclusively rearranged with *TRGJP2*, *TRGVA* exclusively used *TRGJ1/2*, and *TRGV9* and *TRGV10* were rearranged with *TRGJP*. The gene segments *TRGV8-A* and *TRGV11* were found to be rearranged with *TRGJP2* and *TRGJP1* or *TRGJP* and *TRGJP1*, respectively in a comparable frequency. The highest prevalence of multiple clones sharing the same nucleotide sequence was observed in the group of *TRGV8-C* gene segments. This is in contrast to *TRGV11*-carrying clones, where only two out of 17 clones were identical. Accordingly, a different level of polyclonality can be assumed for different populations of γδ T cells. Analysis of the *TRD* repertoire revealed a remarkable preference for *TRDJ4* usage in 97% of all δ chain clones. The *TRDJ3* segment was not used in this setting but was observed in an experiment described in chapter 3.2.2.5. The prevalence of *TRDV1-B*, *TRDV1-G*, *TRDV1-H* and *TRDV3* were higher compared to other V genes in this setting and usage of the *TRDV2* homolog was restricted to a unique clone. In contrast to the *TRG* repertoire, no preference for expanded clones could be seen for *TRDV* gene usage as identical clones could be found in most *TRDV* groups.

In order to provide a comprehensive view of the alpaca *TRG* and *TRD* repertoire, locus representations were created. As all *TRGV*, *TRGJ* and *TRGC* genes were located in one NCBI contig, a complete *TRG* locus could be mapped according to the location of each gene. Conversely, most *TRDV* genes were scattered in single contigs, and thus the genomic organization of three *TRDV* in one case and two *TRDV* and the *TRDD*, *TRDJ* genes, as well as TRDC, could be analyzed.

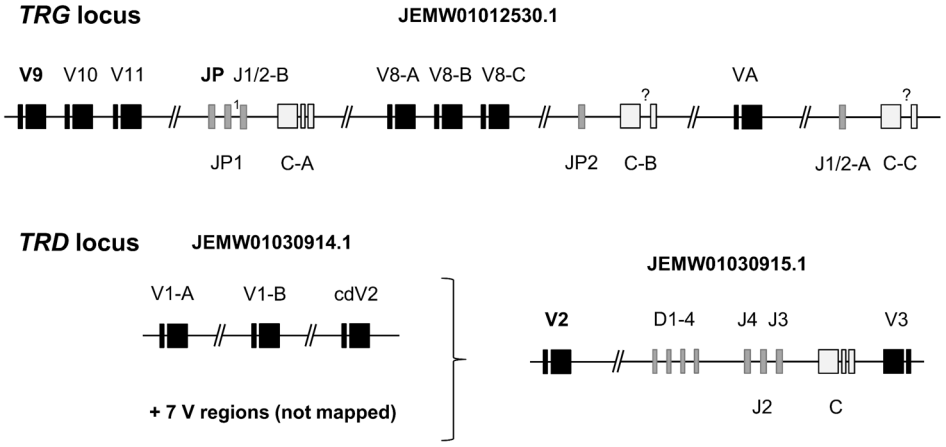

Figure 3.19 *TRG* and partial *TRD* locus representation of *Vicugna pacos*. The genomic organization of *TRG* and *TRD* genes was mapped. The whole genome shotgun contig is indicated for each locus and exons are represented by boxes: variable genes and leader sequences (black), diversity and junctional genes (gray) and constant region genes (white). Potentially missing exons are indicated (?). Variable gene 3 is located in reverse orientation in JEMW01030915.1 and *[1]JP1* was previously described as a homolog for human *JP2* [317].

The results from these experiments and database information were used to develop a schematic view of the TRG and TRD loci in the alpaca as seen in **Figure 3.19**. The *TRG* locus in alpacas could be shown to be organized in a cassette-like structure as described in other species like cattle and sheep (IMGT Locus representations). Thus, preference of certain *TRGJ* and *TRGC* genes can be explained by the genomic organization. The partial *TRD* locus shown here indicates a genomic organization of *TRDV* genes in a linear fashion with clustered *TRDD* and *TRDJ* genes upstream of *TRDC*. The *TRDV3* gene segment is reversely oriented as observed in the human *TRD* locus (IMGT Locus representations).

3.2.2.2 Production of monoclonal antibodies for alpaca Vγ9Vδ2 and BTN3

Due to a lack of reagents to study the BTN3/Vγ9Vδ2 T cell system in alpacas, monoclonal antibodies specific for the two essential parts of this system, the Vγ9Vδ2 T cell receptor and the BTN3 molecule were produced. The hybridoma technology, which was first described by C. Milstein and G. J. F. Köhler, was applied to develop hybridomas as described in chapter 2.2.5.

3.2.2.2.1 Vγ9Vδ2 antibodies

Immunization of BALB/c mice as described in chapter 2.2.5.1 was carried out using mouse permanent cell lines overexpressing an alpaca Vγ9Vδ2 TCR. The mouse B lymphoma cell line M12 and the mouse fibroblast cell line L929 were first transduced with a vector encoding all four subunits of mouse CD3 and sorted on the co-expressed EGFP gene (see 2.2.3.6 and 2.2.3.9). Subsequently, the sorted cells were transduced with alpaca Vγ9 (pEGZ vpVγ9) and Vδ2 (pIH vpVδ2 cl. 9) chains and sorted on mouse CD3 surface expression assessed by flow cytometry staining with an anti-mouse CD3ε antibody (BD Pharmingen). Representative data for CD3 expression on M12 and L929 vpVγ9Vδ2 cells are shown in **Figure 3.20**.

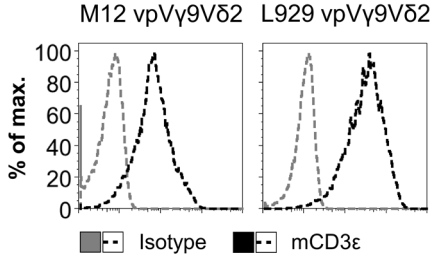

Figure 3.20 CD3 expression of alpaca Vγ9Vδ2 transductants. M12 or L929 cells transduced with mouse CD3 (pMIG II mCD3 δ-F2A-γ-T2A-ε-P2A-ζ), the alpaca Vγ9 TCR chain (pEGZ vpVγ9) and the alpaca Vδ2 TCR chain (pIH vpVδ2 cl. 9). A number of $1*10^5$ cells, previously sorted on GFP^{high} expression, were stained with α-mCD3ε antibody (1 µg/ml, BD Pharmingen) or hamster IgG isotype control (BD Pharmingen) and detected with SA-APC (400 ng/ml, BD Pharmingen). Histograms of a representative staining of mCD3ε of both cell lines are shown.

Transduction of alpaca Vγ9 and Vδ2 TCR chains into the lymphoma cell lines M12 and L929 expressing mouse CD3 resulted in the detection of mouse CD3 via flow cytometry as seen in **Figure 3.20**. Mouse CD3 could only be detected at the surface in combination with TCR chain overexpression which proved surface expression of the alpaca Vγ9Vδ2, without being able to stain this TCR directly. As a proof of concept, a human Vγ9Vδ2 TCR was transduced into both cell lines and stained with an antibody specific for human Vδ2 (data not shown). The L929 vpVγ9Vδ2 TCR transductants were further used to immunize mice and produce hybridomas according to the chapters 2.2.5.1 and 2.2.5.2. Screening of more than 900 hybridoma culture supernatants on M12 vpVγ9Vδ2 cells resulted in the identification of seven positive clones. After subcloning, isotype testing was performed using the Mouse Monoclonal Antibody Isotyping Test Kit (BioRad) and the clones 118.7 (mIgG1, κ), 118.11 (mIgG1, κ), 257.6 (mIgG2a, κ), and 697.3 (mIgG2b, κ) were purified by L. Starick according to the protocol described in chapter 2.2.5.3.

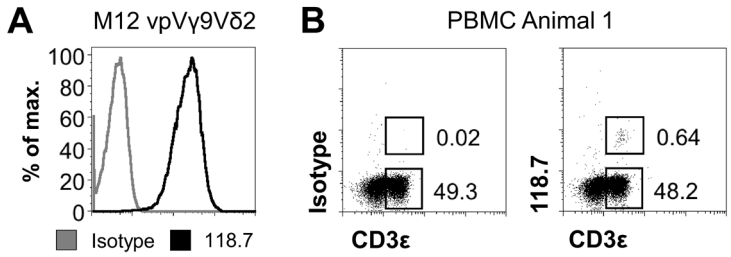

Figure 3.21 The monoclonal antibody 118.7 stains vpVγ9Vδ2 transductants and detects a small population of CD3⁺ alpaca PBMCs. (**A**) The purified mAb 118.7 (0.5 µg/ml, labeled with Fab mIgG1 R-PE) was applied in stainings of M12 vpVγ9Vδ2 transductants (pMIG II mCD3 δ-F2A-γ-T2A-ε-P2A-ζ, pEGZ vpVγ9 and pIH vpVδ2 cl. 9) A representative staining is shown with geometric means of 3.75 (isotype) and 203 (118.7). (**B**) Staining of alpaca PBMCs was performed with the mAb 118.7 (0.5 µg/ml, labeled with Fab mIgG1 R-PE) and the Fixable Viability Dye eFluor® 660 (1:1000, eBioscience), followed by intracellular α-huCD3ε FITC (2 µg/ml, Abd Serotech) staining using the Foxp3/Transcription Factor Staining Buffer Set (eBioscience). The cells were gated on Viability Dye-negative, live cells and the lymphocyte population was determined by FSC (lin) and SSC (log). The frequencies of 118.7⁺ CD3⁺ and 118.7⁻ CD3⁺ cells are indicated in percent of live cells. A representative staining of animal 1 is shown.

A typical staining of 118.7 on M12 cells transduced with an alpaca Vγ9Vδ2 TCR is shown in **Figure 3.21A**. The 118.7 staining, as well as those with all other positive hybridoma supernatants, correlated with mCD3 surface expression tested by antibody staining (data not shown). Additionally, all hybridoma supernatants tested could stain all cell lines overexpressing vpVγ9Vδ2 TCRs with either of two distinct delta chains encoded in pIH vpVδ2 cl.8 (GenBank: KF734083) or pIH vpVδ2 cl.9 (GenBank: KF734084). Those Vδ2 chains had varying CDR3 lengths of 21 and 16 amino acids, respectively, and a glycine (cl.8) or leucine (cl.9) at position δ97 [247, 317]. However, the antibodies were all tested negative for cross-reactivity to the human Vγ9Vδ2 TCR (data not shown). Positive staining of BW cells overexpressing human and alpaca heteromeric TCRs, comprising a human Vγ9 and an alpaca Vδ2 chain, narrowed the potential epitope down to the alpaca Vδ2-chain. The antibody 118.7 was neither cross-reactive to an alpaca TCR with a Vδ2Jδ2 chain overexpressed in BW or 53/4 cells (see 3.2.2.9) nor to Vδ2Jδ3 TCRs as determined by sorting and repertoire analysis (see 3.2.2.5). Therefore, a specificity of 118.7 to alpaca Vδ2Jδ4 chains is likely. The monoclonal antibody 118.7, as well as other hybridoma supernatants (data not shown), were used for PBMC stainings (see 2.2.3.5 and 2.2.3.8) depicted in **Figure 3.21B**. A small but distinct population of alpaca CD3⁺ lymphocytes was stained with the antibody 118.7, and great variations were observed among different animals and some variation between blood samples of the same animal (see **Table A.2**).

3.2.2.2.2 BTN3 antibodies

The strategy for developing a monoclonal antibody for alpaca BTN3 was the same applied for Vγ9Vδ2 in chapter 3.2.2.2.1. First, L929 cells were transduced with the complete coding sequence of alpaca BTN3 cloned into the vector pMIG II as described in 2.2.1.13 and 2.2.3.6. The cells were sorted on the EGFP co-expressed with alpaca BTN3, and BTN3 surface expression was tested with the human anti-BTN3 antibodies 20.1 (agonist) and 103.2 (antagonist) [48, 244]. Those antibodies readily detected alpaca BTN3 when overexpressed in a cell line but did not stain PBMCs.

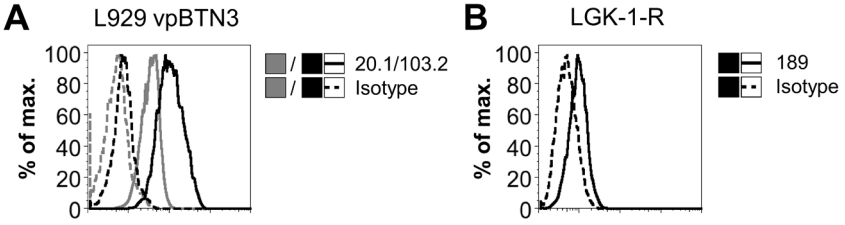

Figure 3.22 BTN3 expression of transduced permanent cell lines and alpaca cells. (**A**) L929 cells transduced with pMIG II vpBTN3 were stained with the α-huBTN3 mAbs 20.1 (3.1 µg/ml) and 103.2 (2.2 µg/ml), and their isotypes mIgG1 (Affymetrix) and mIgG2a (Affymetrix), respectively. The purified antibodies were detected with DαM R-PE (1 µg/ml, Jackson ImmunoResearch). A representative staining of sorted cells is shown, and geometric means of this staining (isotype/antibody) were as follows: 20.1 (4.65/31.8), 103.2 (6.97/103). (**B**) Alpaca kidney primary cells (LGK-1-R) were stained with 50 µl hybridoma cell culture supernatant and isotype control (detected with DαM R-PE, Jackson ImmunoResearch). A representative staining with gating on live cells according to FSC (lin) and SSC (log) is shown and the GMs are 4.65 (isotype) and 8.64 (189).

A representative staining of L929 cells expressing alpaca BTN3 is shown in **Figure 3.22A**. An apparent shift of the sorted cells could be observed, and staining of the mAb 103.2 was superior to that of 20.1. Immunizations of BALB/c mice were carried out with this cell line according to chapter 2.2.5.1 and hybridomas were produced as described in chapter 2.2.5.2. Following HAT-selection, cell culture supernatants were tested for antibody production on Raji cells transduced with alpaca BTN3 (pEGZ vpBTN3) and supernatants of 41 clones were tested positive. Specificity and affinity of those antibodies for endogenous alpaca BTN3 were tested on the alpaca kidney primary cell line LGK-1-R (see 2.2.3.5). Among 41 hybridomas producing antibodies specific for overexpressed alpaca BTN3, only the supernatant of clone 189 contained antibodies that distinctly stained endogenous alpaca BTN3 of the LGK-1R cell line (**Figure 3.22B**). The isotype of clone 189 was subsequently identified as mIgG2b, yet, subcloning was not successful due to contamination with a hybridoma producing mIgG1 antibodies not specific for alpaca BTN3. Single-cell sorting (see 2.2.3.9) of 189 cells on surface mIgG2b using an isotype-specific antibody and subcloning resulted in nine monoclonal hybridomas of which clone 189.21 was single-cell cloned and the single-cell clone 189.21.17 was purified from cell culture supernatants according to chapter 2.2.5.3.

Cross-reactivity of the hybridoma 189 to human BTN3A1 and comparison with 20.1 and 103.2 mAbs was tested using CHO cells overexpressing alpaca or human BTN3-mCherry fusion proteins encoded in the phNGFR mCherry vector (see 2.2.1.13 and 2.2.3.6).

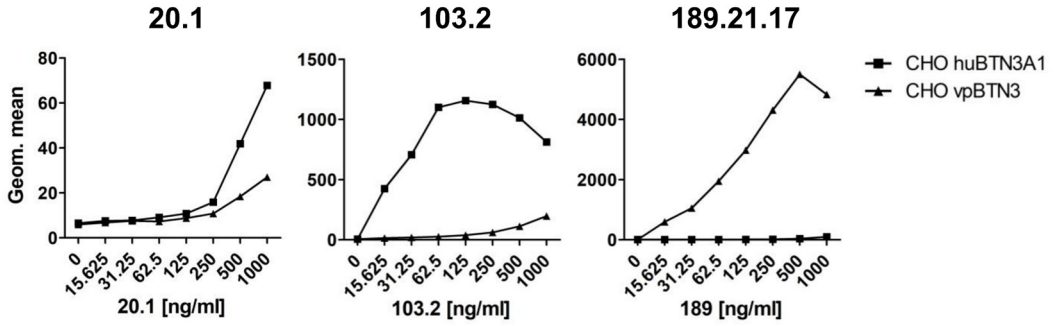

Figure 3.23 Cross-reactivity of BTN3 antibodies to human and alpaca BTN3. CHO cells were transduced with S65T huCD80 and phNGFR mCherry huBTN3A1 or phNGFR mCherry vpBTN3 and sorted for mCherry^{high} cells. 1*10^5 cells per sample were stained with the α-BTN3 antibodies 20.1, 103.2 and the subclone 189.21.17 and detected with DαM R-PE (1 µg/ml, Jackson ImmunoResearch). Live cells were gated on mCherry$^+$ cells (GM: huBTN3A1 54, vpBTN3 74) and GMs of DαM R-PE stainings were calculated. The isotype controls used were mIgG1, mIgG2a and mIgG2b, respectively and are indicated by "0 ng/ml" antibody.

Overexpression of alpaca BTN3 and human BTN3A1 in BTN3-negative CHO cells enabled the comparison of staining performance of the antibodies 20.1, 103.2 and 189 (**Figure 3.23**). Following live cell gating according to FSC/SSC (lin/log), the cells were gated on mCherry$^+$ cells. The cell line overexpressing huBTN3A1 showed slightly lower mCherry levels (GM: 54) compared to vpBTN3 (GM: 74). Titrations of the mAb 20.1 showed 2.5-fold higher geometric means upon staining of huBTN3A1 compared to vpBTN3, even though mCherry levels were lower. Higher affinity of 20.1 to huBTN3A1 can, therefore, be assumed. However, 20.1 stainings were poor compared to the mAb 103.2. This antibody showed a strong staining performance on huBTN3A1 expressed by hamster cells with saturating concentrations starting at 62.5 ng/ml of 103.2 antibody per sample. Cross-reactivity of vpBTN3 was visible, but the staining performance was not nearly as pronounced compared to huBTN3A1. In contrast, staining efficacy of vpBTN3 with the alpaca-specific antibody 189.21.17 showed very high signals on vpBTN3. A saturating dose of 500 ng/ml could be observed. Cross-reactivity to huBTN3A1 could be shown but yielded staining intensities comparable to 20.1 mAb (GM at 1 µg/ml: 99).

Following titrations on permanent cell lines, human and alpaca PBMCs were stained with different concentrations of 20.1, 103.2 and 189.21.17 (1 µg/ml, 100 ng/ml and 10 ng/ml). The histograms of one representative staining are shown in **Figure 3.24**.

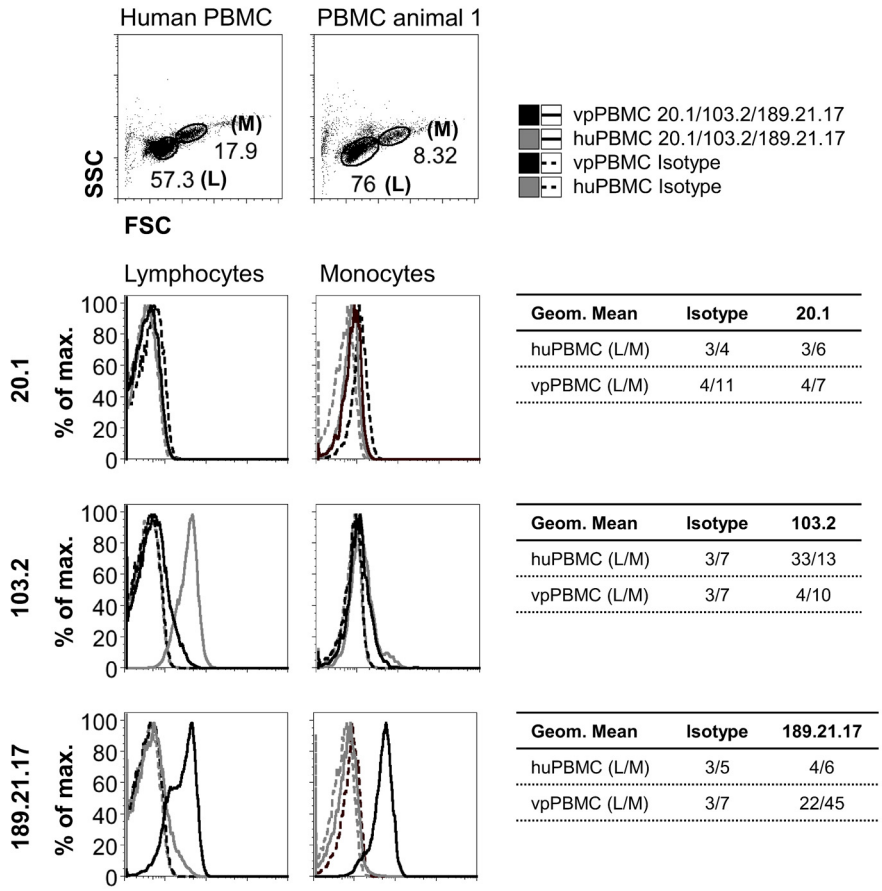

Figure 3.24 BTN3 expression by lymphocytes and monocytes in human and alpaca PBMCs. Human PBMCs (donor 349) and alpaca PBMCs of animal 1 (isolation date 4.4.17) were stained ($1*10^5$ per sample) with the α-BTN3 antibodies 20.1, 103.2 and the subclone 189.21.17 and detected with DαM R-PE (1 µg/ml, Jackson ImmunoResearch). Lymphocytes (L) and monocytes (M) were gated according to size (FSC, lin) and granularity (SSC, log) and frequencies of total events are shown. Histograms for each antibody including isotype controls are depicted for human (hu) and alpaca (vp) PBMCs. The geometric means of all samples are indicated. The isotype controls used were mIgG1, mIgG2a and mIgG2b, respectively.

BTN3 antibody stainings of human and alpaca PBMCs revealed less pronounced staining capacities of all three BTN3-specific antibodies. The lymphocyte and monocyte subsets of both species were analyzed in this experiment (**Figure 3.24**). No distinct staining was observed on human or alpaca PBMCs in stainings with mAb 20.1. This indicates a very low affinity of this antibody for BTN3 on primary cells. In comparison, a clear shift was observed in human lymphocytes when 103.2 was applied. However, no apparent staining of human monocytes and alpaca lymphocytes or monocytes was observed with 103.2. In contrast, alpaca lymphocytes and monocytes were distinctly stained by 189.21.17 mAb. The geometric mean of alpaca monocytes was 2-fold compared to lymphocytes. Human PBMCs could not be stained with this antibody. Therefore, despite cross-reactivity of 20.1 and 103.2 to alpaca BTN3, only the alpaca-specific antibody 189.21.17 can be applied for stainings of alpaca PBMCs.

3.2.2.3 Characterization of alpaca PBMCs

The relative scarcity of information on the expression of surface molecules and potential markers on alpaca cells led us to investigate antibodies specific for llama surface molecules [354]. The antibodies described in that study were developed in mice immunized with llama peripheral blood leukocytes, thymocytes or lymphocytes stimulated with ConA and also included cross-reactive antibodies developed for other species [354]. Flow cytometry was applied by the authors to identify and cluster epitopes recognized by these antibodies, and they have been reported to be cross-reactive for *Vicugna pacos* surface molecules [354]. Assignments of reactivity to molecules equivalent to human clusters were labeled LaCD and antibodies recognizing uncertain epitopes were designated LC. The antibody clones (recognized cluster) used here were first GB45A (BoWC1), an antibody specific for goat WC1 which also shows cross-reactivity to llama, bovine and ovine PBMCs. Antibodies raised against llama epitopes were LT3A, which recognizes CD5-like molecules (LaCD5), LT1A an antibody specific for MHCII in llama, cattle, sheep and goats, LT5A probably reactive to CD8 (LaCD8) and LT10A which recognizes an unknown surface marker on αβ T cells with low expression on B cells (LC1 cluster). The 189 antibody developed in this project (see 3.2.2.2.2) was also used and co-stainings with 118.7 (see 3.2.2.2.1) or anti-CD3 mAb. The stainings were carried out using alpaca PBMCs (see 2.2.3.5) of animal 1 and 2.

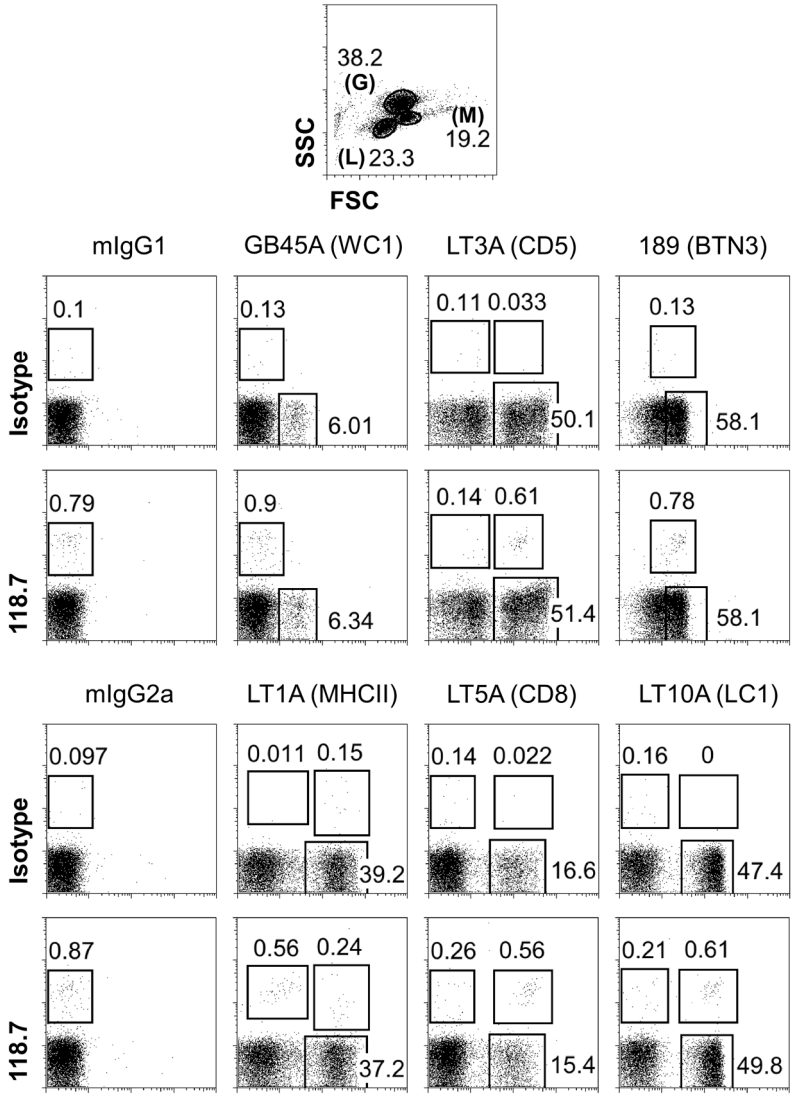

Figure 3.25 Characterization of alpaca 118.7⁺ lymphocytes. PBMCs of animal 1 were stained with the antibodies GB45A (1:8000), LT3A (1:10000), 189 (50 µl supernatant), LT1A (1:10000), LT5A (1:1000), LT10A (1:8000) and the isotypes mIgG1 (Affymetrix) and mIgG2a (Affymetrix) and detected with DαM FITC (3 µg/ml, Jackson ImmunoResearch). Samples were blocked with NmIg (1:100) and stained with mIgG1 or 118.7 pre-incubated with Fab mIgG1 fragments R-PE (0.5 µg/ml, Jackson ImmunoResearch). Cell viability was analyzed with the Fixable Viability Dye eFluor® 660 (1:1000, eBioscience). Gating of Viability Dye-negative, live cells (FSC:lin/SSC:log) is indicated as well as granulocytes (G), monocytes (M) and the lymphocyte gate (L). Lymphocytes were analyzed for surface markers (x-axis) and 118.7 (y-axis). Frequencies of live cells are indicated next to the gates.

The surface expression of WC1, CD5, BTN3, MHC II, CD8 and the staining of a marker for αβ T cells in the context of 118.7 staining is depicted in **Figure 3.25** for PBMCs of animal 1. The same staining was performed with PBMCs of animal 2 (data not shown) and yielded comparable results. The lymphocyte population (L) was defined by size and granularity and CD3 expression patterns. Monocyte populations (M) were verified by co-staining of CD14 and CD3 with an antibody raised against swine CD14 and cross-reactive with llama, bovine, ovine and caprine PBMCs (LaCD14, CAM36A mAb) [354]. Granulocytes (G) did not express CD14 or CD3. In the following, the expression of surface markers on the lymphocyte population will be discussed.

The overall frequency of 118.7^{+} lymphocytes was 0.69-0.77% without background staining, showing a slight variability among samples in one experiment. About 6% of live cells expressed WC1 (GB45A), a marker for γδ T cells in cattle [373-375], but not the Vδ2-chains stained by 118.7. CD5 (LT3A) was expressed by half of all lymphocytes in animal 1 in two distinct levels, and all 118.7^{+} cells express this surface molecule. The CD5 expression of 118.7^{+} T cells could be assigned to the CD5^{low} population of alpaca lymphocytes. BTN3, as stained by the clone 189, was detected on all lymphocytes with 58% of live cells showing a higher expression. The 118.7^{+} population belonged to the BTN3^{high} population of live cells (~58% of live cells). Interestingly, 118.7^{low} cells (0.09% w/o background) were co-stained by the antibody LT1A, a marker for MHC II expression, while 118.7^{high} cells (0.56% w/o background) were not. The overall frequency of MHC II-expressing cells was ~38% in the lymphocyte subset of PBMCs. Staining for the co-receptor CD8 revealed a population of about 16% CD8^{+} cells with a majority of 118.7^{+} (0.54% w/o background) being also CD8^{+}. The last marker tested in this experiment (LT10A), was reported to potentially stain CD2, CD6 or αβ T cells in general, however, the exact surface molecule is not known [354]. Approximately 50% of lymphocytes were stained by LT10A, and again, almost all 118.7^{+} cells were stained, too. To further investigate the surface markers applied here, intracellular CD3 staining was performed.

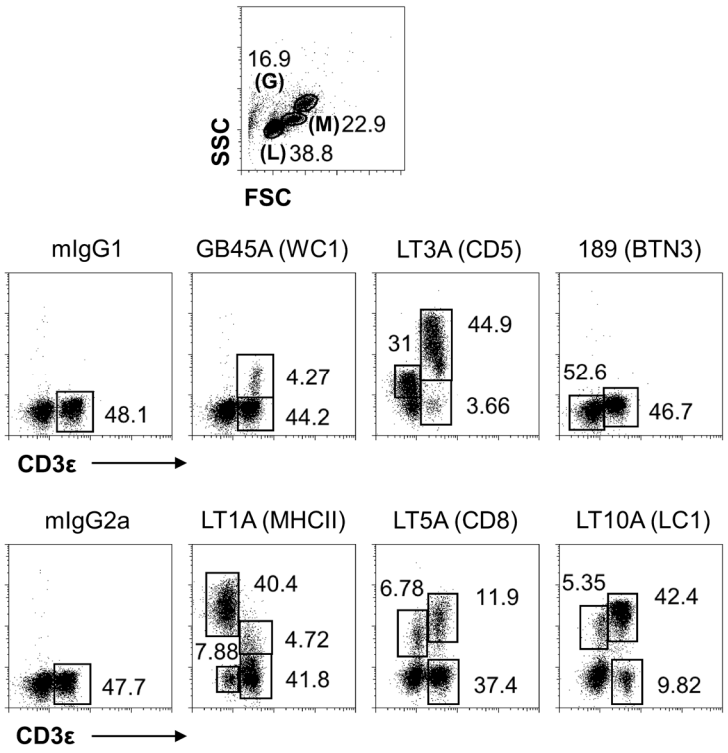

Figure 3.26 Characterization of alpaca lymphocytes with different surface markers and CD3. PBMCs of animal 1 were stained with the antibodies GB45A (1:8000), LT3A (1:10000), 189 (50 µl supernatant), LT1A (1:10000), LT5A (1:1000), LT10A (1:8000) and the isotypes mIgG1 (Affymetrix) and mIgG2a (Affymetrix) and detected with DαM R-PE (1 µg/ml, Jackson ImmunoResearch). Samples were blocked with NmIg (1:100) followed by intracellular staining with α-huCD3ε FITC (2 µg/ml, Abd Serotech) using the Foxp3/Transcription Factor Staining Buffer Set. Cell viability was analyzed with the Fixable Viability Dye eFluor® 660 (1:1000, eBioscience). Gating of Viability Dye-negative, live cells (FSC:lin/SSC:log) is indicated as well as granulocytes (G), monocytes (M) and lymphocytes (L). The lymphocyte gate was analyzed for CD3 (x-axis) and surface markers (y-axis). Frequencies of live cells are indicated next to the gates.

Co-expression of the previously described surface markers with CD3 on alpaca PBMCs is shown in **Figure 3.26** for animal 1. The same staining was carried out on PBMCs of animal 2 and no differences in staining patterns were observed (data not shown). In the following, lymphocytes (L) were analyzed for the expression of a panel of surface markers in context with CD3 expression. Analysis of the lymphocyte population for CD3ε expression revealed CD3 expression on approximately half of the cells. WC1 (GB45A) was detected on 9% of $CD3^+$ cells (about 4% of lymphocytes). LT3A staining revealed a major $LT3A^+CD3^+$ lymphocyte population (92% of $CD3^+$ cells), seemingly divided into two expression levels. A small but distinct population of LT3A-negative $CD3^+$ cells (8% of $CD3^+$ cells) was observed, and 31% of the cells did not express CD3 but were stained in a low fashion with LT3A. This high background staining or low-level expression of CD5 was also observed in co-staining with 118.7 in **Figure 3.25**. Regarding BTN3 expression, T cells showed higher expression of BTN3 (GM: 5.2) in comparison to $CD3^-$ cells (GM: 3.83). In contrast, MHC II was only highly expressed on $CD3^-$ cells (84% of $CD3^-$) and 10% of CD3-expressing cells shifted when stained with LT1A. The remaining $CD3^+$ cells was stained in a low fashion, which could be due to background staining.

Two populations of CD8$^+$ cells with distinct expression levels were observed. One population was positive for CD3 with a higher expression level of CD8, indicating cytotoxic T cells and the other one was CD3$^-$ which could represent NK cells. Finally, LT10A stained most but not all CD3$^+$ T cells and 11% of CD3$^-$ cells. The CD3$^+$ population negative for LT10A staining hints at the total γδ T cell frequency in the PBMCs of this animal. Another llama antibody assumed to be cross-reactive to CD3 [354] was tested on alpaca PBMCs as described before. To confirm CD3-specificity, an intracellular anti-human CD3ε antibody (AbD Serotech) cross-reactive to many species was applied.

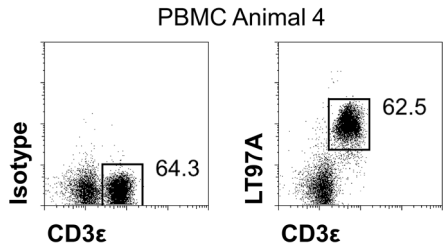

Figure 3.27 The llama antibody LT97A is cross-reactive to alpaca surface CD3. Alpaca PBMCs (1*10^5) were stained with isotype control or LT97A (1:200) and detected with DαM R-PE (1 µg/ml, Jackson ImmunoResearch). The samples were subsequently stained intracellularly with α-huCD3ε FITC (2 µg/ml, Abd Serotech) using the Foxp3/Transcription Factor Staining Buffer Set. Lymphocytes were determined by FSC (lin) and SSC (log) signals and double staining of intracellular CD3ε (x-axis) and LT97A (y-axis) is shown.

Double staining of both antibodies revealed complete overlapping of LT97A$^+$ and CD3ε$^+$ cells (**Figure 3.27**). Thus, the specificity of LT97A to alpaca CD3 was confirmed. FITC labeling of this antibody was performed (data not shown). However, CD3 surface staining of stimulated alpaca PBMCs on day 7 after HMBPP or IL-2 culture was not successful.

3.2.2.4 A subset of alpaca Vδ2$^+$ T cells expands upon HMBPP stimulation

The potential phosphoantigen reactivity of alpaca PBMCs was assessed by culture of PBMCs with the phosphoantigen HMBPP in the presence of hIL-2 as described in chapter 2.2.3.7 and analyzed by a flow cytometry staining with the antibody 118.7 and intracellular staining for CD3ε (see 2.2.3.8). For this, the cells of each well were split into an isotype control and the 118.7 staining. A list of 118.7$^+$ cell frequencies in PBMCs of different animals before and after stimulations with HMBPP is shown in **Table A.2** and **A.3**. In order to study the dose-response of alpaca PBMCs to HMBPP, a stimulation with different concentrations of this antigen was performed in parallel with human PBMCs (donor 346).

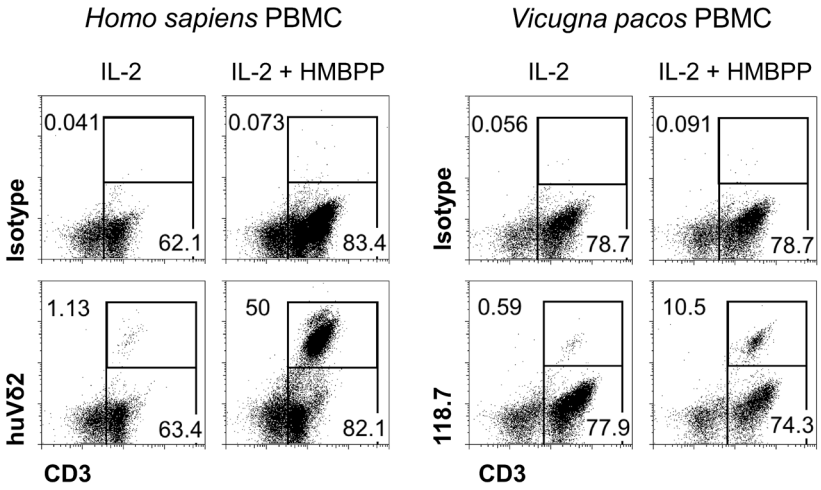

Figure 3.28 Alpaca 118.7⁺ cells increase in frequency upon HMBPP stimulation. Human and alpaca PBMCs (animal 2) were cultured in quadruplicates with a cell density of $1*10^5$ cells per sample (in 200 µl, 96 well plate) in the presence of 50 U/ml hIL2 (Novartis Pharma) with or without 100 nM HMBPP. On day 7, the samples were stained with 118.7 (0.5 µg/ml, labeled with Fab mIgG1 R-PE) for alpaca or huVδ2 PE (400 ng/ml, BD Pharmingen) and the Fixable Viability Dye eFluor® 660 (1:1000, eBioscience), followed by intracellular α-huCD3ε FITC (2 µg/ml, Abd Serotech) staining using the Foxp3/Transcription Factor Staining Buffer Set (eBioscience). The cells were gated on Viability Dye-negative, live cells and the lymphocyte population was determined by FSC/SSC. The CD3 staining is visualized on the x-axis and the isotype/Vδ2/118.7 staining on the y-axis. The frequencies of $Vδ2^+/118.7^+CD3^+$ and $Vδ2^-/118.7^-$ $CD3^+$ cells are indicated in percent of live cells. One staining out of four is shown as a representative dotplot.

The gating strategy applied for the analysis of alpaca and human PBMC stimulations is shown in **Figure 3.28**. The lymphocyte gate was determined by staining with Viability Dye (eBioscience) and FSC/SSC signal, and those cells were then evaluated by 118.7 or Vδ2 staining and CD3 fluorescence. In both species, two levels of CD3 could be observed, and the staining with Vδ2 and 118.7 resulted in a distinct population of $CD3^{high}$ cells in alpaca and human samples. CD3 expression correlated with cell size and $CD3^{high}$ could be assigned to enlarged activated cells, whereas $CD3^{low}$ cells were similar in size to unstimulated lymphocytes. It is noteworthy that not all $CD3^{high}$ cells in the alpaca samples were also positive for 118.7 as seen in the human HMBPP stimulated cells. After seven days of culture, human PBMCs reached a $Vδ2^+$ cell frequency of 50% in the presence of 100 nM HMBPP, and about 1% of cells were positive for Vδ2 in the control samples. In contrast, 10% of alpaca PBMCs were positive for the antibody 118.7 on day 7 of stimulation with 100 nM HMBPP, and 0.5% 118.7^+ T cells could be observed in the IL-2 control. The data obtained from this experiment was summarized in frequencies of $Vδ2^+$ and 118.7^+ cells and total cell numbers in **Figure 3.29**.

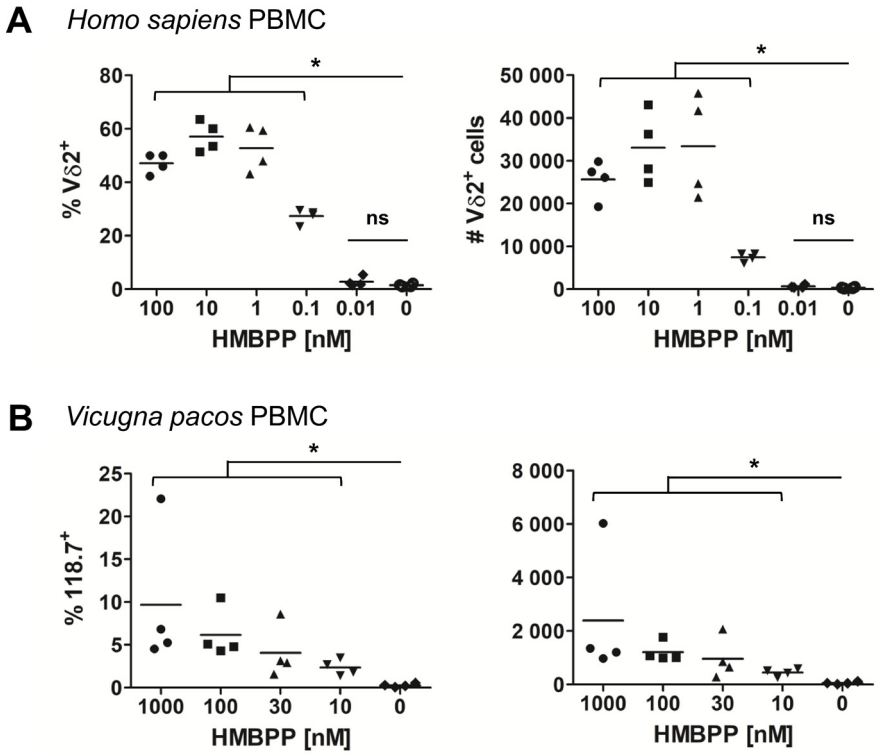

Figure 3.29 Alpaca 118.7⁺ cells proliferate upon HMBPP stimulation. Human and alpaca PBMCs (animal 2) were cultured in quadruplicates with a cell density of $1*10^5$ cells per sample (in 200 µl, 96 well plate) in the presence of 50 U/ml hIL2 (Novartis Pharma) with or without increasing doses of HMBPP. On day 7, the samples were stained with 118.7 (0.5 µg/ml, labeled with Fab mIgG1 R-PE) for alpaca or huVδ2 PE (400 ng/ml, BD Pharmingen) and the Fixable Viability Dye eFluor® 660 (1:1000, eBioscience), followed by intracellular α-huCD3ε FITC (2 µg/ml, Abd Serotech) staining using the Foxp3/Transcription Factor Staining Buffer Set (eBioscience). The cells were gated on Viability Dye-negative, live cells and the lymphocyte population was determined by FSC (lin) and SSC (log). The frequencies of Vδ2⁺/118.7⁺CD3⁺ cells were calculated by subtracting the frequency of the isotype gate (see **Figure 3.28**), and total cell numbers of each sample were measured by Calibrite™ Beads (10^4 per sample, BD). The medians of HMBPP stimulations were compared to the hIL-2 control in a two-tailed Mann-Whitney U test with 95% confidence intervals. Significant differences are indicated by * ($p > 0.05$), no significant difference is indicated by "ns".

The analysis of Vδ2⁺ and 118.7⁺ cell frequencies (w/o background) of alpaca and human PBMCs cultured with HMBPP is summarized in **Figure 3.29**. Here, one experiment was performed in quadruplicates, where each sample was split into isotype control, and 118.7 staining and cell numbers were calculated based on cell counts of both which was measured by Calibrite™ Beads (BD). After stimulation with a range of HMBPP concentrations (0.01-100 µM), human Vδ2 frequencies increased in a dose-dependent manner from around 2% of unstimulated lymphocytes up to more than 60% of live cells at day 7 of stimulation (**Figure 3.29A**). Saturating conditions were observed starting at 1 µM HMBPP, and no significant increase in Vδ2⁺ was detected at 0.01 µM HMBPP compared to the control samples. At the highest dose of HMBPP (100 µM), the frequency of Vδ2⁺ cells decreased compared to 10 and 1 µM doses. This was reflected in the total cell numbers calculated for Vδ2⁺ cells. Up to $4.5*10^4$ live Vδ2⁺ cells could be detected on day 7, indicating a 30-fold increase in cell numbers compared to an estimated number of $1.5*10^2$ Vδ2⁺ cells in $1*10^5$ cells used for stimulations (data not shown). In comparison, alpaca

118.7+ cell frequencies increased in a less pronounced albeit significant manner upon HMBPP stimulation (**Figure 3.29B**). No definite saturating HMBPP dose could be determined, although 10-fold higher concentrations were used. The variance of 118.7+ frequencies among conditions was pronounced in comparison to the human PBMC stimulation. At the highest HMBPP concentration a maximum of 22% of live cells and 6000 total 118.7+ cells were observed. Nonetheless, a 20-fold increase in 118.7+ cells was observed in comparison to stainings of unstimulated lymphocytes of this animal (~300 cells in $1*10^5$ or 0.5% of live cells (see **Table A.2**)). This clearly indicates proliferation of alpaca 118.7+ cells upon HMBPP stimulation.

In addition to the HMBPP dose-response experiment, the effects of BTN3-specific antibodies on the HMBPP reactivity of alpaca PBMCs were studied. For this, the antagonistic antibody 103.2 [48], the agonistic antibody 20.1 [244] and the alpaca BTN3-specific antibody 189 (see 3.2.2.2.2) were added to PBMCs cultured with 100 nM HMBPP and hIL-2.

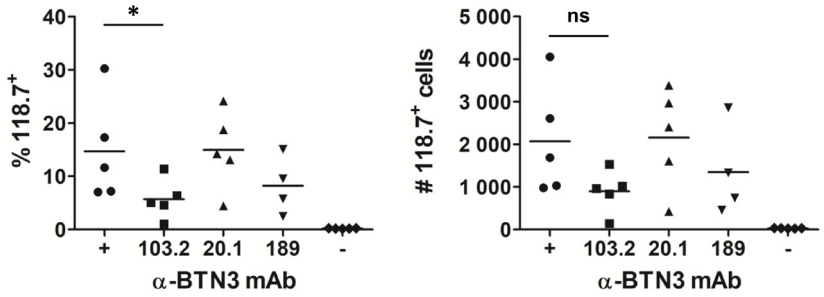

Figure 3.30 Effect of BTN3 antibodies on HMBPP reactivity in PBMC. Alpaca PBMCs (animal 1) were cultured in quadruplicates ($1*10^5$ cells in 200 µl, 96 well plate) in the presence of 50 U/ml hIL2 (Novartis Pharma) with 100 nM HMBPP (+) and the antibodies 103.2 (1 µg/ml), 20.1 (1 µg/ml) or 189 (20 µl culture supernatant). hIL-2 w/o HMBPP was used as a negative control (-). On day 7 samples were stained with 118.7 (0.5 µg/ml, Fab mIgG1 R-PE) and the Fixable Viability Dye eFluor® 660 (1:1000, eBioscience), followed by intracellular α-huCD3ε FITC (2 µg/ml, Abd Serotech) staining. Cells were gated on Viability Dye-, live cells and the lymphocyte population was determined by FSC (lin)/SSC (log). Frequencies of 118.7+CD3+ cells were calculated by subtracting the frequency of the isotype gate (data not shown), and total cell numbers were measured by acquisition of the complete sample. Medians of 103.2, 20.1 and 189 were compared to the HMBPP stimulation in a two-tailed Mann-Whitney U test with 95% confidence intervals. Significant difference is indicated by * ($p > 0.05$), no significant difference is indicated by "ns".

The effect of BTN3-specific antibodies on the HMBPP-dependent increase of 118.7+ cells in alpaca PBMCs is shown in **Figure 3.30**. Among the antibodies used, frequencies of 118.7+ cells were significantly reduced solely upon addition of 103.2 mAb. This was not observed for 118.7+ total cell numbers on day 7 of stimulation. The mAb 20.1 did not have a visible effect on 118.7+ cell proliferation. Yet, the culture supernatants of the alpaca BTN3-specific antibody 189 seemed to reduce the increase of 118.7+ cells slightly. As seen in the HMBPP stimulation of PBMCs of animal 2 in **Figure 3.29**, the variance among quadruplicates in this experiment with PBMCs of animal 1 was pronounced, ranging from less than 10% to around 30% of 118.7+ cells.

3.2.2.5 CDR3 repertoire of unstimulated and expanded alpaca T cells

The presence of *in silico* translatable *TRGV9* and *TRDV2* chains in unstimulated alpaca PBMCs was previously shown by M. Karunakaran [317, 321]. In alpacas, *TRGV9* was found to preferentially rearrange with different variants of *TRGJP* (*JP-A*, *JP-B* or *JP-C*) [317]. The *TRDV2* chain rearranged with a *TRDJ4* homolog in 16 out of 17 clones and in one case with a *TRDJ2* homolog [317]. To investigate this further, the antibody 118.7, specific for alpaca Vδ2 chains, was applied to sort alpaca PBMCs before and after HMBPP stimulation. For this, $3*10^5$ alpaca PBMCs (see 2.2.3.5) were stimulated in a 48 well plate in 1 ml RPMI++ medium with 1 µM HMBPP in the presence of hIL-2 (50 U/ml) for seven days. Cultured and unstimulated PBMCs were sorted on live (Fixable Viability Dye eFluor® 660, eBioscience) 118.7^+ and 118.7^- cells (see 2.2.3.8 and 2.2.3.9) and RNA was isolated as described in chapter 2.2.1.6. First strand cDNA synthesis was performed following the protocol in chapter 2.2.1.8 and *TRGV9* and *TRDV2* chains were amplified in a Phusion PCR (see 2.2.1.10) using primers in the variable and constant regions. The primers used for this experiment were 67 vpVγ9 fwd and 69 vpCγ rev for *TRGV9*/*TRGC* and 68 vpVδ2 fwd as well as 70 vpCδ rev for the amplification of *TRDV2*/*TRDC*. This experiment was performed with PBMCs of animal 1 and 2. Comparison of five conditions (complete PBMCs; unstimulated (-): $118.7^{+/-}$; HMBPP: $118.7^{+/-}$) showed a differential pattern of PCR signal for *TRGV9*/*TRGC* and *TRDV2*/*TRDC* amplifications analyzed by agarose gel electrophoresis (see 2.2.1.1). The *TRGV9*/*TRGC* signal was very weak when cDNA of unstimulated 118.7^+ or 118.7^- cells was used as a template. A difference in *TRGV9* expression between 118.7^+ or 118.7^- cells was observed for animal 2 (118.7^+ signal < 118.7^- signal) but not for animal 1 (118.7^+ signal ~ 118.7^- signal). After seven days of HMBPP stimulation the intensity of the *TRGV9*/*TRGC* PCR products bands increased significantly for both, 118.7^+ or 118.7^- cells (118.7^+ signal > 118.7^- signal). A similar outcome was observed for *TRDV2*/*TRDC* PCR amplifications, with less PCR product in unstimulated cells and a high amount in HMBPP-stimulated cells (118.7^+ signal > 118.7^- signal). In both, animal 1 and 2, only a very faint PCR product band was visible in a PCR with cDNA from unstimulated 118.7^- cells. All PCR products were analyzed by sequencing (see 2.2.1.12), and three different outcomes were observed. One observation was termination of sequences (fwd and rev) by overlapping signals in the CDR3 region indicating the same *TRV* and *TRC* gene but different *TRJ* or CDR3 regions. The second possibility was complete sequence reads indicating a mostly monoclonal composition of the PCR product. In the third case, overlapping signals were observed in the CDR3 region and complete sequence reads of *TRV* to *TRC* or vice versa, were obtained due to similar CDR3 lengths of an oligoclonal PCR product.

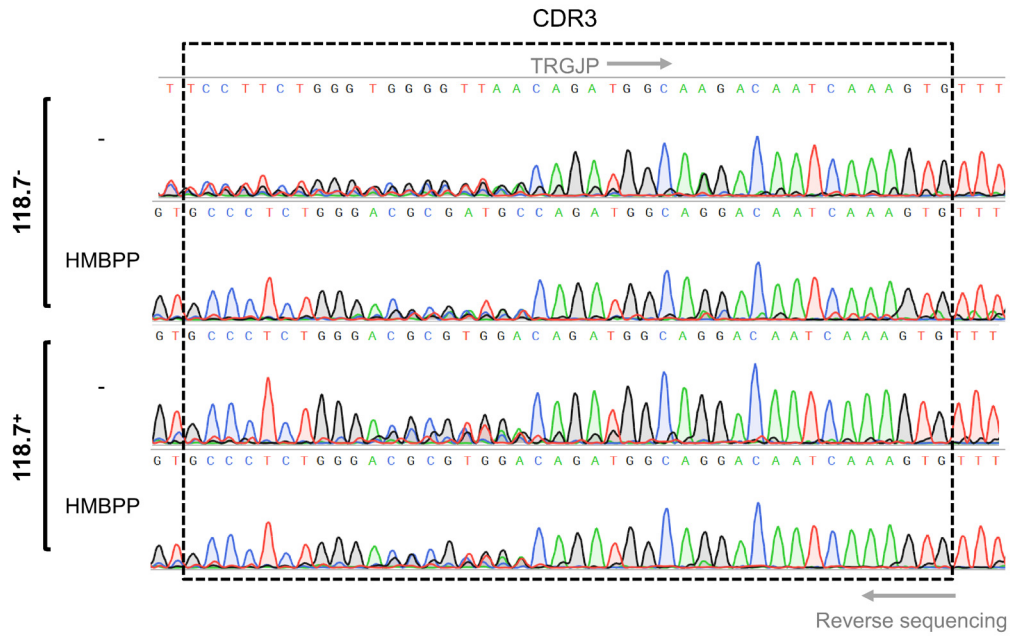

Figure 3.31 *TRGJP* preference in alpaca Vγ9 chains and possible restriction of CDR3 lengths. *TRGV9*/*TRGC* PCR amplifications were performed with cDNA of 118.7^{+} and 118.7^{-} cells of animal 1. These cells were bulk sorted for viable (Fixable Viability Dye eFluor® 660, 1:1000, eBioscience), 118.7$^{+/-}$ unstimulated alpaca PBMCs or PBMCs after 7 days of culture with hIL-2 (50 U/ml) and HMBPP (1 µM). PCR products were sequenced, and chromatogram data (reverse sequence traces) of animal 1 are shown. The DNA nucleobases adenine (green), guanine (black), cytosine (blue) and thymine (red) are color-coded and the sequence encoding the CDR3 region is marked in black according to [358] and the IMGT/DomainGapAlign tool [330, 332]. The start of the *TRGJP* gene segment is indicated.

A representative overview of *TRGV9*/*TRGC* PCR products obtained from all four conditions in animal 1 is depicted in **Figure 3.31**. A preference for *TRGV9*/*TRGJP* rearrangements was observed in all PCR products. Overlapping signals and termination of sequence reads were apparent in the CDR3 region of complete PBMCs and unstimulated 118.7^{-} cells and implied diverse CDR3 lengths. However, in stimulated 118.7^{-} cells overlapping signals in the CDR3 region but no termination of the reads were observed, indicating varying CDR3 sequences but a restriction in CDR3 lengths. The same was true for 118.7^{+} cells, either unstimulated or after HMBPP stimulation. Forward and reverse sequencing of *TRDV2*/*TRDC* PCR products revealed preferential rearrangement of *TRDV2* with *TRDJ4* in complete PBMCs and 118.7^{+} cells (unstimulated or HMBPP-stimulated). Here, the sequence reads indicated varying CDR3 lengths as seen for *TRGV9/TRGC* under some experimental conditions. Analysis of *TRDV2* expression in unstimulated 118.7^{-} cells was not successful with this approach, yet, in stimulated 118.7^{+} cells no variability in CDR3 length and prominence of *TRDV2/TRDJ2* rearrangements was observed. This implies the expression of a very limited number of unique *TRDV2* chains in this condition.

To further investigate these findings, TOPO TA cloning of PCR products was performed according to chapter 2.2.1.11. After transformation (see 2.2.1.3), single-cell clones were chosen for plasmid mini-preparations (see 2.2.1.5) and pCR™4-TOPO® vectors with *TRGV9* and *TRDV2* chains were analyzed by sequencing using the M13 fwd and M13 rev primers. Productive rearrangements were determined by *in silico* translation of *TRGV9* and *TRDV2* sequences. Most *TRDV2* clones were *in silico* translatable, and 90-100% of *TRGV9* clones were productive in 118.7$^+$ cells. The percentage of productive rearrangements in *TRGV9* PCR amplifications from 118.7$^-$ cells was around 60% for unstimulated and HMBPP-stimulated cells. The variation of CDR3 lengths in amino acid sequences of productive rearrangements, determined as described in [358], is summarized in **Figure 3.32**.

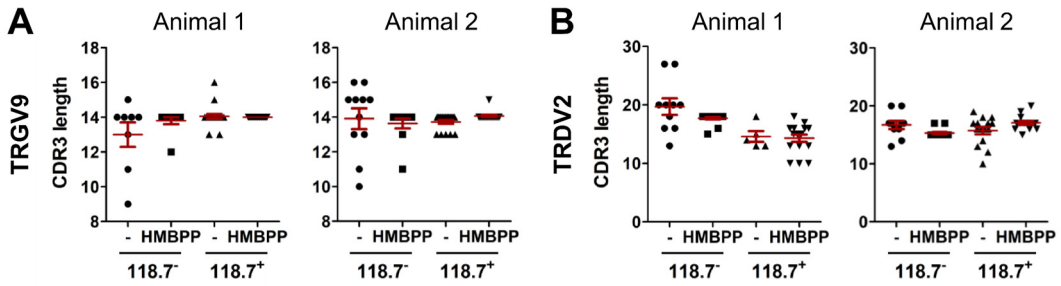

Figure 3.32 CDR3 lengths of Vγ9 and Vδ2 chains in unstimulated alpaca PBMCs and after HMBPP stimulation. *TRGV9*/*TRGC* and *TRDV2*/*TRDC* PCR amplifications were performed with cDNA of 118.7$^+$ and 118.7$^-$ cells. These cells were bulk sorted, viable (Fixable Viability Dye eFluor® 660, 1:1000, eBioscience), unstimulated alpaca PBMCs or PBMCs after 7 days of culture with hIL-2 (50 U/ml) and HMBPP (1 µM). PCR products were cloned into pCR™4-TOPO® vector and clones were analyzed by sequencing. For productive rearrangements, CDR3s were assigned as reported by [358] for human γδ T cells and amino acid sequence length was calculated. Each symbol marks a single clone, mean+SD are indicated in red. *TRGV9*- (*A*) and *TRDV2*-containing chains (**B**) were analyzed for animal 1 and animal 2 in one experiment each.

Analysis of CDR3 lengths of all productive clones obtained from *TRGV9*/*TRGC* and *TRDV2*/*TRDC* PCR amplifications revealed CDR3 length restriction in *TRGV9* but not *TRDV2* chains. CDR3 lengths in *TRGV9* chains of unstimulated 118.7$^-$ cells varied from 9-16 amino acids. A smaller degree of variability could be seen in stimulated 118.7$^-$ cells, where CDR3s were mostly 14 amino acids long. In unstimulated and stimulated 118.7$^+$ cells, only a small fraction of Vγ9 chains carried CDR3s of less than 14 amino acids in both animals. In contrast, Vδ2 chain CDR3s varied in most conditions, except for HMBPP-stimulated 118.7$^-$ cells. This matches the observation of one predominant *TRDV2*/*TRDJ2* clone in this cell subset. The CDR3 and *TRJ* regions of *TRGV9* and *TRDV2* rearrangements were analyzed for frequency and interindividual usage in **Figure 3.33**.

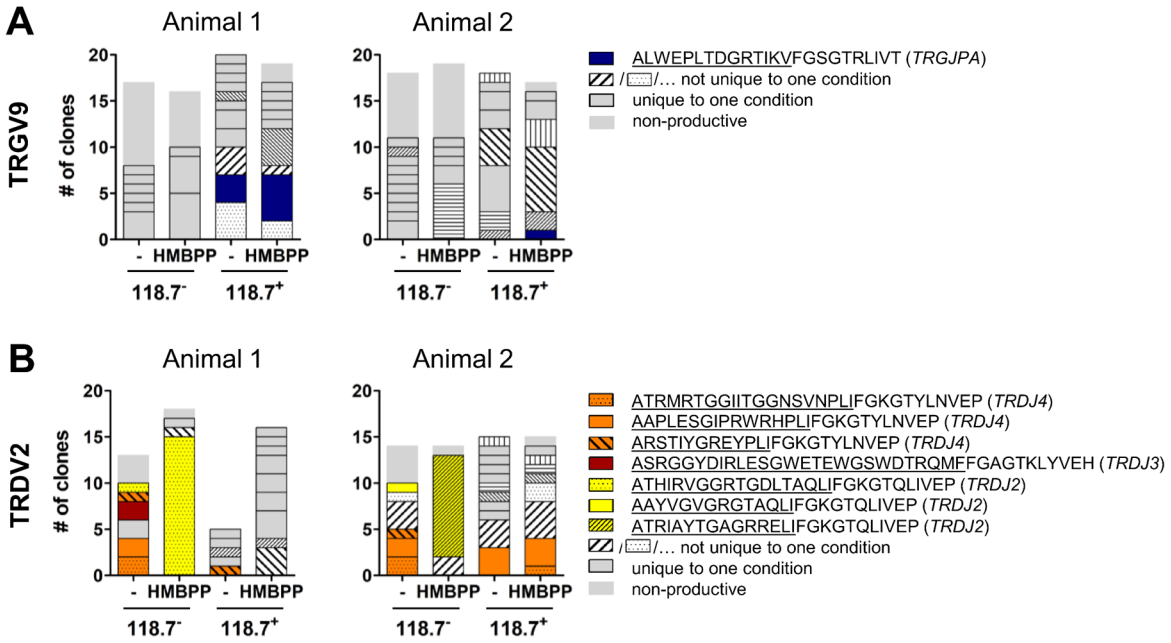

Figure 3.33 CDR3 usage of Vγ9 and Vδ2 chains in unstimulated alpaca PBMCs and after HMBPP stimulation. *TRGV9*/*TRGC* and *TRDV2*/*TRDC* PCR amplifications were performed with cDNA of 118.7$^+$ and 118.7$^-$ cells. These cells were bulk sorted viable (Fixable Viability Dye eFluor® 660, 1:1000, eBioscience) unstimulated alpaca PBMCs or PBMCs after 7 days of culture with hIL-2 (50 U/ml) and HMBPP (1 µM). PCR products were cloned into pCR™4-TOPO® vector and clones were analyzed by sequencing. Clones were analyzed according to their CDR3 and *TRJ* region. (**A**) The frequency of clones carrying the same CDR3 and *TRGJ* is represented by individual boxes, indicating clones unique for one condition (gray), appearing in more than one condition (black and white) and one CDR3+*TRGJP* clone shared by animal 1 and 2 (blue). (**B**) For Vδ2 chains, CDR3+*TRDJ* unique for one condition are marked in black and gray, CDR3+TRDJ appearing in several conditions in one animal are marked in black and white, orange boxes represent sequences shared by both animals, and nonproductive rearrangements are marked in gray. Vδ2 chains using *TRDJ* other than *TRDJ4* are marked in yellow (*TRDJ2*) and red (*TRDJ3*). CDR3 regions appear underscored.

CDR3 and *TRJ* usage of Vγ9 and Vδ2 chains in unstimulated and HMBPP-stimulated alpaca PBMCs sorted on 118.7 staining (**Figure 3.33**) were analyzed with TOPO TA cloning of PCR products. A complete list of all CDR3 and *TRJ* regions is shown for *TRGV9* in **Table A.4** and for *TRDV2* in **Table A.5**. The majority of productively rearranged Vγ9 chains expressed by unstimulated 118.7$^-$ cells of animal 1 preferentially used the *TRGJP-B* isoform, whereas *TRGJP-A* was prevalent in stimulated 118.7$^-$ cells and in 118.7$^+$ cells. One out of nine unique *TRGV9* clones in stimulated 118.7$^+$ cells of animal 1 rearranged with *TRGJP-C*. A different pattern of *TRGJP* usage was observed in animal 2, where mostly *TRGJP-C* was used for rearrangements. Other *TRGJP* used by animal 2 where *TRGJP-A* and a *TRGJP1* homolog. CDR3-*TRGJ* sequences were analyzed according to their occurrence in different conditions in **Figure 3.33A**. Most CDR3-*TRGJ* clones were only observed in one condition, either unstimulated or stimulated cells (gray boxes, each represents a unique clone). Some sequences appeared in more than one condition (black and white boxes) and only one clone was shared by both animals (ALWEPLTDGRTIKVFGSGTRLIVT) which was using a CDR3 of 14 amino acids (underscored). The frequency of unique Vγ9 chains varied among conditions and between animals and no clear distinction of CDR3 or *TRGJ* usage between 118.7$^+$ and 118.7$^-$ cells could be observed.

Analysis of the *TRDV2* clones in **Figure 3.33B** revealed a preference for *TRDJ4* in all conditions except for HMBPP-stimulated 118.7$^-$ cells. In those cells, the majority of pCR™4-TOPO® vectors carried one *TRDV2/TRDJ2* rearrangement with a unique CDR3 in each animal (animal 1: ATHIRVGGRTGDLTAQLIFGKGTQLIVEP; animal 2: ATRIAYTGAGRRELIFGKGTQLIVEP). *TRDV2* chains rearranged with *TRDJ2* (yellow) and once with *TRDJ3* (red) were observed in unstimulated 118.7$^-$ cells but never in 118.7$^+$ cells. This indicates a specificity of mAb 118.7 for Vδ2Jδ4 TCR chains.

The dominance of shared *TRGV9*/*TRGJP* clonotypes between individuals is characteristic for the human Vγ9 chain repertoire [239, 240, 376]. A canonical Vγ9 chain (CDR3: ALWEVQELGKKIKV) produced by rearrangement of germline sequences and no addition of N-nucleotides was described to be an abundant public clonotype in adult humans [376, 377]. The corresponding alpaca germline *TRGV9*/*TRGJP* recombination (CDR3: ALWDALTDGKTIKV) was determined by predicting RSS sites [337] of germline sequences (see 3.2.2.1). This canonical Vγ9 chain was found to be expressed by one clone of 118.7$^-$ unstimulated cells (see **Table A.4**).

3.2.2.6 Alpaca single-cell Vγ9Vδ2 TCR usage

Analysis of the TCR repertoire and clonality of single alpaca Vγ9Vδ2 T cells in peripheral blood were performed by single-cell sorting and subsequent PCR analysis of cells. The method used for these experiments was established for mouse and human γδ cells by [358, 359] and is described in chapter 2.2.1.14. Due to lack of other suitable alpaca Vγ9Vδ2 T cell marker, 118.7 mAb was applied for specific stainings of Vδ2Jδ4 TCR chains (see 3.2.2.2.1, 3.2.2.4 and 3.2.2.5). Single-cell sorting was performed according to chapter 2.2.3.9 and Fixable Viability Dye eFluor® 660 (eBioscience) was used to distinguish viable cells. Two preliminary experiments with unstimulated and stimulated (day 7, 1 µM HMBPP, 50 U/ml rhIL-2) alpaca PBMCs were performed by L. Starick. Analysis of unstimulated PBMCs revealed positive *TRDV2/TRDC* PCR signals in 21 cells. However, *TRGV9/TRGC* amplification was successful in only three of them (14%). These three clones and four randomly chosen *TRGV9/TRGC*-negative clones used rearrangements of the gene segments *TRDV2/TRDJ4* in their Vδ2 chains. A different frequency of Vγ9$^+$ cells was observed in HMBPP-stimulated cells, where 16/17 *TRDV2/TRDC*-positive clones also showed a positive *TRGV9/TRGC* PCR signal. Sequencing of Vδ2 chains revealed usage of productive *TRDV2/TRDJ4* rearrangements for all clones. In contrast to unstimulated cells, sequencing of these *TRGV9/TRGC* PCR products failed entirely in one case and revealed *TRGV9* usage but multiple rearrangements, as indicated by overlapping CDR3 and *TRGJ* signals, in another case. Therefore, pairing of productively rearranged Vγ9 and Vδ2 chains occurred in 82% of the analyzed Vδ2$^+$ clones.

The CDR3 [358] and *TRJ* usage of all Vγ9Vδ2 pairings observed in these experiments is summarized in **Table 3.10**.

Table 3.10 Single-cell usage of alpaca Vγ9Vδ2 TCR. Single-cell sorted viable 118.7$^+$ cells were used for single-cell PCR analysis of *TRGV9/TRDC* and *TRDV2/TRDC*. CDR3 regions (underscored) with *TRJ* usage and CDR3 length for single-cells are shown. The number of clones using these combinations is indicated as well as the total number of *TRDV2*/*TRDC*-positive cells.

Vγ9: CDR3+*TRGJ*	Vδ2: CDR3+*TRDJ*	CDR3 length	*TRGJ*/*TRDJ*	# clones
	Animal 1: 118.7$^+$ unstimulated PBMC			
ALWDARADGRTIKVFGSGTRLIVT	ALPGWSGISKSLIFGKGTYLNVEP	14/13	*JP-A/J4*	1/21
ALWVSLRGRTIKVFGSGTRLIVT	ATPVRYTLESRDPLIFGKGTYLNVEP	13/15	*JP-A/J4*	1/21
ALWAPWTDGRTIKVFGSGTRLIVT	AARVGVGTIYGRGRPLIFGKGTYLNVEP	14/17	*JP-A/J4*	1/21
	Animal 3: 118.7$^+$ HMBPP stimulated PBMC			
ALWAPSLTDGRTIKVFGSGTRLIIT	ATLVGSPTRAGRPLIFGKGTYLNVEP	15/15	*JP-C/J4*	4/17
ALWDARGDGRTIKVFGSGTRLIIT	ATLIRSGWRRGKGPLIFGKGTYLNVEP	14/16	*JP-C/J4*	3/17
ALWDAQADGRTIKVFGSGTRLIIT	AAAGSRMSPLIFGKGTYLNVEP	14/11	*JP-C/J4*	2/17
ALWEPLTDGRTIKVFGSGTRLIIT	ATAVSSLRAGPLIFGKGTYLNVEP	14/13	*JP-C/J4*	3/17
ALWDPLADGRTIKVFGSGTRLIIT	ATTMGLGDRALIFGKGTYLNVEP	14/12	*JP-C/J4*	1/17
ALWARRADGRTIKVFGSGTRLIIT	ATDIRLGDRPLIFGKGTYLNVEP	14/12	*JP-C/J4*	1/17

The analysis of Vγ9Vδ2 pairings in unstimulated and HMBPP-stimulated alpaca PBMCs permitted additional insights into the clonality and CDR3 usage of Vγ9Vδ TCRs (**Table 3.10**). *TRGJ* usage of Vγ9 chains revealed a *TRGJP* preference for successfully sequenced *TRGV9/TRGC* PCR products and the use of one distinct *TRGJP* segment (*JP-A* or *JP-C*) in each animal. Moreover, CDR3 lengths were 14 amino acids in most of the clones. In the case of Vδ2, all chains uniformly used the *TRDJ4* gene segment for rearrangement. In contrast to the CDR3 of Vγ9, CDR3 lengths of Vδ2 chains varied in length (11-17 AA). Some clones in stimulated PBMCs were detected at higher frequencies which were comparable to the results in chapter 3.2.2.6 (see **Table 3.10**, **Table A.4** and **Table A.5**). In all cases, unique Vγ9 chains were paired with a unique Vδ2 chain. However, no *TRGV9/TRGC* PCR signal was observed for two Vδ2 chains (CDR3: ATPVRYTLESRDPLI and ATAVSSLRAGPLI) in unstimulated and stimulated PBMCs, respectively, even though they were paired with a productive *TRGV9/TRGJP* rearrangement in other clones. Therefore, the efficiency of the *TRGV9*/*TRGC* PCR amplification remains to be investigated and seems less robust compared to the *TRDV2*/*TRDC* setup.

3.2.2.7 Molecule/s X conserved in *Vicugna pacos*

Previous studies reported a requirement of human chromosome 6 for phosphoantigen-mediated activation of Vγ9Vδ2 T cells [48, 304]. One molecule on chromosome 6 shown to be essential for phosphoantigen reactivity is human BTN3A1 [48, 49]. However, rodent cells are not able to present PAgs to human Vγ9Vδ2 T cells when transduced with human BTN3A1 [315].

In contrast, activation of human Vγ9Vδ2 T cells in co-culture with rodent cells expressing human BTN3A1 is possible using the BTN3-specific antibody 20.1 which activates Vγ9Vδ2 T cells in the absence of phosphoantigens [315]. This indicates the expression of a functional BTN3 molecule but additional molecules encoded on chromosome 6 seem to be necessary to confer the ability of HMBPP reactivity [315]. To investigate the conservation of these molecules in the alpaca and the compatibility of these with the human system, the alpaca primary kidney cell line LGK-1-R was used. This cell line was retrovirally transduced with human CD80 (S65T huCD80) and human BTN3A1 (pEGZ huBTN3A1) as described in chapter 2.2.3.6 and surface expression of huCD80 (data not shown) and huBTN3A1 was determined in a flow cytometry experiment (see 2.2.3.8).

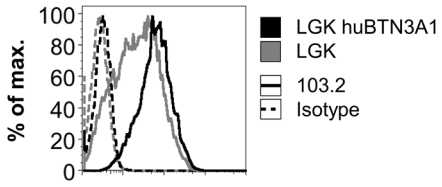

Figure 3.34 Overexpression of human BTN3A1 in an alpaca primary kidney cell line. The alpaca kidney cell line LGK-1-R was retrovirally transduced with huCD80 (S65T huCD80) and huBTN3A1 (pEGZ huBTN3A1). Overexpression of huBTN3A1 in LGK-1-R huBTN3A1 cells (black) was confirmed with 103.2 antibody staining (2.2 µg/ml, DαM R-PE). LGK-1-R cells overexpressing huCD80 were used as a control (gray). Geometric means of isotype (dashed line) and 103.2 (solid line) were: LGK (3/19) and LGK huBTN3A1 (3/57).

The cross-reactive antibody 103.2 specific for human BTN3 was used to show surface expression of alpaca BTN3 and human BTN3A1 in **Figure 3.34**. This antibody staining was performed with LGK-1-R cells overexpressing huBTN3A1 together with human CD80 (LGK huBTN3A1) and LGK-1-R cells overexpressing only human CD80 (LGK) as a control. A distinct shift of all LGK cells was observed after staining with 103.2 mAb (GM: 19), indicating the endogenous expression of alpaca BTN3. This signal was amplified almost 3-fold, when human BTN3A1 was overexpressed in those cells (GM: 57).

The ability of LGK huBTN3A1 cells to mediate phosphoantigen reactivity was assessed by stimulation assays with murine reporter cell lines overexpressing human Vγ9Vδ2 TCRs that release mIL-2 upon antigen recognition. The previously described murine αβ TCR-bearing 53/4 rat/mouse CD28 (r/mCD28) cell line was used as a reporter cell line for γδ TCR overexpression by retroviral transduction [369]. The r/m chimeric CD28 molecule leads to an increased mIL-2 release of responder cells (BW58 or 53/4 transductants) upon binding to counter-ligands like CD80 on the antigen-presenting cell line [156, 345]. In addition, CD28 is essential for phosphoantigen-dependent mIL-2 production of murine reporter cell lines expressing a human Vγ9Vδ2 TCR in co-culture with Raji cells [378]. In this experimental setup, LGK huBTN3A1 cells were used as antigen-presenting cells and 53/4 huVγ9Vδ2 transductants (see 2.1.10) as responder cells. A stimulation assay of permanent cell lines with increasing doses of the BTN3-specific antibody 20.1 or HMBPP was performed as described in chapter 2.2.3.7.

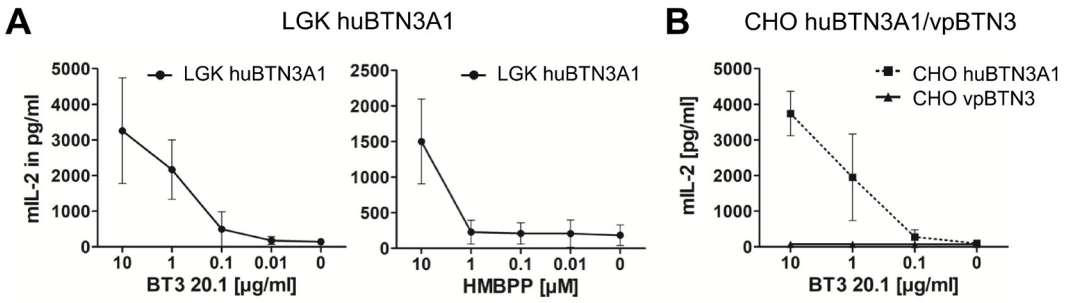

Figure 3.35 Alpaca but not hamster cells provide molecules essential for HMBPP reactivity. (**A**) LGK huBTN3A1 cells ($1*10^4$) were plated overnight in 50 µl RPMI++ in a 96 well tissue culture plate. Human responder cells (53/4 huVγ9Vδ2) in RPMI++ were added (50 µl, $5*10^4$ cells) and 100 µl of a dilution of the mAb 20.1 or HMBPP in RPMI++ to reach the final concentrations indicated. RPMI++ was used as a control, and the experiment was done in duplicates. Supernatants were tested for mIL-2 after 22 h with an mIL-2 ELISA. Means of four independent experiments are shown with standard deviations. (**B**) Stimulation of human responder cells as described in A with CHO cells overexpressing huBTN3A1 (phNGFR mCherry huBTN3A1) or alpaca BTN3 (phNGFR mCherry vpBTN3). Mean+SD of three independent experiments are shown.

The effect of overexpression of human BTN3A1 in an alpaca primary cell line on human Vγ9Vδ2 activation via 20.1 or HMBPP is summarized in **Figure 3.35A**. The mAb 20.1 was reported to induce activation via BTN3 in an HMBPP-independent manner [244]. In the presence of 20.1 huVγ9Vδ2 transductants produced a substantial amount of mIL-2 in a dose-dependent manner in co-culture with LGK huBTNA1 cells. This was not observed in LGK cells without huBTN3A1 and the amount of IL-2 released was 10-fold higher at 10 µg/ml of 20.1 compared to the same setup with Raji cells (data not shown). HMBPP reactivity of Vγ9Vδ2 transductants was only observed at 10 µM HMBPP, however, the magnitude of mIL-2 release was comparable to the one observed in co-culture with Raji cells (data not shown). Only a very minor IL-2 production was observed when LGK cells were used in co-culture with responder cells and HMBPP (data not shown). This demonstrates PAg recognition by human BTN3A1 overexpressed in alpaca cells and therefore compatibility of additional molecules required for HMBPP-mediated activation of Vγ9Vδ2 cells. Stimulations with LGK cells overexpressing human BTN3A1 and responder cells with alpaca Vγ9Vδ2 TCRs (53/4 huVγ9vpVδ2 cl.8 or vpVδ2 cl.9) did not result in HMBPP- or 20.1-dependent mIL-2 release. To investigate the effect of the agonistic activity of the human BTN3-specific antibody 20.1 in cells expressing alpaca BTN3, hamster cells (CHO) incapable of PAg recognition [315] were used for transduction (see 2.2.3.6) of alpaca BTN3 (phNGFR mCherry vpBTN3) and human BTN3A1 (phNGFR mCherry huBTN3A1). In this setup, CHO cells with human BTN3A1 or alpaca BTN3 were co-cultured with the murine responder cell line 53/4 huVγ9Vδ2 and increasing doses of 20.1 mAb (**Figure 3.35B**). In the presence of human BTN3A1, a robust mIL-2 production of murine responder cells overexpressing human TCRs was shown. In contrast, no activation was observed with alpaca BTN3. This indicates either a failure of alpaca BTN3 recognition by human Vγ9Vδ2 TCR transductants and/or no agonistic activity of 20.1.

3.2.2.8 Phosphoantigen-sensing of alpaca B30.2

Although the precise molecular mechanism of phosphoantigen recognition by human Vγ9Vδ2 T cells is not yet known, the human BTN3A1 molecule has been found to be essential for phosphoantigen reactivity of Vγ9Vδ2 T cells [49]. In addition, a shallow basic phosphoantigen-binding pocket was described, which is located in the intracellular B30.2 domain of human BTN3A1 [308]. The amino acids necessary for the formation of this pocket (H351, H378, K393, R412, R418, R469) are conserved in the only BTN3 isoform of alpacas [267, 308]. Moreover, additional, not yet identified molecules essential for phosphoantigen recognition are preserved in the alpaca system (see 3.2.2.7). To study the ability of alpaca BTN3 to recognize phosphoantigens, *in vitro* stimulation assays as described in the chapters 2.2.3.7 and 3.2.2.7 were used. An established model involving 293T cells as APCs and mouse responder cells transduced with a human Vγ9Vδ2 TCR was used. For analysis of responder cell activity, mIL-2 was measured by ELISA as described in chapter 2.2.2.2.3. The 293T cells in these assays were complete BTN3 knock out or BTN3A1 knock out cells produced with the CRISPR/Cas9 system by M. Karunakaran. Those knock out cells were reconstituted by retroviral transduction (see 2.2.3.6) with human BTN3A1, alpaca BTN3 or the two chimeric BTN3 molecules hu/vpBTN3 and vp/huBTN3 described in chapter 2.2.1.13. The chimeric BTN3 molecules comprised the human or alpaca Ig-like domains BTN3-V and BTN3-C with the transmembrane, juxtamembrane and B30.2 domain of the other species. All BTN3 molecules were expressed as fusion proteins with mCherry (phNGFR mCherry vector) and sorted on similar mCherry levels. To test the ability of alpaca BTN3 and the chimeric molecules to reconstitute HMBPP or 20.1 reactivity, the mIL-2 production of murine responder cells expressing a human TCR (53/4 huVγ9Vδ2) was measured.

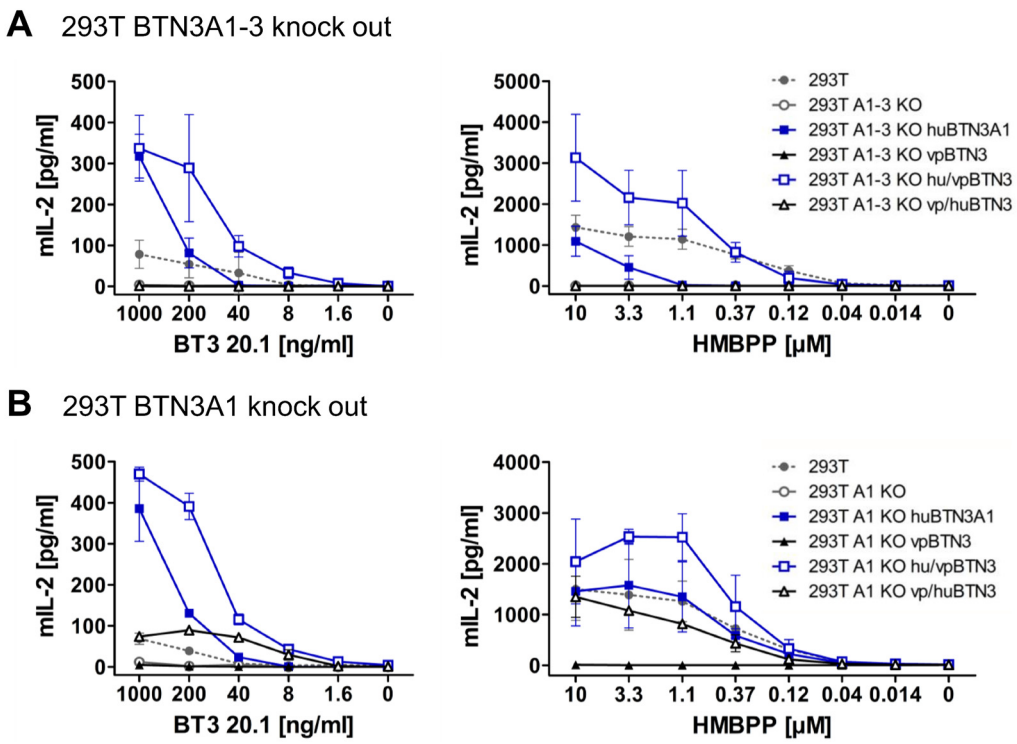

Figure 3.36 The alpaca B30.2 domain can sense phosphoantigens. (**A**) 293T BTN3 complete knock out cells (293T A1-3 ko) were transduced with huBTN3A1, vpBTN3 or the chimeric BTN3 molecules hu/vpBTN3 or vp/huBTN3 (all in phNGFR mCherry). Sorted cells ($1*10^4$, similar mCherry level) were plated overnight in 50 µl RPMI++ in a 96 well tissue culture plate. Human responder cells (53/4 huVγ9Vδ2) in RPMI++ were added (50 µl, $5*10^4$ cells) and 100 µl of a dilution of the mAb 20.1 or HMBPP in RPMI++ to reach the indicated final concentrations. RPMI++ was used as a control, and the experiment was done in duplicates. Supernatants were tested for mIL-2 after 22 h with an mIL-2 ELISA. Means of three independent experiments are shown with standard deviations. (**B**) Stimulation of human responder cells as described in **A** with 293T BTN3A1 knock out cells (293T A1 KO) overexpressing huBTN3A1, vpBTN3, hu/vpBTN3 or vp/huBTN3 (phNGFR mCherry). BTN3 transductants were sorted on similar mCherry levels. Means and standard deviations of three independent experiments are shown.

The IL-2 production of responder cells upon stimulation with the antibody 20.1 or HMBPP and different antigen-presenting cells is shown in **Figure 3.36**. Complete knock out of all BTN3 isoforms (293T A1-3 KO) resulted in a total loss of IL-2 production of responder cells upon 20.1 or HMBPP stimulation. Overexpression of human BTN3A1 fully replenished the 20.1-mediated IL-2 production but failed to reach levels of mIL-2 observed upon HMBPP stimulation in co-culture with 293T cells (**Figure 3.36A**). HMBPP reactivity using 293T A1-3 KO huBTN3A1 cells was only achieved at high levels of HMBPP (>3.3 µM). Alpaca BTN3 and the chimeric molecule vp/huBTN3 were not able to rescue HMBPP or 20.1 reactivity in this stimulation assay. Here, failure of recognition by the human Vγ9Vδ2 TCR seems evident. Yet, HMBPP recognition and agonistic effects of 20.1 were restored entirely through overexpression of the second chimeric molecule hu/vpBTN3A1. Similar effects were observed when 293T BTN3A1 knock out cells (293T A1 KO) were used (**Figure 3.36B**). BTN3A1 knock out in APCs resulted in a complete lack of mIL-2 after HMBPP or 20.1 stimulation. Overexpression of human BTN3A1 could fully reconstitute both, HMBPP and 20.1 reactivity, measured by IL-2

amounts similar or greater than levels observed with 293T wild-type APCs. The chimeric molecule hu/vpBTN3 was also able to rescue IL-2 production of responder cells completely. Alpaca BTN3 did not have any effect in this model, however, vp/huBTN3 resulted in mIL-2 production similar to the 293T setting.

3.2.2.9 Expression of phosphoantigen-reactive alpaca TCRs

Formal proof of phosphoantigen-reactive alpaca Vγ9Vδ2 TCRs was provided by the expression of Vγ9Vδ2 TCRs in murine responder cells. For this purpose, different alpaca Vγ9 and Vδ2 TCR chains were expressed in different combinations in the murine responder cells 53/4 r/mCD28 as described in chapter 3.2.2.7.

Table 3.11 List of alpaca Vγ9 and Vδ2 chains used for expression in permanent cell lines. Vγ9 chains were cloned into pEGZ and Vδ2 into pIH vectors. The CDR3 region appears underscored, and CDR3 lengths are indicated as well as the amino acid at position δ97 [247]. The *TRJ* segment used in Vγ9 and Vδ2 chains is indicated, and the clone used for amplification during cloning is given.

Vγ9 TCR chain	**CDR3 + *TRGJ***	**CDR3 length**	***TRGJ***	**clone**
vpVγ9	ALWAAADGRTIKVFGSGTRLIVT	13	*JP-A*	described in [317]
vpVγ9 14aa	ALWDARADGRTIKVFGSGTRLIVT	14	*JP-A*	(animal 1 118.7$^+$ & single cell PCR)
Vδ2 TCR chain	**CDR3+ *TRDJ***	**CDR3 length**	***TRDJ***	**clone**
vpVδ2 cl.8	ATS**G**GIYGGISLRGRESRPLIFGKGTYLNVEP	21	*J4*	described in [317]
vpVδ2 cl.9	AMW**L**ESDYTDWEYPLIFGKGTYLNVEP	16	*J4*	described in [317]
vpVδ2Jδ2	ATH**I**RVGGRTGDLTAQLIFGKGTQLIVEP	18	*J2*	Jδ2 usage (animal 1 cl. 23)

The alpaca TCR chains Vγ9, Vδ2 cl.8 and Vδ2 cl.9 (**Table 3.11**) have already been described by Karunakaran et al. and can form a functional TCR, as tested by CD3 cross-linking assays [317]. Two additional alpaca TCR chains have been cloned into expression vectors by L. Starick using the protocol described in chapter 2.2.1.13, and retroviral transduction of 53/4 r/mCD28 cells was performed according to chapter 2.2.3.6. TCR transductants using all six combinations of Vγ9 and Vδ2 TCR chains (**Table 3.11**) were generated and pairings of all chains were successfully detected on the cell surface with the alpaca-specific antibody 118.7 and vector-encoded EGFP. One exception was the vpVδ2Jδ2 TCR chain, which is not stained by 118.7 and no direct verification of TCRs with this Vδ2 chain was possible on 53/4 r/mCD28 cells. In addition to the use of strong selection markers, TCRs using vpVδ2Jδ2 were overexpressed in parallel in TCR$^-$ BW58 cells and surface expression was tested with CD3 staining which indicates TCR chain pairing and TCR complex formation. Stimulation assays comparable to the assays described in chapter 2.2.3.7, 3.2.2.7 and 3.2.2.8 were performed by A. Nöhren using HMBPP and agonistic or antagonistic BTN3 antibodies (20.1 and 103.2). The antagonistic antibody 103.2 completely abolished HMBPP-mediated activation of human Vγ9Vδ2 T cells in the presence of

human BTN3 [48, 303] and the agonist antibody 20.1 mediates human BTN3-dependent, HMBPP-independent activation of human Vγ9Vδ2 T cells [244]. The potential phosphoantigen reactivity of alpaca TCR transductants was tested on the alpaca cell line LGK-1-R and cross-reactivity with human BTN3 was tested on 293T cells.

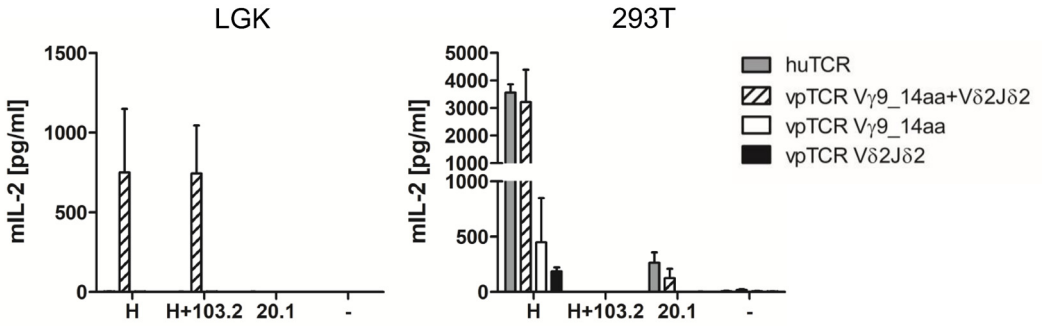

Figure 3.37 Phosphoantigen-reactive alpaca Vγ9Vδ2 TCR pairings. 293T cells or alpaca LGK-1-R cells were seeded at a density of $1*10^4$ cells per well in flat bottom 96 well cell culture plates o.n. The stimuli HMBPP (H, 10 µM), HMBPP+103.2 (0.5 µg/ml 103.2), 20.1 (1 µg/ml) or medium (-) were added. Responder cells were used at a cell number of $5*10^4$ per well. 53/4 r/mCD28 overexpressing huVγ9Vδ2 (huTCR), transduced with pEGZ vpVγ9 14aa and pIH vpVδ2 cl.8 (vpTCR Vγ914aa), transduced with pEGZ vpVγ9 14aa and pIH vpVδ2Jδ2 (vpTCR Vγ9_14aa+Vδ2Jδ2) or pEGZ vpVγ9 and pIH vpVδ2Jδ2 were used. Mouse IL-2 in cell culture supernatants was tested via mIL-2 ELISA and three independent experiments were carried out for HMBPP, HMBPP+103.2 and medium. 20.1 stimulations were carried out in two independent experiments. Mean+SD are shown.

Only one alpaca Vγ9Vδ2 TCR pairing showed phosphoantigen-dependent activation in co-culture with cells expressing alpaca BTN3 (**Figure 3.37**). Secretion of around 750 pg/ml mIL-2 was measured upon HMBPP stimulation of responder cells expressing vpVγ9 14aa paired with vpVδ2Jδ2. This TCR used a Vγ9 chain with a CDR3 length of 14 amino acids and a Vδ2Jδ2 chain using isoleucine at position δ97 (vpTCR Vγ9_14aa+Vδ2Jδ2). Both characteristics have been predicted to be of importance in the study of Vγ9 and Vδ2 repertoires described in chapter 3.2.2.5 and 3.2.2.6. No effect of the antagonist antibody 103.2 was observed, indicating that the affinity of this antibody is too low to affect alpaca BTN3-dependent γδ TCR activation (see 3.2.2.2.2). A pronounced cross-reactivity of the same TCR to human BTN3A1 expressed by 293T was observed reaching levels of mIL-2 production of the control. In contrast, no cross-reactivity of the human TCR to alpaca BTN3 was observed in this setting. Two other alpaca Vγ9Vδ2 TCRs showed HMBPP-dependent activation in co-culture with 293T cells. One using the Vδ2Jδ2 chain paired with a different vpVγ9 chain (vpTCR Vδ2Jδ2) and the other using a Vδ2Jδ4 chain with glycine at position δ97 (vpVδ2 cl.8) paired with vpVγ9 14aa (vpTCR Vγ9_14aa). Both responder cells showed slight cross-reactivity to human BTN3A1 which was more than seven-fold lower compared to human Vγ9Vδ2 or vpTCR Vγ9_14aa+Vδ2Jδ2. The antagonistic antibody 103.2 inhibited HMBPP-dependent mIL-2 production mediated by human BTN3A1. This indicates a similar mode of BTN3A1 recognition for human Vγ9Vδ2 TCRs and

cross-reactive alpaca TCRs. BTN3-dependent and HMBPP-independent activation of Vγ9Vδ2 responder cells via mAb 20.1 was only successful in co-culture with 293T for human TCRs and vpTCR Vγ9_14aa+Vδ2Jδ2. The other pairings of alpaca Vγ9 and Vδ2 TCR chains did not produce mIL-2 in co-culture with LGK-1-R or 293T cells upon HMBPP stimulation. Hence, phospho-antigen-reactive Vγ9Vδ2 TCRs are most likely expressed by alpacas, however, the pairing of certain Vγ9 and Vδ2 chains seems to be crucial for the functionality of these cells.

4 Discussion

4.1 The CD1d/iNKT cell system in cotton rats

The cotton rat (*Sigmodon hispidus*) is used as an animal model due to its susceptibility to human pathogens like influenza virus, human parainfluenza virus, human respiratory virus and measles virus [234]. Pre-clinical testing of antiviral reagents and vaccines is performed in this model, but lack of reagents and genomic sequence information hampers more detailed research [232, 233]. The goal of this study was to investigate the presence and functionality of the glycolipid-reactive iNKT cell subset. For this purpose, the molecular prerequisites, the expression of a CD1d-like molecule and the characteristic semi-invariant TCR α chain, as well as the homolog for rat Vβ8 TCR chains, were studied.

4.1.1 A functional homolog of CD1d is expressed in cotton rats

The antigen-presenting molecule CD1d was cloned from cotton rat cDNA using PCR and RACE PCR approaches. The analysis of multiple clones from spleen (4 clones) and thymus (10 clones) revealed expression of one uniform CD1d transcript. Comparison of the complete cotton rat CD1d to other species showed higher sequence conservation of cotton rat CD1d with rodent sequences (e.g., rat, mouse and hamster) as opposed to human CD1d (see 3.1.1.1). Hamster and cotton rat CD1d were more similar compared to cotton rat identities with mouse or rat CD1d. This can be explained by the evolutionary split of the murid, containing mice and rats, and the cricetid group, containing hamster and cotton rat as well as the split of groups containing hamster (Arvicolinae-Cricetinae) and cotton rats (Sigmodontinae-Netominae). According to Steppan et al., the first split of murid and cricetid groups happened 23.3 to 24.7 million years ago, whereas the split between groups of hamsters and cotton rats happened at a later time, 18.7 to 19.6 million years ago [379]. No evidence for other CD1 molecules was found on the mRNA level of cotton rats. Database analysis of *Cricetus griseus* and *Mesocricetus auratus* using mouse CD1d and human CD1a-e (data not shown) revealed only one CD1 isoform (CD1d) as seen in cotton rats. As primates and other non-muroid groups possess more than one CD1 isoform, the deletion of these molecules could have occurred 24.5 to 25.9 million years ago before the latest basal radiation of Muroidea (contains cotton rat and hamster) and Muridae (contains mouse and rat) [379].

To study the surface expression of cotton rat CD1d in different tissues, several antibodies raised against mouse or rat CD1d were tested for cross-reactivity. Human B cell lymphomas (Raji) were used to overexpress the cloned cotton rat CD1d and the antibodies 1B1, WTH-1 and WTH-2 were tested by flow cytometry (see 3.1.1.2). A slight reactivity was observed for the rat anti-mouse 1B1 antibody. WTH-1 and WTH-2, rat CD1d-specific antibodies generated in *CD1d* knock out mice, showed a differential reactivity to cotton rat CD1d. No cross-reactivity was observed for WTH-1, which detected only rat and mouse CD1d. Epitope mapping of WTH-1 revealed the epitope to be in the loop linking the α1 and α2 domain with important contributions of the aspartic acid at position 92 of rat and 93 of mouse CD1d [355]. In cotton rat CD1d, a histidine is encoded at this location. Hamster CD1d did not show a substitution like that and could potentially be detected by WTH-1. The epitope of the second rat-specific antibody WTH-2 is not yet mapped but equal recognition of rat, mouse and cotton rat CD1d indicates conservation of the epitope for this antibody. WTH-2 was subsequently used to determine the tissue surface expression of cotton rat CD1d in direct comparison to C57BL/6 mice (see 3.1.1.3). A distinct pattern of CD1d surface expression, with homogenous expression in the thymus and varying CD1d expression levels in spleen and lymph nodes, was observed in cotton rats. Differences in the transmembrane and intracellular domain of cotton rat CD1d in comparison to mouse CD1d could potentially result in varying cellular expression. These variations could also influence antigen sampling, cellular trafficking and half-life of the CD1d molecule. As cotton rats most likely possess only the CD1d isoform of the CD1 family, it is particularly interesting to discuss potential consequences of this distinct CD1d expression. The markedly lower CD1d expression levels in the thymus of cotton rats in comparison to mouse CD1d (see **Figure 3.3**) could impact the development of iNKT cells in this organism, as iNKT cells were reported to be positively selected on immature thymocytes [185, 206]. Moreover, lower CD1d expression on the cells selecting developing iNKT cells could potentially result in different iNKT TCR affinity or density. Similarly, the difference in CD1d expression between B and T cells (see **Figure 3.4**) possibly influences the cross-talk of those cell types with iNKT cells in cotton rats. In general, expression of CD1 molecules can differ considerably between species owing to the specialization of certain CD1 molecules to present antigens to distinct T cell subpopulations. In addition, CD1 molecules could be involved in processes other than antigen presentation, as exocrine acinar cells in the rat pancreas express high levels of CD1d [355]. Expression on hematopoietic cells was reported to be similar for murine species [355] but more distinct for distantly related species.

4.1.2 Glycolipid recognition by a cotton rat iNKT cell-like cell population

An essential tool for the investigation of iNKT cells is the detection of those cells by glycolipid-loaded CD1d oligomers [123, 126, 127, 360, 380]. CD1d dimers were produced by fusion of cotton rat CD1d onto a mIgG antibody base as described in chapter 2.2.4 and 3.1.2.1. This allowed the study of antigen presentation by cotton rat CD1d and CD1d recognition by iNKT TCRs. By applying cotton rat CD1d dimers, the ability of CD1d to present a typical iNKT cell antigen and activate iNKT TCRs was shown and cross-reactivity to rat iNKT TCRs was observed (see **Figure 3.5** and **Figure 3.6**). Moreover, the glycolipid-loading capacities of cotton rat CD1d dimers have been extensively studied and compared to other species [381]. This study showed, that CD1d of human, mouse, rat and cotton rat required distinct surfactants for optimal loading and that modifications of the typical glycolipid antigen αGC resulted in differential loading efficiencies.

Cotton rat CD1d dimers as well as rat CD1d dimers were subsequently applied to detect glycolipid-specific and CD1d-restricted cells in cotton rat hematopoietic tissues (see 3.1.2.2). In splenocytes, a mean of 0.23% of live cells was detected by PBS57-loaded CD1d dimers. This cell subset was characterized by CD3 expression and thus most likely an iNKT cell-like population in the cotton rat. *In vitro* expansion of cotton rat iNKT cells in splenocytes and IHLs was attempted as described before in the rat model [149]. However, expansion of CD1d dimer-positive cells was highly variant and not reliably reproducible (data not shown). This could indicate different requirements for ideal stimulation conditions with glycolipid antigens in the cotton rat system as compared to rats. Besides proliferation upon activation, another important feature of iNKT cells is the rapid production of the inflammatory cytokines INF-γ and IL-4 [126]. To further prove the existence of an iNKT cell-like subset in cotton rats, the response of splenocytes to the typical glycolipid antigens αGC and PBS57 was tested (see 3.1.2.3). A substantial amount of IFN-γ and a less pronounced production of IL-4 were observed after stimulation with αGC or PBS57 in cotton rat splenocytes. IFN-γ levels were 100-fold higher and IL-4 production was twice compared to cytokine levels shown for F344 rat splenocytes in a similar experiment [149]. This difference could be explained by a greater frequency of iNKT cells in cotton rats (~ 10-fold) on the one hand or by indirect effects like NK cell activation by iNKT cells and subsequent IFN-γ production on the other hand [382]. In contrast to cytokine production following *in vitro* stimulation assays of primary cell cultures, no serum increases of IFN-γ or IL-4 could be detected in cotton rats i.p. injected with αGC. This phenomenon is similar to clinical data, which report no increase in serum levels of IL-4 upon intravenous injection of KRN7000 [383]. In that study, in one cancer patient with initially high iNKT cell numbers,

increased serum-IFN-γ levels were observed at a single time point (8 h) after drug administration. This is in stark contrast to mice, where a strong IFN-γ response was reported [384, 385]. Hence, the lack of a systemic IFN-γ response resembles data in the human system and could make cotton rats an even more valuable model to study the iNKT cell subset.

4.1.3 Family members of *AV14* and *BV8* in the cotton rat

Evidence for an iNKT cell-like population in cotton rats detected by CD1d dimers raised the question of conservation of semi-invariant TCRs characteristic for these cells. To investigate this on the molecular level, cotton rat homologs for the characteristic iNKT α chain using an *AV14*/*AJ18* rearrangement and the Vβ8 TCR chain associated with mouse and rat iNKT α chains [126] were studied as described in the chapters 3.1.3.1 and 3.1.3.2.

Functional cotton rat *AV14*/*AJ18* rearrangements were identified with the amplification of partial *AV14*/*TRAC* fragments from IHL cDNA and subsequent 5' and 3' RACE PCR approaches (see 3.1.3.1). The expression of a homolog of the canonical *AV14*/*AJ18* rearrangement further supports the existence of an iNKT cell-like subset. Homologies to a hamster *AV14*/*AJ18* rearrangement (predicted), mouse, rat and human iNKT α chains were calculated and dependent on evolutionary relationships. The gene segment *AJ18* was found to be highly conserved among species. Furthermore, multiple variants of *AV14* segments were expressed in cotton rats. The investigation of *AV14* gene segments on the genomic level revealed six unique members of the *AV14* family (**Figure 3.10**) with three unique types of transcripts using the corresponding genomic variants. This occurrence of multiple family members for *AV14* is therefore not a peculiarity of rats [125, 149, 349, 363]. Substitutions at the VJ junction, which are another feature of mouse and rat *AV14*/*AJ18* rearrangements, are also conserved in cotton rats. Some transcripts encoded for valine or alanine instead of glycine 93 (G93V) or valine 92 (V92A), respectively. In mice and rats, substitutions in those positions were found to affect ligand binding [219, 349].

The same approach was applied for the amplification of *BV8* homologs from cotton rat cDNA as described in chapter 3.1.3.2. The analysis of 16 cotton rat *BV8* clones in the expression vector S65T revealed nine unique productive rearrangements using multiple *TRBJ* segments and CDR3 diversity. This polyclonal TCR β chain usage is consistent with findings in mice, rats and human [126, 130, 149]. Two distinct variable gene segments were used in these clones which share 81% amino acid identity and differ in 21 amino acids. Two clones (clone 1 and 7) carrying those variable regions were used to analyze homologies to *BV8* of rat, mouse and the human homolog BV11. Sequence conservation of the variable gene segment was more pronounced

among the rodents considered in this analysis with overall amino acid identities of more than 75% between cotton rat and rat or mouse β chains. In-depth analysis of the cotton rat *BV8*-like gene segments with the IMGT/DomainGapAlign tool [330, 332] revealed closer homology (78.9%/80%) to the mouse *BV8.1* gene segment (IMGT: *TRGV13-3*01*). A comparison with the rat *BV8* family members *8.1*, *8.2*, *8.3* and *8.4* showed the highest sequence conservation of each cotton rat clone 1 and 7 (74% and 79%) with rat *BV8.4*. Constant region usage was restricted to two distinct *TRBC* genes differing in 9 amino acids, and two more *BV8* family members were found to be pseudogenes. In summary, these results prove the existence of at least six members of the cotton rat *AV14*-like family and four distinct *BV8* gene segments and show remarkable similarities to mice and rats.

4.1.4 Expression of a functional cotton rat iNKT TCR

The ability of the newly identified cotton rat iNKT α and β chains to form a functional iNKT TCR was tested by expression of those chains in a TCR^- fibroblast cell line (L929). Random invariant Vα14Jα18 and Vβ8 chains were chosen for this experiment to test whether pairing of those chains was possible. Therefore, these pairings do not represent bona fide iNKT TCRs used *in vivo* but allow *in vitro* studies of structural and functional conservation. Expression of two distinct cotton rat α chains in combination with two cotton rat β chains is described in chapter 3.1.3.3. As both chains are essential for glycolipid recognition mediated by CD1d [171, 199, 201], detection of these TCRs with antigen-loaded CD1d multimers was used to mimic glycolipid recognition and study iNKT TCR functionality *in vitro*. All combinations of cotton rat iNKT TCR chains were successfully detected on the surface of transduced cell lines with the help of cotton rat and rat dimers as well as rat tetramers. Differences in staining intensities of α and β chain combinations were more pronounced with the application of rat tetramers indicating more efficient staining. The application of rat tetramers for stainings of primary cells should be considered to reevaluate iNKT cell numbers. Usage of α chain clone 8 improved staining with rat CD1d tetramers loaded with PBS57. This is surprising, as valine is used in position 93, which was shown to diminish CD1d multimer staining in rats [349]. Differential usage of β chain clone 1 and 7 with different *BV8* and *TRBJ* segments did not markedly change glycolipid recognition. Natural variations in the Vα14Jα18 chain VJ-junction and influence on glycolipid recognition are characteristic for iNKT TCRs in humans, mice and rats [219, 349, 386, 387], and it would be worthwhile to study these in cotton rats. For some cotton rat iNKT TCRs, stainings with cotton rat CD1d dimers might be superior due to species-specificities. Overall, the proof of functional pairings of typical iNKT TCRs in the cotton rat that recognize glycolipid antigens presented by CD1d emphasizes the conservation of this system.

4.1.5 Outlook: The CD1d/iNKT cell system in cotton rats

A first identification of the CD1d/iNKT cell system in the cotton rat was performed in this study. Cotton rats express a fully functional antigen-presenting CD1d molecule and multiple family members of *AV14*- and *BV8*-like genes. Moreover, expression of cotton rat Vα14Jα18 and Vβ8 TCR chains proved lipid:CD1d dimer recognition of iNKT TCRs *in vitro*. In addition, tools and methods developed in other rodent models have been established in the cotton rat. Although glycolipid recognition by cotton rat iNKT TCRs could be shown, no information is available on endogenous ligands in the cotton rat system and the investigation of effector functions of cotton rat iNKT cells is still pending. For this, comparative transcriptomics could be applied to study conserved features. In summary, the novel reagents presented in this project allow the further study of the immune function of the iNKT cell subset in infectious disease models such as infections with human respiratory virus or measles virus, thus combining the natural susceptibility of cotton rats with tools developed in this setting.

4.2 Vγ9Vδ2 T cells in non-primate animal models

4.2.1 The armadillo as a witness for coevolution of BTN3 and Vγ9Vδ2 T cells

In this thesis, the nine-banded armadillo (*Dasypus novemcinctus*) was analyzed for functional expression of the essential components of the BTN3/Vγ9Vδ2 T cell system and the results were published [326]. Previous studies of the distribution of *TRGV9*, *TRDV2* and *BTN3* genes among mammals identified the armadillo as candidate species for this particular system [267, 317] and expression of those genes was investigated in this setting. Expression of productive *TRDV2* rearrangements which preferentially used *TRDJ4* homologs (see 3.2.1.2) was observed in armadillo cDNA, however, no corresponding *TRGV9* rearrangements were found (see 3.2.1.3). Phosphoantigen-reactive *TRDV2*-chains in humans commonly use *TRDJ1*, *2* or *3* [241], however, pairing of *TRDV2* with a *TRDJ4*-like gene segment has been shown in alpaca [317]. Surface expression of armadillo Vδ2-like chains could be shown for heteromeric TCRs with a human Vγ9 chain and TCR signaling was observed (see 3.2.1.2). This indicates conservation of structural features that allow pairing of Vδ2 with a Vγ9 chain. In humans, Vδ2 chains also pair with γ chains different from Vγ9 [388], but some γδ pairings are not expressed [389]. Phosphoantigen reactivity of these human/armadillo TCRs was not observed although not surprising, as all CDRs contribute to PAg-mediated activation of the human Vγ9Vδ2 TCR [241]. Nevertheless, armadillo Vδ2 chains could be used for functional studies, e.g., by exchanging the CDR regions for the human counterparts. In addition, a curious finding was the expression of the amino acids isoleucine or valine at position δ97 in one-third of all clones (see **Figure 3.15**). Therefore, this apparently common use of the proposed hydrophobic amino acids essential for PAg recognition leads to the question whether this is a suitable indicator caused by selection for structural requirements or a more random characteristic [247, 317].

Moreover, no full-length *BTN3* transcripts were found to be expressed in armadillo cDNA in this setting (see 3.2.1.1). Using genomic database information, armadillo *BTN3* loci could be mapped, and there is evidence for a multigene *BTN3*-like family. However, no assessment of gene numbers can be made due to lack of genomic data and transcripts. One locus was strikingly like the human *BTN3A3* locus, and another carried deletions of transmembrane parts and B30.2, indicating a *BTN3A2*-like gene. No signal sequences were found indicating a loss of function previous to duplication events. In contrast, two successive duplications occurred in primates leading to three BTN3 isoforms [298]. This and the observation of multiple deletions and frameshifts, speak for non-functional armadillo *BTN3* transcripts. Interestingly, the codons of the six proposed PAg-binding sites of the B30.2 domain of BTN3A1 are preserved in the armadillo B30.2 domain which, together with the fact of a translatable *TRGV9* gene, suggests the loss of structural elements of PAg sensing in an armadillo ancestor [308].

4.2.2 Alpacas possess a functional BTN3/Vγ9Vδ2 T cells system

4.2.2.1 The *TRG* and *TRD* repertoire in *Vicugna pacos*

As a first step towards a more comprehensive overview of the γδ T cell repertoire in alpacas and an additional reference point for the study of Vγ9Vδ2 cells in this animal model, the *TRG* and *TRD* repertoire were studied in unstimulated alpaca PBMCs (see 3.2.2.1). A first glance at the *TRG* and *TRD* repertoire in unstimulated alpaca blood cells has been given for the first time in this study. The results shown here are subject to limitations and errors due to sequencing, PCR reactions and lack of complete genomic information. Therefore, assignments of *TRV* and *TRJ* segments are preliminary and based upon human homologies.

Here, we report a cassette-like organization of the *TRG* locus with clustering of *TRGV9*, *TRGV10* and *TRGV11* homologs with *TRGJP*, *TRGJP1, TRGJ1/2-B* (potential pseudogene) and *TRGC-A*, three variants of *TRGV8*-like genes with *TRGJP2* and *TRGC-B*, and a *TRGVA* homolog with *TRGJ1/2* and *TRGC-C* genes segments, respectively. Rearrangements found in unstimulated alpaca blood cells support this genomic organization due to differential *TRGC* and *TRGJ* usage as described in chapter 3.2.2.1. This cassette-like organization is also found in other artiodactyls like sheep (*Ovis aries*) and cattle (*Bos taurus*) [390] as well as in dogs (*Canis lupus*) [391] and mice (*Mus musculus*) [392]. The three *TRGC* segments in alpacas seem to diverge in exon-intron organization, as *TRGC-A* seemed to be organized in three exons and only two exons were found through homology searches (alpaca and human *TRGC* regions) for *TRGC-C/-B*. The last exon including a termination codon was identical for all three isoforms. Therefore, exons used by *TRGC-B* and *TRGC-C* genes could have been overlooked. No evidence for constant region pseudogenes was observed in this context and *TRGC-A, -B,* and *-C* were used in alpaca transcripts, however, only full-length spliced *TRGC-A* transcripts have been proven so far [317]. Splicing defects or missing exons of *TRGC-B* or *TRGC-C* cannot be ruled out without performing 3' RACE experiments to determine the 3' end of both. The same was true for variable regions and junctional segments, as no apparent defects in gene structure were observed. No obvious preference of specific *TRGJ* segments was observed in this experiment. Rearrangements of *TRGV* genes with *TRGJ* of another cassette were possible as in the case of *TRGV8-A* genes of the second cluster rearranged with *TRGJ1/2* of the third V-J-C structure. However, *TRGJ* segments were always spliced to the *TRGC* gene of the same cassette. Only minor observations could be made in terms of frequency of certain *TRGV* genes or *TRGJ* preferences. The most abundant *TRGV* genes in unstimulated alpaca PBMCs were *TRGV8-C* and *TRGV11*. Interestingly, the clonality of *TRGV8-C* seemed restricted in comparison to *TRGV11* (see **Figure 3.18**). Moreover, only one clone among 39 γ chains used *TRGV9* in a rearrangement with *TRGJP*. This indicates a very low frequency of *TRGV9* transcripts in unstimulated PBMCs.

In the case of the *TRD* repertoire, no complete locus could be constructed from the genomic information available to this date. Here, homologs to the human *TRDV2* and *TRDV3* genes and 12 members of a *TRDV1*-like family were found in total among expressed transcripts and genomic database entries. If similar but not more than 98% identical *TRDV1* gene segments were found, a new group was formed, as no data was available to study polymorphisms or alleles of the same gene. In addition, one *TRDV* gene (*cdTRDV2*) could not be assigned to a human counterpart but was identified as a homolog (92% amino acid identity) of the camelid *TRDV2.1*01* gene [372]. An expanded family of *TRDV1*-like genes has been reported for other artiodactyl species like sheep [62], cattle (annotation of *TRD* locus described in [393]) and camels [372]. The question arises whether alpacas can be considered a "γδ high" species as described in chapter 1.3.3.2. Evidence justifying this lies in the existence of a multimember *TRDV* family and the relatively high frequency of $WC1^+$ cells (see 3.2.2.3). However, the lack of specific antibodies for other γδ T cell subsets in alpacas renders a definite assignment difficult.

Analysis of alpaca δ chain transcripts within the clones studied here showed usage of *TRDV1* members in almost 80% of unique rearrangements which is also comparable to studies in camelid species [372]. Other frequent *TRDV* genes found were *TRDV3* and *cdTRDV2*. Interestingly, as seen for *TRGV9*, the *TRDV2* homolog in alpacas was found in only one clone, indicating very low frequencies of cells carrying this gene segment. In terms of *TRDD* gene usage, all D genes were found to be used in the δ chains in this experiment and usage of multiple D segments was common. A strong preference for the use of the *TRGJ4* homolog and very low prevalence of *TRGJ2* or *TRGJ3* (see 3.2.2.5) gene segments was observed. This is also in context with findings in camelid species [372] and armadillos (see 3.2.1.2). In contrast to the γ chain repertoire, no conclusions about clonality could be made in this setting, as expanded clones with nucleotide-identical sequences were found throughout all δ chains.

An interesting observation in this experiment was the very low frequency of non-productive rearrangements (2 clones for γ chains, 1 clone for δ chains). In other experimental setups, the prevalence of non-productive rearrangements was higher, especially for *TRGV*/*TRGJ* rearrangements (see 3.2.1.3 and 3.2.2.5). Other studies report non-productive γ chain rearrangements of cells that later commit to the αβ lineage [377, 394]. Here, the reason for lack of non-productive rearrangements could be the modification of RNA transcripts to add an RNA oligo to the 5' end with a known sequence for amplification (see 2.2.1.9). As uncapped mRNAs are not ligated to this RNA oligo, it is possible that capping is different for productive and non-productive rearrangements. This could be verified by the 5' RACE amplification with a *TRGC* primer and amplifications of *TRGV/TRGC* using the same cDNA, as uncapped mRNAs do not possess the RNA oligo but are still transcribed in cDNA.

Another aspect of *TRG* and *TRD* repertoires in the alpaca are somatic hypermutations that were described for *Camelus dromedarius*, a close relative of *Vicugna pacos* [372]. These could not be confirmed in the alpaca. Analysis of nucleotide differences in constant and variable regions of the *TRG* and *TRD* repertoires revealed no apparent difference in nucleotide mismatch numbers in this setting and clones with the same rearrangement were always nucleotide-identical in the *TRGV* region.

4.2.2.2 Monoclonal antibodies specific for alpaca γδ TCR and BTN3

As no alpaca-specific antibodies for the study of alpaca Vγ9Vδ2 T cells and BTN3 are available, the aim of this thesis included the generation of hybridomas producing specific monoclonal antibodies for both surface markers. Four different antibodies, raised against the Vγ9Vδ2 T cell receptor, were successfully purified from hybridoma culture supernatants (118.7, 118.11, 257.6 and 697.3) as described in chapter 3.2.2.2.1. The epitope recognized by all of them was deduced to be on the Vδ2 chain, as human Vγ9/alpaca Vδ2 heteromeric TCRs were still recognized whereas no cross-reactivity was observed for human Vγ9Vδ2 TCRs. No staining of 118.7 was observed on alpaca TCRs using a *TRDV2/TRDJ2* δ chain, however, δ chains using the *TRDJ4* segments were stained irrespective of CDR3 usage or length (see 3.2.2.5). This indicates a specificity of 118.7 for alpaca *TRDV2/TRDJ4* δ chains. The antibody 118.7 was routinely used for stainings of alpaca PBMCs before and after stimulation assays (see 3.2.2.3, 3.2.2.4 and 3.2.2.5) and successfully applied in single cell sorting (see 3.2.2.6). A small but distinct $118.7^{+}CD3^{+}$ lymphocyte population could be observed in alpaca PBMCs with frequencies of 0.2 to 1.4% of T cells and high variation between individual animals (see **Table A.2**). Repertoire analysis of Vγ9 and Vδ2 chains in 118.7^{+} and 118.7^{-} cells also indicated an epitope of 118.7 on Vδ2 chains using *TRDJ4* gene segments, as Vδ2 chains using another J segments (*TRDJ2* or *TRDJ3*) were never 118.7^{+}. The mIgG1 heavy and κ light chain of the 118.7 monoclonal antibody were cloned by D. Chheng as part of a B.Sc. thesis project by application of degenerate primers for variable regions and 5' RACE PCR. The gene segments used by 118.7 were *IGHV1-37*01* rearranged with *IGHJ4*01* for the heavy chain and *IGK4-79*01/IGKJ1*02* was used by the κ light chain. The cloned antibody chains were retrovirally transduced into SP2/0 cells and antibodies could be purified from cell culture supernatant. Considering the lack of specificity of 118.7 for alpaca Vδ2Jδ2 chains, other hybridomas obtained from the same immunization (e.g., 257.6, 118.11 and 697.3) should be tested on Vδ2Jδ2 TCRs.

The second monoclonal antibody was raised against alpaca BTN3 overexpressed in L929 cells as described in chapter 3.2.2.2.2. Here, a curious phenomenon was observed as 41 hybridomas produced antibodies recognizing vpBTN3 when expressed by cell lines like RAJI, CHO or 293T

but no staining was detectable on alpaca PBMCs for all but one of 41 clones. This could be either due to differential expression of endogenous and overexpressed alpaca BTN3 leading to a masked epitope or simply due to lower affinities of most clones that are not efficient at detecting endogenous BTN3. The hybridoma clone 189 (mIgG2b) showed high affinity for alpaca BTN3 on PBMCs but could only be purified after single cell sorting on surface mIgG2b due to contamination with hybridoma cells producing non-specific mIgG1 antibodies. However, hybridoma supernatants of 189 were not cross-reactive to human BTN3A1, whereas the human antibodies 20.1 and 103.2 could be used to detect transduced alpaca BTN3 on the surface of several cell lines. The epitopes of both antibodies specific for human BTN3 were studied by single-chain versions of 20.1 (20.1 scFV and 103.2 scFV) [303]. The epitope for the 20.1 antibody specific for human BNT3 [244] has been mapped to the amino acids E64, Q74, V75, the motif EDRQSAP (amino acids 86-92) and R94 [303] in the BTN3-V region of human BTN3A1 (numbering according to [309]). Sequence analysis of alpaca BTN3 revealed two amino acid changes in the epitope of 20.1, namely S90I and P92E, which disturb but do not completely abolish antibody binding to alpaca BTN3 expressed by rodent or human cell lines. Epitope mapping of 103.2 revealed the amino acids S59, E61, T62, A80, D81, G81, R101 and D102 as contact sites for 103.2. Alpaca BTN3 possesses a mostly conserved epitope with one amino acid change of D81G. Titrations of 20.1, 103.2 and 189.21.17 on CHO cells expressing human BTN3A1 or alpaca BTN3 revealed differential staining capacities of those antibodies. A certain cross-reactivity of 20.1 and 103.2 to alpaca BTN3 and minimal or unspecific staining of huBTN3A1 with 189.21.17 was observed, however, 20.1 staining was poor in comparison to 103.2 and 189. Therefore, 103.2 is a valuable antibody for stainings of human BTN3 and evaluation of differential BTN3 expression levels on lymphocytes and monocytes was possible. The same is true for the staining of alpaca BTN3 with 189.21.17 revealing BTN3 expression levels of alpaca lymphocytes and monocytes distinct from human.

4.2.2.3 Characterization of alpaca blood lymphocytes

Limited data on the expression of surface markers in alpaca PBMCs is available to this date. A selection of antibodies raised against llama surface markers was studied on llama and alpaca PBMCs by Davis et al. [354]. Frequencies of granulocytes, monocytes and lymphocytes varied among the alpaca samples used in this study and sometimes granulocytes frequencies were higher than 50% of live cells. This is in context with findings in llama PBMCs with 60-80% of granulocytes [354] and could be due to different densities of camelid granulocytes in comparison to human. The use of Histopaque®-1077 for alpaca PBMC isolations might not be ideal, and other density gradients should be explored.

Several antibodies described in the llama study have been used in co-stainings with 118.7 and a CD3 antibody cross-reactive for alpaca as described in chapter 3.2.2.3. The newly developed alpaca BTN3-specific antibody 189 was also applied. Alpaca lymphocytes of two animals were characterized in this setting and frequencies varied among individuals. Cells stained with GB45A, an antibody for bovine WC1, were $CD3^+$ and amounted to 6-15% (animal 1/2) of lymphocytes. Llama and alpaca PBMCs have been shown to express on average 16% $WC1^+$ cells which could be confirmed here [354]. WC1 expression has been shown to be unique to γδ T cells and has not been proven in humans or mice but cattle, swine and sheep cells [373-375, 395, 396]. The surface marker CD5 is expressed by human αβ T cells and B cells, and expression of CD5 as stained by the antibody LT3A varied between 50%-70% (animal 1/2) of lymphocytes and was a little higher compared to previous results in llama studies [354]. Most $CD5^+$ cells expressed CD3 and CD5 was also expressed by 60% of $CD3^-$ lymphocytes. MHC II expression was detected by LT1A antibody staining on 22-38% (animal 2/1) and could be assigned to the majority of $CD3^-$ cells, most likely B cells (22-40% of lymphocytes animal 2/1) and a small fraction of $CD3^+$ cells, probably activated T cells [397]. In addition, a small MHC II^- $CD3^-$ population of 8-10% (animal 1/2) was detected. Again, comparison with total MHC II frequencies observed in llama PBMCs revealed similar expression patterns [354]. LT5A, a llama-specific antibody assigned to CD8, stained around 16% of live cells in both animals. CD3 staining revealed 3-7% of lymphocytes to be $LT5A^+CD3^-$ and most likely NK cells and approximately 12% $LT5A^+CD3^+$ cells representing cytotoxic T cells. Similarly, llama PBMCs have been observed to comprise about 13% $CD8^+$ cells [354]. Surface expression of BTN3 was studied by the newly developed mAb 189 and could be detected on all lymphocytes (see 3.2.2.2.2 and 3.2.2.3). A slight difference in expression levels was detected on $CD3^+$ and $CD3^-$ cells, with a higher expression on T cells.

All the markers applied in these stainings were co-stained with 118.7 mAb to further characterize the cell subset stained by this antibody. 118.7^+ cells were observed to be $CD3^+$, $CD5^{low}$ and $BTN3^{high}$. Interestingly, 118.7^+ cells were not stained by GB45A specific for WC1, a marker for γδ T cells. This is not surprising, as WC1 expression in ruminants is associated with the distinct usage of *TRGV* segments that associate with the *TRGC5* cassette of constant regions [398]. As discussed in chapter 4.2.2.1, $WC1^+$ cell frequencies of around 16% are reminiscent of "γδ high" species and the existence of $WC1^+$ cells and $WC1^-$ γδ T cells provides further evidence. However, not all γδ T cells in ruminants express this marker [399] and 118.7^+ cells could simply represent a distinct γδ subset from alpaca $GB45A^+$ cells. Investigation of $GB45A^+$ cells in the alpaca seems to be worthwhile especially concerning the *TRG* and *TRD* usage of this population. The antibodies LT1A (MHC II) and LT5A (CD8) stained subsets of 118.7^+ cells, with most cells being $CD8^+$ and MHC II^-. MHC II expression correlated with 118.7 expression levels, as

118.7^{low} cells expressed MHC II. This could be an indicator for activated 118.7^{+} cells because the expression of all MHC II isotypes was found to be induced in activated human T cells [397]. A small population of 118.7^{+} cells was observed to be CD8^{-} and the surface marker stained by LT10A was expressed by the majority but not all 118.7^{+} cells. As the specificity of 118.7 mAb was narrowed down to an epitope on δ chains using the *TRDV2/TRDJ4* gene rearrangement and therefore Vδ2Jδ4 chains, differences in expression of certain cell surface markers could be explained by the state of activation of these cells or differential pairing with γ chains.

The characterization of alpaca PBMCs should be expanded by co-stainings of other surface markers like GB45A together with LT3A (CD5), LT5A (CD8) or LT10A (LC1 cluster) to further characterize the composition of WC1^{+} cells in alpaca PBMCs. Furthermore, testing of more antibodies specific to llama PBMCs should be considered, as to this date, no CD4 staining was possible. More knowledge on BTN3 expression levels could be gained by co-stainings of biotinylated or labeled 189 antibodies with markers for B cells, MHC II (LT1A) and WC1 (GB45A). The lymphocyte composition in peripheral blood of alpacas was further characterized in this experimental setup and shows striking similarities to expression patterns in llama PBMCs, as previously reported by Davis et al. [354].

4.2.2.4 A subset of alpaca PBMCs show HMBPP reactivity

In this study, phosphoantigen reactivity of PBMCs from *Vicugna pacos*, the first non-primate species expressing Vγ9Vδ2 T cells, could be shown. Frequencies and cell numbers of 118.7^{+} cells increased in alpaca PBMCs after seven days of stimulation with the phosphoantigen HMBPP (see 3.2.2.4). Frequencies of alpaca Vδ2Jδ4^{+} cells increased from 0.5% of live cells to around 22%. The Vδ2^{+} cell population in human PBMCs increased in frequency to 60% in a parallel experiment at the highest dose of 1 nM HMBPP. In comparison to human PBMCs, where a saturating dose of HMBPP could be observed at 1 nM concentrations, HMBPP was possibly not used in a saturating dose for alpaca PBMCs (1 µM). Yet, considering the specificity of 118.7 for Vδ2Jδ4 TCR chains, phosphoantigen-reactive Vγ9Vδ2 T cells potentially using other Jδ could have been overlooked. Interestingly, 118.7^{+} cell frequencies in control samples with only hIL-2 seemed to drop compared to day 0 which indicates decreased viability without stimulus. However, cell proliferation upon stimulation with the phosphoantigen HMBPP seemed evident, as calculated cell numbers of 118.7^{+} cells increased 30-fold compared to day 0 stainings. This implies not only enhanced survival of Vδ2Jδ4 T cells in alpaca PBMCs but proliferation upon stimulation with the phosphoantigen HMPBP.

While establishing alpaca PBMC stimulations, a variety of culture conditions was tested. Due to lack of recombinant alpaca IL-2, recombinant human IL-2 was used. Addition of this human cytokine promoted dose-dependent cell survival in comparison to cells cultivated in medium only. The addition of culture supernatant of ConA-stimulated alpaca PBMCs instead of hIL-2 did not promote cell survival as well. The use of culture mediums specifically manufactured for human PBMC culture like X-Vivo 10 or X-Vivo 15 with or without supplements (10% FCS, SC supplement) did in fact decrease frequencies of Vδ2Jδ4^{+} cells in alpaca. Therefore, RPMI1640 with 10% FCS and SC supplement (RPMI++) was routinely used. Variation of responses at different cell densities were studied and the outcome of cultivation in 48 or 96 well plates was examined. The parameters yielding the best results were cultivation for seven days in 96 well plates (no difference was observed between round or flat bottom to this date) in 200 µl RPMI++ and added hIL-2 (50 U/ml). A variety of factors could explain the outcome of alpaca PBMC stimulations in comparison to human PBMCs. One observation was a pronounced variability among individuals where no increase in 118.7^{+} cell frequency could be shown (animal 4) and others with varying frequencies of 118.7^{+} cells on day 7 (animal 1-3 and 5-8) (see selection of experiments in **Table A.3**). This is in agreement with observations in humans where inter-individual differences can be observed upon *in vitro* stimulation of PBMCs with aminobisphosphonates or HMBPP [400-402]. The cell viability of alpaca PBMCs decreased rapidly after day 7 which is surprising since human PBMCs can be stimulated and Vγ9Vδ2 T cells expanded with either aminobisphosphonates (NBP) or HMBPP and cultured for more than 14 days [71, 313]. The major limitation was the viability and numbers of cells isolated from alpaca blood samples. Recovery of viable cells after Histopaque®-1077 PBMC isolation varied greatly among animals and time points of blood draw. In general, lower yield of PBMCs was observed in blood samples of female alpacas compared to male individuals. Lymphocytes recovered from some samples displayed enhanced cell death in cultures and very low numbers of live lymphocytes (0.3-1*10^{4}) were observed on day 7 in contrast to more than 3*10^{4} in other stimulations. This could be due to subclinical infections of alpacas and pre-activation of lymphocytes or due to differences in cell viability caused by isolation procedures. This drawback of alpaca PBMC stimulations should be investigated by testing of various isolation protocols, e.g. different density gradients, and low cell recovery could be improved by using higher quantities of blood. One hint at differential behavior of alpaca PBMCs compared to human PBMCs was a pilot experiment using higher temperatures for cell culture incubation (data not shown). Body temperatures of healthy alpaca range between 37.5 and 38.9°C [403, 404], therefore stimulation assays of alpaca PBMCs of animal 3 with 50 U/ml rhIL-2 and 1 µM HMBPP were incubated at 37°C or 39°C, respectively. A two-fold increase in 118.7^{+} cells was observed at 39°C compared to 37°C, although there was no marked difference in cell viability. However, higher incubation

temperatures could result in enhanced survival and/or proliferation of 118.7$^+$ cells. In summary, a phosphoantigen reactivity of alpaca PBMCs could be proven in this setting but efficient stimulation conditions still need to be established. Once a reliable stimulation protocol is established, a characterization of the expanded cells with alpaca-specific surface markers should be performed as well as testing for proliferation (CFSE or Ki67) and/or activation markers should be considered.

Two antibodies have been described for human BTN3 that have been found to be cross-reactive to alpaca BTN3 (see 3.2.2.2.2). The antibody 20.1 is an agonist antibody that mediates BTN3-dependent and phosphoantigen-independent activation of Vγ9Vδ2 T cells [244] and the mAb 103.2 specifically inhibits phosphoantigen-dependent activation of Vγ9Vδ2 T cells by binding BTN3 [48, 303]. Addition of 20.1 mAb to alpaca PBMCs did not result in an increased frequency of 118.7$^+$ cells or visible stimulation of cells (size and granularity by FSC/SSC). The antibody 103.2, however, mediated a significant reduction of 118.7$^+$ frequencies in a stimulation assay with HMBPP (see **Figure 3.30**). This was in contrast to the human system, where 103.2 almost completely abrogated Vγ9Vδ2 activation. This could be due to the lower affinity of 103.2 to alpaca BTN3 as observed in chapter 3.2.2.2.2. The newly developed antibody 189 (clone 189.21.17) resulted in a lower frequency of 118.7$^+$ cells in cultures with HMBPP, however, no significant effect was observed. Yet, cell culture supernatants of the 189 hybridoma contaminated with another unspecific hybridoma were used (see 3.2.2.2.2), and low concentrations of 189 could be the reason for a diminished effect. Therefore, the purified clone 189.21.17 should be tested for its inhibitory capacity on phosphoantigen-mediated activation of alpaca and human cells.

4.2.2.5 Vγ9 and Vδ2 usage in unstimulated and expanded PBMCs

The expression of productive alpaca Vγ9 and Vδ2 chains was first described by Karunakaran et al. [317]. This study also described a *TRGJP* preference of *TRGV9* gene segments and a CDR3 length variation of ± 2 amino acids. In addition, the majority of *TRDV2* gene segments was rearranged with a *TRDJ4* homolog [317]. Due to the availability of the newly synthesized mAb 118.7 specific for Vδ2Jδ4 chains, a more in-depth repertoire analysis of alpaca Vγ9Vδ2 chains in unstimulated and HMBPP-stimulated PBMCs was performed (see 3.2.2.5). In addition, single-cell Vγ9Vδ2 TCR usage was studied in unstimulated PBMCs and PBMCs after seven days of culture with HMBPP (see 3.2.2.6).

Here, the previously reported preference for *TRGJP* in Vγ9 chains and the gene segment *TRDJ4* in Vδ2 chains could be confirmed [317]. Analysis of CDR3 lengths in TOPO TA clones of *TRGV9*/*TRGC* and *TRDV2*/*TRDC* PCR products revealed a pronounced bias of *TRGV9* chains for CDR3 of 14 amino acids in 118.7$^+$ cells and 118.7$^-$ cells after stimulation with HMBPP, whereas no length restriction of CDR3 regions was observed in *TRDV2*-carrying chains. A certain bias for CDR3 lengths of 13 or 14 amino acids has also been reported for the bottlenose dolphin [325]. As already discussed in chapter 3.2.2.1, three variants of *TRGJP* segments were found in the study by M. Karunakaran and colleagues (*JP-A*, *JP-B* and *JP-C*) and usage of these was different for individuals [317]. Here, the same variants of *TRGJP* were observed and the two animals showed distinct biases for different *TRGJP* variants (animal 1: *TRGJP-B*; animal 2: *TRGJP-C*). Not more than two variants were used per animal which indicates allelic versions of the same gene. The 118.7$^-$ cell population was observed to be nearly monoclonal after HMBPP stimulation, whereas a difference in clonality was less pronounced for 118.7$^+$ cells before and after HMBPP stimulation. Reasons for the increased number of clones sharing the same clonotype in stimulated 118.7$^-$ PBMCs were most likely the activation and proliferation of phosphoantigen-reactive cells and/or reduced viability of non-reactive cells. The only clear differences observed between *TRGV9* and *TRDV2* usage in 118.7$^-$ and 118.7$^+$ cells were the occurrence of *TRDV2* in rearrangement with other *TRDJ*s in 118.7$^-$ cells and the prominence of a single *TRDV2*/*TRDJ2* clone, with different CDR3 regions in animal 1 and 2, in the 118.7$^-$ subset after HMBPP stimulation. This implies the existence of a highly phosphoantigen-reactive Vδ2Jδ2$^+$ cell subset that cannot be detected in PBMC stimulations to this date due to the specificity of 118.7 for Vδ2Jδ4 chains (see 3.2.2.4) and could also explain the lower response of alpaca PBMCs to HMBPP as measured by increase of cells stained by mAb 118.7. Therefore, to study the full effect of phosphoantigen recognition in alpaca PBMCs, it would be worthwhile to develop other antibodies specific for Vδ2Jδ2 or even pan-Vδ2. Curiously, Vδ2Jδ4 chains were also observed in 118.7$^-$ cells although 118.7 seems to be specific for these δ chains. The occurrence of this can be explained by cross-contamination of cells during sorting and very low frequencies of *TRDV2*/*TRDC* transcripts in unstimulated 118.7$^-$ cells.

An important feature of phosphoantigen-reactive Vδ2 chains in humans is the use of a hydrophobic amino acid (L, I or V) at position δ97 [241, 247]. Alpaca Vδ2 chains showed conservation of these amino acids in some but not all Vδ2 chains, and interindividual differences were observed. In general, 40-77% of unique clones used leucine, isoleucine or valine at δ97. The frequency of clones carrying these residues seemed less in the unstimulated 118.7$^-$ subset. However, both Vδ2Jδ2 clones observed at high frequencies in stimulated cells showed isoleucine at position δ97. This indicates importance of these residues in alpaca, however, a definite influence on phosphoantigen reactivity needs to be examined. Here, site-directed

mutagenesis should be considered, and the effect on phosphoantigen recognition by alpaca TCRs should be studied (see 3.2.2.9). Another aspect of TCR repertoires is the existence of clonotypes shared by different individuals. The dominance of public *TRGV9*/*TRGJP* clonotypes is characteristic for the human Vγ9 chain repertoire [239, 240, 376]. In the alpaca, only one clonotype (CDR3: ALWEPLTDGRTIKV) was shared by both animals. Therefore, one can only speculate that this characteristic feature of Vγ9 chains is conserved in alpaca and should be further investigated by Next Generation Sequencing (NGS). The canonical *TRGV9*/*TRGJP* rearrangement in humans (CDR3: ALWEVQELGKKIKV) was described as a major public clonotype in adult humans [376, 377]. In contrast, the alpaca germline *TRGV9*/*TRGJP* recombination (CDR3: ALWDALTDGKTIKV) was found to be expressed by only one clone of 118.7^{-} unstimulated cells.

These results indicate conservation of characteristic features of human Vγ9 and Vδ2 repertoires in alpacas and provide insights into the possible TCR usage of phosphoantigen-reactive alpaca γδ T cells. However, they do not prove a pairing of Vγ9 and Vδ2 chains in alpaca PBMCs. For this purpose, single-cell PCR experiments were performed using the mAb 118.7 (see 3.2.2.6). Interestingly, Vδ2 chains seemed to not always pair with Vγ9 chains, especially in unstimulated PBMCs. Only 14% of Vδ2 chains were positive for a *TRGV9*/*TRGC* transcript in unstimulated 118.7^{+} cells, whereas 82% of HMBPP-stimulated cells where Vγ9Vδ2^{+}. This is a clear indication of proliferation or selective survival of cells with Vγ9Vδ2 pairings upon HMBPP stimulation. Vδ2 pairing is not restricted to Vγ9 in humans [388], therefore other γ chains could be associated with Vδ2 in alpacas. This should be investigated by single-cell PCR of Vδ2Jδ4^{+} cells using primers specific for the most frequent *TRGV* gene segments used in alpacas (*TRGV11* and *TRGV8-C*). The features of alpaca *TRGV9* and *TRDV2* rearrangements observed in chapter 3.2.2.5 could be confirmed in the single-cell PCR experiments. *TRGJP* preference and preferred CDR3 lengths of 14 amino acids were observed. Oligoclonality of the Vγ9Vδ2 cell subset can be assumed, as even with the small sample size used in this pilot experiment, some clonotypes were detected in multiple single-cells. Overlapping signals of *TRGV9* CDR3 regions were detected in one single-cell clone. This indicates for multiple Vγ9 chain transcripts expressed by one cell, especially since only one Vδ2 chain was observed. However, the expression of multiple transcripts of γ chains and lack of allelic exclusion has been described for mice and humans [405-407]. Single-cell PCR experiments with alpaca PBMCs indicate low Vγ9Vδ2 frequencies in unstimulated PBMCs and an increase of Vγ9Vδ2 pairings after HMBPP stimulation. These results need to be viewed under the caveat that this experimental setup still needs to be adequately established. Especially the robustness of the *TRGV9*/*TRGC* PCR amplification remains questionable and could lead to an underestimation of Vγ9 transcripts.

4.2.2.6 Conservation of prerequisites for phosphoantigen recognition in alpaca

Phosphoantigen reactivity of human Vγ9Vδ2 T cells is mediated by human BTN3A1 [48, 49, 304, 308] and other unknown molecules encoded on human chromosome 6 [315]. Hamster cells (CHO) lack the ability to activate human Vγ9Vδ2 T cells when transduced with human BTN3A1, however, this is reconstituted in somatic hybrid cell lines (CHO huChr. 6) carrying a human chromosome 6 [315]. Here, expression of human BTN3A1 in an alpaca cell line lead to phosphoantigen recognition by human Vγ9Vδ2 TCRs (see 3.2.2.7). Although phosphoantigen reactivity in this experiment required higher doses of HMBPP compared to human cell lines expressing endogenous BTN3, the conservation of additional factors necessary for PAg recognition in the alpaca seems evident.

The alpaca BTN3 exists in only one isoform in alpacas in contrast to humans where two successive duplications led to the isoforms BTN3A1, BTNA2 and BTN3A3 [298]. The only human isoform able to sense phosphoantigens is BTN3A1, as BTN3A2 lacks the B30.2 domain and BTN3A3 has one amino acid change in the B30.2 domain that abolishes phosphoantigen binding [48]. Alpaca BTN3 possesses a BTN3-V and BTN3-C domain more like BTN3-V and BTN3-C of human BTN3A1 and A2. The intracellular juxtamembrane domain and the B30.2 domain, however, are more like BTN3A3. Interestingly, the transmembrane region is very much like the human BTN3A1 homolog and is the most conserved region in the whole molecule.

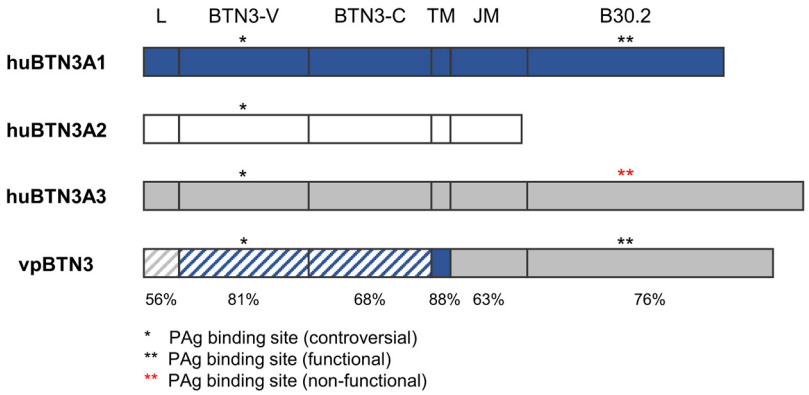

Figure 4.1 Similarities of alpaca BTN3 domains with human BTN3 isoforms. The regions of BTN3 amino acid sequences leader (L), variable Ig-like region (BTN3-V), constant Ig-like region (BTN3-C), transmembrane (TM), juxtamembrane (JM) and intracellular B30.2 domain (B30.2). Lengths are represented by the size of boxes. Amino acid identities of alpaca BTN3 regions to counterparts in human isoforms were calculated with NCBI blastp. Alpaca BTN3 regions were color-coded according to similarities with human isoforms (blue: BTN3A1, white: BTN3A2, gray: BTN3A3 or striped: similar to more than one isoform).

The functionality of alpaca BTN3 was assessed using chimeric alpaca/human BTN3 molecules due to the lack of an alpaca *in vitro* system. For this, chimeric molecules with the human BTN3-V and BTN3-C, and the alpaca transmembrane, juxtamembrane and B30.2 region and vice versa were cloned and expressed in 293T cells lacking BTN3A1 or all isoforms (see 3.2.2.8).

The 293T BTN3A1 and complete BTN3A1-3 knock out cell lines were developed by M. Karunakaran using the CRISPR/Cas9 system and both cell lines were not able to mediate phosphoantigen recognition or 20.1-dependent activation in culture with human Vγ9Vδ2 TCR transductants (unpublished data). These 293T KO cells were transduced with human BTN3A1, alpaca BTN3 or the chimeric BTN3 molecules hu/vpBTN3 or vp/huBTN3 as mCherry fusion proteins and an established in vitro model with murine responder cells carrying human Vγ9Vδ2 TCRs was used (see 3.2.2.8). Reconstitution of 293T BTN3A1-3 KO cells with human BTN3A1 rescued 20.1 mAb-mediated IL-2 production but could not replenish HMBPP-mediated IL-2 release, whereas huBTN3A1 expression in 293T BTN3A1 KO cells fully rescued 20.1 and HMBPP-dependent activation. This is in context with other findings that report a reduced function of human BTN3A1 without help from the other isoforms (unpublished data M. Karunakaran and T. Herrmann and [310]). Overexpression of alpaca BTN3 did not result in any activation of human Vγ9Vδ2 TCR transductants in both 293T KO cell lines. The same outcome was observed when vp/huBTN3 was expressed in 293T BTN3A1-3 KO cells. Lack of recognition of alpaca BTN3 by responder cells carrying human TCRs and therefore no cross-reactivity seems evident This is not surprising as Vγ9Vδ2 TCR require cell-cell contact for stimulation [249, 250] and differences in the extracellular parts of human and alpaca BTN3 could abolish binding of TCRs. Surprisingly, vp/huBTN3 mediated rescue of 20.1 and HMBPP effects in 293T BTN3A1 KO cells. Here, as no recognition of alpaca extracellular domains by the human Vγ9Vδ2 TCR seems evident, heterodimers of vp/huBTN3 and human BTN3A2 or BTN3A3 could mediate TCR recognition while vp/huBTN3 replaces the function of huBTN3A1 [310]. The BTN3-C region has been implied to be important for the formation of heterodimers of human BTN3A1 with BTN3A2 or BTN3A3 and BTN3A1 homodimers have been reported [303, 310]. Yet, the formation of human BTN3A1 homodimers could not be replicated in lipid nanodisks [312]. In this experimental setup, wild-type vpBTN3 was not recognized in 293T huBTN3A1 knock out cells by the human γδ TCR, whereas vp/huBTN3 enabled PAg-mediated activation of responder cells. As both chimeric molecules possess the alpaca BTN3-C region, potential heterodimers of vp/huBTN3 and endogenous human BTN3A2 or BTN3A3 must be formed by different interactions and an importance of the transmembrane and intracellular domains seems evident. Therefore, the development of chimeric alpaca BTN3 molecules carrying the human transmembrane, juxtamembrane or B30.2 domain of BTN3A1 should be considered to map interacting regions using the 293T huBTN3A1 knock out system.

A chimeric molecule with the human extracellular part of BTN3A1 together with alpaca BTN3 intracellular domains (hu/vpBTN3) rescued 20.1- and HMBPP-mediated activation of responder cells in both BTN3 KO cell lines. Hence, the alpaca B30.2 domain seems to be able to sense phosphoantigens in the human *in vitro* system and transmembrane and juxtamembrane

domains seem to be conserved enough to allow the complete functionality of the chimeric hu/vpBTN3. Moreover, in collaboration with the group of E. Adams, the interaction of the phosphoantigens IPP and HMBPP with the alpaca B30.2 domain has been investigated using isothermal titration calorimetry and was shown to be similar to human B30.2. This indicates that differences in phosphoantigen recognition in the human and alpaca system are not primarily linked to variations in phosphoantigen binding to the B30.2 domains.

The formation of BTN3 heteromers seems necessary for efficient recognition of PAg and inside-out signaling [310]. However, it remains to be studied how the single isoform of BTN3 in alpacas can unite the features of the human system in one molecule. In terms of evolution, the alpaca BTN3 can be described as the more primordial form of BTN3 described by Afrache et al. [298]. This primordial form of BTN3 can be found in *Otolemur garnettii* (Prosimians) which has to this date not been shown to possess a functional Vγ9Vδ2 T cell subset [298]. One peculiarity of the alpaca transmembrane domain is the amino acid change of L259C compared to human BTN3A1 (see **Figure A.2**). This change was not observed in *Otolemur garnettii* BTN3. A cysteine in the transmembrane region could play a role in dimerization or functionality of alpaca BTN3. Interestingly, the same amino acid change is found in dolphin BTN3. As both animals possess only one isoform of BTN3, it would be worthwhile to study a potential involvement of this residue in BTN3 functionality using site-directed mutagenesis.

The results obtained in this study of alpaca BTN3 were used to develop a proposed model for phosphoantigen recognition based on what is known in the human system.

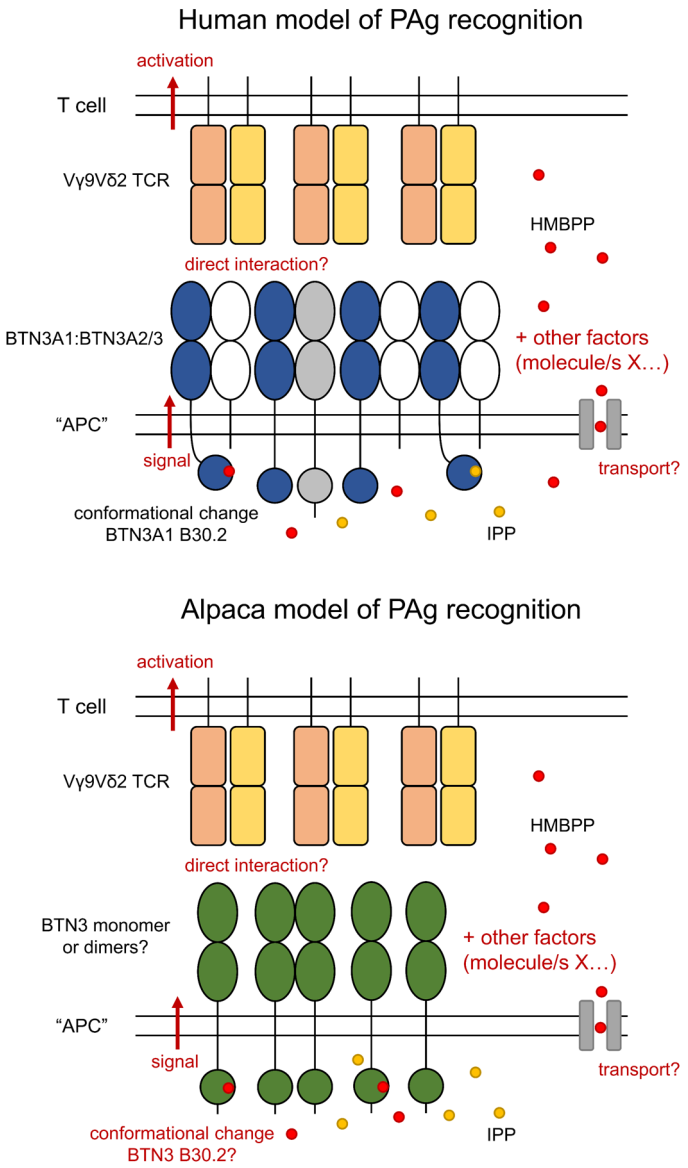

Figure 4.2 Proposed model of phosphoantigen recognition in humans and alpacas.

The activation of Vγ9Vδ2 T cells in alpacas seems to be mediated by the single BTN3 isoform expressed in this species. Whether or not homodimers are formed comparable to human heterodimers is not known yet. Assumingly, a conformational change could happen in the alpaca BTN3 upon binding of phosphoantigen to the alpaca B30.2 domain. The signal translation to the surface is not well studied in humans but clustering of BTN3 molecules could occur leading to direct binding of the Vγ9Vδ2 TCR or recognition by the TCR is dependent on other unknown molecules. Conservation of molecule/s X, other unknown factors that are essential for phosphoantigen recognition in humans and are not found in rodents, could be confirmed in the alpaca.

4.2.2.7 Phosphoantigen-reactive alpaca TCRs

A formal proof of phosphoantigen-reactive alpaca Vγ9Vδ2 TCRs is shown in chapter 3.2.2.9 using an *in vitro* model of phosphoantigen stimulation [369]. Only one out of six combinations of alpaca Vγ9 and Vδ2 TCR chains (vpVγ9_14aa+vpVδ2Jδ2) was observed to react in a phosphoantigen-dependent manner in co-culture with cells expressing endogenous alpaca BTN3 (LGK-1-R). However, a cross-reactivity of this TCR and two others, one carrying the same Vδ2 chain and one using the same Vγ9 chain, to human BTN3A1 was detected. In the case of vpVγ9_14aa+vpVδ2Jδ2, mIL-2 production was of similar magnitude as observed for human responder cells indicating a similar efficiency of recognition. The lacking reactivity of alpaca TCRs to endogenous BTN3 (LGK-1-R) and higher reactivity in a xenogenous model as well as the overall scarcity of PAg-reactive clonotypes (1 out of 6) indicates an extreme importance of the right Vγ9 and Vδ2 pairing in the alpaca BTN3/Vγ9Vδ2 T cell system. This observation could be explained by various levels of affinity leading to a stronger response of certain Vγ9Vδ2 TCRs compared to a lower response of other clonotypes. In this experimental setting, the use of a Vγ9 TCR with a CDR3 of 14 amino acids or the use of a Vδ2Jδ2 TCR chain seemed to be beneficial for PAg reactivity. Combination of both resulted in the expression of a very potent alpaca Vγ9Vδ2 TCR. One could speculate that the *TRDJ2* gene segment used in rearrangement with *TRDV2* leads to a higher reactivity of the alpaca TCR *in vitro*, however, this is only the case in combination with the vpVγ9_14aa TCR chain. In general, the *TRDJ4* gene segment is more prevalent in alpaca δ chains (see 3.2.2.1 and 3.2.2.5) and *TRDJ2* usage is rare but could be more suitable for PAg recognition. Therefore, the frequency of potent PAg-reactive Vγ9Vδ2 TCRs could be very low. Investigation of Vδ2 chains using other *TRDJ* gene segments like *TRDJ3* should be considered to gain a better understanding of PAg-reactive Vδ2 chains in the alpaca. The K108R and K109T substitutions in the alpaca *TRGJP-A* gene segment as compared to human *TRGJP* did not disrupt PAg recognition in alpacas (see 1.6.5). Here, the influence of other variants of the alpaca *TRGJP* gene segment on phosphoantigen reactivity should be investigated. The fact that Vδ2Jδ4 chains did not react to phosphoantigens in co-culture with LGK-1-R cells could be due to inefficient stimulatory capacities of LGK-1-R cells or a requirement of higher TCR affinities in this setting. BTN3 antibody-dependent activation by 20.1 and inhibition of mIL-2 production by 103.2 was only observed in the human *in vitro* model using 293T cells but not with LGK-1-R. This is not surprising considering the lower affinities of both antibodies to alpaca BTN3 (see 3.2.2.2.2). The agonist antibody 20.1 is able to activate specific alpaca clonotypes in context with human BTN3 whereas others do not react. This is reminiscent of human Vγ9Vδ2 TCRs which show differential reactivity to 20.1 mAb [369]. Inhibition by 103.2 was not observed for the alpaca Vδ2Jδ2 TCR, however, inhibition of 118.7^{+} Vδ2Jδ4 T cells seemed evident in a different preliminary stimulation (see 3.2.2.4).

The effect of 103.2 on Vδ2Jδ2 T cells should, therefore, be examined in PBMC stimulation experiments. In addition, antibody-dependent inhibition or activation of the alpaca BTN3-specific mAb 189.21.17 needs to be investigated.

The existence of phosphoantigen-reactive Vγ9Vδ2 TCRs could be proven in this study. However, dose-dependent reactivity to HMBPP and other stimuli like aminobisphosphonates (zoledronate) should be tested as well as other alpaca BTN3 expressing cell lines. Clonotypes from alpaca single-cell PCRs should be tested for antigen reactivity to investigate combinations of Vγ9 and Vδ2 chains used *in vivo*. Considering the lack of cross-reactivity of a human Vγ9Vδ2 TCR, it would be interesting to study how the recognition of alpaca BTN3 differs from that of human BTN3 isoforms. For this purpose, heterodimeric TCRs or chimeric BTN3 molecules could be produced to test for molecular determinants of BTN3 or the TCR specifically. More precisely, what are the determinants that are missing to enable a human Vγ9Vδ2 TCR to recognize alpaca BTN3?

4.2.3 Outlook: The BTN3/Vγ9Vδ2 T cell system in non-primate species

Phylogenetic studies showed the conservation of *TRGV9*, *TRDV2* and *BTN3* genes in several non-primate species and led to the hypothesis of emergence of this system with placental mammals. These genes have been lost in some species and lost or retained function in other placental mammals. Two candidate species for functional BTN3/Vγ9Vδ2 T cell systems have been studied in this thesis. The nine-banded armadillo revealed a most likely non-functional BTN3/Vγ9Vδ2 T cell system at closer inspection and can be described as a witness for co-evolution, whereas the alpaca is the first non-primate candidate species proven to possess a phosphoantigen-reactive Vγ9Vδ2 T cells system and a BTN3-like molecule functionally similar to the human BTN3 isoforms.

Several steps can be taken to investigate the structural requirements of the BTN3/Vγ9Vδ2 T cell system using both species. First, the armadillo BTN3 isoforms should be verified on the genomic level, and number and structure of these should be studied. Moreover, the B30.2 domain of the armadillo could be reconstructed to a functional ORF, and it would be interesting if phosphoantigen interactions with this domain are still possible and comparable to human or alpaca B30.2 domains. In addition, the phosphoantigen-sensing ability of this armadillo B30.2 domain could be investigated within a chimeric BTN3 molecule using *in vitro* stimulation assays with Vγ9Vδ2 responder cells. Armadillo Vδ2 chains could provide a valuable tool in the study of heteromeric TCRs and their PAg-mediated activation.

The alpaca can be considered a developing model for a BTN3/Vγ9Vδ2 T cell system and will help to identify common determinants of Vγ9Vδ2 and BTN3 interactions between species. In general, alpaca Vγ9Vδ2 T cells can be phosphoantigen-reactive, and the alpaca BTN3 molecule is able to interact with phosphoantigens. The outstanding advantage of this model will be the existence of only one BTN3 isoform and lacking recognition of this BTN3 by human Vγ9Vδ2 TCRs. This enables the study of interaction partners using chimeric molecules. A functional study of alpaca Vγ9Vδ2 TCR and BTN3 interactions is possible as specific TCRs have the ability to recognize endogenous alpaca BTN3. This *in vitro* system needs to be thoroughly established, and the interactions of different alpaca TCRs with chimeric human/alpaca BTN3 molecules should be investigated. A reliable protocol for the isolation and phosphoantigen stimulation of alpaca PBMCs needs to be established, and identification of phosphoantigen-reactive PBMCs should be repeated with antibodies specific for Vδ2Jδ4 and Vδ2Jδ2 TCRs. NGS studies could provide a valuable tool to investigate TCR usage of alpaca Vγ9Vδ2 T cells further. We hypothesize that the conserved phosphoantigen recognition of this system in the alpaca correlates with effector functions comparable to the human system. This could be investigated by transcriptomics of cell subset due to a general lack of other suitable reagents in this model organism.

4.3 Conclusions

Three species, alpaca, nine-banded armadillo and cotton rat were investigated in this thesis for the conservation of non-conventional T cell subsets. First, the cotton rat was shown to express functional iNKT-like cells and their antigen-presenting molecule CD1d is homologous to CD1d of established mouse and rat models. Moreover, an expanded family of *AV14* TCR α chain genes was found. This first identification of the immunomodulating iNKT cell subset contributed to a better characterization of the cotton rat immune system, and this knowledge can now be used to study the role of iNKT cells in virus infections. Hence, this added a variety of tools to study infectious diseases in an already valuable animal model for human respiratory virus infections. Second, the expression of genes necessary for a functional subset of the major human γδ T cell subpopulation Vγ9Vδ2 was studied in the nine-banded armadillo, an animal model used in leprosy research and a natural reservoir of *Mycobacterium leprae*. According to the findings of this project, the functional conservation of the BTN3/Vγ9Vδ2 T cell system in this species does not seem likely. However, insights into the evolutionary rise of the BTN3/Vγ9Vδ2 T cell system in a common ancestor of placental mammals could be gained, and the armadillo animal model can be applied to study the importance of structural features for the functionality of those cells

in *in vitro* studies with chimeric molecules. Last, the alpaca was further investigated for Vγ9Vδ2 T cell populations, reactivity to phosphoantigens and conservation of a functional BTN3 molecule. All of these aspects could be confirmed to be existent in the alpaca, and interesting differences to the human Vγ9Vδ2 T cell system were observed. The alpaca animal model is the first non-primate species with a conserved BTN3/Vγ9Vδ2 T cell system and promises to be a valuable tool in the understanding of this system in placental mammals.

5 Summary

Non-human species have been used for a long time in most scientific fields including immunology, virology, oncology, infectious diseases and behavioral biology. Today, inbred mouse strains are the go-to method for most of medical research that requires a model system. However, other species that could prove to be essential tools for the study of specific cell subsets remain to be evaluated and tested for conservation of functionality. In this thesis, three species were investigated for the conservation of two non-conventional T cell systems, the CD1d/ iNKT cell system and the BTN3/ Vγ9Vδ2 T cell system. Non-conventional T cells are αβ or γδ T cells that do not fit into the classical mode of antigen recognition and adaptive responses. These T cells recognize antigens different from classical peptide antigens and are not restricted to the polymorphic MHC molecules but rather to non-polymorphic antigen-presenting molecules. They usually show a limited TCR repertoire and tissue-specific localization can be observed as well as higher frequencies of subsets compared to αβ clonotypes.

The iNKT cell subset is restricted by the lipid antigen-presenting molecule CD1d and carries out immunomodulatory functions by rapid cytokine secretion. This cell subset is characterized by the expression of a semi-invariant αβ TCR using an α chain with an *AV14*/*AJ18* rearrangement in mice and rats while human iNKT cells use the homologous *AV24*/*AJ18* gene rearrangement. These α chains associate with a limited number of different β chains which show diversity in the β chain junctional region. A role for iNKT cells has been described in various microbial infection, autoimmunity, cancer and virus infections. Research in the cotton rat, a model organism for infections with human respiratory viruses and measles virus, was somewhat hampered by lack of genomic information and tools for the detailed study of iNKT cells during virus infections. Therefore, the conservation of the iNKT cell subset and its antigen-presenting molecule CD1d was investigated in this model organism. The molecular basis of this system, the semi-invariant iNKT TCR chains and CD1d were proven to be expressed and compared to homologs in human and rodents. Cotton rats possess multiple members of the *AV14* and *BV8* family and only one isoform of CD1d which is comparable to findings in the rat. Moreover, the reactivity of primary cells to glycolipid antigens could be shown, and an iNKT cell-like population was detected in primary cells using newly developed cotton rat CD1d oligomers. These were also applied to test the capacity of CD1d to present typical glycolipid antigens to iNKT TCR transductants. In addition, expression of cotton rat iNKT TCR α and β chains in TCR-negative cell lines was used to show successful pairing and detection of glycolipids in the context of CD1d. In summary, the conservation of a functional CD1d/iNKT cell system in the cotton rat could be shown, and tools were developed to study this cell subset in the course of infectious diseases.

The Vγ9Vδ2 T cell subset is the major γδ T cell subset in human peripheral blood and has the unique ability to contribute to immune surveillance by detecting pyrophosphorylated metabolites of isoprenoid synthesis, also termed phosphoantigens, that indicate cell stress, transformation or infection. These cells are characterized by the usage of the TCR gene segments *TRGV9*/*TRGJP* and *TRDV2* and phosphoantigen recognition is mediated by members of the BTN3 family. Up to this date, phosphoantigen-reactive γδ T cells have only been shown in primate species. However, evidence for the existence and functional conservation of the genes implied in the BTN3/Vγ9Vδ2 T cell system was found in several placental mammal species, and two candidate species were chosen for further investigation.

The nine-banded armadillo, a valuable model for leprosy research, was shown to possess homologous genes to *TRGV9*, *TRDV2* and *BTN3*. In this study, the expression of productive rearrangements of *TRDV2* gene segments could be shown in peripheral blood samples, but no evidence was found for the expression of a functional *TRGV9* rearrangement or BTN3 molecules. Interestingly, evidence for duplication of *BTN3* genes was shown, and the genetic organization was strikingly similar to human *BTN3*, even though *BTN3* genes in the armadillo are most likely pseudogenes. Moreover, determinants of phosphoantigen-reactive Vγ9Vδ2 T cells and functional BTN3 molecules were found to still be prevalent in armadillo genes. This makes the armadillo an interesting model to study the structural determinants that allow phosphoantigen recognition by a functional Vγ9Vδ2 T cell subset although this species is merely a witness for a functional system in a placental mammal ancestor.

In contrast, alpacas were shown to express functional Vγ9Vδ2 T cells which conserved many features of the human counterpart including *TRGJP* usage and CDR3γ length restriction. Expression of Vγ9Vδ2 pairings could be shown by single-cell PCR and functional phosphoantigen-reactive pairings were observed. This phosphoantigen reactivity was also shown in PBMC cultures with a newly developed antibody specific for alpaca Vδ2Jδ4 chains. Moreover, a more detailed study of the alpaca TCR repertoire showed similarities to "γδ high" species like camelids and cattle which possess an extended family of *TRDV* genes. The γ and δ loci of alpaca TCR genes were drafted based on genomic information and cDNA studies and provide an overview for more detailed studies. Conservation of phosphoantigen recognition by the single BTN3 molecule of alpacas was shown in 293T knock out cell lines, and BTN3 detection on PBMCs was investigated with a newly developed alpaca BTN3-specific antibody. These findings prove the existence of a functional BTN3-dependent phosphoantigen-reactive Vγ9Vδ2 T cell subset and provide a basis for the future study of this cell system in a non-primate species.

Moreover, as the first non-primate candidate species with the BTN3/Vγ9Vδ2 T cell system the alpaca is an important outgroup for research in this field. The use of a single BTN3 variant in contrast to three human isoforms that work together renders the alpaca a unique and to this date indispensable model for Vγ9Vδ2 T cells.

In conclusion, this study provides an overview of the applicability of new animal models in the study of the non-conventional T cell subsets iNKT cells and Vγ9Vδ2 T cells and leads the way for a better understanding of structural and functional relationships.

6 Zusammenfassung

Nicht-menschliche Spezies werden seit langer Zeit in den meisten naturwissenschaftlichen Feldern wie Immunologie, Virologie, Onkologie, Infektionsforschung und Verhaltensforschung verwendet. Wenn ein Modelsystem benötigt wird, werden heutzutage in der medizinischen Forschung bevorzugt Experimente in Maus-Inzuchtlinien durchgeführt. Im Gegensatz dazu gibt es viele nicht-murine Spezies, die als wichtige Instrumente in der Untersuchung von speziellen Zellpopulationen dienen könnten und in Bezug auf Koservierung der Funktionalität dieser Zellen untersucht und evaluiert werden sollten. In dieser Arbeit wurden drei Spezies hinsichtlich ihrer Konservierung von unkonventionellen T-Zellen und ihren Interaktionspartnern, dem CD1d/iNKT-Zellsystem und dem BTN3/Vγ9Vδ2 T-Zellsystem, untersucht. Nicht-konventionelle T-Zellen sind αβ oder γδ T-Zellen, die nicht in das klassische Schema der adaptiven Immunantwort und Peptidantigenerkennung via MHC passen. Diese speziellen T-Zellen erkennen andere Antigene und unterliegen nicht der MHC-Restriktion, sondern interagieren mit meist nicht-polymorphen antigenpräsentierenden Molekülen. Zudem verwenden unkonventionelle T-Zellen oft ein limitiertes TCR-Genrepertoire, weisen eine gewebsspezifische Lokalisierung auf und existieren in höheren Frequenzen als einzelne peptidspezifische αβ T-Zell-Klonotypen.

iNKT-Zellen erkennen Lipide, die von CD1d präsentiert werden, und führen immunmodulatorische Funktionen durch schnelle Zytokinproduktion aus. Charakteristisch ist die Expression einer semi-invarianten TCR α-Kette mit einer *AV14/AJ18*-Umlagerung in Mäusen und Ratten und der homologen Umlagerung *AV24/AJ18* im Menschen. Diese α-Kette liegt gepaart mit bestimmten β-Ketten vor, die Diversität in der CDR3 Region aufweisen. iNKT-Zellen wird eine Bedeutung in diversen mikrobiellen und viralen Infektionen, Autoimmunität und Krebs zugeschrieben. Die Erforschung von iNKT-Zellen in der Baumwollratte, einem Modellorganismus für Infektionen mit humanen Viren, war bislang durch das Fehlen von genomischen Daten und Methoden eingeschränkt. Daher wurde die Konservierung von iNKT-Zellen und ihrem antigenpräsentierenden Molekül CD1d in der Baumwollratte untersucht. Die Expression der molekularen Bestandteile dieses Systems, die iNKT α-Kette, typische β-Ketten und CD1d, konnte bestätigt werden und mit den homologen Molekülen in Menschen und Nagern verglichen werden. Baumwollratten besitzen, vergleichbar mit Ratten, mehrere Mitglieder der *AV14*- und *BV8*-Familie und nur eine CD1d Variante. Zudem konnte die Reaktivität von primären Baumwollrattenzellen gegenüber typischen iNKT-Zell-Antigenen gezeigt werden und iNKT-Zellpopulationen in primären Zellen wurden mithilfe von CD1d-Multimeren gefärbt. Diese wurden auch zum Test der Funktionalität von CD1d herangezogen. Zusätzlich wurden iNKT TCR-Ketten in TCR-negativen Zelllinien exprimiert und so Paarung und Glykolipiderkennung gezeigt.

Zusammenfassend konnte die Konservierung des CD1d/iNKT-Zellsystems in der Baumwollratte bewiesen werden Methoden entwickelt werden, die eine Erforschung der Bedeutung von iNKT-Zellen in Virusinfektionen in diesem Modellorganismus ermöglichen.

Vγ9Vδ2 T-Zellen sind die Hauptpopulation von γδ T-Zellen im Blut des Menschen und haben die einzigartige Fähigkeit Metabolite des Isoprenoidstoffwechsels, die Phosphoantigene, zu erkennen und dadurch zur Immunüberwachung beizutragen. Diese Moleküle sind ein Indiz für Zellstress, Transformation oder Infektionen. Charakteristische Merkmale von Vγ9Vδ2 T-Zellen sind die Verwendung einer *TRGV9*/*TRGJP*-Umlagerung in der γ-Kette und eines *TRDV2*-Gensegments in der δ-Kette. Phosphoantigen-Erkennung wird durch Mitglieder der BTN3 Familie ermöglicht. Bis jetzt wurden funktionelle Vγ9Vδ2 T-Zellen nur in Vertretern der Primaten gezeigt, die Gene dieses Systems sind allerdings in mehreren höheren Säugetieren konserviert. Zwei Kandidaten für ein funktionelles BTN3/Vγ9Vδ2 T-Zellsystem wurden in dieser Arbeit näher betrachtet.

Das Neunbinden-Gürteltier ist ein Modellorganismus der Lepraforschung und die Konservierung von *TRGV9*, *TRDV2* und *BTN3* Homologen wurde in dieser Spezies gezeigt. Die Expression von produktiven *TRDV2*-Umlagerungen konnte im Blut dieser Tiere nachgewiesen werden, es wurde jedoch kein Hinweis auf die Expression von γ-Ketten mit *TRGV9* Gensegmenten oder BTN3 Transkripten gefunden. Interessanterweise konnte eine Duplikation von BTN3 Genen und eine erstaunliche Ähnlichkeit der genomischen Organisation von BTN3 Loci zum Menschen gezeigt werden. Allerdings liegen im Fall des Neunbinden-Gürteltiers eher BTN3 Pseudogene vor. Zusätzlich konnten charakteristische Merkmale von Phosphoantigen-reaktiven menschlichen Vγ9Vδ2 T-Zellen und BTN3 gefunden werden, die immer noch im Gürteltier angelegt sind. Dadurch bietet sich das Neunbinden-Gürteltier als Modell für die Erforschung von strukturellen Faktoren an, die Phosphoantigen-Erkennung durch funktionelle Vγ9Vδ2 T-Zellen ermöglichen. Generell ist dieser Modellorganismus aber eher ein Zeuge für ein funktionelles BTN3/VγVδ2 T-Zellsystem in einem gemeinsamen Vorfahren.

Im Gegensatz dazu wurden in Alpakas funktionelle Vγ9Vδ2 T-Zellen nachgewiesen, die viele Charakteristiken menschlicher Phosphoantigen-reaktiver Vγ9Vδ2 T-Zellen, z.B. *TRGJP* Verwendung und CDR3 Längenrestriktion, aufweisen. Die Expression von Vγ9Vδ2 Paarungen im Alpaka konnte durch Einzelzell-PCR gezeigt werden und einige Paarungen waren in der Lage Phosphoantigene zu erkennen. Diese Reaktivität wurde, mithilfe von neu entwickelten Vδ2Jδ4-spezifischen Antikörpern, auch in PBMC Kulturen nachgewiesen. Weiterhin wurden Ähnlichkeiten des Alpakas mit „γδ high“ Spezies, z. B. Kamele und Rinder, durch eine erweiterte Untersuchung des TCR-Repertoires aufgezeigt. Schematische Darstellungen der TCR-γ und -δ Loci wurden basierend auf genomischen Daten und cDNA Analysen angefertigt und ermöglichen

eine Übersicht für genauere Untersuchungen. Die Konservierung der Phosphoantigen-Bindung zu Alpaka BTN3 konnte durch Gen Knock-out Zelllinien bestätigt werden und die BTN3 Expression wurde mit neuen Alpaka BTN3-spezifischen Antikörpern untersucht. Diese Ergebnisse beweisen die Existenz einer BTN3-abhängigen Phosphoantigen-reaktiven Vγ9Vδ2 T-Zellpopulation im Alpaka und liefern eine Basis für zukünftige Studien dieses Systems. Weiterhin ist das Alpaka als erste nicht-Primaten Spezies eine wichtige Außengruppe für die Forschung in diesem Feld und ein bis jetzt einzigartiges und unersetzliches Modell für die Verwendung nur einer BTN3 Isoform in einem funktionellen BTN3/Vγ9Vδ2 T-Zellsystem.

Abschließend lässt sich sagen, dass in dieser Arbeit eine Übersicht der Eignung von neuen Tiermodellen für die Untersuchung zweier nicht-konventioneller T-Zellpopulationen, der iNKT und Vγ9Vδ2 T-Zellen, geschaffen wurde. Dies ermöglicht weitere Untersuchungen zum besseren Verständnis von strukturellen und funktionellen Interaktionen.

List of Figures

Appendix

List of Tables

Appendix

Appendix

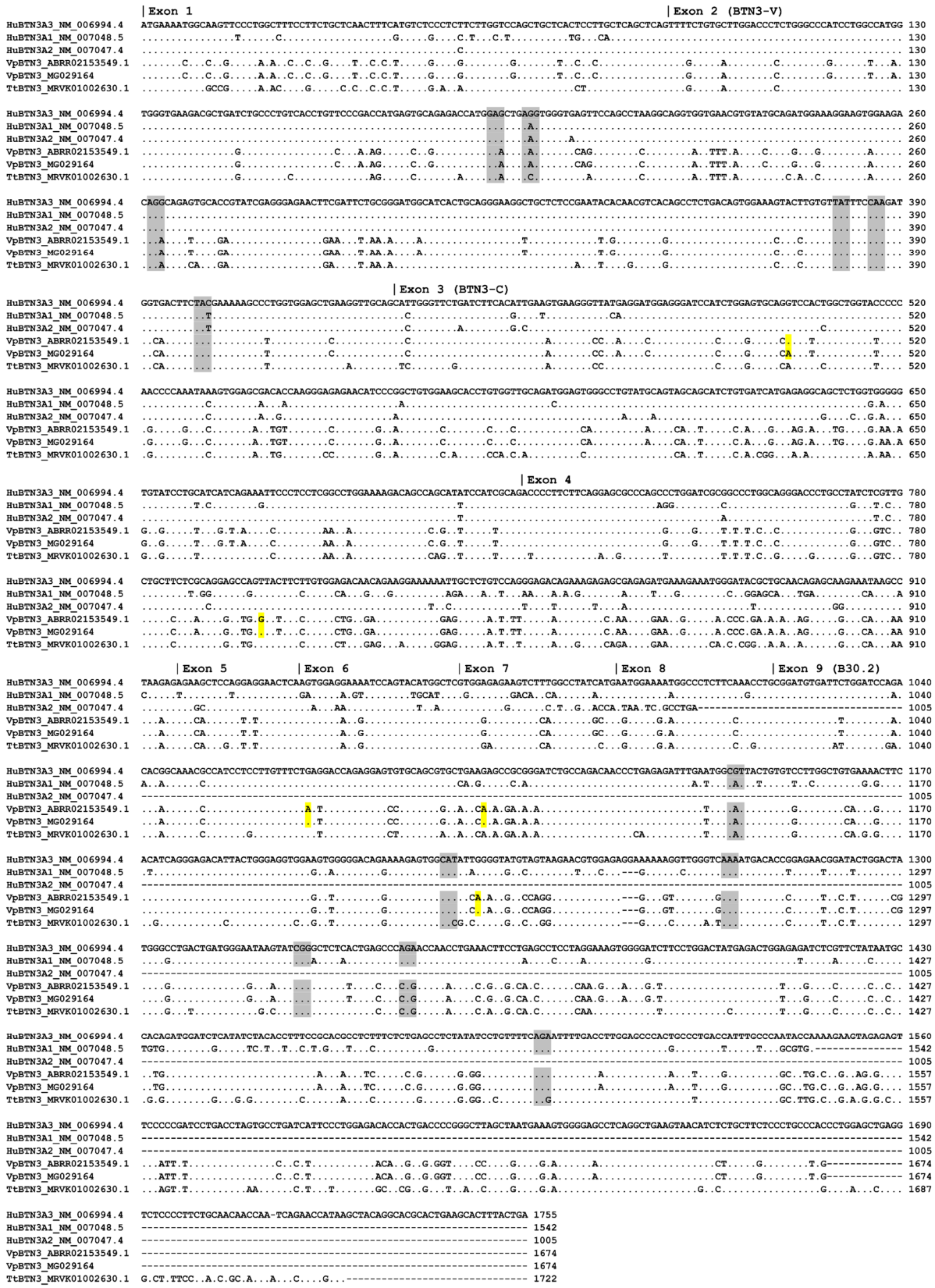

Figure A.1 Continued

Figure A.1 Nucleotide alignment of full-length *BTN3* transcripts/predicted *BTN3* sequences of human, alpaca and dolphin. The transcripts of human *BTN3A3* (GenBank: NM_006994.4), human *BTN3A1* (GenBank: NM_007048.5), human *BTN3A2* (GenBank:NM_007047.4) and alpaca (GenBank: MG029164) were aligned with the *in silico* spliced *BTN3*-like sequences of alpaca (*Vicugna pacos* whole genome shotgun contig ABRR02153549.1) and dolphin (*Tursiops truncatus* whole genome shotgun contig MRVK01002630.1) obtained from the NCBI database. Clustal Omega was used to calculate the nucleotide alignment. Identical nucleotides (dots), gaps (dashes) and the first nucleotide of each domain (following exon organization) are indicated. Codons for amino acids implied in recognition of phosphoantigens [304, 308] are highlighted in gray, polymorphisms found in the two alpaca BTN3 transcripts are marked in yellow. Abbreviations: transmembrane domain (TM), juxtamembrane domain (JM). Figure and figure legend adapted from [326].

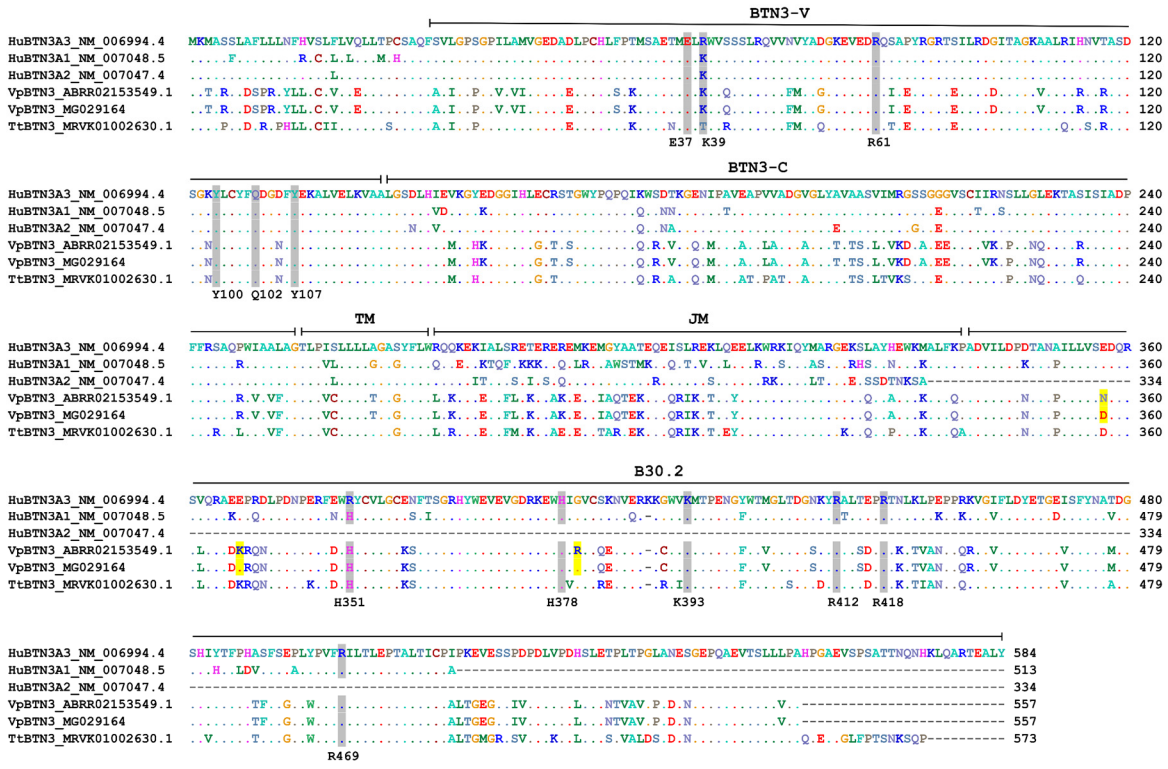

Figure A.2 Amino acid alignment of *BTN3* sequences of human, alpaca and dolphin. Nucleotide sequences described in **Figure A.1** were translated and aligned using the Clustal Omega tool. Identical amino acids (dots), gaps (dashes) and polymorphisms in the alpaca sequences (yellow) are indicated. The domains of *BTN3* were determined according to human *BTN3A1* as described before [309] and proposed phosphoantigen binding residues are highlighted in gray [304, 308]. Abbreviations: TM (transmembrane), JM (juxtamembrane). Figure and figure legend adapted from [326].

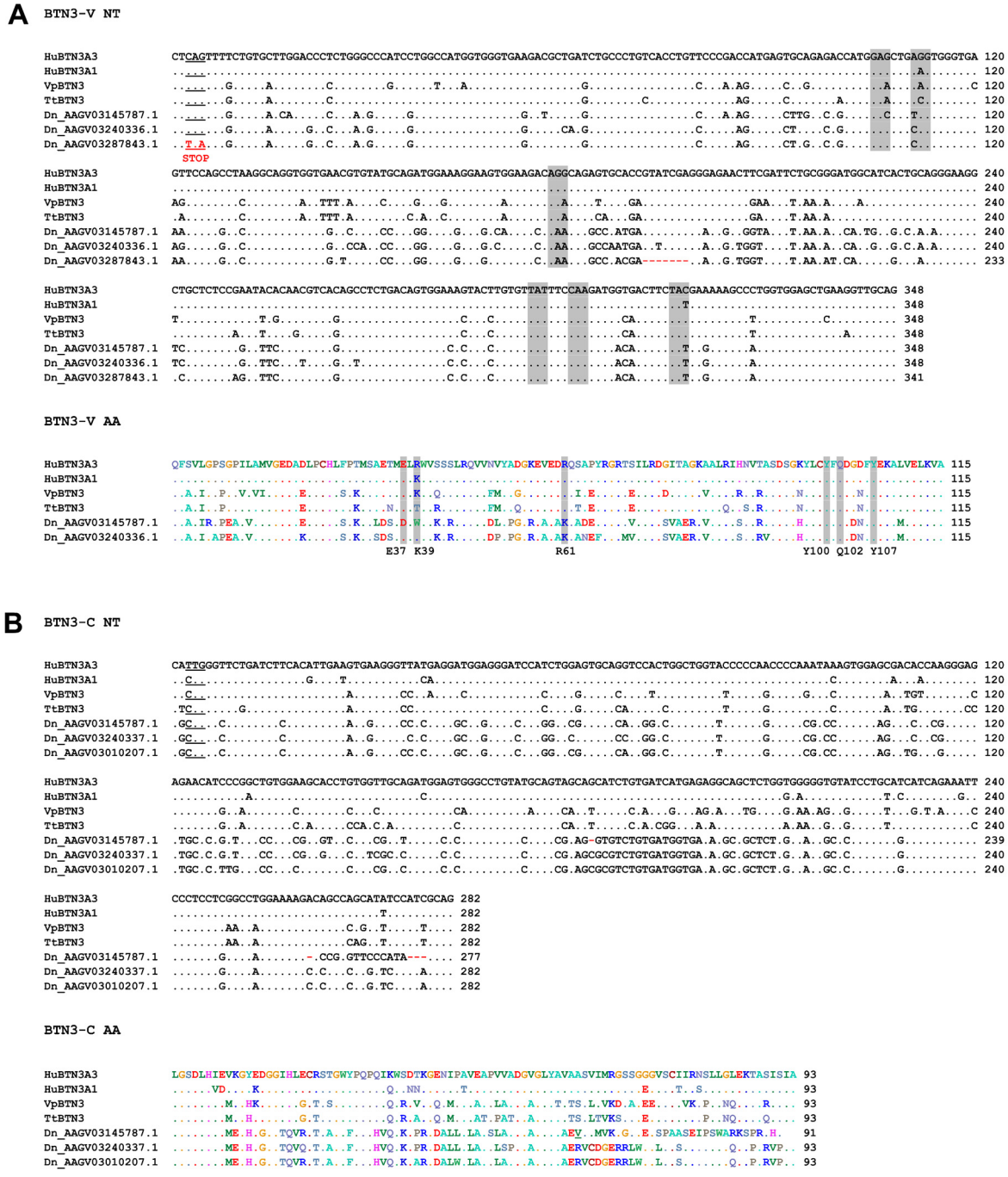

Figure A.3 Alignment of the proposed armadillo *BTN3-V* and *BTN3-C* sequences with human, alpaca and dolphin. (A) The *BTN3-V* regions of human *BTN3A1* and *BTN3A3*, alpaca *BTN3* (ABRR02153549.1) and dolphin *BTN3* were determined according to the exon structure obtained via splicing prediction and aligned with three *BTN3-V* homologous sequences found by NCBI BLAST analysis (using human *BTN3A3*) of armadillo wgs (AAGV03145787.1 (corresponding to **Figure 3.14E**); AAGV03240336.1 (**Figure 3.14F**); AAGV03287843.1 (**Figure 3.14G**)). **(B)** The *BTN3-C* regions were determined as described for *BTN3-V* and compared to the homologous armadillo sequences (AAGV03145787.1 (**Figure 3.14E**); AAGV03240337.1 (**Figure 3.14F**); AAGV03010207.1 (**Figure 3.14G**)). The nucleotide/amino acid sequences were aligned using Clustal Omega. Identical nucleotides/amino acids appear as dots, gaps are indicated by dashes, and phosphoantigen binding residues are highlighted in gray. The first codon used to *in silico* translate the nucleotide sequences appears underscored. The termination codon preventing the full-length translation of *BTN3-V* in the contig AAGV03287843.1 and the missing nucleotides disturbing the reading frame of the *BTN3-V* in AAGV03287843.1, and the *BTN3-C* in AAGV03145787.1 are highlighted in red. Figure and figure legend adapted from [326].

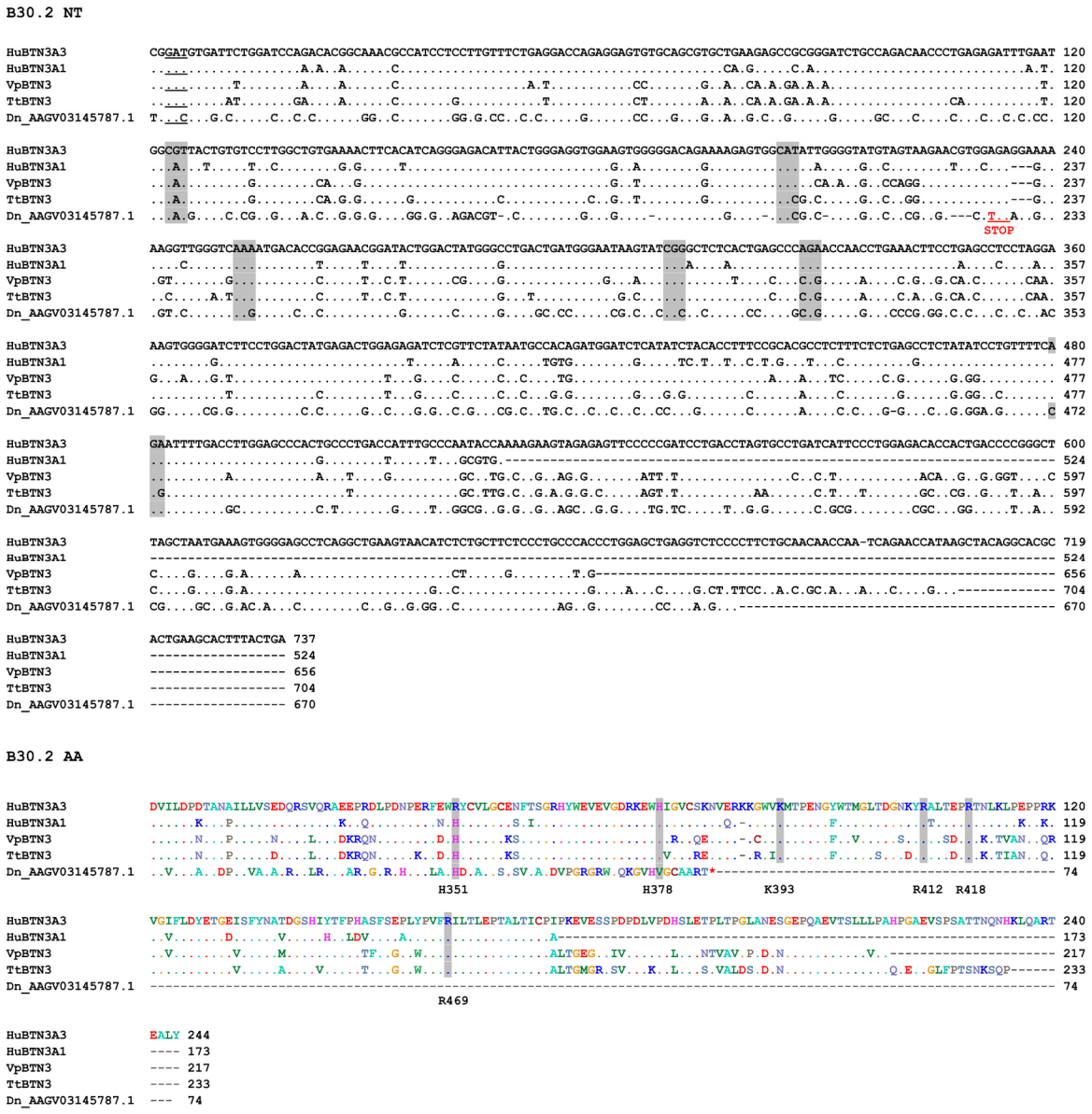

Figure A.4 Alignment of the predicted B30.2-like domain of armadillo with human, alpaca and dolphin. The single B30.2-like domain obtained from one contig in the armadillo wgs database (AAGV03145787.1, (**Figure 3.14E**)) was aligned with human, alpaca and dolphin BTN3 B30.2 domains determined by splicing prediction. The nucleotide/amino acid sequences were aligned using Clustal Omega. Identical nucleotides/amino acids appear as dots, gaps are indicated by dashes, and phosphoantigen binding residues are highlighted in gray. The first codon used to *in silico* translate the nucleotide sequences appears underscored. The termination codon preventing the full-length translation the armadillo B30.2 domain is highlighted in red in the nucleotide sequence and indicated in the amino acid sequence (*). Adapted from [326].

Figure A.5 Organization of genomic regions in *Dasypus novemcinctus* contigs. (**A**) AAGV03145787.1 (**Figure 3.14E**) and (**B**) AAGV03240337.1 (**Figure 3.14F**). The human BTN3A3 nucleotide sequence was used for an NCBI Blast search in the armadillo wgs database. The exons 2, 3, 4, 6 and 9 (highlighted in color) could be determined in the contig AAGV03145787.1 and the exons 3 and 4 (highlighted in color) in the contig AAGV03240337.1. The remaining exons were found by NCBI Blast of human non-coding regions between exon 4 and 9 to the armadillo contig AAGV03145787.1. The exons 6 and 7 in AAGV03240337.1 were assigned via homologies to AAGV03145787.1. Partial alignments are shown below. The exon-intron organization (marked by //) was determined by consensus splice donor and acceptor sites or homologies to human *BTN3* exons. No termination codon was identified for exon 9 in contig AAGV03145787.1, and no splice site could be determined for exon 4 in the contig AAGV03240337.1. Adapted from [326].

A *Dasypus novemcinctus* Contig AAGV03145787.1 (**Figure 3.14E**)

Genomic regions homologous to:
Exon 1 (not found), 2 (BTN3-V), 3 (BTN3-C), 4, 5 (not found), 6, 7, 8, 9 (B30.2)

>AAGV03145787.1 *Dasypus novemcinctus* isolate 3-136 Contig145889, whole genome shotgun sequence (length: 29470; region shown: 1855-8962)

ATTGGGCCATGTCATTAGGGCATTTTGTCCCCTGGCAGCCCCAGCTCCAGCCCCCTCTAATGGCACGTCCCCCTTTTGCTGAGCAG//CTC
AGTTTGCTGTGATCAGACCCCCTGAGGCCATCGTGGCCATGGTGGGTGAGGATGCTGAGCTGCCCTGTCACCTGTCCCCAAAGATGAGCTT
GGACAGCATGGACCTGTGGTGGGTGAAATCCAGGCTCAGGCAGGTGGTGGACCTGTACCCAGGGGGAAGGGAGGCAGAAGCCAAACAGGCC
GATGAGTATCGAGGAAGGACGGTAATTTTAAGAGACAGTGTCGCCGAAAGGAAGGTCGCTCTCCGGATTTCCAACGTCAGAGCCTCTGACA
GTGGACACTACCTGTGTTATTTCCAAGATGACAACTTCTATGAGAAAGCCATGGTGGAGCTGAAGGTTGCAG//GCGAGCCCCTGGCTTTT
GCATAAGCTCCTTCCCCTGTGAGACCTGGGGTGGGTACAGGCTTCGGGCTCTCAACCCACCTGCAGCCCTCCTGGTAGCCACGAGGAGCTG
CCACCATTGCCTCCCGGTAGCCACAAGGAGCTGCCACCGTTGCCTCCTGGTAGCCACGAGGAGCTGCCACCATTGCCTCCTGGTAGCCACG
AGGAGCTGCCACCGTTGCCTCCTGGTAGCCACGAGGAGCTGCCACCGTTGCTTCCTGGCAGCCACGAGGAGCTGCTGCCGTTGCCTCCTGG
TAGCCACGAGGAGCTGCCGCCGTTGCCTCCTGGCAGCCACGAGGAGCTGCCGCCGTTGCCTCCTGGTAGCCACGAGGAGCTGCCGCCATTG
CCTCCTGGTAGCCACGAGGAGCTGCCACCGTTGCCTCCCTGGGCTTAAGAAGGAGACCTGGGCTTTCTACCAGGAAGAAGTCCTACTGCAG
CCGACATGGTCAAGCTCAGAACTCCATCATGGTGGCCAGCAGGGGTCCAAGCAGGGAAGGAGAACGAGAGGTGGTTGGTGGGGTGTTCTGG
TTCAGGGGTGGGCTGGGGGCCTGTATGACTGTTCTCCAGCCAGGGGTGTCACTGAGGGAGAAGGCCCACCATGGGAGGCCGGGGGCCTCAG
GAAGAGGGTGTCAGCCTGGTGTTAGGGCCTTTGGGGGGTGGTTCACACAAGTGGGGCCGCTGTCAGGAAGGAGGGGGTAATTCTGGGAGTG
GGTCTCTTAGTAAATCTCACCTAGGGGGAAGGAAGACGAGGGCGAGGGTGAGGCTGAAGCTGTGATGGGTGGTGAGGCTGCACGGTCATCT
TGTGGTGGCTCGTGGTTGCCTCCACGCTCAGCCACCGCTGGGCAGTGCTCTTGTTCCCGTGATAATCTGTAAAGGTGCCAAAGCGCACCAT
TGGACATGATGCTCGGAGACATTGTGTCTGTTCAACAGCGCTGTGAGTGCCAGGCCGGCTCCCGGGTGCCAGGGCTGCCTTTCTCCGTTCT
CAGGCATGCCCTTGCCCTGCGGCTTCTGGTGGGGTTTGGTCCATGGGGAGCCCCAGCAGGAGGTGGAGGGAGGGAGAAAGGAGGCAGCGGT
GCCTGGAGCTGGCAGCGTCCTCTCCAGGACTCTCCTCTTGGGGCTTCGGAAGAGCGTCCTCTCCTCCTCTCTTGGAGCTTTGGGGTGGCCG
CTCTGCTCTCGTTGGCCCTGGGGTGCTGCAGTACCCCATGCCATTTCCCCTCACCACTCCCACTTTGGGAATCCGCTCCTTAGTTCAGTCG
CTCTGAATGAGTTCCTGTGAGTGAGCCATCGGGTCTCCTTGCGGCCCTGCCTGGTGCCGAAGGCTCCCAAGAATTCAGCACGTGCTTCCTC
CGCAG//CGCTGGGCTCTGATCTCCACATTGAAATGGAGGGCCACGAGGGCGGGGGGACCCAGGTGCGGTGCACATCGGCCGGCTGGTTCC
CCCAGCCCCACGTCCAGTGGAAGGACCCCCGGGGAGATGCCCTGCTGGCCCTGGCGGCGTCTCTGGCGGCTGATGGCGCGGGCCTGTACGC
AGCGGAGGTGTCTGTGATGGTGAAAGGCGGCTCTGGGGAGGGCTCTCCTGCAGCATCAGAAATTCCCTCCTGGGCCAGGAAAAGCCCGCGT
TCCCATAGCAG//GGCAGTGCCCGCTCAGCCTCGGCGTGCTCTGCCAGCTGGGGCTGCTGACAGGAGGAGGTGAGGCTGAGTCCCAGCTGC
TGGTTTGGGCCTTTCCAGGACCTGGAGGCTTCTCCTTGCTCCAGGGACGCTTCTCTCCCCCATAAAACCGTTGTGCCACAGGCGTTTCCTC
TGTCCTGTGTACTGGAAACTGTGGCAGGCAATGGGAATTGAACTGAAATAGTTAAGATCAAATCTTTAAACATGTCAAAGGATGGAATGCA
AAAAAATAATTACAACTCCTATTACAAGGAAAGAGCTAAGCCACTTAGGATAACTCAGTAGAAAAATGAGCAAAGAGCACGAATCATTAAT
TCTCAGAAGCAGAAATATACTCAATCTCATGCTTTGGAGAAATGTATATTAAAACTTTTCCATCATGAGGTTGGCAAAATTAAAAGGGGGA
AGAGGTTGATAACATATTCTGATGGCAGAGAACATGGGGACGCAGGCCCTCTTACGCATTTGTTGATGTAATTGGTGTATTTTTGGTATAA
ATTGGTACAGCCTCTATGGAGGACAATACAGTGATTATTCAAACTACTTGTTCATTGATCTGAAATCCTGTTTCTGGGCATTTGTCTGGCT
GATACGTGGGCACTTGCATGAAATGAGTCATTAAATGGCGATTTATTATACTATTGAGGATAAGAGTGAAAAGTTAGAAACGGTGGAAACG
TTCCTCAAGAGGGGCTTCTAGTGTGGAATATGACACAGCAGTGAGGAAGGACACACGGTCCCTAACACGGAAAGTTCCCTGAGCTGTACCA
TGAACAGGAGAAGCAAGATTCAGGCCAGAGCGTGTAGAAGCCTGTTTTGGTGTTAAAATAAGAATATAGAATGGTTATTTATAATTTTTTA
AACGTAACAAACCCTTGGATAGCACTCACTGTGTGCTGGGCACTTTATAAACAGTGATTTGTTGTTGATTACATTTTAGTTTGTTTTTTTT
TTAAAGAGGCTTTAGGTTACATAAATGTTTAATTCCCTCTGACTCCGTGTAGTAGGTGCCATTACCACTCCCATTTTACAGAGAAGGACAC
TGAAAAACAGAGAGGCTAAGAAACTAGTCTAGGGTCACACTTCCACCGCAAGGAGCCAATTTAAACCAGAACTTAAACCAGGGCCCTTCTG
GCTCCGGAGTTCCCCAAGCTGACTAATAAGCTACTAAGTGGGGGCGGAAAGGCTGGGTGGATGGAGGAATTGGACGATTTGGGGTATATTT
CTGTGATTTGAACCATGTAAATAAGTTCAGTATTTGAAAACTTAAATTATGTTTTAAGTTTAAGAAACTTAAAATATTTAAGAAAACTGTC
TGATTGATGCTCGAGGAGCTCTTTCCACGGGGGTGGCAGCACTTCTGGCTGGGCCGCAGGTTGTACCAGTTTCCCAGGCGCCTGGTCCCCA
GTGCTCCCAGACCTCAGGAAAAGGCAGCGCAGTTCACCTGTGGATAACCACGGGCTCCCTGCCCTGCGGGAAGAGGGCCAAGGCCATGCGG
CCCCCCACCCTGTCCCTCTTGCAG//ACCCCTTCTTCCAGAGCGCCGGGCCCTGGGTGGCAGCCTTCGCGGCCACGCTGCCCACCCTGCTG
CAGCTCTCGTGGGAGCCGGTTACTTCCTGTGACGACAGCAGAAG//GTCCAAGAGGCCGTAGTCCAGGAGAAAGAGAGGGCGTGTGAGAGG
AGGAGGAAAAGGAACGGACAGAGAAGGAGAGGGAGGGAGTGGCGTGCGCATTTAAGCGCCTTCATGACTCCTCGCCCTTTATTCCTTGCAG
//AGTGGAGGAAGGTCCAGTACATGACTC//GTGAGTGGCGCCGGCATCTCCTGAGTCAGGACTCTCCTCTCTGTCACTTTGCAGGCCCTT
TCTCTTTAGCCAGGGCTGGGAAGGGCCCTGGAGCCCTTTCTGGGGGAAGAAAGTTAGGATGGCTGATTGCAGGAAGGACAGGGGGAGCTTT
TCTTTCTATAAAAGGAAAAAAAACTACCGTCCATCTCTCTCCACAAGAGGCCCACATGCTCTCTAGCCCTGCGAGATGCTGAGGAATATCT
AGGGGTGCACTTCAAATAAAGGGGCTGAGGAGGATGGAGCCCCGTAGGTGAGCTGGCCTCCTTGTGCCAGCAGACTGCCAGCTGCTTTACA
TCTCTGGAGGCTGCAGAGAACTTAAAAAAAGGAAAGATTAAAAGGACTGAGGAAGGCAGAGACGGAGGATGGGGAACAGTGTTTCTCATGA
AGAGAAGAGTGGCGCAGTGGTTACAGATTTATTGCACCCGCCTTTAAAAATTAGTGTCTGCAATGGCCTCATCAAGTTTCTCAAATTCTTT
TCTGAAATAAGCGGGAAACAATATAAATTGAGAAAGATGGATTCTAGTATACCTACTGTGTGCAAGCAACACCTGCACCCAGGTATGGGGC
ACACACGGTGCCCTACTCGGTGCCTGTGACAACATCAGCTCGTGAGCGGTGCTCGCCAGCCTGCTGTCGGGGAGGAGAGGGGATGGACTTG
AACCTGCAGAGGCAGGAGGTCGGGGTGGGCTGGGCCTAAGGAGAGGCTGGAGGGAGGCGAGGGGAAGAGAAAGGCAGGGAGTCAGCACACG
TGGTCCAGGTGACAGTTCCGCCTTTCTCCCAACGCAG//GAGGGAAGAAGTCCCCGCACTACCATG//GTGAGTGGTACTGACTTTGCAGG

GGCACTGAGCCCTGACACGTTCCTCCGTGGTCAGGGCTCCCAAGAGAAATAATCACATCCAGCACAGAAGCTCTTTTCCGTGGGAGGGGTG
ACACCTGCTTTTCGAGACCCGAGAGGAACTTCCAGATGCAGCCTCCGTGTGTCTTTGGCTGTAGCCGCGGCTAGCGCACACGCAGGCACCC
AGCCGTGTCTGATCTGTCAGCGCTCTGCAGAGGGGAGGCATTGGGAGATATTCCGAAGGGAGAGAGAAAAGAAAGAAAGAGTGGGAGAGGT
GGGGGGTGAGCCTAAATAATGGCCTGTTTTTCATCTCGCCTCCTTTTCAG//AGTGGAAGGCGGCCCTCTTCCAAGCTG//GGGAGTGAAG
TGCAGGCTAATGACCAAGGGACCTTCCCCCTTTTCTCCTCCAACTCCTGAGATCCTGGGGAAAGAAGCCATTGCACCCTGCGCCTTCCAGC
TGAGAGCCCAGAGAGTCAGGGAGAAGGGCTCTCCTCTGTGGGTGGAGCCGGGGAAAGGGAGGGAGACAGAACTGGAATGCAGGGAGAGCGA
GGTGACCATGACGCAGGAGAAGGCAGTGTGCCAAGAGCGCAGCCTTCCCATGGCCCCCCACTAACTCCTCGAGTTACCTAAGGCCTCTGTG
CTTTAGAATCCTCATTCTTAGGTAGTGCGCATAATTACCAGTTCACAGGGGTTGGGGTGAAGACTGAATGAGGTCAAGGCTGAAGGGGAGG
GGAAGGGCCATTCGGGAGCCAAGGGGGCCCTGGTCCCAGGGGAGGCCTGCGGGCAGCAGGCTTGCCTTGCTTAGCTGCTGGCAGGGAGGAA
GCAGGGAGAAGAAGGGCTCTGCTCCTCTCTCTTTCCTGTTCCAATCTTCTGCCAAACCCAACAGGAAAGCAGAGGCAAGGGAGCTGTCCAG
GAAGTCCTATTCCTAGAGCTAGGATGAGGGTGGAAAAGGGTGGAGAGGGCAGTGGAGCACAAACGCCCCACCTGGTCCCGAGTACAGAGTA
GGCATGGCAGGGCTGCAGCCTCCGGCACGTCCTCGGGTGTGCCCTTCTCTAGTGTGTTCCCTGTGTTAGCACAGTCAACCCCAGAGAACGG
TCTTAGCCCCAGTTTTCAGATGAGGAACAGGAGGCTAGAGGTACGTGGGTGTCATCTGAGTTGGATCTATGGAAAGAGCATGCATTGTTAA
AAGGAAAAGCCTCCCAGCCAGGCGTGGCAGAGCTGAGGCTAAAAGCACAGGTGGCCAGAGCCAGTTGAGGAACAGGAAGCAAGAAAGTGGA
AGAAGGGCGCCGTTCTGCCACGTGAGCCCACGCCAGGTCAGGAAGGCGTGTGTGGCATCTCACCACCACCCCCTTCACACGAACACTGGAC
CTCCCAGCTTTCTCTCTGGGGGTTGCAGGGAGGATCACTTTCAGGGCAGGCTGGGGACCCCAGGCTCTGGACTCGGGCCCTGGAGGCTCTG
AGGTCCAGGCAGACGGGCTGAGCCCACGGGCCACCCTCGAGCCCCTCCAG//TGGACGTGGTCCTGGACCCCGCCACGGCGGACCCCATCC
TGGTGGCCTCCGCGGACCGGAGGAGCCTGCGGCGGGCAGAGGCGCGGCGGGGTCTGCGCGACCACCCCGAGCGACTCGCCTGGCATGACTG
CGCGCTGGGCAGCGAGAGCGTCACGGCGGGAGACGTTCCTGGGAGGGGGAGGTGGGGACAGAAAGGAGTGCACGTCGGGTGTGCAGCGAGG
ACGTGAAGAGAAAGTGCTGGGTCAAGATGACCCCCGAGAACGGATGCTGGACCATGGGGCTGAGCGCCGGGAACGACTACCGCGCCCTCAC
CCAGCCGCGGACCAAGCTGCCCGTGGCCGCGCCCCCCAGACGGGTGGGCGTGTTCCTGGACCACGAGACGGGCGAGGTGTCCTGCTACGAC
GCTGCCGACGGCTCCCACCTCTGCACCTTCCCGCACACCTCCTCCTCGGGCCCCTGTGGACGGTTTTCCGAATTTTGACGCTGGAGCCCAC
CGTCCTGACCGTTTGTCCGGCGCCGAGAGGAGAGCAGGGGTCCCTGGTCCCTGATCTGGGGCCTGACCGCGCCCTGGAGCGCCCAGGGACC
CTGGACTCGGCTAGCGAGAACGAGGACCCTCAGGCCGAGGTGAGGTCCCTGCTTCTCCCTGAGCAGCCTGGAGCCCAGGACGCCCGCCCCG
CCCACCTTAAGTCGCTGTGGGCTCGCGGGTTCCAAGCTCCTGCTCCCAGTACTTCAGCTACGCCACGTAACGACTCTGTGACTCTGGTACC
CCTTTAGTACCCTCTTTTTTTATTTTTAATGAGTAT

<u>Homologous Exons not found by NCBI Blast of human BTN3A3 to armadillo wgs:</u>

Exon 7: NCBI BLAST of human and armadillo contig AAGV03145787.1 non-coding region upstream of B30.2 and downstream of exon 6

```
AAGV03145787.1          AGGAGGGAAGAAGTCCCCGCACTACCATGGTGAGTG
                        ||| ||  |||||||   |  ||| ||||||||||||
HuBTN3A3                AGGTGGAGAGAAGTCTTTGGCCTATCATGGTGAGTG
```

Exon 8: NCBI BLAST of human and armadillo contig AAGV03145787.1 non-coding region upstream of B30.2 and downstream of exon 6

```
HuBTN3A3                AAATACTGACCTTTTTCTTATCTGTGTCTCCTTCCTTTCAGAATGGAAAATGGCCCTCTT  399
                        |||||  ||  |||  |||  |  ||||   |  ||||||    ||||||  |||||    |||||||||
AAGV03145787.1          AAATAATGGCCTGTTTTTCATCTC-GCCTCCTT---TTCAGAGTGGAAGGCGGCCCTCTT  349

HuBTN3A3                CAAACCTGGTGAGTAAATCACTGTATGTTCCCTGGATCAACAACCTGAGGGACTATATTC  459
                        |  ||  |||| ||||  ||         ||    | ||  |  ||  |||  ||||||  |   |
AAGV03145787.1          CCAAGCTGGGGAGTGAAG-------TG----CAGGCT-AATGACCA-AGGGACCTTCCCC  396

HuBTN3A3                CTTTCTCCTCCTCCAACTCTTGTGAT  485
                        ||||   ||||||||||| ||  |||
AAGV03145787.1          CTTTT--CTCCTCCAACTCCTGAGAT  420
```

B *Dasypus novemcinctus* Contig AAGV03240337.1 (**Figure 3.14F**)

Genomic regions homologous to:
Exon 1 (not found), 2 (BTN3-V, corresponding exon 2 in AAGV03240336.1), 3 (BTN3-C), 4 (truncated, deletion), 5 (not found, deletion), 6, 7, 8 (not found, deletion), 9 (B30.2, not found, deletion)

>AAGV03240337.1 *Dasypus novemcinctus* isolate 3-136 Contig240580, whole genome shotgun sequence (length: 24370; region shown: 716- 3834)

GGGAAGGGCTCCTTAGTTCAGTCGCTCTGAATGAGTTCCTGTGAGTGAGCCATCGGGTCTCCTTGCGGCCCTGCCTGGTGCCGAAGGCTCC
CAAGAATTCAGCACGTGCTTCCTCCGCAG//CGCTGGGCTCTGATCTCCACATTGAAATGGAGGGTCACGAGGGCGGGGGGACCCAGGTGC
AGTGCACCTCGGCCGGCTGGTTCCCCCAGCCCCACGTCCAGTGGAAGGACCCCCGGGGAGATGCCCTGCTGGCCCTGGCGGCGCCTCTGTC
GCCCGATGGCGCGGGCCTGTACGCAGCGGAGCGCGTCTGTGATGGTGAAAGGCGGCTCTGGGGAGGGCTCTCCTGCAGCATCAGAAATTCC
CTCCTGGGCCAGGAAAAGCCCGCCCGCGTTCCCATAGCAG//GGCAGTGCCCGCTCAGCCTCGGCGTGCTCTGCCAGCTGGGGCTGCTGTG
AGGAGGAGGTGAGGCTGAGTCCCAGCTGCTGGTTTGGGCCTTTCCAGGACCTGAGGCTTCTCCTTGCTCCAGGGACGCTTCTCTCCCCCAT
AAAACCGTTGTGCCACAGGCGTTTCCTCTGTCCTGTGTACTGGAAACTGCGGCAGGCAATGGGAATTGAGCTGAAATAGTTAAGATCAGAT
CTTTAAACATGTCAAAGGACGGAATGCAAAAAAATAATTACAACTCCTATCACAACAAAGAAGGAAACCTCCTTAAAACAGAAAAGCTCTT
ACGACAACTCAGAAGAAAAATGAGCAAAGAACATGAATTATTCACTCTCAAACAGAAATACACTCAATCTCATGCTTTGGAGAAATGTATA
TTAAAACATTTTCCATCCTGAGATTGGCAAAATATGAAATTAAAAGGGGGAAGAGGTTGATAACATATTCTGATGGCAGAGAACATGGGGA
CGCAGGCCCTCTTACGCATTTGTTGATGTAATTTGGCATATTTTTGGTATAAATTGGTACAGCCTCCATGGAGGACAATACAGTGATTATT
CAAACTACTTGTTTCTTGATCTAAAGTCCTATTTCTGGGCATTTGTCTGACTAATACATGGGCACTTGCATGAAATGAGCCATTAAATGAC
TATTTATTATACTATTGAGGATAAGAGTGAAAAGTTAGAAACGGTGGAAATGTTCCTCAAGAGAGGCTTCCAGCATGGAATACGACACAGC
AGTGAAGAAGGACACACAGTCCCACCACGGAGAGAGCCCTGAGCTGTGCCATGAACAGGAGAAGCAAGATTCAGGCCAGAGCATTTAGAAG
CCTGTTTTGGTGTAAAAATAAGAATATAGATTGGTATTATAATTTTTATATGTAACGAACCCTTGGATGGCACTCACTGTGTGCCAGGCAC
TTTACAAACAGTGATTTGTTGTTGTTGTAGATTACATTTTACTTTTTTTCTTTAAAGAGGCTTTAGGTATCATAAATGTTTAATCCCTCTG
ACTCCCTGAGATAGGTGTTATTACCACTCCCATTTTACAGATGAGTATGCCTGCGGAACAGAGAGGCTAAGTAACTAGTCTAGAGTCACAC
ATCCTCAGCCAGGAGCCAGAATTTAAATCGTTGCCCTCCTGGCTCCAGAGTTCCCCACACCAACTAATAACAAGCTACTAAGTGGGGAGGG
GAAAGGCTGGGTAGATGGAGGAATTGGACGACTTTGGCTATTTTTCTGTGATTTGAACCATGTAAATGAGTTCAGTATTTGAAAAGTTAAA
TCAGAAAACTGTCTGATGCTCGAGGAGCTCATTCCATGGGGGCCGCAGGTTGTGCCAGTTTCCCGGGCGCCTGGTCCCCAGCGCTCCCAGA
CCTCAGGAAAAGGCGGCCCAGGTCACCTGTGGATAACCGTGGACTCCCGGCCCGGAGGGAGGAGGGGCGAGGCTTCGAGGACCCCCGCCCT
TTCCCCCTGGCAG//ACCCCTTCTTCCGGAGCACCGAGCCCTGGGCGGCGGCCTTCGCGGCCACGCTGCCCACCCTGCTGCAGCTCCTCGC
CATTTATTCCTCGCAG//ATGGAGGAAGATGCAGTACATGACTC//GTGAGTGGCGCCGGCACCTCCTCTGAGTCAGGACTCTCCTCTTGA
TCACTTTGCAGTCCTGGAGCCCTTTCCCCTGGGGAAGAAAGCTAGGATGGCGATTGCGGGAAGGAGAGGGGGAGCCTTTCTTTCTTTAAAA
AGAAAAGTGCCGTCCATCTCTCTCCACAAGAGGCCCACAGGCTCTCTAGCCCTGCAAGATGCTGAGGAATATCCAGGGCTGCACTTCAAAT
AAAGGGGGTGAGGAGGATGGAGCCCCGTAAGTGAGCTGGCCTCCTTGTGCCAGGAGCCTAGTGAGCTGCTTTACATCTCTGTAGGCTGCAG
AGAATTTAAAATAAGGAAAGATTAAAAGGAATGAGGAAAGCAGAGACAGAGGATGAGATACGGTGTTTCTCATAAAGAGGAGAAGAGTGGT
GCAGTGGTTACAGATTGCACCTGCCTTTAAAATTAGTGTCTGAAATGGCCTCGTTGAGTTTCTCAAATTCTTTTCCAAAATAAGCGGGAAA
CAATATAAATTGAGAAAGACGGATTCTAGTATACCTACTATGTACAAGCAACACCTGCGCCCAGGTATGGGGCACACACAGTGCCCTACTC
GGGTACCCTGTGACAACATCAGCTCGTGAGCGGAGCTCCCAGGCCTGCTGTCGGGGAGGAGAGGAGATGGACTTGGACCTGCAGAGGCAGG
AGGTCGGGGTGGGCTGGGCCTAAGGAGAGGCTGGAGGGAGCAAGGGGAAGAGAAAGGCAGGGAGTCGGCGCGCGTGGTCCAGGTGACAGCT
CTGCCTTTCTCCCAACGCAG//GAGGGAAGAAGTCCCTGCACTACGCTG//CTGAGTGGTGCTGACTCCGCAGGGGCGCTGAGCCCTGACA
CTTTCCTCCTCGGTCAGGGCTCCCAAAGGAATAATCACATCCAGTACAGAAGCGCTTTTCGGAGGGAGGGGCGATGACTGCTTTTTGAAAC
CCAAGAGGGACTTCCAGATATGGCCTCTGGGTATTTTGGCCACAGCAGCTCCTGGTGCACAGGCACGCACCCAGCTGTGTCTCATCTGTCA
GCATTCTGGAGTGGGGAGGCACTGGGAGATATTCTGAA

Exon 6: NCBI BLAST of armadillo contigs AAGV03145787.1 and AAGV03240337.1

```
AAGV03145787.1          TTTATTCCTTGCAGAGTGGAGGAAGGTCCAGTACATGACTCGTGAGTGGCGCCGG
                        ||||||||| ||||| ||||||||| | ||||||||||||||||||||||||||
AAGV03240337.1          TTTATTCCTCGCAGA-TGGAGGAAGATGCAGTACATGACTCGTGAGTGGCGCCGG
```

Exon 7: NCBI BLAST of armadillo contigs AAGV03145787.1 and AAGV03240337.1

```
AAGV03145787.1          GCAGGGAGTCAGCACACGTGGTCCAGGTGACAGTTCCGCCTTTCTCCCAACGCAGGAGGG
                        |||||||||| || | |||||||||||||||| || ||||||||||||||||||||||||
AAGV03240337.1          GCAGGGAGTCGGCGCGCGTGGTCCAGGTGACAGCTCTGCCTTTCTCCCAACGCAGGAGGG

AAGV03145787.1          AAGAAGTCCCCGCACTACCATGGTGAGTGGTACTGACTTTGCAGGGGCACTGAGCCCTGA
                        ||||||||| ||||||| || |||||||| ||||||  |||||||| ||||||||||
AAGV03240337.1          AAGAAGTCCCTGCACTACGCTGCTGAGTGGTGCTGACTCCGCAGGGGCGCTGAGCCCTGA
```

Table A.1 CDR3 regions and *TRDD* usage of unstimulated alpaca PBMCs. CDR3 regions were determined with the IMGT/DomainGapAlign tool [330, 332]. *TRDV* regions and *TRDD* usage (***D1/3***, *D2*, *D4*) are marked. The CDR3 length in amino acids was calculated and the clone numbers are indicated ("/" indicates identical clones and "n.p." non-productive rearrangements).

TRDV	CDR3 (IMGT)	*TRDD*	CDR3 length (AA)	clone #
V2	GCAGCCGCGAGGGCACGGGAGACTCCACTGATA	*D4*	11	94
V3	GCTCCTTTCGTATACGGACGTTGGAGTGGGATGCTGGGAGACCGGATGGATCCACTGATA	*D4*	20	63/68
V3	GCTCTGGAGTACGGGAGGCAGTATCCACTGATA	-	11	72
V3	GCTCTGGAGTAC**GGTGGGA**CGCCCATCGGTCCACTGATA	***D1/3***	13	85
V3	GCTCTTGGGCGGCTGGGGTATCCACTGATA	-	10	92
V3	GCTCTGGAGTACCGGGTGCTATACGGACGGCGGGAGTGGTTGGAGTCGGACTGGGATCCACTGATA	*D2*	22	95
V3	GCTCTGGGCCGCTCGTTGGA**GTGGGATT**GGGGACTACTGATA	***D1/3***	14	98
cdV2	GCTCTCTGGCTCAGAGGAGGTGGAAAGTGGTTGGAGTCGA**GGGATTT**GCTGGGAGCCCAACTGATA	*D2*. ***D1/3***	22	53
cdV2	GCTCTCTGGGTTACCCCTGGGATATACGGACTGGGAGACCCACTGATA	*D4*	16	56/76
cdV2	GCTCTCTGGGACTACGATATACGGACGGTGGTTGGA**GTGGGATT**GTACGATATACGGACGAGACAGTATC CACTGATA	*D2*, ***D1/3***	26	58
V1-B	GCTCTCAGAGAAGGCCCATACGGACGAGACGCTCCACTGATA	-	14	55
V1-B2	GCTCTCAGAGAAAGCCCACCCGGAGTCGAGGGATACGATATACGGACGGGAGATCCACTGATA	*D4*	21	57
V1-B2	GCTCTCAGAGATGGCGATATACGGTATCCACTGATA	-	12	59
V1-B2	GCTCTAACGGTTGGAGTCGGGATTGGGAGATATGATCCACTGATA	*D4*	15	61
V1-B2	GCTCTCAGAGAAAGCTGGCCCTACGATCTAGTGGTTGGA**GTGGGATTT**CCGTATCCACTGATA	*D2*, ***D1/3***	21	66
V1-B2	GCTCTCAGAGGGTCGTGGTTGGAGTC**TGGGATT**ACGGAGGGAGACCGGTATCCACTGATA	*D2*, ***D1/3***	20	69/75
V1-B2	GCTCTCAGGGGTGATATACGGAGTGGTTGGAGTC**TGGGATT**CCCCGGGCGGTATCCACTGATA	*D2*, ***D1/3***	21	77
V1-C2	GCTCTCTGGGAAAGGTCCAGGGATACTGGGAGACCGTATCCACTGATA	*D4*	14	67
V1-D	GCTCTAGAAGAAGTTCCCGCCGGGTCCCCACTGATA	-	12	96/99
V1-E	GCTCTCAGAGAGATATGCTGGGAGTATCCACTGATA	*D4*	12	62
V1-E	GCTCTCACTTGGCGATATACGGAGTGGTTGGAGTCTGGCGCTGGGTCGCAGTATCCACTGATA	*D2*	21	83
V1-G	GCTTTCGGGGGAGAGAGCACAGCTTATC	*D4*	9	74/87
V1-G	GCTTTCGATGGAGCCTCCCGACGGAGTGGTTGGAGTGGACCCCTACGGAGGTATCCACTGATA	*D2*	21	73/86
V1-G	GCTTTCGCTACGGCGATATACGGGTTGGAGTGGGATACGGACTGGGAGACAGTATCCACTGATA	*D2*, *D4*	n.p.	81
V1-G	GCTTTCGATGGAAGCCGTGCGATACGGAC**GTGGGATTT**GGTTGGA**GTGGGATT**GGGAGACCCACTGATA	*2x**D1/3***	23	93
V1-G	GCTTTCGATGGAAGGGGGACGGAC**GGGATTT**TTG**GGTGGGATTT**ACGGCGCTGGGAGTATCCACTGATA	*2x**D1/3***, *D4*	23	97
V1-H	GCTCTCTGGGACAGCTTCGCCGGAAAGTGGTTGGAGGCTGGGAGACCGGGACCACTGATA	*D4*	20	51
V1-H	GCTCGGTATACGGAC**GGGATTT**CGTTG**GGTGGGA**TGCTGGGAGACCCACTGATA	*2x**D1/3***, *D4*	18	52
V1-H	GCTCTCTGGGACAGTTGCGGATATACGGGT**GGTGGG**GCT	***D1/3***	13	60
V1-H	GCTCTCTGGGACAGCCTGGACGGTTGGAGTCGA**GGGATTT**TATACGGGGGATATCCACTGATA	*D2*, ***D1/3***	21	64/70
V1-H	GCTCTCTGCGCTCCCCCCCGTACGATATACGTTGGAGTGGGAGATCCACTGATA	*D2*, *D4*	18	65
V1-H	GCTCTCTGGGACGCCGAGTCGTTGGAGGGATTTGGGAATCCACTGATA	*D2*	16	71
V1-H	GCTCTCTGGGACCAAAGCCAGGGTTGGAGTC**GGGATTT**GGGGTTAAATCCACTGATA	*D2*, ***D1/3***	19	78
V1-K	GCTCTCAGAGAACCGGGATATGGAGTCGAGAGACTCCGGTATCCACTGATA	*D2*	17	80/82
V1-K2	GCTCTCAGAGAAATACG**GTGGGATT**GGA**GTGGGATTT**GGAGACAGTATCCACTGATA	*2x **D1/3***	19	84

Table A.2 List of 118.7 frequencies in alpaca PBMCs. Unstimulated PBMCs (1*10^5 per sample) were stained with isotype control or 118.7 mAb ([1]Fab R-PE labeled, [2]DαM R-PE labeled) with (percentage of live cells indicated) or without (-) intracellular CD3ε staining. The flow cytometry stainings were carried out as described in chapter 3.2.2.4. Live cells were determined by [4]FSC/SSC. In some samples, Fixable Viability Dye eFluor® 660 (1:1000, eBioscience) was used to identify dead cells ([3]). The animal and PBMC isolation date are indicated as well as 118.7$^+$ frequencies of live cells (corrected for background staining) and CD3 frequencies if applicable. The frequency of 118.7$^+$ cells among CD3$^+$ cells was calculated in those cases.

Isolation date	Animal	Experiment	% 118.7$^+$	% 118.7$^+$/CD3$^+$	% CD3$^+$
19.07.16	1	20.07.16	0.64[2,4]	1.12	57
19.07.16/22.09.16	1	29.09.16	0.87[2,4]	-	-
19.07.16/22.09.16	1	15.11.16	0.72[1,4]	-	-
19.07.16/22.09.16	1	23.11.16	0.80[2,4]	-	-
19.07.16/22.09.16	1	12.01.17	0.75[2,3]	-	-
04.04.17	1	05.04.17	0.56[1,3]	-	-
27.06.17	1	27.06.17	1.98[1,4]	-	-
27.09.17	1	28.09.17	1.75[1,4]	-	-
19.07.16	2	20.07.16	0.52[2,4]	-	-
22.09.16	2	20.03.17	0.44[2,3]	0.85	51.65
22.09.16	2	20.03.17	0.68[1,3]	-	-
15.02.17	2	22.03.17	0.70[2,3]	1.36	53.9
04.04.17	2	05.04.17	0.65[1,3]	-	-
27.09.17	3	28.09.17	0.98[1,4]	-	-
19.07.16	4	20.07.16	0.22[2,4]	0.34	64.45
19.07.16	4	25.08.16	0.24[2,4]	0.36	65.95
22.09.16	5	31.01.17	0.12[2,4]	0.26	45.35
22.09.16	5	13.02.17	0.12[2,3]	0.26	46.10
27.03.12	7	27.06.16	0.14[2,4]	0.20	68.95
27.06.17	6	27.06.17	0.91[1,4]	-	-
27.03.12	8	27.04.16	0.31[2,4]	0.5	61.75
27.03.12	8	27.06.16	0.19[2,4]	0.31	60.85
27.06.17	8	27.06.17	3.94[1,4]	-	-

Table A.3 List of alpaca PBMC stimulation results. PBMCs (1*10^5 per well) were stimulated in 96 well flat bottom suspension culture plates for seven days. Concentrations of hIL2 and HMBPP are indicated. On day 7, each well was divided and 118.7/isotype stainings ([1]Fab R-PE labeled, [2]DαM R-PE labeled) with (percentage of live cells indicated) or without (-) intracellular CD3ε staining were carried out. Fixable Viability Dye eFluor® 660 (1:1000, eBioscience) was used to identify dead cells. The animal and PBMC isolation date are indicated as well as 118.7$^+$ frequencies of live cells (corrected for background staining) and CD3 frequencies if applicable. The frequency of 118.7$^+$ cells among CD3$^+$ cells was calculated in those cases. Total cell numbers were estimated by using [5]Calibrite™ Beads (10^4 per sample, BD) or by the acquisition of the complete sample by flow cytometry[6]. The cell numbers of isotype and 118.7 staining were taken together. If available, means of replicates were calculated and the number of replicates (n=x) is indicated.

Isolation date	Animal	Experiment	% 118.7$^+$	% 118.7$^+$/CD3$^+$	% CD3$^+$	Live cells	Stimulation conditions (IL2 [U/ml]/HMBPP [nM]
04.04.17	1	11.04.17	0.54[1,n=4]	-	-	6156[5]	50/0
04.04.17	1	11.04.17	12.11[1,n=4]	-	-	8132[5]	50/1000
27.06.17	1	04.07.17	1.07[1,n=2]	-	-	22889[5]	50/0
27.06.17	1	04.07.17	8.80[1,n=2]	-	-	16389[5]	50/100
04.04.17	1	20.07.17	0.00[1]	-	-	2676[6]	50/0
04.04.17	1	20.07.17	2.13[1]	-	-	2120[6]	50/100
27.09.17	1	04.10.17	0.10[1,n=2]	-	-	22363[5]	50/0
27.09.17	1	04.10.17	1.42[1,n=2]	-	-	23342[5]	50/100
22.09.16	2	24.11.16	0,15[1]	0.18	82.80	-	100/0
22.09.16	2	24.11.16	7.30[1,n=2]	8.78	83.10	-	100/1000
22.09.16	2	24.11.16	0.14[1]	0.18	78.00	-	0/100
22.09.16	2	24.11.16	12.36[1]	14.56	84.90	-	25/100
22.09.16	2	24.11.16	6.14[1]	7.45	82.45	-	50/100
22.09.16	2	24.11.16	5.52[1]	6.80	81.20	-	100/100
22.09.16	2	24.11.16	6.26[1]	7.49	83.55	-	200/100
22.09.16	2	08.12.16	0.19[1]	0.25	76.80	40976[6]	0/100
22.09.16	2	08.12.16	1.26[1]	1.54	81.79	68379[6]	3.125/100
22.09.16	2	08.12.16	3.17[1]	3.88	81.78	76576[6]	6.25/100
22.09.16	2	08.12.16	3.06[1]	3.76	81.37	76748[6]	12.5/100
22.09.16	2	08.12.16	1.69[1]	2.07	81.66	43898[6]	25/100
22.09.16	2	08.12.16	2.81[1]	3.47	81.00	51898[6]	50/100
15.02.17	2	23.02.17	0.41[1,n=3]	-	-	11603[6]	50/0
15.02.17	2	23.02.17	28.72[1,n=3]	-	-	15403[6]	50/1000
22.09.16	2	02.03.17	0.23[1,n=3]		84,35	22990[6]	50/0
22.09.16	2	02.03.17	0.78[1,n=4]		81.81	25407[6]	50/1
22.09.16	2	02.03.17	2.79[1,n=4]		82.90	24110[6]	50/10
22.09.16	2	02.03.17	10.42[1,n=4]		86.23	27575[6]	50/100
22.09.16	2	02.03.17	10.10[1,n=4]		86.11	26021[6]	50/1000
04.04.17	2	11.04.17	0.05[1,n=4]	-	-	7738[5]	50/0
04.04.17	2	11.04.17	35.96[1,n=4]	-	-	6036[5]	50/1000
27.09.17	2	04.10.17	0.16[1]	-	-	8883[5]	50/0
27.09.17	2	04.10.17	11.95[1]	-	-	11410[5]	50/100
15.02.17	3	23.02.17	0.95[1,n=3]	-	-	3390[6]	50/0
15.02.17	3	23.02.17	2.05[1,n=3]	-	-	5329[6]	50/1000
27.09.17	3	04.10.17	0.03[1,n=2]	-	-	34430[5]	50/0
27.09.17	3	04.10.17	33.11[1,n=2]	-	-	34818[5]	50/100
27.06.17	6	04.07.17	0.22[1,n=2]	-	-	15365[5]	50/0
27.06.17	6	04.07.17	1.04[1,n=2]	-	-	13270[5]	50/100
27.06.17	8	04.07.17	0.21[1,n=2]	-	-	17675[5]	50/0
27.06.17	8	04.07.17	3.28[1,n=2]	-	-	9679[5]	50/100

Table A.4 List of *TRGV9* CDR3 and *TRGJ* regions obtained by *TRGV9*/*TRGC* PCR. *TRGV9*/*TRGC* PCR amplifications were performed with cDNA of 118.7^{+} or 118.7^{-} unstimulated or stimulated cells (cell viability: Fixable Viability Dye eFluor® 660, 1:1000, eBioscience). Stimulation was carried out for 7 days of with hIL-2 (50 U/ml) and HMBPP (1 µM). PCR products were cloned into pCR™4-TOPO® vector and clones were analyzed by sequencing. Clones were analyzed according to their CDR3 and *TRGJ* region. CDR3 regions (underscored) together with *TRGJ* amino acid sequences are listed for each condition. The frequencies of unique CDR3+*TRGJ* sequences among translatable clones is indicated as well as CDR3 lengths and *TRGJ* types according to [317] were assigned.

Animal 1				Animal 2			
TRGV9*: CDR3+*TRGJ	**CDR3 length**	***TRGJ***	**# Clones**	***TRGV9*: CDR3+*TRGJ***	**CDR3 length**	***TRGJ***	**# Clones**
118.7^{-} unstimulated				**118.7^{-} unstimulated**			
ALWDTLTDGKTIKVFGSGTRLIIT	14	*JP-B*	3/8	ALWDALRKDGRTIKVFGSGTRLIIT	15	*JP-C*	2/11
ALWERLGTDGKTIKVFGSGTRLIIT	15	*JP-B*	1/8	ALWDARLLTDGRTIKVFGSGTRLIIT	16	*JP-C*	1/11
ALWDALTDGKTIKVFGSGTRLIIT	14	*JP-B*	1/8	ALWDPRTDGRTIKVFGSGTRLIIT	14	*JP-C*	1/11
ALWDVIDGKTIKVFGSGTRLIIT	13	*JP-B*	1/8	APTDGRTIKVFGSGTRLIIT	10	*JP-C*	1/11
ALWEDGRTIKVFGSGTRLIVT	11	*JP-A*	1/8	ALWAARDGRTIKVFGSGTRLIIT	13	*JP-C*	1/11
APPPRTIKVFGSGTRLIVT	9	*JP-A*	1/8	ALWDAPVTDGRTIKVFGSGTRLIIT	15	*JP-C*	1/11
				ALWDAQNGRTIKVFGSGTRLIVT	13	*JP-A*	1/11
				ALWDAPRLTDGRTIKVFGSGTRLIVT	16	*JP-A*	1/11
				ALWDARINGGRTIKVFGSGTRLIVT	15	*JP-A*	1/11
				ALWNTSGWIKIFGEGTKLIVIPP	11	*JP1*	1/11
118.7^{-} HMBPP-stimulated				**118.7^{-} HMBPP-stimulated**			
ALWDALPDGRTIKVFGSGTRLIVT	14	*JP-A*	5/10	ALWDRWADGRTIKVFGSGTRLIIT	14	*JP-C*	6/11
ALWDLMTDGRTIKVFGSGTRLIVT	14	*JP-A*	4/10	ALWDARTDGRTIKVFGSGTRLIIT	14	*JP-C*	2/11
ALWDADGKTIKVFGSGTRLIIT	12	*JP-B*	1/10	ALWDHGRTIKVFGSGTRLIIT	11	*JP-C*	1/11
				ALWAGQPTGRTIKVFGSGTRLIIT	14	*JP-C*	1/11
				ALCRGPTSGWIKIFGEGTKLIVIPP	13	*JP1*	1/11
118.7^{+} unstimulated				**118.7^{+} unstimulated**			
ALWDARSDGRTIKVFGSGTRLIVT	14	*JP-A*	4/20	ALWDARDGRTIKVFGSGTRLIIT	13	*JP-C*	5/18
ALWEPLTDGRTIKVFGSGTRLIVT	14	*JP-A*	3/20	ALWAPQTDGRTIKVFGSGTRLIIT	14	*JP-C*	4/18
ALWDARADGRTIKVFGSGTRLIVT	14	*JP-A*	3/20	ALWDPLPDGRTIKVFGSGTRLIIT	14	*JP-C*	2/18
ALWVSLRGRTIKVFGSGTRLIVT	13	*JP-A*	2/20	ALWDRWADGRTIKVFGSGTRLIIT	14	*JP-C*	2/18
ALWDALADGRTIKVFGSGTRLIVT	14	*JP-A*	2/20	ALWDSLTDGRTIKVFGSGTRLIIT	14	*JP-C*	2/18
ALWDALTDGRTIKVFGSGTRLIVT	14	*JP-A*	1/20	ALWDVRTDGRTIKVFGSGTRLIIT	14	*JP-C*	1/18
ALWDARLTDGRTIKVFGSGTRLIVT	15	*JP-A*	1/20	ALWDPRTDGRTIKVFGSGTRLIIT	14	*JP-C*	1/18
ALWDPLTDGRTIKVFGSGTRLIVT	14	*JP-A*	1/20	ALWDGITDGRTIKVFGSGTRLIVT	14	*JP-A*	1/18
ALWDSTGLTDGRTIKVFGSGTRLIVT	16	*JP-A*	1/20				
ALWDARTDGRTIKVFGSGTRLIVT	14	*JP-A*	1/20				
ALWDAAADGKTIKVFGSGTRLIIT	14	*JP-B*	1/20				
118.7^{+} HMBPP-stimulated				**118.7^{+} HMBPP-stimulated**			
ALWEPLTDGRTIKVFGSGTRLIVT	14	*JP-A*	5/17	ALWAPQTDGRTIKVFGSGTRLIIT	14	*JP-C*	7/16
ALWDAAADGKTIKVFGSGTRLIIT	14	*JP-B*	4/17	ALWDGITDGRTIKVFGSGTRLIVT	14	*JP-A*	3/16
ALWDARSDGRTIKVFGSGTRLIVT	14	*JP-A*	2/17	ALWDALADGRTIKVFGSGTRLIIT	14	*JP-C*	2/16
ALWDAAADGKTIKVFGSGTRLIVT	14	*JP-A/B*	1/17	ALWDPRTDGRTIKVFGSGTRLIIT	14	*JP-C*	2/16
ALWDSRSDGRTIKVFGSGTRLIVT	14	*JP-A*	1/17	ALWDARRADGRTIKVFGSGTRLIVT	15	*JP-A*	1/16
ALWDPRSDGRTIKVFGSGTRLIVT	14	*JP-A*	1/17	ALWEPLTDGRTIKVFGSGTRLIVT	14	*JP-A*	1/16
ALWDSRADGRTIKVFGSGTRLIVT	14	*JP-A*	1/17				
ALWDARADGRTIKVFGSGTRLIVT	14	*JP-A*	1/17				
ALWDAAADGRTIKVFGSGTRLIIT	14	*JP-C*	1/17				

Table A.5 List of *TRDV2,* CDR3 and *TRDJ* regions. *TRDV2*/*TRDC* PCR amplifications were performed with cDNA of 118.7^{+} or 118.7^{-} unstimulated or stimulated cells (cell viability: Fixable Viability Dye eFluor® 660, 1:1000, eBioscience). Stimulation was carried out for 7 days with hIL-2 (50 U/ml) and HMBPP (1 µM). PCR products were cloned into pCR™4-TOPO® vector and clones were analyzed by sequencing. Clones were analyzed according to their CDR3 and J-region. CDR3 regions (underscored) together with *TRDJ* amino acid sequences are listed for each condition. The frequencies of unique CDR3+*TRDJ* sequences among translatable clones is indicated as well as CDR3 lengths and *TRDJ* were named according to homologies to human *TRDJ*. The amino acid in position δ97 is marked in bold [247].

Animal 1				**Animal 2**			
TRDV2*: CDR3+*TRDJ	**CDR3 length**	***TRDJ***	**# Clones**	***TRDV2*: CDR3+*TRDJ***	**CDR3 length**	***TRDJ***	**# Clones**
118.7^{-} unstimulated				**118.7^{-} unstimulated**			
ATR**M**RTGGIITGGNSVNPLIFGKGTYLNVEP	20	J4	2/10	ARS**T**IYGREYPLIFGKGTYLNVEP	13	J4	1/10
AAP**L**ESGIPRWRHPLIFGKGTYLNVEP	16	J4	2/10	AAP**L**ESGIPRWRHPLIFGKGTYLNVEP	16	J4	2/10
ATR**Q**GYGWSRDWIRVTAQLIFGKGTQLIVEP	20	J2	2/10	ATR**I**RYTDVETRLRPLIFGKGTYLNVEP	17	J4	3/10
ASR**G**GYDIRLESGWETEWGSWDTRQMFFGAGTKLYVEH	27	J3	2/10	ATR**M**RTGGIITGGNSVNPLIFGKGTYLNVEP	20	J4	2/10
ATH**I**RVGGRTGDLTAQLIFGKGTQLIVEP	18	J2	1/10	ATR**A**VRYRLGGAGRNLIFGKGTYLNVEP	17	J4	1/10
ARS**T**IYGREYPLIFGKGTYLNVEP	13	J4	1/10	AAY**V**GVGRGTAQLIFGKGTQLIVEP	14	J2	1/10
118.7^{-} HMBPP-stimulated				**118.7^{-} HMBPP-stimulated**			
ATH**I**RVGGRTGDLTAQLIFGKGTQLIVEP	18	J2	15/17	ATR**I**AYTGAGRRELIFGKGTQLIVEP	15	J2	11/13
ATK**A**RWSRLGDRPLIFGKGTYLNVEP	15	J4	1/17	ATR**I**RYTDVETRLRPLIFGKGTYLNVEP	17	J4	2/13
ATT**C**VGVGYDIRTPLIFGKGTYLNVEP	16	J4	1/17				
118.7^{+} unstimulated				**118.7^{-} unstimulated**			
ASL**M**VGGGGRGELIFGKGTYLNVEP	14	J4	1/5	ATR**I**RYTDVETRLRPLIFGKGTYLNVEP	17	J4	3/15
ATA**V**RSGWSRDGRPRPLIFGKGTYLNVEP	18	J4	1/5	AAP**L**ESGIPRWRHPLIFGKGTYLNVEP	16	J4	3/15
ARS**T**IYGREYPLIFGKGTYLNVEP	13	J4	1/5	ATK**V**GFRERGASLIFGKGTYLNVEP	14	J4	1/15
ATS**G**WSRGFEPLIFGKGTYLNVEP	13	J4	1/5	AST**I**YGRGETPLIFGKGTYLNVEP	13	J4	1/15
ASK**V**GWSRLGDRPLIFGKGTYLNVEP	15	J4	1/5	ATS**V**RVGGFRETKGPLIFGKGTYLNVEP	17	J4	1/15
				ATR**M**TTGVVGVGLVRGPLIFGKGTYLNVEP	19	J4	1/15
				ATT**G**LKRGGPLIFGKGTYLNVEP	12	J4	1/15
				ATK**I**RRGPLIFGKGTYLNVEP	10	J4	1/15
				ATP**I**RSGWRDGRRPLIFGKGTYLNVEP	16	J4	1/15
				AIK**M**VGFRYTDWEPRPLIFGKGTYLNVEP	18	J4	1/15
				ANP**I**VRYTPGLGVRGPLIFGKGTYLNVEP	18	J4	1/15
118.7^{+} HMBPP-stimulated				**118.7^{+} HMBPP-stimulated**			
ATK**A**RWSRLGDRPLIFGKGTYLNVEP	15	J4	3/16	ATR**I**RYTDVETRLRPLIFGKGTYLNVEP	17	J4	4/14
ATK**L**VVGIRTWETPLIFGKGTYLNVEP	16	J4	3/16	AAP**L**ESGIPRWRHPLIFGKGTYLNVEP	16	J4	3/14
ATA**L**RRGRLIFGKGTYLNVEP	10	J4	2/16	ATR**A**VRYRLGGAGRNLIFGKGTYLNVEP	17	J4	2/14
ATT**I**YGRGRYPLIFGKGTYLNVEP	13	J4	2/16	ATR**M**TTGVVGVGLVRGPLIFGKGTYLNVEP	19	J4	1/14
ARA**I**TAYGQTPSERLIFGKGTYLNVEP	16	J4	2/16	ATS**V**RVGGFRETKGPLIFGKGTYLNVEP	17	J4	1/14
ATG**V**RYTASGWRSGPLIFGKGTYLNVEP	17	J4	1/16	ATR**V**GVGVRGQYPLIFGKGTYLNVEP	15	J4	1/14
AAR**A**RETPLIFGKGTYLNVEP	10	J4	1/16	ATR**M**RTGGIITGGNSVNPLIFGKGTYLNVEP	20	J4	1/14
ATT**I**RSRGRDILIFGKGTYLNVEP	13	J4	1/16	ANP**I**VRYTPGLGVRGPLIFGKGTYLNVEP	18	J4	1/14
ATA**V**RSGWSRDGRPRPLIFGKGTYLNVEP	18	J4	1/16				

References

[1] **Abbas AK, Lichtman AH, Pillai S** (2014) *Cellular and molecular immunology*. 8th ed. Philadelphia: Saunders/Elsevier.

[2] **Murphy K, Weaver C** (2017) *Janeway's Immunobiology*. 9th ed. New York: Garland Science/Taylor & Francis.

[3] **Ericsson AC, Crim MJ, Franklin CL** (2013) *A Brief History of Animal Modeling*. Mo Med, 110(3):201-5.

[4] **Marrack P, Scott-Browne JP, Dai S, Gapin L, Kappler JW** (2008) *Evolutionarily Conserved Amino Acids That Control TCR-MHC Interaction*. Annu Rev Immunol, 26(1):171-203.

[5] **Carding SR, Egan PJ** (2002) *Gammadelta T cells: functional plasticity and heterogeneity*. Nat Rev Immunol, 2(5):336-45.

[6] **Straube F, Herrmann T** (2000) *Expression of functional CD8alpha Beta heterodimer on rat gamma delta T cells does not correlate with the CDR3 length of the TCR delta chain predicted for MHC class I-restricted antigen recognition*. Eur J Immunol, 30(12):3562-8.

[7] **Vantourout P, Hayday A** (2013) *Six-of-the-best: unique contributions of gammadelta T cells to immunology*. Nat Rev Immunol, 13(2):88-100.

[8] **Chien YH, Jores R, Crowley MP** (1996) *Recognition by gamma/delta T cells*. Annu Rev Immunol, 14:511-32.

[9] **Born WK, Kemal Aydintug M, O'brien RL** (2013) *Diversity of gammadelta T-cell antigens*. Cell Mol Immunol, 10(1):13-20.

[10] **Adams EJ, Chien Y-H, Garcia KC** (2005) *Structure of a γδ T Cell Receptor in Complex with the Nonclassical MHC T22*. Science, 308(5719):227-31.

[11] **Wingren C, Crowley MP, Degano M, Chien Y-H, Wilson IA** (2000) *Crystal Structure of a γδ T Cell Receptor Ligand T22: A Truncated MHC-Like Fold*. Science, 287(5451):310-4.

[12] **Matis LA, Fry AM, Cron RQ, Cotterman MM, Dick RF, Bluestone JA** (1989) *Structure and specificity of a class II MHC alloreactive gamma delta T cell receptor heterodimer*. Science, 245(4919):746-9.

[13] **Xu B, Pizarro JC, Holmes MA, Mcbeth C, Groh V, Spies T, et al.** (2011) *Crystal structure of a γδ T-cell receptor specific for the human MHC class I homolog MICA*. Proc Natl Acad Sci U S A, 108(6):2414-9.

[14] **Kong Y, Cao W, Xi X, Ma C, Cui L, He W** (2009) *The NKG2D ligand ULBP4 binds to TCRγ9/δ2 and induces cytotoxicity to tumor cells through both TCRγδ and NKG2D*. Blood, 114(2):310-7.

[15] **Groh V, Steinle A, Bauer S, Spies T** (1998) *Recognition of Stress-Induced MHC Molecules by Intestinal Epithelial γδ T Cells*. Science, 279(5357):1737-40.

[16] **Bai L, Picard D, Anderson B, Chaudhary V, Luoma A, Jabri B, et al.** (2012) *The majority of CD1d-sulfatide-specific T cells in human blood use a semiinvariant Vδ1 TCR*. Eur J Immunol, 42(9):2505-10.

[17] **Agea E, Russano A, Bistoni O, Mannucci R, Nicoletti I, Corazzi L, et al.** (2005) *Human CD1-restricted T cell recognition of lipids from pollens*. The Journal of Experimental Medicine, 202(2):295-308.

[18] **Russano AM, Bassotti G, Agea E, Bistoni O, Mazzocchi A, Morelli A, et al.** (2007) *CD1-restricted recognition of exogenous and self-lipid antigens by duodenal gammadelta+ T lymphocytes*. J Immunol, 178(6):3620-6.

[19] **Russano AM, Agea E, Corazzi L, Postle AD, De Libero G, Porcelli S, et al.** (2006) *Recognition of pollen-derived phosphatidyl-ethanolamine by human CD1d-restricted gamma delta T cells*. J Allergy Clin Immunol, 117(5):1178-84.

[20] **Dieudé M, Striegl H, Tyznik AJ, Wang J, Behar SM, Piccirillo CA, et al.** (2011) *Cardiolipin Binds to CD1d and Stimulates CD1d-Restricted γδ T Cells in the Normal Murine Repertoire*. J Immunol, 186(8):4771-81.

[21] **Willcox CR, Pitard V, Netzer S, Couzi L, Salim M, Silberzahn T, et al.** (2012) *Cytomegalovirus and tumor stress surveillance by binding of a human γδ T cell antigen receptor to endothelial protein C receptor*. Nat Immunol, 13:872.

[22] **Zeng X, Wei YL, Huang J, Newell EW, Yu H, Kidd BA, et al.** (2012) *gammadelta T cells recognize a microbial encoded B cell antigen to initiate a rapid antigen-specific interleukin-17 response*. Immunity, 37(3):524-34.

[23] **Rust CJ, Verreck F, Vietor H, Koning F** (1990) *Specific recognition of staphylococcal enterotoxin A by human T cells bearing receptors with the V gamma 9 region*. Nature, 346(6284):572-4.

[24] **Johnson RM, Lancki DW, Sperling AI, Dick RF, Spear PG, Fitch FW, et al.** (1992) *A murine CD4-, CD8- T cell receptor-gamma delta T lymphocyte clone specific for herpes simplex virus glycoprotein I*. J Immunol, 148(4):983-8.

[25] **Kozbor D, Cassatella MA, Lessin S, Kagan J, Finver S, Faust J, et al.** (1990) *Expression and function of gamma delta- and alpha beta-T cell receptor heterodimers on human somatic T cell hybrids*. J Immunol, 144(10):3677-83.

[26] **Kozbor D, Trinchieri G, Monos DS, Isobe M, Russo G, Haney JA, et al.** (1989) *Human TCR-gamma+/delta+, CD8+ T lymphocytes recognize tetanus toxoid in an MHC-restricted fashion*. J Exp Med, 169(5):1847-51.

[27] **Born W, Hall L, Dallas A, Boymel J, Shinnick T, Young D, et al.** (1990) *Recognition of a peptide antigen by heat shock--reactive gamma delta T lymphocytes*. Science, 249(4964):67-9.

[28] **O'brien RL, Fu YX, Cranfill R, Dallas A, Ellis C, Reardon C, et al.** (1992) *Heat shock protein Hsp60-reactive gamma delta cells: a large, diversified T-lymphocyte subset with highly focused specificity*. Proc Natl Acad Sci U S A, 89(10):4348-52.

[29] **Fu YX, Vollmer M, Kalataradi H, Heyborne K, Reardon C, Miles C, et al.** (1994) *Structural requirements for peptides that stimulate a subset of gamma delta T cells*. J Immunol, 152(4):1578-88.

[30] **Zhang L, Jin N, Nakayama M, O'brien RL, Eisenbarth GS, Born WK** (2010) *Gamma delta T cell receptors confer autonomous responsiveness to the insulin-peptide B:9-23*. J Autoimmun, 34(4):478-84.

[31] **Pfeffer K, Schoel B, Gulle H, Kaufmann SHE, Wagner H** (1990) *Primary responses of human T cells to mycobacteria: a frequent set of γ/δ T cells are stimulated by protease-resistant ligands*. Eur J Immunol, 20(5):1175-9.

[32] **Morita CT, Jin C, Sarikonda G, Wang H** (2007) *Nonpeptide antigens, presentation mechanisms, and immunological memory of human Vgamma2Vdelta2 T cells: discriminating friend from foe through the recognition of prenyl pyrophosphate antigens*. Immunol Rev, 215:59-76.

[33] **Adams EJ, Gu S, Luoma AM** (2015) *Human gamma delta T cells: Evolution and ligand recognition*. Cell Immunol, 296(1):31-40.

[34] **Vermijlen D, Gatti D, Kouzeli A, Rus T, Eberl M** (2018) *gammadelta T cell responses: How many ligands will it take till we know?* Semin Cell Dev Biol.

[35] **Famili F, Wiekmeijer AS, Staal FJ** (2017) *The development of T cells from stem cells in mice and humans*. Future Sci OA, 3(3):FSO186.

[36] **Gibbons DL, Haque SF, Silberzahn T, Hamilton K, Langford C, Ellis P, et al.** (2009) *Neonates harbour highly active gammadelta T cells with selective impairments in preterm infants*. Eur J Immunol, 39(7):1794-806.

[37] **Vermijlen D, Brouwer M, Donner C, Liesnard C, Tackoen M, Van Rysselberge M, et al.** (2010) *Human cytomegalovirus elicits fetal gammadelta T cell responses in utero*. J Exp Med, 207(4):807-21.

[38] **Dimova T, Brouwer M, Gosselin F, Tassignon J, Leo O, Donner C, et al.** (2015) *Effector Vgamma9Vdelta2 T cells dominate the human fetal gammadelta T-cell repertoire*. Proc Natl Acad Sci U S A, 112(6):E556-65.

[39] **Schmolka N, Wencker M, Hayday AC, Silva-Santos B** (2015) *Epigenetic and transcriptional regulation of gammadelta T cell differentiation: Programming cells for responses in time and space*. Semin Immunol, 27(1):19-25.

[40] **Dudley EC, Girardi M, Owen MJ, Hayday AC** (1995) *Alpha beta and gamma delta T cells can share a late common precursor*. Curr Biol, 5(6):659-69.

[41] **Ciofani M, Knowles GC, Wiest DL, Von Boehmer H, Zuniga-Pflucker JC** (2006) *Stage-specific and differential notch dependency at the alphabeta and gammadelta T lineage bifurcation*. Immunity, 25(1):105-16.

[42] **Pereira P, Boucontet L, Cumano A** (2012) *Temporal predisposition to alphabeta and gammadelta T cell fates in the thymus*. J Immunol, 188(4):1600-8.

[43] **Hayday AC** (2000) *[gamma][delta] cells: a right time and a right place for a conserved third way of protection*. Annu Rev Immunol, 18:975-1026.

[44] **Ramsburg E, Tigelaar R, Craft J, Hayday A** (2003) *Age-dependent requirement for gammadelta T cells in the primary but not secondary protective immune response against an intestinal parasite*. J Exp Med, 198(9):1403-14.

[45] **Prinz I, Silva-Santos B, Pennington DJ** (2013) *Functional development of gammadelta T cells*. Eur J Immunol, 43(8):1988-94.

[46] **Pang DJ, Neves JF, Sumaria N, Pennington DJ** (2012) *Understanding the complexity of gammadelta T-cell subsets in mouse and human*. Immunology, 136(3):283-90.
[47] **Di Marco Barros R, Roberts NA, Dart RJ, Vantourout P, Jandke A, Nussbaumer O, et al.** (2016) *Epithelia Use Butyrophilin-like Molecules to Shape Organ-Specific gammadelta T Cell Compartments*. Cell, 167(1):203-18 e17.
[48] **Harly C, Guillaume Y, Nedellec S, Peigne CM, Monkkonen H, Monkkonen J, et al.** (2012) *Key implication of CD277/butyrophilin-3 (BTN3A) in cellular stress sensing by a major human gammadelta T-cell subset*. Blood, 120(11):2269-79.
[49] **Wang H, Henry O, Distefano MD, Wang YC, Raikkonen J, Monkkonen J, et al.** (2013) *Butyrophilin 3A1 plays an essential role in prenyl pyrophosphate stimulation of human Vgamma2Vdelta2 T cells*. J Immunol, 191(3):1029-42.
[50] **Melichar HJ, Narayan K, Der SD, Hiraoka Y, Gardiol N, Jeannet G, et al.** (2007) *Regulation of gammadelta versus alphabeta T lymphocyte differentiation by the transcription factor SOX13*. Science, 315(5809):230-3.
[51] **Kang J, Volkmann A, Raulet DH** (2001) *Evidence that gammadelta versus alphabeta T cell fate determination is initiated independently of T cell receptor signaling*. J Exp Med, 193(6):689-98.
[52] **Hayes SM, Li L, Love PE** (2005) *TCR signal strength influences alphabeta/gammadelta lineage fate*. Immunity, 22(5):583-93.
[53] **Turchinovich G, Hayday AC** (2011) *Skint-1 identifies a common molecular mechanism for the development of interferon-gamma-secreting versus interleukin-17-secreting gammadelta T cells*. Immunity, 35(1):59-68.
[54] **Barbee SD, Woodward MJ, Turchinovich G, Mention JJ, Lewis JM, Boyden LM, et al.** (2011) *Skint-1 is a highly specific, unique selecting component for epidermal T cells*. Proc Natl Acad Sci U S A, 108(8):3330-5.
[55] **Jin Y, Xia M, Saylor CM, Narayan K, Kang J, Wiest DL, et al.** (2010) *Cutting edge: Intrinsic programming of thymic gammadeltaT cells for specific peripheral tissue localization*. J Immunol, 185(12):7156-60.
[56] **Chennupati V, Worbs T, Liu X, Malinarich FH, Schmitz S, Haas JD, et al.** (2010) *Intra- and intercompartmental movement of gammadelta T cells: intestinal intraepithelial and peripheral gammadelta T cells represent exclusive nonoverlapping populations with distinct migration characteristics*. J Immunol, 185(9):5160-8.
[57] **Edelblum KL, Shen L, Weber CR, Marchiando AM, Clay BS, Wang Y, et al.** (2012) *Dynamic migration of gammadelta intraepithelial lymphocytes requires occludin*. Proc Natl Acad Sci U S A, 109(18):7097-102.
[58] **Wurbel MA, Malissen M, Guy-Grand D, Meffre E, Nussenzweig MC, Richelme M, et al.** (2001) *Mice lacking the CCR9 CC-chemokine receptor show a mild impairment of early T- and B-cell development and a reduction in T-cell receptor gammadelta(+) gut intraepithelial lymphocytes*. Blood, 98(9):2626-32.
[59] **Garcia-Peydro M, De Yebenes VG, Toribio ML** (2003) *Sustained Notch1 signaling instructs the earliest human intrathymic precursors to adopt a gammadelta T-cell fate in fetal thymus organ culture*. Blood, 102(7):2444-51.
[60] **Van De Walle I, Waegemans E, De Medts J, De Smet G, De Smedt M, Snauwaert S, et al.** (2013) *Specific Notch receptor-ligand interactions control human TCR-alphabeta/gammadelta development by inducing differential Notch signal strength*. J Exp Med, 210(4):683-97.
[61] **De Rosa SC, Andrus JP, Perfetto SP, Mantovani JJ, Herzenberg LA, Herzenberg LA, et al.** (2004) *Ontogeny of gamma delta T cells in humans*. J Immunol, 172(3):1637-45.
[62] **Hein WR, Dudler L** (1993) *Divergent evolution of T cell repertoires: extensive diversity and developmentally regulated expression of the sheep gamma delta T cell receptor*. EMBO J, 12(2):715-24.
[63] **Holderness J, Hedges JF, Ramstead A, Jutila MA** (2013) *Comparative biology of gammadelta T cell function in humans, mice, and domestic animals*. Annu Rev Anim Biosci, 1:99-124.
[64] **Shekhar S, Milling S, Yang X** (2012) *Migration of gammadelta T cells in steady-state conditions*. Vet Immunol Immunopathol, 147(1-2):1-5.
[65] **Geginat J, Paroni M, Maglie S, Alfen JS, Kastirr I, Gruarin P, et al.** (2014) *Plasticity of human CD4 T cell subsets*. Front Immunol, 5:630.
[66] **Hayday AC** (2009) *Gammadelta T cells and the lymphoid stress-surveillance response*. Immunity, 31(2):184-96.
[67] **Bonneville M, O'brien RL, Born WK** (2010) *Gammadelta T cell effector functions: a blend of innate programming and acquired plasticity*. Nat Rev Immunol, 10(7):467-78.

[68] **Qin G, Mao H, Zheng J, Sia SF, Liu Y, Chan PL, et al.** (2009) *Phosphoantigen-expanded human gammadelta T cells display potent cytotoxicity against monocyte-derived macrophages infected with human and avian influenza viruses*. J Infect Dis, 200(6):858-65.

[69] **Dieli F, Troye-Blomberg M, Ivanyi J, Fournie JJ, Krensky AM, Bonneville M, et al.** (2001) *Granulysin-dependent killing of intracellular and extracellular Mycobacterium tuberculosis by Vgamma9/Vdelta2 T lymphocytes*. J Infect Dis, 184(8):1082-5.

[70] **Munk ME, Gatrill AJ, Kaufmann SH** (1990) *Target cell lysis and IL-2 secretion by gamma/delta T lymphocytes after activation with bacteria*. J Immunol, 145(8):2434-9.

[71] **Rincon-Orozco B, Kunzmann V, Wrobel P, Kabelitz D, Steinle A, Herrmann T** (2005) *Activation of Vγ9Vδ2 T Cells by NKG2D*. J Immunol, 175(4):2144-51.

[72] **Ansel KM, Ngo VN, Hyman PL, Luther SA, Forster R, Sedgwick JD, et al.** (2000) *A chemokine-driven positive feedback loop organizes lymphoid follicles*. Nature, 406(6793):309-14.

[73] **Brandes M, Willimann K, Moser B** (2005) *Professional antigen-presentation function by human gammadelta T Cells*. Science, 309(5732):264-8.

[74] **Chodaczek G, Papanna V, Zal MA, Zal T** (2012) *Body-barrier surveillance by epidermal gammadelta TCRs*. Nat Immunol, 13(3):272-82.

[75] **Strid J, Roberts SJ, Filler RB, Lewis JM, Kwong BY, Schpero W, et al.** (2008) *Acute upregulation of an NKG2D ligand promotes rapid reorganization of a local immune compartment with pleiotropic effects on carcinogenesis*. Nat Immunol, 9(2):146-54.

[76] **Latha TS, Reddy MC, Durbaka PV, Rachamallu A, Pallu R, Lomada D** (2014) *gammadelta T Cell-Mediated Immune Responses in Disease and Therapy*. Front Immunol, 5:571.

[77] **Martin B, Hirota K, Cua DJ, Stockinger B, Veldhoen M** (2009) *Interleukin-17-producing gammadelta T cells selectively expand in response to pathogen products and environmental signals*. Immunity, 31(2):321-30.

[78] **Su D, Shen M, Li X, Sun L** (2013) *Roles of gammadelta T cells in the pathogenesis of autoimmune diseases*. Clin Dev Immunol, 2013:985753.

[79] **Sutton CE, Lalor SJ, Sweeney CM, Brereton CF, Lavelle EC, Mills KH** (2009) *Interleukin-1 and IL-23 induce innate IL-17 production from gammadelta T cells, amplifying Th17 responses and autoimmunity*. Immunity, 31(2):331-41.

[80] **Lockhart E, Green AM, Flynn JL** (2006) *IL-17 production is dominated by gammadelta T cells rather than CD4 T cells during Mycobacterium tuberculosis infection*. J Immunol, 177(7):4662-9.

[81] **Girardi M, Oppenheim DE, Steele CR, Lewis JM, Glusac E, Filler R, et al.** (2001) *Regulation of cutaneous malignancy by gammadelta T cells*. Science, 294(5542):605-9.

[82] **Gao Y, Yang W, Pan M, Scully E, Girardi M, Augenlicht LH, et al.** (2003) *Gamma delta T cells provide an early source of interferon gamma in tumor immunity*. J Exp Med, 198(3):433-42.

[83] **Lanca T, Costa MF, Goncalves-Sousa N, Rei M, Grosso AR, Penido C, et al.** (2013) *Protective role of the inflammatory CCR2/CCL2 chemokine pathway through recruitment of type 1 cytotoxic gammadelta T lymphocytes to tumor beds*. J Immunol, 190(12):6673-80.

[84] **Silva-Santos B, Serre K, Norell H** (2015) *gammadelta T cells in cancer*. Nat Rev Immunol, 15(11):683-91.

[85] **Zou C, Zhao P, Xiao Z, Han X, Fu F, Fu L** (2017) *γδ T cells in cancer immunotherapy*. Oncotarget, 8(5):8900-9.

[86] **Rei M, Pennington DJ, Silva-Santos B** (2015) *The emerging Protumor role of gammadelta T lymphocytes: implications for cancer immunotherapy*. Cancer Res, 75(5):798-802.

[87] **Lawand M, Dechanet-Merville J, Dieu-Nosjean MC** (2017) *Key Features of Gamma-Delta T-Cell Subsets in Human Diseases and Their Immunotherapeutic Implications*. Front Immunol, 8:761.

[88] **Ribot JC, Debarros A, Pang DJ, Neves JF, Peperzak V, Roberts SJ, et al.** (2009) *CD27 is a thymic determinant of the balance between interferon-gamma- and interleukin 17-producing gammadelta T cell subsets*. Nat Immunol, 10(4):427-36.

[89] **Turchinovich G, Pennington DJ** (2011) *T cell receptor signalling in gammadelta cell development: strength isn't everything*. Trends Immunol, 32(12):567-73.

[90] **Jensen KD, Su X, Shin S, Li L, Youssef S, Yamasaki S, et al.** (2008) *Thymic selection determines gammadelta T cell effector fate: antigen-naive cells make interleukin-17 and antigen-experienced cells make interferon gamma*. Immunity, 29(1):90-100.

[91] **Ribot JC, Ribeiro ST, Correia DV, Sousa AE, Silva-Santos B** (2014) *Human gammadelta thymocytes are functionally immature and differentiate into cytotoxic type 1 effector T cells upon IL-2/IL-15 signaling*. J Immunol, 192(5):2237-43.

[92] **Dieli F, Poccia F, Lipp M, Sireci G, Caccamo N, Di Sano C, et al.** (2003) *Differentiation of effector/memory Vdelta2 T cells and migratory routes in lymph nodes or inflammatory sites*. J Exp Med, 198(3):391-7.
[93] **Lieber MR** (1991) *Site-specific recombination in the immune system*. FASEB J, 5(14):2934-44.
[94] **Arstila TP, Casrouge A, Baron V, Even J, Kanellopoulos J, Kourilsky P** (1999) *A direct estimate of the human alphabeta T cell receptor diversity*. Science, 286(5441):958-61.
[95] **Davis MM** (1990) *T cell receptor gene diversity and selection*. Annu Rev Biochem, 59:475-96.
[96] **Davis MM, Bjorkman PJ** (1988) *T-cell antigen receptor genes and T-cell recognition*. Nature, 334(6181):395-402.
[97] **Laydon DJ, Bangham CR, Asquith B** (2015) *Estimating T-cell repertoire diversity: limitations of classical estimators and a new approach*. Philos Trans R Soc Lond B Biol Sci, 370(1675).
[98] **Godfrey DI, Uldrich AP, Mccluskey J, Rossjohn J, Moody DB** (2015) *The burgeoning family of unconventional T cells*. Nat Immunol, 16(11):1114-23.
[99] **Kasmar AG, Van Rhijn I, Magalhaes KG, Young DC, Cheng TY, Turner MT, et al.** (2013) *Cutting Edge: CD1a tetramers and dextramers identify human lipopeptide-specific T cells ex vivo*. J Immunol, 191(9):4499-503.
[100] **Kasmar AG, Van Rhijn I, Cheng TY, Turner M, Seshadri C, Schiefner A, et al.** (2011) *CD1b tetramers bind alphabeta T cell receptors to identify a mycobacterial glycolipid-reactive T cell repertoire in humans*. J Exp Med, 208(9):1741-7.
[101] **Ly D, Kasmar AG, Cheng TY, De Jong A, Huang S, Roy S, et al.** (2013) *CD1c tetramers detect ex vivo T cell responses to processed phosphomycoketide antigens*. J Exp Med, 210(4):729-41.
[102] **De Lalla C, Lepore M, Piccolo FM, Rinaldi A, Scelfo A, Garavaglia C, et al.** (2011) *High-frequency and adaptive-like dynamics of human CD1 self-reactive T cells*. Eur J Immunol, 41(3):602-10.
[103] **Bourgeois EA, Subramaniam S, Cheng TY, De Jong A, Layre E, Ly D, et al.** (2015) *Bee venom processes human skin lipids for presentation by CD1a*. J Exp Med, 212(2):149-63.
[104] **De Jong A, Pena-Cruz V, Cheng TY, Clark RA, Van Rhijn I, Moody DB** (2010) *CD1a-autoreactive T cells are a normal component of the human alphabeta T cell repertoire*. Nat Immunol, 11(12):1102-9.
[105] **De Jong A, Cheng TY, Huang S, Gras S, Birkinshaw RW, Kasmar AG, et al.** (2014) *CD1a-autoreactive T cells recognize natural skin oils that function as headless antigens*. Nat Immunol, 15(2):177-85.
[106] **Treiner E, Duban L, Bahram S, Radosavljevic M, Wanner V, Tilloy F, et al.** (2003) *Selection of evolutionarily conserved mucosal-associated invariant T cells by MR1*. Nature, 422(6928):164-9.
[107] **Ussher JE, Klenerman P, Willberg CB** (2014) *Mucosal-associated invariant T-cells: new players in anti-bacterial immunity*. Front Immunol, 5:450.
[108] **Eckle SB, Birkinshaw RW, Kostenko L, Corbett AJ, Mcwilliam HE, Reantragoon R, et al.** (2014) *A molecular basis underpinning the T cell receptor heterogeneity of mucosal-associated invariant T cells*. J Exp Med, 211(8):1585-600.
[109] **Kjer-Nielsen L, Patel O, Corbett AJ, Le Nours J, Meehan B, Liu L, et al.** (2012) *MR1 presents microbial vitamin B metabolites to MAIT cells*. Nature, 491(7426):717-23.
[110] **Patel O, Kjer-Nielsen L, Le Nours J, Eckle SB, Birkinshaw R, Beddoe T, et al.** (2013) *Recognition of vitamin B metabolites by mucosal-associated invariant T cells*. Nat Commun, 4:2142.
[111] **Corbett AJ, Eckle SB, Birkinshaw RW, Liu L, Patel O, Mahony J, et al.** (2014) *T-cell activation by transitory neo-antigens derived from distinct microbial pathways*. Nature, 509(7500):361-5.
[112] **Rahimpour A, Koay HF, Enders A, Clanchy R, Eckle SB, Meehan B, et al.** (2015) *Identification of phenotypically and functionally heterogeneous mouse mucosal-associated invariant T cells using MR1 tetramers*. J Exp Med, 212(7):1095-108.
[113] **Dusseaux M, Martin E, Serriari N, Peguillet I, Premel V, Louis D, et al.** (2011) *Human MAIT cells are xenobiotic-resistant, tissue-targeted, CD161hi IL-17-secreting T cells*. Blood, 117(4):1250-9.
[114] **Le Bourhis L, Martin E, Peguillet I, Guihot A, Froux N, Core M, et al.** (2010) *Antimicrobial activity of mucosal-associated invariant T cells*. Nat Immunol, 11(8):701-8.
[115] **Gold MC, Cerri S, Smyk-Pearson S, Cansler ME, Vogt TM, Delepine J, et al.** (2010) *Human mucosal associated invariant T cells detect bacterially infected cells*. PLoS Biol, 8(6):e1000407.
[116] **Budd RC, Miescher GC, Howe RC, Lees RK, Bron C, Macdonald HR** (1987) *Developmentally regulated expression of T cell receptor beta chain variable domains in immature thymocytes*. J Exp Med, 166(2):577-82.

[117] **Fowlkes BJ, Kruisbeek AM, Ton-That H, Weston MA, Coligan JE, Schwartz RH, et al.** (1987) *A novel population of T-cell receptor αβ-bearing thymocytes which predominantly expresses a single Vβ gene family*. Nature, 329:251.
[118] **Makino Y, Kanno R, Ito T, Higashino K, Taniguchi M** (1995) *Predominant expression of invariant V alpha 14+ TCR alpha chain in NK1.1+ T cell populations*. Int Immunol, 7(7):1157-61.
[119] **Sykes M** (1990) *Unusual T cell populations in adult murine bone marrow. Prevalence of CD3+CD4-CD8- and alpha beta TCR+NK1.1+ cells*. J Immunol, 145(10):3209-15.
[120] **Dasgupta S, Kumar V** (2016) *Type II NKT cells: a distinct CD1d-restricted immune regulatory NKT cell subset*. Immunogenetics, 68(8):665-76.
[121] **Godfrey DI, Macdonald HR, Kronenberg M, Smyth MJ, Van Kaer L** (2004) *NKT cells: what's in a name?* Nat Rev Immunol, 4(3):231-7.
[122] **Porcelli S, Yockey CE, Brenner MB, Balk SP** (1993) *Analysis of T cell antigen receptor (TCR) expression by human peripheral blood CD4-8- alpha/beta T cells demonstrates preferential use of several V beta genes and an invariant TCR alpha chain*. J Exp Med, 178(1):1-16.
[123] **Lantz O, Bendelac A** (1994) *An invariant T cell receptor alpha chain is used by a unique subset of major histocompatibility complex class I-specific CD4+ and CD4-8- T cells in mice and humans*. J Exp Med, 180(3):1097-106.
[124] **Dellabona P, Padovan E, Casorati G, Brockhaus M, Lanzavecchia A** (1994) *An invariant V alpha 24-J alpha Q/V beta 11 T cell receptor is expressed in all individuals by clonally expanded CD4-8- T cells*. J Exp Med, 180(3):1171-6.
[125] **Matsuura A, Kinebuchi M, Chen HZ, Katabami S, Shimizu T, Hashimoto Y, et al.** (2000) *NKT cells in the rat: organ-specific distribution of NK T cells expressing distinct V alpha 14 chains*. J Immunol, 164(6):3140-8.
[126] **Bendelac A, Savage PB, Teyton L** (2007) *The biology of NKT cells*. Annu Rev Immunol, 25:297-336.
[127] **Koseki H, Imai K, Nakayama F, Sado T, Moriwaki K, Taniguchi M** (1990) *Homogenous junctional sequence of the V14+ T-cell antigen receptor alpha chain expanded in unprimed mice*. Proc Natl Acad Sci U S A, 87(14):5248-52.
[128] **Paletta D**. The variability of the rat iNKT TCR. Würzburg: Julius-Maximilians-Universität Würzburg; 2015.
[129] **Gapin L** (2010) *iNKT cell autoreactivity: what is 'self' and how is it recognized?* Nat Rev Immunol, 10(4):272-7.
[130] **Matsuda JL, Gapin L, Fazilleau N, Warren K, Naidenko OV, Kronenberg M** (2001) *Natural killer T cells reactive to a single glycolipid exhibit a highly diverse T cell receptor beta repertoire and small clone size*. Proc Natl Acad Sci U S A, 98(22):12636-41.
[131] **Kawano T, Cui J, Koezuka Y, Toura I, Kaneko Y, Motoki K, et al.** (1997) *CD1d-restricted and TCR-mediated activation of valpha14 NKT cells by glycosylceramides*. Science, 278(5343):1626-9.
[132] **Godfrey DI, Stankovic S, Baxter AG** (2010) *Raising the NKT cell family*. Nat Immunol, 11(3):197-206.
[133] **Bendelac A, Lantz O, Quimby ME, Yewdell JW, Bennink JR, Brutkiewicz RR** (1995) *CD1 recognition by mouse NK1+ T lymphocytes*. Science, 268(5212):863-5.
[134] **Godfrey DI, Kronenberg M** (2004) *Going both ways: immune regulation via CD1d-dependent NKT cells*. J Clin Invest, 114(10):1379-88.
[135] **Brigl M, Brenner MB** (2010) *How invariant natural killer T cells respond to infection by recognizing microbial or endogenous lipid antigens*. Semin Immunol, 22(2):79-86.
[136] **Tupin E, Kinjo Y, Kronenberg M** (2007) *The unique role of natural killer T cells in the response to microorganisms*. Nat Rev Microbiol, 5(6):405-17.
[137] **Novak J, Lehuen A** (2011) *Mechanism of regulation of autoimmunity by iNKT cells*. Cytokine, 53(3):263-70.
[138] **Meyer EH, Dekruyff RH, Umetsu DT** (2007) *iNKT cells in allergic disease*. Curr Top Microbiol Immunol, 314:269-91.
[139] **Vivier E, Ugolini S, Blaise D, Chabannon C, Brossay L** (2012) *Targeting natural killer cells and natural killer T cells in cancer*. Nat Rev Immunol, 12(4):239-52.
[140] **Brennan PJ, Brigl M, Brenner MB** (2013) *Invariant natural killer T cells: an innate activation scheme linked to diverse effector functions*. Nat Rev Immunol, 13(2):101-17.
[141] **De Santo C, Salio M, Masri SH, Lee LY, Dong T, Speak AO, et al.** (2008) *Invariant NKT cells reduce the immunosuppressive activity of influenza A virus-induced myeloid-derived suppressor cells in mice and humans*. J Clin Invest, 118(12):4036-48.

[142] **Paget C, Ivanov S, Fontaine J, Blanc F, Pichavant M, Renneson J, et al.** (2011) *Potential role of invariant NKT cells in the control of pulmonary inflammation and CD8+ T cell response during acute influenza A virus H3N2 pneumonia*. J Immunol, 186(10):5590-602.
[143] **Ho L-P, Denney L, Luhn K, Teoh D, Clelland C, Mcmichael AJ** (2008) *Activation of invariant NKT cells enhances the innate immune response and improves the disease course in influenza A virus infection*. Eur J Immunol, 38(7):1913-22.
[144] **Guillonneau C, Mintern JD, Hubert F-X, Hurt AC, Besra GS, Porcelli S, et al.** (2009) *Combined NKT cell activation and influenza virus vaccination boosts memory CTL generation and protective immunity*. Proc Natl Acad Sci U S A, 106(9):3330-5.
[145] **Godfrey DI, Hammond KJ, Poulton LD, Smyth MJ, Baxter AG** (2000) *NKT cells: facts, functions and fallacies*. Immunol Today, 21(11):573-83.
[146] **Esteban LM, Tsoutsman T, Jordan MA, Roach D, Poulton LD, Brooks A, et al.** (2003) *Genetic control of NKT cell numbers maps to major diabetes and lupus loci*. J Immunol, 171(6):2873-8.
[147] **Lee PT, Putnam A, Benlagha K, Teyton L, Gottlieb PA, Bendelac A** (2002) *Testing the NKT cell hypothesis of human IDDM pathogenesis*. J Clin Invest, 110(6):793-800.
[148] **Monzon-Casanova E**. Rat iNKT Cells: Phenotype and Function [Doctoral thesis]. Würzburg: Julius-Maximilians-Universität Würzburg; 2010.
[149] **Monzon-Casanova E, Paletta D, Starick L, Muller I, Sant'angelo DB, Pyz E, et al.** (2013) *Direct identification of rat iNKT cells reveals remarkable similarities to human iNKT cells and a profound deficiency in LEW rats*. Eur J Immunol, 43(2):404-15.
[150] **Rocha-Campos AC, Melki R, Zhu R, Deruytter N, Damotte D, Dy M, et al.** (2006) *Genetic and functional analysis of the Nkt1 locus using congenic NOD mice: improved Valpha14-NKT cell performance but failure to protect against type 1 diabetes*. Diabetes, 55(4):1163-70.
[151] **Chen H, Huang H, Paul WE** (1997) *NK1.1+ CD4+ T cells lose NK1.1 expression upon in vitro activation*. J Immunol, 158(11):5112-9.
[152] **Matsuda JL, Naidenko OV, Gapin L, Nakayama T, Taniguchi M, Wang CR, et al.** (2000) *Tracking the response of natural killer T cells to a glycolipid antigen using CD1d tetramers*. J Exp Med, 192(5):741-54.
[153] **Gumperz JE, Miyake S, Yamamura T, Brenner MB** (2002) *Functionally distinct subsets of CD1d-restricted natural killer T cells revealed by CD1d tetramer staining*. J Exp Med, 195(5):625-36.
[154] **Benlagha K, Weiss A, Beavis A, Teyton L, Bendelac A** (2000) *In vivo identification of glycolipid antigen-specific T cells using fluorescent CD1d tetramers*. J Exp Med, 191(11):1895-903.
[155] **Schumann J, Voyle RB, Wei BY, Macdonald HR** (2003) *Cutting edge: influence of the TCR V beta domain on the avidity of CD1d:alpha-galactosylceramide binding by invariant V alpha 14 NKT cells*. J Immunol, 170(12):5815-9.
[156] **Pyz E, Naidenko O, Miyake S, Yamamura T, Berberich I, Cardell S, et al.** (2006) *The complementarity determining region 2 of BV8S2 (V beta 8.2) contributes to antigen recognition by rat invariant NKT cell TCR*. J Immunol, 176(12):7447-55.
[157] **Barral DC, Brenner MB** (2007) *CD1 antigen presentation: how it works*. Nat Rev Immunol, 7(12):929-41.
[158] **Mcmichael AJ, Pilch JR, Fabre JW, Mason DY, Galfré G, Milstein C** (1979) *A human thymocyte antigen defined by a hybrid myeloma monoclonal antibody*. Eur J Immunol, 9(3):205-10.
[159] **Calabi F, Milstein C** (1986) *A novel family of human major histocompatibility complex-related genes not mapping to chromosome 6*. Nature, 323:540.
[160] **Brigl M, Brenner MB** (2004) *CD1: Antigen Presentation and T Cell Function*. Annu Rev Immunol, 22(1):817-90.
[161] **Calabi F, Jarvis JM, Martin L, Milstein C** (1989) *Two classes of CD1 genes*. Eur J Immunol, 19(2):285-92.
[162] **Facciotti F, Cavallari M, Angénieux C, Garcia-Alles LF, Signorino-Gelo F, Angman L, et al.** (2011) *Fine tuning by human CD1e of lipid-specific immune responses*. Proc Natl Acad Sci U S A, 108(34):14228-33.
[163] **Bradbury A, Belt KT, Neri TM, Milstein C, Calabi F** (1988) *Mouse CD1 is distinct from and co-exists with TL in the same thymus*. EMBO J, 7(10):3081-6.
[164] **Kasmar A, Van Rhijn I, Moody DB** (2009) *The evolved functions of CD1 during infection*. Curr Opin Immunol, 21(4):397-403.
[165] **Ichimiya S, Kikuchi K, Matsuura A** (1994) *Structural analysis of the rat homologue of CD1. Evidence for evolutionary conservation of the CD1D class and widespread transcription by rat cells*. J Immunol, 153(3):1112-23.

[166] **Katabami S, Matsuura A, Chen HZ, Imai K, Kikuchi K** (1998) *Structural organization of rat CD1 typifies evolutionarily conserved CD1D class genes*. Immunogenetics, 48(1):22-31.
[167] **Zeng Z, Castano AR, Segelke BW, Stura EA, Peterson PA, Wilson IA** (1997) *Crystal structure of mouse CD1: An MHC-like fold with a large hydrophobic binding groove*. Science, 277(5324):339-45.
[168] **Moody DB, Zajonc DM, Wilson IA** (2005) *Anatomy of CD1–lipid antigen complexes*. Nat Rev Immunol, 5:387.
[169] **Fichtner AS, Paletta D, Starick L, Schumann RF, Niewiesk S, Herrmann T** (2015) *Function and expression of CD1d and invariant natural killer T-cell receptor in the cotton rat (Sigmodon hispidus)*. Immunology, 146(4):618-29.
[170] **Ly D, Moody DB** (2014) *The CD1 size problem: lipid antigens, ligands, and scaffolds*. Cell Mol Life Sci, 71(16):3069-79.
[171] **Rossjohn J, Pellicci DG, Patel O, Gapin L, Godfrey DI** (2012) *Recognition of CD1d-restricted antigens by natural killer T cells*. Nat Rev Immunol, 12(12):845-57.
[172] **De Silva AD, Park JJ, Matsuki N, Stanic AK, Brutkiewicz RR, Medof ME, et al.** (2002) *Lipid protein interactions: the assembly of CD1d1 with cellular phospholipids occurs in the endoplasmic reticulum*. J Immunol, 168(2):723-33.
[173] **Park J-J, Kang S-J, De Silva AD, Stanic AK, Casorati G, Hachey DL, et al.** (2004) *Lipid–protein interactions: Biosynthetic assembly of CD1 with lipids in the endoplasmic reticulum is evolutionarily conserved*. Proc Natl Acad Sci U S A, 101(4):1022-6.
[174] **Dougan SK, Salas A, Rava P, Agyemang A, Kaser A, Morrison J, et al.** (2005) *Microsomal triglyceride transfer protein lipidation and control of CD1d on antigen-presenting cells*. J Exp Med, 202(4):529-39.
[175] **Brozovic S, Nagaishi T, Yoshida M, Betz S, Salas A, Chen D, et al.** (2004) *CD1d function is regulated by microsomal triglyceride transfer protein*. Nat Med, 10(5):535-9.
[176] **Kang SJ, Cresswell P** (2002) *Calnexin, calreticulin, and ERp57 cooperate in disulfide bond formation in human CD1d heavy chain*. J Biol Chem, 277(47):44838-44.
[177] **Bauer A, Hüttinger R, Staffler G, Hansmann C, Schmidt W, Majdic O, et al.** (1997) *Analysis of the requirement for β2-microglobulin for expression and formation of human CD1 antigens*. Eur J Immunol, 27(6):1366-73.
[178] **Brutkiewicz RR, Bennink JR, Yewdell JW, Bendelac A** (1995) *TAP-independent, beta 2-microglobulin-dependent surface expression of functional mouse CD1.1*. J Exp Med, 182(6):1913-9.
[179] **Lawton AP, Prigozy TI, Brossay L, Pei B, Khurana A, Martin D, et al.** (2005) *The mouse CD1d cytoplasmic tail mediates CD1d trafficking and antigen presentation by adaptor protein 3-dependent and -independent mechanisms*. J Immunol, 174(6):3179-86.
[180] **Kang SJ, Cresswell P** (2004) *Saposins facilitate CD1d-restricted presentation of an exogenous lipid antigen to T cells*. Nat Immunol, 5(2):175-81.
[181] **Zhou D, Cantu C, 3rd, Sagiv Y, Schrantz N, Kulkarni AB, Qi X, et al.** (2004) *Editing of CD1d-bound lipid antigens by endosomal lipid transfer proteins*. Science, 303(5657):523-7.
[182] **Yuan W, Qi X, Tsang P, Kang S-J, Illarionov PA, Besra GS, et al.** (2007) *Saposin B is the dominant saposin that facilitates lipid binding to human CD1d molecules*. Proc Natl Acad Sci U S A, 104(13):5551-6.
[183] **Brossay L, Jullien D, Cardell S, Sydora BC, Burdin N, Modlin RL, et al.** (1997) *Mouse CD1 is mainly expressed on hemopoietic-derived cells*. J Immunol, 159(3):1216-24.
[184] **Roark JH, Park SH, Jayawardena J, Kavita U, Shannon M, Bendelac A** (1998) *CD1.1 expression by mouse antigen-presenting cells and marginal zone B cells*. J Immunol, 160(7):3121-7.
[185] **Bendelac A** (1995) *Positive selection of mouse NK1+ T cells by CD1-expressing cortical thymocytes*. J Exp Med, 182(6):2091-6.
[186] **Geissmann F, Cameron TO, Sidobre S, Manlongat N, Kronenberg M, Briskin MJ, et al.** (2005) *Intravascular immune surveillance by CXCR6+ NKT cells patrolling liver sinusoids*. PLoS Biol, 3(4):e113.
[187] **Liu Y, Goff RD, Zhou D, Mattner J, Sullivan BA, Khurana A, et al.** (2006) *A modified alpha-galactosyl ceramide for staining and stimulating natural killer T cells*. J Immunol Methods, 312(1-2):34-9.
[188] **Natori T, Morita M, Akimoto K, Koezuka Y** (1994) *Agelasphins, novel antitumor and immunostimulatory cerebrosides from the marine sponge Agelas mauritianus*. Tetrahedron, 50(9):2771-84.
[189] **Birkholz AM, Kronenberg M** (2015) *Antigen specificity of invariant natural killer T-cells*. Biomed J, 38(6):470-83.

[190] **Aspeslagh S, Li Y, Yu ED, Pauwels N, Trappeniers M, Girardi E, et al.** (2011) *Galactose-modified iNKT cell agonists stabilized by an induced fit of CD1d prevent tumour metastasis*. EMBO J, 30(11):2294-305.
[191] **Venkataswamy MM, Porcelli SA** (2010) *Lipid and glycolipid antigens of CD1d-restricted natural killer T cells*. Semin Immunol, 22(2):68-78.
[192] **Miyamoto K, Miyake S, Yamamura T** (2001) *A synthetic glycolipid prevents autoimmune encephalomyelitis by inducing TH2 bias of natural killer T cells*. Nature, 413:531.
[193] **Zhou D, Mattner J, Cantu C, 3rd, Schrantz N, Yin N, Gao Y, et al.** (2004) *Lysosomal glycosphingolipid recognition by NKT cells*. Science, 306(5702):1786-9.
[194] **Porubsky S, Speak AO, Luckow B, Cerundolo V, Platt FM, Grone HJ** (2007) *Normal development and function of invariant natural killer T cells in mice with isoglobotrihexosylceramide (iGb3) deficiency*. Proc Natl Acad Sci U S A, 104(14):5977-82.
[195] **Porubsky S, Speak AO, Salio M, Jennemann R, Bonrouhi M, Zafarulla R, et al.** (2012) *Globosides but Not Isoglobosides Can Impact the Development of Invariant NKT Cells and Their Interaction with Dendritic Cells*. J Immunol, 189(6):3007-17.
[196] **Godfrey DI, Mccluskey J, Rossjohn J** (2005) *CD1d antigen presentation: treats for NKT cells*. Nat Immunol, 6(8):754-6.
[197] **Koch M, Stronge VS, Shepherd D, Gadola SD, Mathew B, Ritter G, et al.** (2005) *The crystal structure of human CD1d with and without alpha-galactosylceramide*. Nat Immunol, 6(8):819-26.
[198] **Zajonc DM, Cantu C, 3rd, Mattner J, Zhou D, Savage PB, Bendelac A, et al.** (2005) *Structure and function of a potent agonist for the semi-invariant natural killer T cell receptor*. Nat Immunol, 6(8):810-8.
[199] **Pellicci DG, Patel O, Kjer-Nielsen L, Pang SS, Sullivan LC, Kyparissoudis K, et al.** (2009) *Differential recognition of CD1d-alpha-galactosyl ceramide by the V beta 8.2 and V beta 7 semi-invariant NKT T cell receptors*. Immunity, 31(1):47-59.
[200] **Mallevaey T, Selvanantham T** (2012) *Strategy of lipid recognition by invariant natural killer T cells: 'one for all and all for one'*. Immunology, 136(3):273-82.
[201] **Borg NA, Wun KS, Kjer-Nielsen L, Wilce MC, Pellicci DG, Koh R, et al.** (2007) *CD1d-lipid-antigen recognition by the semi-invariant NKT T-cell receptor*. Nature, 448(7149):44-9.
[202] **Patel O, Pellicci DG, Uldrich AP, Sullivan LC, Bhati M, Mcknight M, et al.** (2011) *Vbeta2 natural killer T cell antigen receptor-mediated recognition of CD1d-glycolipid antigen*. Proc Natl Acad Sci U S A, 108(47):19007-12.
[203] **Benlagha K, Wei DG, Veiga J, Teyton L, Bendelac A** (2005) *Characterization of the early stages of thymic NKT cell development*. J Exp Med, 202(4):485-92.
[204] **Gapin L, Matsuda JL, Surh CD, Kronenberg M** (2001) *NKT cells derive from double-positive thymocytes that are positively selected by CD1d*. Nat Immunol, 2(10):971-8.
[205] **Dashtsoodol N, Shigeura T, Aihara M, Ozawa R, Kojo S, Harada M, et al.** (2017) *Alternative pathway for the development of Valpha14(+) NKT cells directly from CD4(-)CD8(-) thymocytes that bypasses the CD4(+)CD8(+) stage*. Nat Immunol, 18(3):274-82.
[206] **Guo J, Hawwari A, Li H, Sun Z, Mahanta SK, Littman DR, et al.** (2002) *Regulation of the TCRalpha repertoire by the survival window of CD4(+)CD8(+) thymocytes*. Nat Immunol, 3(5):469-76.
[207] **Stanic AK, De Silva AD, Park JJ, Sriram V, Ichikawa S, Hirabyashi Y, et al.** (2003) *Defective presentation of the CD1d1-restricted natural Va14Ja18 NKT lymphocyte antigen caused by beta-D-glucosylceramide synthase deficiency*. Proc Natl Acad Sci U S A, 100(4):1849-54.
[208] **Brennan PJ, Tatituri RV, Brigl M, Kim EY, Tuli A, Sanderson JP, et al.** (2011) *Invariant natural killer T cells recognize lipid self antigen induced by microbial danger signals*. Nat Immunol, 12(12):1202-11.
[209] **Pei B, Speak AO, Shepherd D, Butters T, Cerundolo V, Platt FM, et al.** (2011) *Diverse endogenous antigens for mouse NKT cells: self-antigens that are not glycosphingolipids*. J Immunol, 186(3):1348-60.
[210] **Fox LM, Cox DG, Lockridge JL, Wang X, Chen X, Scharf L, et al.** (2009) *Recognition of lyso-phospholipids by human natural killer T lymphocytes*. PLoS Biol, 7(10):e1000228.
[211] **Facciotti F, Ramanjaneyulu GS, Lepore M, Sansano S, Cavallari M, Kistowska M, et al.** (2012) *Peroxisome-derived lipids are self antigens that stimulate invariant natural killer T cells in the thymus*. Nat Immunol, 13(5):474-80.
[212] **Kain L, Webb B, Anderson BL, Deng S, Holt M, Costanzo A, et al.** (2014) *The identification of the endogenous ligands of natural killer T cells reveals the presence of mammalian alpha-linked glycosylceramides*. Immunity, 41(4):543-54.

[213] **Chung B, Aoukaty A, Dutz J, Terhorst C, Tan R** (2005) *Signaling lymphocytic activation molecule-associated protein controls NKT cell functions*. J Immunol, 174(6):3153-7.
[214] **Griewank K, Borowski C, Rietdijk S, Wang N, Julien A, Wei DG, et al.** (2007) *Homotypic interactions mediated by Slamf1 and Slamf6 receptors control NKT cell lineage development*. Immunity, 27(5):751-62.
[215] **Nichols KE, Hom J, Gong SY, Ganguly A, Ma CS, Cannons JL, et al.** (2005) *Regulation of NKT cell development by SAP, the protein defective in XLP*. Nat Med, 11(3):340-5.
[216] **Pasquier B, Yin L, Fondaneche MC, Relouzat F, Bloch-Queyrat C, Lambert N, et al.** (2005) *Defective NKT cell development in mice and humans lacking the adapter SAP, the X-linked lymphoproliferative syndrome gene product*. J Exp Med, 201(5):695-701.
[217] **Chun T, Page MJ, Gapin L, Matsuda JL, Xu H, Nguyen H, et al.** (2003) *CD1d-expressing dendritic cells but not thymic epithelial cells can mediate negative selection of NKT cells*. J Exp Med, 197(7):907-18.
[218] **Pellicci DG, Uldrich AP, Kyparissoudis K, Crowe NY, Brooks AG, Hammond KJ, et al.** (2003) *Intrathymic NKT cell development is blocked by the presence of alpha-galactosylceramide*. Eur J Immunol, 33(7):1816-23.
[219] **Bedel R, Berry R, Mallevaey T, Matsuda JL, Zhang J, Godfrey DI, et al.** (2014) *Effective functional maturation of invariant natural killer T cells is constrained by negative selection and T-cell antigen receptor affinity*. Proc Natl Acad Sci U S A, 111(1):E119-28.
[220] **Savage AK, Constantinides MG, Han J, Picard D, Martin E, Li B, et al.** (2008) *The transcription factor PLZF directs the effector program of the NKT cell lineage*. Immunity, 29(3):391-403.
[221] **Benlagha K, Kyin T, Beavis A, Teyton L, Bendelac A** (2002) *A thymic precursor to the NK T cell lineage*. Science, 296(5567):553-5.
[222] **Hammond KJ, Pellicci DG, Poulton LD, Naidenko OV, Scalzo AA, Baxter AG, et al.** (2001) *CD1d-restricted NKT cells: an interstrain comparison*. J Immunol, 167(3):1164-73.
[223] **Van Kaer L** (2007) *NKT cells: T lymphocytes with innate effector functions*. Curr Opin Immunol, 19(3):354-64.
[224] **Park SH, Benlagha K, Lee D, Balish E, Bendelac A** (2000) *Unaltered phenotype, tissue distribution and function of Valpha14(+) NKT cells in germ-free mice*. Eur J Immunol, 30(2):620-5.
[225] **Reilly EC, Wands JR, Brossay L** (2010) *Cytokine dependent and independent iNKT cell activation*. Cytokine, 51(3):227-31.
[226] **Matsuda JL, Gapin L, Baron JL, Sidobre S, Stetson DB, Mohrs M, et al.** (2003) *Mouse V alpha 14i natural killer T cells are resistant to cytokine polarization in vivo*. Proc Natl Acad Sci U S A, 100(14):8395-400.
[227] **Mattner J, Debord KL, Ismail N, Goff RD, Cantu C, 3rd, Zhou D, et al.** (2005) *Exogenous and endogenous glycolipid antigens activate NKT cells during microbial infections*. Nature, 434(7032):525-9.
[228] **Paget C, Mallevaey T, Speak AO, Torres D, Fontaine J, Sheehan KC, et al.** (2007) *Activation of invariant NKT cells by toll-like receptor 9-stimulated dendritic cells requires type I interferon and charged glycosphingolipids*. Immunity, 27(4):597-609.
[229] **Leite-De-Moraes MC, Hameg A, Arnould A, Machavoine F, Koezuka Y, Schneider E, et al.** (1999) *A distinct IL-18-induced pathway to fully activate NK T lymphocytes independently from TCR engagement*. J Immunol, 163(11):5871-6.
[230] **Park SH, Kyin T, Bendelac A, Carnaud C** (2003) *The contribution of NKT cells, NK cells, and other gamma-chain-dependent non-T non-B cells to IL-12-mediated rejection of tumors*. J Immunol, 170(3):1197-201.
[231] **Eberl G, Macdonald HR** (1998) *Rapid death and regeneration of NKT cells in anti-CD3epsilon- or IL-12-treated mice: a major role for bone marrow in NKT cell homeostasis*. Immunity, 9(3):345-53.
[232] **Niewiesk S, Prince G** (2002) *Diversifying animal models: the use of hispid cotton rats (Sigmodon hispidus) in infectious diseases*. Lab Anim, 36(4):357-72.
[233] **Faith RE, Montgomery CA, Durfee WJ, Aguilar-Cordova E, Wyde PR** (1997) *The cotton rat in biomedical research*. Lab Anim Sci, 47(4):337-45.
[234] **Boukhvalova MS, Prince GA, Blanco JC** (2009) *The cotton rat model of respiratory viral infections*. Biologicals, 37(3):152-9.
[235] **Green MG, Huey D, Niewiesk S** (2013) *The cotton rat (Sigmodon hispidus) as an animal model for respiratory tract infections with human pathogens*. Lab Anim, 42(5):170-6.
[236] **Borst J, Wicherink A, Van Dongen JJ, De Vries E, Comans-Bitter WM, Wassenaar F, et al.** (1989) *Non-random expression of T cell receptor gamma and delta variable gene segments in functional T lymphocyte clones from human peripheral blood*. Eur J Immunol, 19(9):1559-68.

[237] **Casorati G, De Libero G, Lanzavecchia A, Migone N** (1989) *Molecular analysis of human gamma/delta+ clones from thymus and peripheral blood*. J Exp Med, 170(5):1521-35.
[238] **Kabelitz D, He W** (2012) *The multifunctionality of human Vgamma9Vdelta2 gammadelta T cells: clonal plasticity or distinct subsets?* Scand J Immunol, 76(3):213-22.
[239] **Delfau M-H, Hance AJ, Lecossier D, Vilmer E, Grandchamp B** (1992) *Restricted diversity of Vγ9-JP rearrangements in unstimulated human γ/δ T lymphocytes*. Eur J Immunol, 22(9):2437-43.
[240] **Pauza CD, Cairo C** (2015) *Evolution and function of the TCR Vgamma9 chain repertoire: It's good to be public*. Cell Immunol, 296(1):22-30.
[241] **Wang H, Fang Z, Morita CT** (2010) *Vgamma2Vdelta2 T Cell Receptor recognition of prenyl pyrophosphates is dependent on all CDRs*. J Immunol, 184(11):6209-22.
[242] **Bukowski JF, Morita CT, Band H, Brenner MB** (1998) *Crucial Role of TCRγ Chain Junctional Region in Prenyl Pyrophosphate Antigen Recognition by γδ T Cells*. J Immunol, 161(1):286-93.
[243] **Fournie JJ, Bonneville M** (1996) *Stimulation of gamma delta T cells by phosphoantigens*. Res Immunol, 147(5):338-47.
[244] **Compte E, Pontarotti P, Collette Y, Lopez M, Olive D** (2004) *Frontline: Characterization of BT3 molecules belonging to the B7 family expressed on immune cells*. Eur J Immunol, 34(8):2089-99.
[245] **Allison TJ, Winter CC, Fournie JJ, Bonneville M, Garboczi DN** (2001) *Structure of a human gammadelta T-cell antigen receptor*. Nature, 411(6839):820-4.
[246] **Miyagawa F, Tanaka Y, Yamashita S, Mikami B, Danno K, Uehara M, et al.** (2001) *Essential contribution of germline-encoded lysine residues in Jgamma1.2 segment to the recognition of nonpeptide antigens by human gammadelta T cells*. J Immunol, 167(12):6773-9.
[247] **Yamashita S, Tanaka Y, Harazaki M, Mikami B, Minato N** (2003) *Recognition mechanism of non-peptide antigens by human gammadelta T cells*. Int Immunol, 15(11):1301-7.
[248] **Evans PS, Enders PJ, Yin C, Ruckwardt TJ, Malkovsky M, Pauza CD** (2001) *In vitro stimulation with a non-peptidic alkylphosphate expands cells expressing Vgamma2-Jgamma1.2/Vdelta2 T-cell receptors*. Immunology, 104(1):19-27.
[249] **Morita CT, Beckman EM, Bukowski JF, Tanaka Y, Band H, Bloom BR, et al.** (1995) *Direct presentation of nonpeptide prenyl pyrophosphate antigens to human gamma delta T cells*. Immunity, 3(4):495-507.
[250] **Lang F, Peyrat MA, Constant P, Davodeau F, David-Ameline J, Poquet Y, et al.** (1995) *Early activation of human V gamma 9V delta 2 T cell broad cytotoxicity and TNF production by nonpeptidic mycobacterial ligands*. J Immunol, 154(11):5986-94.
[251] **De Libero G** (1999) *Control of gammadelta T cells by NK receptors*. Microbes Infect, 1(3):263-7.
[252] **Moris A, Rothenfusser S, Meuer E, Hangretinger R, Fisch P** (1999) *Role of gammadelta T cells in tumor immunity and their control by NK receptors*. Microbes Infect, 1(3):227-34.
[253] **Ribot JC, Debarros A, Silva-Santos B** (2011) *Searching for "signal 2": costimulation requirements of gammadelta T cells*. Cell Mol Life Sci, 68(14):2345-55.
[254] **Panchamoorthy G, Mclean J, Modlin RL, Morita CT, Ishikawa S, Brenner MB, et al.** (1991) *A predominance of the T cell receptor V gamma 2/V delta 2 subset in human mycobacteria-responsive T cells suggests germline gene encoded recognition*. J Immunol, 147(10):3360-9.
[255] **Huang D, Chen CY, Zhang M, Qiu L, Shen Y, Du G, et al.** (2012) *Clonal immune responses of Mycobacterium-specific gammadelta T cells in tuberculous and non-tuberculous tissues during M. tuberculosis infection*. PLoS One, 7(2):e30631.
[256] **Qaqish A, Huang D, Chen CY, Zhang Z, Wang R, Li S, et al.** (2017) *Adoptive Transfer of Phosphoantigen-Specific gammadelta T Cell Subset Attenuates Mycobacterium tuberculosis Infection in Nonhuman Primates*. J Immunol, 198(12):4753-63.
[257] **Shen Y, Zhou D, Qiu L, Lai X, Simon M, Shen L, et al.** (2002) *Adaptive immune response of Vgamma2Vdelta2+ T cells during mycobacterial infections*. Science, 295(5563):2255-8.
[258] **Li B, Rossman MD, Imir T, Oner-Eyuboglu AF, Lee CW, Biancaniello R, et al.** (1996) *Disease-specific changes in gammadelta T cell repertoire and function in patients with pulmonary tuberculosis*. J Immunol, 157(9):4222-9.
[259] **Janis EM, Kaufmann SH, Schwartz RH, Pardoll DM** (1989) *Activation of gamma delta T cells in the primary immune response to Mycobacterium tuberculosis*. Science, 244(4905):713-6.
[260] **Modlin RL, Pirmez C, Hofman FM, Torigian V, Uyemura K, Rea TH, et al.** (1989) *Lymphocytes bearing antigen-specific gamma delta T-cell receptors accumulate in human infectious disease lesions*. Nature, 339(6225):544-8.
[261] **Ryan-Payseur B, Frencher J, Shen L, Chen CY, Huang D, Chen ZW** (2012) *Multieffector-functional immune responses of HMBPP-specific Vgamma2Vdelta2 T cells in nonhuman primates inoculated with Listeria monocytogenes DeltaactA prfA**. J Immunol, 189(3):1285-93.

[262] **Ho M, Webster HK, Tongtawe P, Pattanapanyasat K, Weidanz WP** (1990) *Increased gamma delta T cells in acute Plasmodium falciparum malaria*. Immunol Lett, 25(1-3):139-41.
[263] **De Paoli P, Basaglia G, Gennari D, Crovatto M, Modolo ML, Santini G** (1992) *Phenotypic profile and functional characteristics of human gamma and delta T cells during acute toxoplasmosis*. J Clin Microbiol, 30(3):729-31.
[264] **Wucherpfennig KW, Newcombe J, Li H, Keddy C, Cuzner ML, Hafler DA** (1992) *Gamma delta T-cell receptor repertoire in acute multiple sclerosis lesions*. Proc Natl Acad Sci U S A, 89(10):4588-92.
[265] **Andreu JL, Trujillo A, Alonso JM, Mulero J, Martinez C** (1991) *Selective expansion of T cells bearing the gamma/delta receptor and expressing an unusual repertoire in the synovial membrane of patients with rheumatoid arthritis*. Arthritis Rheum, 34(7):808-14.
[266] **Holoshitz J, Koning F, Coligan JE, De Bruyn J, Strober S** (1989) *Isolation of CD4- CD8- mycobacteria-reactive T lymphocyte clones from rheumatoid arthritis synovial fluid*. Nature, 339(6221):226-9.
[267] **Karunakaran MM, Herrmann T** (2014) *The Vgamma9Vdelta2 T Cell Antigen Receptor and Butyrophilin-3 A1: Models of Interaction, the Possibility of Co-Evolution, and the Case of Dendritic Epidermal T Cells*. Front Immunol, 5:648.
[268] **Pont F, Familiades J, Dejean S, Fruchon S, Cendron D, Poupot M, et al.** (2012) *The gene expression profile of phosphoantigen-specific human gammadelta T lymphocytes is a blend of alphabeta T-cell and NK-cell signatures*. Eur J Immunol, 42(1):228-40.
[269] **Caccamo N, La Mendola C, Orlando V, Meraviglia S, Todaro M, Stassi G, et al.** (2011) *Differentiation, phenotype, and function of interleukin-17-producing human Vgamma9Vdelta2 T cells*. Blood, 118(1):129-38.
[270] **Casetti R, Agrati C, Wallace M, Sacchi A, Martini F, Martino A, et al.** (2009) *Cutting edge: TGF-beta1 and IL-15 Induce FOXP3+ gammadelta regulatory T cells in the presence of antigen stimulation*. J Immunol, 183(6):3574-7.
[271] **Wesch D, Glatzel A, Kabelitz D** (2001) *Differentiation of resting human peripheral blood gamma delta T cells toward Th1- or Th2-phenotype*. Cell Immunol, 212(2):110-7.
[272] **Zheng J, Liu Y, Lau Y-L, Tu W** (2012) *γδ-T cells: an unpolished sword in human anti-infection immunity*. Cell Mol Immunol, 10:50.
[273] **Harly C, Peigne CM, Scotet E** (2014) *Molecules and Mechanisms Implicated in the Peculiar Antigenic Activation Process of Human Vgamma9Vdelta2 T Cells*. Front Immunol, 5:657.
[274] **Morita CT, Mariuzza RA, Brenner MB** (2000) *Antigen recognition by human gamma delta T cells: pattern recognition by the adaptive immune system*. Springer Semin Immunopathol, 22(3):191-217.
[275] **Brandes M, Willimann K, Lang AB, Nam KH, Jin C, Brenner MB, et al.** (2003) *Flexible migration program regulates gamma delta T-cell involvement in humoral immunity*. Blood, 102(10):3693-701.
[276] **Scotet E, Nedellec S, Devilder MC, Allain S, Bonneville M** (2008) *Bridging innate and adaptive immunity through gammadelta T-dendritic cell crosstalk*. Front Biosci, 13:6872-85.
[277] **Nussbaumer O, Gruenbacher G, Gander H, Thurnher M** (2011) *DC-like cell-dependent activation of human natural killer cells by the bisphosphonate zoledronic acid is regulated by gammadelta T lymphocytes*. Blood, 118(10):2743-51.
[278] **Eberl M, Moser B** (2009) *Monocytes and gammadelta T cells: close encounters in microbial infection*. Trends Immunol, 30(12):562-8.
[279] **Fournie JJ, Sicard H, Poupot M, Bezombes C, Blanc A, Romagne F, et al.** (2013) *What lessons can be learned from gammadelta T cell-based cancer immunotherapy trials?* Cell Mol Immunol, 10(1):35-41.
[280] **Fisher JPH, Heuijerjans J, Yan M, Gustafsson K, Anderson J** (2014) *γδ T cells for cancer immunotherapy: A systematic review of clinical trials*. Oncoimmunology, 3:e27572.
[281] **Tanaka Y, Sano S, Nieves E, De Libero G, Rosa D, Modlin RL, et al.** (1994) *Nonpeptide ligands for human gamma delta T cells*. Proc Natl Acad Sci U S A, 91(17):8175-9.
[282] **Gober HJ, Kistowska M, Angman L, Jeno P, Mori L, De Libero G** (2003) *Human T cell receptor gammadelta cells recognize endogenous mevalonate metabolites in tumor cells*. J Exp Med, 197(2):163-8.
[283] **Tanaka Y, Morita CT, Tanaka Y, Nieves E, Brenner MB, Bloom BR** (1995) *Natural and synthetic non-peptide antigens recognized by human gamma delta T cells*. Nature, 375(6527):155-8.
[284] **Kuzuyama T** (2002) *Mevalonate and nonmevalonate pathways for the biosynthesis of isoprene units*. Biosci Biotechnol Biochem, 66(8):1619-27.

[285] **Kohler S, Delwiche CF, Denny PW, Tilney LG, Webster P, Wilson RJ, et al.** (1997) *A plastid of probable green algal origin in Apicomplexan parasites*. Science, 275(5305):1485-9.
[286] **Thompson K, Rogers MJ** (2004) *Statins Prevent Bisphosphonate-Induced γ,δ-T-Cell Proliferation and Activation In Vitro*. J Bone Miner Res, 19(2):278-88.
[287] **Eberl M, Hintz M, Reichenberg A, Kollas AK, Wiesner J, Jomaa H** (2003) *Microbial isoprenoid biosynthesis and human gammadelta T cell activation*. FEBS Lett, 544(1-3):4-10.
[288] **Begley M, Gahan CG, Kollas AK, Hintz M, Hill C, Jomaa H, et al.** (2004) *The interplay between classical and alternative isoprenoid biosynthesis controls gammadelta T cell bioactivity of Listeria monocytogenes*. FEBS Lett, 561(1-3):99-104.
[289] **Hamano Y, Dairi T, Yamamoto M, Kuzuyama T, Itoh N, Seto H** (2002) *Growth-phase dependent expression of the mevalonate pathway in a terpenoid antibiotic-producing Streptomyces strain*. Biosci Biotechnol Biochem, 66(4):808-19.
[290] **Kuzuyama T, Takagi M, Takahashi S, Seto H** (2000) *Cloning and characterization of 1-deoxy-D-xylulose 5-phosphate synthase from Streptomyces sp. Strain CL190, which uses both the mevalonate and nonmevalonate pathways for isopentenyl diphosphate biosynthesis*. J Bacteriol, 182(4):891-7.
[291] **Zhang Y, Song Y, Yin F, Broderick E, Siegel K, Goddard A, et al.** (2006) *Structural studies of Vgamma2Vdelta2 T cell phosphoantigens*. Chem Biol, 13(9):985-92.
[292] **Espinosa E, Belmant C, Sicard H, Poupot R, Bonneville M, Fournie JJ** (2001) *Y2K+1 state-of-the-art on non-peptide phosphoantigens, a novel category of immunostimulatory molecules*. Microbes Infect, 3(8):645-54.
[293] **Reichenberg A, Hintz M, Kletschek Y, Kuhl T, Haug C, Engel R, et al.** (2003) *Replacing the pyrophosphate group of HMB-PP by a diphosphonate function abrogates Its potential to activate human gammadelta T cells but does not lead to competitive antagonism*. Bioorg Med Chem Lett, 13(7):1257-60.
[294] **Rhodes DA, Stammers M, Malcherek G, Beck S, Trowsdale J** (2001) *The cluster of BTN genes in the extended major histocompatibility complex*. Genomics, 71(3):351-62.
[295] **Henry J, Miller MM, Pontarotti P** (1999) *Structure and evolution of the extended B7 family*. Immunol Today, 20(6):285-8.
[296] **Rhodes DA, Reith W, Trowsdale J** (2016) *Regulation of Immunity by Butyrophilins*. Annu Rev Immunol, 34:151-72.
[297] **Rhodes DA, De Bono B, Trowsdale J** (2005) *Relationship between SPRY and B30.2 protein domains. Evolution of a component of immune defence?* Immunology, 116(4):411-7.
[298] **Afrache H, Pontarotti P, Abi-Rached L, Olive D** (2017) *Evolutionary and polymorphism analyses reveal the central role of BTN3A2 in the concerted evolution of the BTN3 gene family*. Immunogenetics, 69(6):379-90.
[299] **Abeler-Dorner L, Swamy M, Williams G, Hayday AC, Bas A** (2012) *Butyrophilins: an emerging family of immune regulators*. Trends Immunol, 33(1):34-41.
[300] **Afrache H, Gouret P, Ainouche S, Pontarotti P, Olive D** (2012) *The butyrophilin (BTN) gene family: from milk fat to the regulation of the immune response*. Immunogenetics, 64(11):781-94.
[301] **Messal N, Mamessier E, Sylvain A, Celis-Gutierrez J, Thibult ML, Chetaille B, et al.** (2011) *Differential role for CD277 as a co-regulator of the immune signal in T and NK cells*. Eur J Immunol, 41(12):3443-54.
[302] **Yamashiro H, Yoshizaki S, Tadaki T, Egawa K, Seo N** (2010) *Stimulation of human butyrophilin 3 molecules results in negative regulation of cellular immunity*. J Leukoc Biol, 88(4):757-67.
[303] **Palakodeti A, Sandstrom A, Sundaresan L, Harly C, Nedellec S, Olive D, et al.** (2012) *The molecular basis for modulation of human Vgamma9Vdelta2 T cell responses by CD277/butyrophilin-3 (BTN3A)-specific antibodies*. J Biol Chem, 287(39):32780-90.
[304] **Vavassori S, Kumar A, Wan GS, Ramanjaneyulu GS, Cavallari M, El Daker S, et al.** (2013) *Butyrophilin 3A1 binds phosphorylated antigens and stimulates human gammadelta T cells*. Nat Immunol, 14(9):908-16.
[305] **Wang H, Morita CT** (2015) *Sensor Function for Butyrophilin 3A1 in Prenyl Pyrophosphate Stimulation of Human Vgamma2Vdelta2 T Cells*. J Immunol, 195(10):4583-94.
[306] **Hsiao CH, Lin X, Barney RJ, Shippy RR, Li J, Vinogradova O, et al.** (2014) *Synthesis of a phosphoantigen prodrug that potently activates Vgamma9Vdelta2 T-lymphocytes*. Chem Biol, 21(8):945-54.
[307] **Rhodes DA, Chen HC, Price AJ, Keeble AH, Davey MS, James LC, et al.** (2015) *Activation of human gammadelta T cells by cytosolic interactions of BTN3A1 with soluble phosphoantigens and the cytoskeletal adaptor periplakin*. J Immunol, 194(5):2390-8.

[308] **Sandstrom A, Peigne CM, Leger A, Crooks JE, Konczak F, Gesnel MC, et al.** (2014) *The intracellular B30.2 domain of butyrophilin 3A1 binds phosphoantigens to mediate activation of human Vgamma9Vdelta2 T cells*. Immunity, 40(4):490-500.
[309] **Nguyen K, Li J, Puthenveetil R, Lin X, Poe MM, Hsiao CC, et al.** (2017) *The butyrophilin 3A1 intracellular domain undergoes a conformational change involving the juxtamembrane region*. FASEB J, 31(11):4697-706.
[310] **Vantourout P, Laing A, Woodward MJ, Zlatareva I, Apolonia L, Jones AW, et al.** (2018) *Heteromeric interactions regulate butyrophilin (BTN) and BTN-like molecules governing γδ T cell biology*. Proc Natl Acad Sci U S A.
[311] **Salim M, Knowles TJ, Baker AT, Davey MS, Jeeves M, Sridhar P, et al.** (2017) *BTN3A1 Discriminates gammadelta T Cell Phosphoantigens from Nonantigenic Small Molecules via a Conformational Sensor in Its B30.2 Domain*. ACS Chem Biol, 12(10):2631-43.
[312] **Gu S, Sachleben JR, Boughter CT, Nawrocka WI, Borowska MT, Tarrasch JT, et al.** (2017) *Phosphoantigen-induced conformational change of butyrophilin 3A1 (BTN3A1) and its implication on Vgamma9Vdelta2 T cell activation*. Proc Natl Acad Sci U S A, 114(35):E7311-E20.
[313] **Peigne CM, Leger A, Gesnel MC, Konczak F, Olive D, Bonneville M, et al.** (2017) *The Juxtamembrane Domain of Butyrophilin BTN3A1 Controls Phosphoantigen-Mediated Activation of Human Vgamma9Vdelta2 T Cells*. J Immunol, 198(11):4228-34.
[314] **Sebestyen Z, Scheper W, Vyborova A, Gu S, Rychnavska Z, Schiffler M, et al.** (2016) *RhoB Mediates Phosphoantigen Recognition by Vgamma9Vdelta2 T Cell Receptor*. Cell Rep, 15(9):1973-85.
[315] **Riano F, Karunakaran MM, Starick L, Li J, Scholz CJ, Kunzmann V, et al.** (2014) *Vgamma9Vdelta2 TCR-activation by phosphorylated antigens requires butyrophilin 3 A1 (BTN3A1) and additional genes on human chromosome 6*. Eur J Immunol, 44(9):2571-6.
[316] **Kazen AR, Adams EJ** (2011) *Evolution of the V, D, and J gene segments used in the primate gammadelta T-cell receptor reveals a dichotomy of conservation and diversity*. Proc Natl Acad Sci U S A, 108(29):E332-40.
[317] **Karunakaran MM, Gobel TW, Starick L, Walter L, Herrmann T** (2014) *Vgamma9 and Vdelta2 T cell antigen receptor genes and butyrophilin 3 (BTN3) emerged with placental mammals and are concomitantly preserved in selected species like alpaca (Vicugna pacos)*. Immunogenetics, 66(4):243-54.
[318] **O'leary MA, Bloch JI, Flynn JJ, Gaudin TJ, Giallombardo A, Giannini NP, et al.** (2013) *The placental mammal ancestor and the post-K-Pg radiation of placentals*. Science, 339(6120):662-7.
[319] **Springer MS, Stanhope MJ, Madsen O, De Jong WW** (2004) *Molecules consolidate the placental mammal tree*. Trends Ecol Evol, 19(8):430-8.
[320] **Wang H, Lee HK, Bukowski JF, Li H, Mariuzza RA, Chen ZW, et al.** (2003) *Conservation of Nonpeptide Antigen Recognition by Rhesus Monkey Vγ2Vδ2 T Cells*. J Immunol, 170(7):3696-706.
[321] **Karunakaran MM**. The Evolution of Vγ9Vδ2 T cells. Würzburg: Julius-Maximilians-Universität Würzburg; 2014.
[322] **Kirchheimer WF, Storrs EE** (1971) *Attempts to establish the armadillo (Dasypus novemcinctus Linn.) as a model for the study of leprosy. I. Report of lepromatoid leprosy in an experimentally infected armadillo*. Int J Lepr Other Mycobact Dis, 39(3):693-702.
[323] **Truman R** (2005) *Leprosy in wild armadillos*. Lepr Rev, 76(3):198-208.
[324] **Scollard DM, Adams LB, Gillis TP, Krahenbuhl JL, Truman RW, Williams DL** (2006) *The continuing challenges of leprosy*. Clin Microbiol Rev, 19(2):338-81.
[325] **Linguiti G, Antonacci R, Tasco G, Grande F, Casadio R, Massari S, et al.** (2016) *Genomic and expression analyses of Tursiops truncatus T cell receptor gamma (TRG) and alpha/delta (TRA/TRD) loci reveal a similar basic public gammadelta repertoire in dolphin and human*. BMC Genomics, 17(1):634.
[326] **Fichtner AS, Karunakaran MM, Starick L, Truman RW, Herrmann T** (2018) *The Armadillo (Dasypus novemcinctus): A Witness but Not a Functional Example for the Emergence of the Butyrophilin 3/Vγ9Vδ2 System in Placental Mammals*. Front Immunol, 9(265).
[327] **Zhang Z, Schwartz S, Wagner L, Miller W** (2000) *A greedy algorithm for aligning DNA sequences*. J Comput Biol, 7(1-2):203-14.
[328] **Altschul SF, Madden TL, Schaffer AA, Zhang J, Zhang Z, Miller W, et al.** (1997) *Gapped BLAST and PSI-BLAST: a new generation of protein database search programs*. Nucleic Acids Res, 25(17):3389-402.
[329] **Lefranc MP** (2011) *IMGT, the International ImMunoGeneTics Information System*. Cold Spring Harb Protoc, 2011(6):595-603.

[330] **Ehrenmann F, Kaas Q, Lefranc M-P** (2010) *IMGT/3Dstructure-DB and IMGT/DomainGapAlign: a database and a tool for immunoglobulins or antibodies, T cell receptors, MHC, IgSF and MhcSF*. Nucleic Acids Res, 38(suppl_1):D301-D7.
[331] **Ehrenmann F, Lefranc MP** (2011) *IMGT/DomainGapAlign: IMGT standardized analysis of amino acid sequences of variable, constant, and groove domains (IG, TR, MH, IgSF, MhSF)*. Cold Spring Harb Protoc, 2011(6):737-49.
[332] **Ehrenmann F, Lefranc MP** (2012) *IMGT/DomainGapAlign: the IMGT(R) tool for the analysis of IG, TR, MH, IgSF, and MhSF domain amino acid polymorphism*. Methods Mol Biol, 882:605-33.
[333] **Zerbino DR, Achuthan P, Akanni W, Amode M r, Barrell D, Bhai J, et al.** (2018) *Ensembl 2018*. Nucleic Acids Res, 46(D1):D754-D61.
[334] **Mcwilliam H, Li W, Uludag M, Squizzato S, Park YM, Buso N, et al.** (2013) *Analysis Tool Web Services from the EMBL-EBI*. Nucleic Acids Res, 41(W1):W597-W600.
[335] **Gasteiger E, Gattiker A, Hoogland C, Ivanyi I, Appel RD, Bairoch A** (2003) *ExPASy: the proteomics server for in-depth protein knowledge and analysis*. Nucleic Acids Res, 31(13):3784-8.
[336] **Desmet F-O, Hamroun D, Lalande M, Collod-Béroud G, Claustres M, Béroud C** (2009) *Human Splicing Finder: an online bioinformatics tool to predict splicing signals*. Nucleic Acids Res, 37(9):e67-e.
[337] **Merelli I, Guffanti A, Fabbri M, Cocito A, Furia L, Grazini U, et al.** (2010) *RSSsite: a reference database and prediction tool for the identification of cryptic Recombination Signal Sequences in human and murine genomes*. Nucleic Acids Res, 38(Web Server issue):W262-W7.
[338] **Pietschmann T, Heinkelein M, Heldmann M, Zentgraf H, Rethwilm A, Lindemann D** (1999) *Foamy virus capsids require the cognate envelope protein for particle export*. J Virol, 73(4):2613-21.
[339] **Knodel M, Kuss AW, Lindemann D, Berberich I, Schimpl A** (1999) *Reversal of Blimp-1-mediated apoptosis by A1, a member of the Bcl-2 family*. Eur J Immunol, 29(9):2988-98.
[340] **Soneoka Y, Cannon PM, Ramsdale EE, Griffiths JC, Romano G, Kingsman SM, et al.** (1995) *A transient three-plasmid expression system for the production of high titer retroviral vectors*. Nucleic Acids Res, 23(4):628-33.
[341] **Lindemann D, Patriquin E, Feng S, Mulligan RC** (1997) *Versatile retrovirus vector systems for regulated gene expression in vitro and in vivo*. Mol Med, 3(7):466-76.
[342] **Holst J, Wang H, Eder KD, Workman CJ, Boyd KL, Baquet Z, et al.** (2008) *Scalable signaling mediated by T cell antigen receptor-CD3 ITAMs ensures effective negative selection and prevents autoimmunity*. Nat Immunol, 9(6):658-66.
[343] **Dal Porto J, Johansen TE, Catipovic B, Parfiit DJ, Tuveson D, Gether U, et al.** (1993) *A soluble divalent class I major histocompatibility complex molecule inhibits alloreactive T cells at nanomolar concentrations*. Proc Natl Acad Sci U S A, 90(14):6671-5.
[344] **Hebell T, Ahearn JM, Fearon DT** (1991) *Suppression of the immune response by a soluble complement receptor of B lymphocytes*. Science, 254(5028):102-5.
[345] **Kreiss M, Asmuss A, Krejci K, Lindemann D, Miyoshi-Akiyama T, Uchiyama T, et al.** (2004) *Contrasting contributions of complementarity-determining region 2 and hypervariable region 4 of rat BV8S2+ (Vbeta8.2) TCR to the recognition of myelin basic protein and different types of bacterial superantigens*. Int Immunol, 16(5):655-63.
[346] **Bueler H, Mulligan RC** (1996) *Induction of antigen-specific tumor immunity by genetic and cellular vaccines against MAGE: enhanced tumor protection by coexpression of granulocyte-macrophage colony-stimulating factor and B7-1*. Mol Med, 2(5):545-55.
[347] **Luhder F, Huang Y, Dennehy KM, Guntermann C, Muller I, Winkler E, et al.** (2003) *Topological requirements and signaling properties of T cell-activating, anti-CD28 antibody superagonists*. J Exp Med, 197(8):955-66.
[348] **Letourneur F, Malissen B** (1989) *Derivation of a T cell hybridoma variant deprived of functional T cell receptor alpha and beta chain transcripts reveals a nonfunctional alpha-mRNA of BW5147 origin*. Eur J Immunol, 19(12):2269-74.
[349] **Paletta D, Fichtner AS, Hahn AM, Starick L, Beyersdorf N, Monzon-Casanova E, et al.** (2015) *The hypervariable region 4 (HV4) and position 93 of the alpha chain modulate CD1d-glycolipid binding of iNKT TCRs*. Eur J Immunol, 45(7):2122-33.
[350] **Warburton D, Gersen S, Yu MT, Jackson C, Handelin B, Housman D** (1990) *Monochromosomal rodent-human hybrids from microcell fusion of human lymphoblastoid cells containing an inserted dominant selectable marker*. Genomics, 6(2):358-66.
[351] **Oi VT, Morrison SL, Herzenberg LA, Berg P** (1983) *Immunoglobulin gene expression in transformed lymphoid cells*. Proc Natl Acad Sci U S A, 80(3):825-9.

[352] **Sanford KK, Earle WR, Likely GD** (1948) *The growth in vitro of single isolated tissue cells*. J Natl Cancer Inst, 9(3):229-46.
[353] **Griffith IJ, Nabavi N, Ghogawala Z, Chase CG, Rodriguez M, Mckean DJ, et al.** (1988) *Structural mutation affecting intracellular transport and cell surface expression of murine class II molecules*. J Exp Med, 167(2):541-55.
[354] **Davis WC, Heirman LR, Hamilton MJ, Parish SM, Barrington GM, Loftis A, et al.** (2000) *Flow cytometric analysis of an immunodeficiency disorder affecting juvenile llamas*. Vet Immunol Immunopathol, 74(1-2):103-20.
[355] **Monzon-Casanova E, Steiniger B, Schweigle S, Clemen H, Zdzieblo D, Starick L, et al.** (2010) *CD1d expression in paneth cells and rat exocrine pancreas revealed by novel monoclonal antibodies which differentially affect NKT cell activation*. PLoS One, 5(9).
[356] **Pyz E**. Identification of rat NKT cells and molecular analysis of their surface receptor mediated activation. Würzburg: Univeristy of Würzburg; 2004.
[357] **Fichtner AS**. CD1d and iNKT cells in cotton rats [M.Sc. Thesis]. Würzburg: University of Würzburg; 2013.
[358] **Ravens S, Schultze-Florey C, Raha S, Sandrock I, Drenker M, Oberdorfer L, et al.** (2017) *Human gammadelta T cells are quickly reconstituted after stem-cell transplantation and show adaptive clonal expansion in response to viral infection*. Nat Immunol, 18(4):393-401.
[359] **Kashani E, Föhse L, Raha S, Sandrock I, Oberdörfer L, Koenecke C, et al.** (2015) *A clonotypic Vγ4Jγ1/Vδ5Dδ2Jδ1 innate γδ T-cell population restricted to the CCR6+CD27− subset*. Nat Commun, 6:6477.
[360] **Exley M, Garcia J, Balk SP, Porcelli S** (1997) *Requirements for CD1d recognition by human invariant Valpha24+ CD4-CD8- T cells*. J Exp Med, 186(1):109-20.
[361] **Schneck JP, Slansky JE, O'herrin SM, Greten TF** (2001) *Monitoring antigen-specific T cells using MHC-Ig dimers*. Curr Protoc Immunol, Chapter 17:Unit 17 2.
[362] **Lebowitz MS, O'herrin SM, Hamad AR, Fahmy T, Marguet D, Barnes NC, et al.** (1999) *Soluble, high-affinity dimers of T-cell receptors and class II major histocompatibility complexes: biochemical probes for analysis and modulation of immune responses*. Cell Immunol, 192(2):175-84.
[363] **Kinebuchi M, Matsuura A** (2004) *Rat T-cell receptor TRAV11 (Valpha14) genes: further evidence of extensive multiplicity with homogeneous CDR1 and diversified CDR2 by genomic contig and cDNA analysis*. Immunogenetics, 55(11):756-62.
[364] **Smith LR, Kono DH, Theofilopoulos AN** (1991) *Complexity and sequence identification of 24 rat V beta genes*. J Immunol, 147(1):375-9.
[365] **Torres-Nagel NE, Gold DP, Hunig T** (1993) *Identification of rat Tcrb-V8.2, 8.5, and 10 gene products by monoclonal antibodies*. Immunogenetics, 37(4):305-8.
[366] **Asmuss A, Hofmann K, Hochgrebe T, Giegerich G, Hunig T, Herrmann T** (1996) *Alleles of highly homologous rat T cell receptor beta-chain variable segments 8.2 and 8.4: strain-specific expression, reactivity to superantigens, and binding of the mAb R78*. J Immunol, 157(10):4436-41.
[367] **Huppi KE, D'hoostelaere LA, Mock BA, Jouvin-Marchel E, Behlke MA, Chou HS, et al.** (1988) *T-cell receptor VTβ genes in natural populations of mice*. Immunogenetics, 27(1):51-6.
[368] Solovyev VV. Statistical approaches in Eukaryotic gene prediction. In: Balding D. CC, Bishop M., editor. Handbook of statistical genetics. 3rd ed: Wiley-Interscience; 2007.
[369] **Starick L, Riano F, Karunakaran MM, Kunzmann V, Li J, Kreiss M, et al.** (2017) *Butyrophilin 3A (BTN3A, CD277)-specific antibody 20.1 differentially activates Vgamma9Vdelta2 TCR clonotypes and interferes with phosphoantigen activation*. Eur J Immunol, 47(6):982-92.
[370] **Pelicci P, Subar M, Weiss A, Dalla-Favera R, Littman D** (1987) *Molecular diversity of the human T-gamma constant region genes*. Science, 237(4818):1051-5.
[371] **Band H, Hochstenbach F, Parker CM, Mclean J, Krangel MS, Brenner MB** (1989) *Expression of human T cell receptor-gamma delta structural forms*. J Immunol, 142(10):3627-33.
[372] **Antonacci R, Mineccia M, Lefranc M-P, Ashmaoui HME, Lanave C, Piccinni B, et al.** (2011) *Expression and genomic analyses of Camelus dromedarius T cell receptor delta (TRD) genes reveal a variable domain repertoire enlargement due to CDR3 diversification and somatic mutation*. Mol Immunol, 48(12):1384-96.
[373] **Clevers H, Machugh ND, Bensaid A, Dunlap S, Baldwin CL, Kaushal A, et al.** (1990) *Identification of a bovine surface antigen uniquely expressed on CD4−CD8− T cell receptor γ/δ+ T lymphocytes*. Eur J Immunol, 20(4):809-17.
[374] **Wijngaard PL, Metzelaar MJ, Machugh ND, Morrison WI, Clevers HC** (1992) *Molecular characterization of the WC1 antigen expressed specifically on bovine CD4-CD8- gamma delta T lymphocytes*. J Immunol, 149(10):3273-7.

[375] **Morrison WI, Davis WC** (1991) *Differentiation antigens expressed predominantly on CD4– CD8– T lymphocytes (WC1, WC2)*. Vet Immunol Immunopathol, 27(1):71-6.
[376] **Cairo C, Armstrong CL, Cummings JS, Deetz CO, Tan M, Lu C, et al.** (2010) *Impact of age, gender and race on circulating gammadelta T cells*. Hum Immunol, 71(10):968-75.
[377] **Sherwood AM, Desmarais C, Livingston RJ, Andriesen J, Haussler M, Carlson CS, et al.** (2011) *Deep sequencing of the human TCRgamma and TCRbeta repertoires suggests that TCRbeta rearranges after alphabeta and gammadelta T cell commitment*. Sci Transl Med, 3(90):90ra61.
[378] **Li J-Q**. Modulating the expression of enzymes of isoprenoid synthesis: effects on Vgamma9Vdelta2 T cell activation and tumor cell growth 2010.
[379] **Steppan S, Adkins R, Anderson J** (2004) *Phylogeny and divergence-date estimates of rapid radiations in muroid rodents based on multiple nuclear genes*. Syst Biol, 53(4):533-53.
[380] **Benlagha K, Bendelac A** (2000) *CD1d-restricted mouse V alpha 14 and human V alpha 24 T cells: lymphocytes of innate immunity*. Semin Immunol, 12(6):537-42.
[381] **Paletta D, Fichtner AS, Starick L, Porcelli SA, Savage PB, Herrmann T** (2015) *Species Specific Differences of CD1d Oligomer Loading In Vitro*. PLoS One, 10(11):e0143449.
[382] **Eberl G, Macdonald HR** (2000) *Selective induction of NK cell proliferation and cytotoxicity by activated NKT cells*. Eur J Immunol, 30(4):985-92.
[383] **Giaccone G, Punt CJ, Ando Y, Ruijter R, Nishi N, Peters M, et al.** (2002) *A phase I study of the natural killer T-cell ligand alpha-galactosylceramide (KRN7000) in patients with solid tumors*. Clin Cancer Res, 8(12):3702-9.
[384] **Singh N, Hong S, Scherer DC, Serizawa I, Burdin N, Kronenberg M, et al.** (1999) *Cutting edge: activation of NK T cells by CD1d and alpha-galactosylceramide directs conventional T cells to the acquisition of a Th2 phenotype*. J Immunol, 163(5):2373-7.
[385] **Burdin N, Brossay L, Kronenberg M** (1999) *Immunization with alpha-galactosylceramide polarizes CD1-reactive NK T cells towards Th2 cytokine synthesis*. Eur J Immunol, 29(6):2014-25.
[386] **Sanderson JP, Waldburger-Hauri K, Garzon D, Matulis G, Mansour S, Pumphrey NJ, et al.** (2012) *Natural variations at position 93 of the invariant Valpha24-Jalpha18 alpha chain of human iNKT-cell TCRs strongly impact on CD1d binding*. Eur J Immunol, 42(1):248-55.
[387] **Scott-Browne JP, Matsuda JL, Mallevaey T, White J, Borg NA, Mccluskey J, et al.** (2007) *Germline-encoded recognition of diverse glycolipids by natural killer T cells*. Nat Immunol, 8:1105.
[388] **Solomon KR, Krangel MS, Mclean J, Brenner MB, Band H** (1990) *Human T cell receptor-gamma and -delta chain pairing analyzed by transfection of a T cell receptor-delta negative mutant cell line*. J Immunol, 144(3):1120-6.
[389] **Boucontet L, Grana M, Alzari PM, Pereira P** (2009) *Mechanisms determining cell membrane expression of different gammadelta TCR chain pairings*. Eur J Immunol, 39(7):1937-46.
[390] **Miccoli MC, Antonacci R, Vaccarelli G, Lanave C, Massari S, Cribiu EP, et al.** (2003) *Evolution of TRG Clusters in Cattle and Sheep Genomes as Drawn from the Structural Analysis of the Ovine TRG2@ Locus*. J Mol Evol, 57(1):52-62.
[391] **Massari S, Bellahcene F, Vaccarelli G, Carelli G, Mineccia M, Lefranc MP, et al.** (2009) *The deduced structure of the T cell receptor gamma locus in Canis lupus familiaris*. Mol Immunol, 46(13):2728-36.
[392] **Vernooij BTM, Lenstra JA, Wang K, Hood L** (1993) *Organization of the Murine T-Cell Receptor γ Locus*. Genomics, 17(3):566-74.
[393] **Herzig CTA, Lefranc M-P, Baldwin CL** (2010) *Annotation and classification of the bovine T cell receptor delta genes*. BMC Genomics, 11(1):100.
[394] **Alexandre D, Lefranc MP** (1992) *The human gamma/delta + and alpha/beta + T cells: a branched pathway of differentiation*. Mol Immunol, 29(4):447-51.
[395] **Mackay CR, Beya MF, Matzinger P** (1989) *Gamma/delta T cells express a unique surface molecule appearing late during thymic development*. Eur J Immunol, 19(8):1477-83.
[396] **Carr MM, Howard CJ, Sopp P, Manser JM, Parsons KR** (1994) *Expression on porcine gamma delta lymphocytes of a phylogenetically conserved surface antigen previously restricted in expression to ruminant gamma delta T lymphocytes*. Immunology, 81(1):36-40.
[397] **Ko HS, Fu SM, Winchester RJ, Yu DT, Kunkel HG** (1979) *Ia determinants on stimulated human T lymphocytes. Occurrence on mitogen- and antigen-activated T cells*. J Exp Med, 150(2):246-55.
[398] **L Blumerman S, Herzig C, Rogers A, C Telfer J, Baldwin C** (2006) *Differential TCR gene usage between WC1 and WC1 ruminant γδ T cell subpopulations including those responding to bacterial antigen*. 680-92 p.

[399] **Machugh ND, Mburu JK, Carol MJ, Wyatt CR, Orden JA, Davis WC** (1997) *Identification of two distinct subsets of bovine gamma delta T cells with unique cell surface phenotype and tissue distribution*. Immunology, 92(3):340-5.
[400] **Kunzmann V, Bauer E, Feurle J, Tony FW, Hans-Peter, Wilhelm M** (2000) *Stimulation of γδ T cells by aminobisphosphonates and induction of antiplasma cell activity in multiple myeloma*. Blood, 96(2):384-92.
[401] **Wilhelm M, Kunzmann V, Eckstein S, Reimer P, Weissinger F, Ruediger T, et al.** (2003) *γδ T cells for immune therapy of patients with lymphoid malignancies*. Blood, 102(1):200-6.
[402] **Mariani S, Muraro M, Pantaleoni F, Fiore F, Nuschak B, Peola S, et al.** (2005) *Effector γδ T cells and tumor cells as immune targets of zoledronic acid in multiple myeloma*. Leukemia, 19:664.
[403] **Fowler ME** (1998) *Medicine and surgery of South American camelids: llama, alpaca, vicuna, guanaco*: Iowa State University Press.
[404] **Mattiello S, Formis E, Barbieri S** (2011) *Thermoregulation of alpacas bred in Italy*. Int J Biometeorol, 55(2):213-8.
[405] **Koning F, Yokoyama WM, Maloy WL, Stingl G, Mcconnell TJ, Cohen DI, et al.** (1988) *Expression of C gamma 4 T cell receptors and lack of isotype exclusion by dendritic epidermal T cell lines*. J Immunol, 141(6):2057-62.
[406] **Heilig JS, Tonegawa S** (1987) *T-cell gamma gene is allelically but not isotypically excluded and is not required in known functional T-cell subsets*. Proc Natl Acad Sci U S A, 84(22):8070-4.
[407] **Ezquerra A, Wilde DB, Mcconnell TJ, Sturmhöfel K, Valas RB, Shevach EM, et al.** (1992) *Mouse autoreactive γ/δ T cells II. Molecular characterization of the T cell receptor*. Eur J Immunol, 22(2):491-8.

Abbreviations

(D)PBS	(Dulbecco's) Phosphate buffered saline
(E)GFP	(enhanced) Green Fluorescent Protein
(i)NKT	(invariant) Natural killer T cell
(RLM) RACE	(RNA ligase-mediated) Rapid amplification of cDNA ends
°C	Degree Celsius
µ-	Micro- (10^{-6})
A (Ala)	Alanine
A	Adenine (nucleobase)
AA	Acrylamide
AA	Amino acid/s
Acetyl-CoA	Acetyl coenzyme A
AF	Alexa Fluor®
APC	Antigen-presenting cell
APS	Ammonium persulfate
ATV	Antibiotic-Trypsin-Versene
BCR	B cell receptor
BD	Becton&Dickinson
bio	Biotinylated
BLAST	Basic Local Alignment Search Tool
bo	Bovine
bp	Base pairs
BSA	Bovine Serum Albumin
BSS	Buffered Sodium Salts
BTN	Butyrophilin
BTN3-C	BTN3 IgC region
BTN3-V	BTN3 IgV region
BTNL	Butyrophilin-like
C (Cys)	Cysteine
c	Concentration
C	Cytosine (nucleobase)
CD	Cluster of differentiation
cDNA	Complementary deoxyribonucleic acid
CDR	Complementarity-Determining-Region
CHO	Chinese hamster ovary cell
Chr.	Chromosome
CLIP	Class II-associated invariant chain peptide
cm	Centimeter (10^{-2} m)
cm^2	Square centimeter
CMV	Cytomegalovirus
CO_2	Carbon dioxide
ConA	Concanavalin A
cr	Cotton rat
D (Asp)	Aspartic acid
Da	Dalton
DAMP	Damage-associated molecular pattern
DC	Dendritic cell
ddNTP	Dideoxyribonucleotide triphosphate
DEPC	Diethyl pyrocarbonate
DETC	Dendritic epidermal T cell
dH_2O	Distilled water
DMAPP	Dimethylallyl pyrophosphate
DMEM	Dulbecco's Modified Eagle Medium
DMSO	Dimethyl sulfoxide
dn	Armadillo
DN	Double-negative
DNA	Deoxyribonucleic acid

dNTP	Deoxyribonucleotide triphosphate
DOXP	1-Deoxy-D-xylulose 5-phosphate
DP	Double-positive
DαM	Donkey anti-mouse
E (Glu)	Glutamic acid
E. coli	*Escherichia coli*
EDTA	Ethylenediaminetetraacetic acid
EGFP	Enhanced Green Fluorescent Protein
ELISA	Enzyme-linked Immunosorbent Assay
EPCR	Endothelial protein C receptor
ER	Endoplasmic reticulum
et al.	et alii
EtBr	Ethidium bromide
EtOH	Ethanol
F (Phe)	Phenylalanine
F	Farad
FACS	Fluorescence activated cell sorting
FBS	Fetal Bovine Serum
FCS	Fetal Calf Serum
FITC	Fluorescein isothiocyanate
FPPS	Farnesyl pyrophosphate synthase
FSC	Forward Scatter
fwd	Forward
G (Gly)	Glycine
g	Gram
G	Guanine (nucleobase)
gDNA	Genomic deoxyribonucleic acid
GM	Geometric mean
gpMBP	Guinea pig Myelin Basic Protein
GSP	Gene-specific primer
GTP	Guanosine-5'-triphosphate
GαM	Goat anti-mouse
H (His)	Histidine
h	Hour/s
H_2O	Water
ha	Hamster
HAT	Hypoxanthine-aminopterin-thymidine
HBS	HEPES-buffered saline
HEK	Human embryonal kidney cells
HEPES	4-(2-Hydroxyethyl)-1-piperazineethanesulfonic acid
HF	High fidelity
HLA	Human leukocyte antigen
HMBPP	(E)-4-hydroxy-3-methyl-but-2-enyl pyrophosphate
HMG-CoA	β-Hydroxyl-β-methylglutaryl-coenzyme A
HPIV	Human parainfluenzavirus
HSC	Hematopoietic stem cell
HSV	Herpes simplex virus
HT	Hypoxanthine-thymidine
hu	Human
HV4	Hypervariable region 4
I (Ile)	Isoleucine
i.p.	Intraperitoneal
i.v.	Intravenous
ICOS(L)	Inducible costimulatory (ligand)
ID	Intracellular domain
IFN-γ	Interferon-γ
Ig	Immunoglobulin
iGb3	Isoglobotrihexosylceramide
IgC	Immunoglobulin-like constant region

IgV	Immunoglobulin-like variable region
IHL	Intrahepatic lymphocytes
iIEL	Intestinal intraepithelial T cells
IL-	Interleukin-
IPP	Isopentenyl pyrophosphate
IRES	Internal Ribosomal Entry Site
ITAM	Immunoreceptor tyrosine-based activation motif
JM	Juxtamembrane domain
K (Lys)	Lysine
k-	Kilo- (10^3)
L (Leu)	Leucine
l	Liter
la	Llama
LB	Lysogeny Broth
lin	Linear scale
log	Logarithmic scale
M (Met)	Methionine
m-	Milli- (10^{-3})
M	Molar concentration/Molarity
m	Mouse
mAb	Monoclonal antibody
mAb	Monoclonal antibody
MAIT	Mucosal-associated invariant T cell
MALT	Mucosal-associated tissue
MCS	Multiple cloning site
MEP	2-C-methyl-D-erythritol 4-phosphate
MHC	Major histocompatibility complex
MHC I/II	Major histocompatibility complex class I/II
min	Minute/s
mRNA	Messenger ribonucleic acid
MTTP	Microsomal triglyceride transfer protein
MuLV	Murine Leukemia Virus
MVA	Mevalonate
MW	Molecular Weight
MWCO	Molecular Weight Cut Off
N (Asn)	Asparagine
n-	Nano- (10^{-9})
N	Normality
NCBI	National Center for Biotechnology Information
NGS	Next generation sequencing
NK	Natural killer cell
NmIg	Normal mouse serum immunoglobulin
NT	Nucleotide/s
OD	Optic density
P (Pro)	Proline
PAg	Phosphoantigen
PAMP	Pathogen-associated molecular pattern
PBMC	Peripheral blood monocytic cells
PCR	Polymerase chain reaction
PE	Phycoerythrin
PEG	Polyethylene glycol
pH	Potential of hydrogen
PLC	Peptide-loading complex
PLZF	Promyelocytic leukaemia zinc finger protein
PRR	Pattern recognition receptor
pur.	Purified
Q (Gln)	Glutamine
R (Arg)	Arginine
r	Rat

RAG-1/2	Recombination-activating gene-1/2
rcf/ x g	Relative centrifugal force/Centrifuge G-force
rev	Reverse
RNA	Ribonucleid acid
rpm	Revolutions per minute
RPMI	Roswell Park Memorial Institute
RSS	Recombination signal sequence
RSV	Respiratory syncytial virus
RT	Room temperature
S (Ser)	Serine
s	Second/s
S.O.C	Super Optimal Broth with Catabolite repression
SA-APC	Streptavidin-allophycocyanin
SD	Standard deviation
SDS	Sodium dodecyl sulfate
SDS-PAGE	SDS-polyacrylamide gel electrophoresis
SEM	Standard error of means
SOB	Super Optimal Broth
SP	Single-positive
SSC	Side Scatter
T (Thr)	Threonine
T	Thymine (nucleobase)
TAE	Tris-acetate-EDTA buffer
TAP1/2	Transporter associated with antigen processing-1/2
TCR	T cell receptor
TdT	Terminal deoxynucleotidyl transferase
TE	Tris-EDTA buffer
TEMED	Tetramethylethylenediamine
TGS	Tris-Glycine-SDS buffer
TM	Transmembrane domain
TNF	Tumor Necrosis Factor
TRAIL	TNF-Related Apoptosis Inducing Ligand
TRC	T cell receptor constant gene segment
TRD	T cell receptor diversity gene segment
TRIM	Tripartite motif-containing proteins
TRJ	T cell receptor junctional gene segment
TRV	T cell receptor variable gene segment
U	Units
V (Val)	Valine
V	Volt
vp	Alpaca
W (Trp)	Tryptophan
w/o	Without
wgs	Whole genome shotgun contigs
Y (Tyr)	Tyrosine
z. B.	Zum Beispiel
αGC	α-Galactosylceramide
β_2m	β_2-Microglobuline

Affidavit

I hereby confirm that my thesis entitled "*Alpaca, armadillo and cotton rat as new animal models for non-conventional T cells: Identification of cell populations and analysis of antigen receptors and ligands*" is the result of my own work. I did not receive any help or support from commercial consultants. All sources and/or materials applied are listed and specified in this thesis.

Furthermore, I confirm that this thesis has not yet been submitted as part of another examination process neither in identical nor in similar form.

Würzburg, April 18, 2018 ……..
(Alina Suzann Fichtner)

Eidesstattliche Erklärung

Hiermit erkläre ich an Eides statt, dass die Dissertation „*Alpaka, Gürteltier und Baumwollratte als neue Tiermodelle für nicht-konventionelle T-Zellen: Identifikation von Zellpopulationen und Analyse von Antigenrezeptoren und Liganden*" eigenständig, d.h. insbesondere selbstständig und ohne Hilfe eines kommerziellen Promotionsberaters, angefertigt und keine anderen als die von mir angegeben Quellen und Hilfsmittel verwendet zu haben.

Ich erkläre außerdem, dass die Dissertation weder in gleicher noch in ähnlicher Form bereits in einem anderen Prüfungsverfahren vorgelegt wurde.

Würzburg, 18. April 2018 ……..
(Alina Suzann Fichtner)

Curriculum Vitae

Acknowledgments

Most of all, I want to thank Prof. Dr. Thomas Herrmann for the opportunity to complete my doctorate under his supervision. I am very grateful for his encouragement, support, lengthy discussions and his mentorship that helped me to become the inquisitive scientist I am today.

Furthermore, I want to thank Prof. Dr. Stefan Niewiesk for the opportunity to complete the cotton rat project under his great supervision at the Ohio State University. I would like to take this opportunity to also thank our collaborators Prof. Dr. Thomas Göbel and Prof. Dr. Richard Truman.

Moreover, I would like to express my gratitude to my committee members PD Dr. Heike Hermanns and PD Dr. Niklas Beyersdorf who contributed to this project with their valuable input and advice.

A big thank you to my colleagues in the laboratory of Prof. Dr. Thomas Herrmann; it was a wonderful time. Thank you, Lisa, for your friendship, guidance and help in the course of many projects. I also greatly appreciate Daniel, Mohindar and Anna for their help and friendship. Thanks to everyone at the institute who helped me with this project and encouraged me along the way and thank you Devra and Gia for supporting me during my time at the Ohio State University.

Last but not least, I want to thank my parents and family for teaching me to be curious and their support along the way and thanks to all my friends who were there for me in good and tough times.

Finally, I want to dedicate the last lines to Michael who is always by my side and encourages me every day.